

CHARACTERISATION OF SAPPI SAICCOR PULP MILL'S EFFLUENT

BY

BRENDA MOODLEY
BSc. (HONS) (Natal)

Submitted in partial fulfilment of the requirements
for the degree of
Master of Science
in the
School of Pure and Applied Chemistry,
University of Natal,
Durban
2001

*For my family :
Dad, Mum, Chantal and Christel*

*'Happy is the man that findeth
wisdom, and the man that getteth understanding.
For the merchandise of it is better than the
merchandise of silver, and the gain thereof
than fine gold.'*

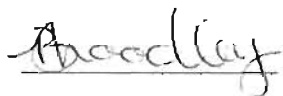
Proverbs : 3 : v 13-14

Preface

The experimental work described in this thesis was carried out in the School of Pure and Applied Chemistry, University of Natal, Durban, South Africa under the supervision of of Professor J. Marsh and Professor D. A. Mulholland.

This study represents original work by the author and has not been submitted in any other form to another university. Where use was made of the work of others, it has been duly acknowledged in the text.

Signed :

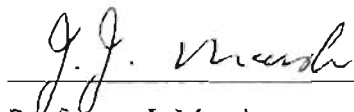


B. Moodley

BSc, BSc (HONS) (Natal)

I hereby certify that the above statement is correct.

Signed :



Professor J. Marsh

Ph.D. (RAU)



Professor D. A. Mulholland

Ph.D. (Natal)

ACKNOWLEDGEMENTS

I would firstly like to thank my supervisor, Professor D. A. Mulholland for all her advice and guidance during the course of this year. She has allowed me to work independently but with continuous support and has always made time to help me through any problem. I have been truly blessed to have you as my supervisor.

I would also like to thank, my supervisor, Professor J. Marsh for his continuous support and encouragement during this year. Thank you for organising the many necessary meetings and trips down to SAPPI SAICCOR and as well as for allowing me to learn from your vast industrial experience.

Thank you to Professor M. Laing and Dr. A. Kindness for their assistance in interpreting the XRD spectrum and thank you to Roy and Pat from the Geology department of the University of Natal – Durban for the running of the XRD and XRF spectra.

A very big thank you to my colleagues in the Natural Products Research Group. Thank you to Peter Cheplogoi for his constant encouragement and support and to Phil Coombes who was never too busy to offer assistance when I needed it. Thank you to Nivan Moodley and Dashnie Naidoo, Angela Langlois and Kathryn McFarland for creating a pleasant working environment. A special thank you to my sister, Chantal, and to Neil for their continuous support and advice and for encouraging me to continue with my postgraduate studies.

Many thanks must go to both the academic and technical staff in the School of Pure and Applied Chemistry who have assisted me in some way during the course of this year.

In particular, I would like to thank Bret Parel for his constant help in the laboratory and for the running of the mass spectra. Thank you for never being too busy to assist me. Thank you also to Dilip Jagjivan for his efficient running of the NMR spectra and thank you to Zarina Sayed-Ally and Saroj Naidoo for their assistance in the running of the UV

spectra. Thank you to Ernest Mchunu for providing a clean and comfortable working environment. Thank you also to Marion Horn from the University of Natal – Pietermaritzburg for her assistance in running optical rotations.

I would also like to thank John Thubron from SAPPI SAICCOR for all his assistance during this year. Thank you John for always making the time in your busy schedule to see me during my site visits and for your many tours through the plant. Thank you for organising the many samples I requested during this year and for providing all the essential information concerning the plant process and laboratory analyses. Thank you also to Tracy Pohl for readily providing information on the species of wood milled and for transporting samples from SAICCOR to the laboratory.

I would like to place on record my appreciation and gratitude to SAPPI SAICCOR for their financial assistance.

But most of all I would like to thank my family, Dad, Mum, Christel and Chantal, for always being there for me and for allowing me the privilege to once again return to campus and continue with my studies. Thank you for your patience and support and not forgetting your prayers – without you I would never have been able to achieve what I have thus far.

And most importantly, I would like to thank the Lord Jesus Christ, who has been my strength and guide for it is only through him I can do all things.

LIST OF ABBREVIATIONS

^1H NMR spectroscopy – proton nuclear magnetic resonance spectroscopy

^{13}C NMR spectroscopy – carbon-13 nuclear magnetic resonance spectroscopy

COSY – correlated spectroscopy

HETCOR – heteronuclear shift correlation nuclear magnetic resonance

NOESY – nuclear Overhauser effect spectroscopy

HMBC – heteronuclear multiple bond coherence

HSQC – heteronuclear multiple quantum coherence

LRMS – low resolution mass spectrometry

I.R. – infrared

UV – ultraviolet/visible

Mp – melting point

TLC – thin layer chromatography

PTLC – preparative thin layer chromatography

GC/MS – gas chromatography/mass spectrometry

pr. – pressure

L-Phe – L-phenylalanine

NADPH – nicotinamide adenine dinucleotide phosphate

SAM – S-adenosylmethionine

W-M – **W**agner-**M**eerwein

ATP – adenosine triphosphate

ADP – adenosine diphosphate

UDP – uridine diphosphate

β -D-Glcp – β -D-glucopyranose

β -D-Manp – β -D-mannopyranose

β -D-Xylp – β -D-xylopyranose

4-O-Me- α -D-GlcpU – pyranoid 4-O-Me- α -D-glucuronic

s – singlet

d – doublet

t – triplet

q – quartet

m – multiplet

Hz – Hertz

LIST OF FIGURES

	Page No.
FIGURE 1: Wood chipping	8
FIGURE 2: Cooking of wood chips in a digester	9
FIGURE 3: Viscose fibres	11
FIGURE 4: Cellophane wrapping	11
FIGURE 5: Simplified structure of a woody cell	14
FIGURE 6: Structures of biologically important lignans and the cancer drug etoposide	18
FIGURE 7: Structures of squalene and squalene epoxide	23
FIGURE 8: Structures of common triterpenoids, eg., cholesterol, campesterol and sitosterol	23
FIGURE 9: Structures of a common monosaccharide and disaccharide	31
FIGURE 10: Structures of linear and branched polysaccharides	35
FIGURE 11: Structures of some common naturally occurring polysaccharides	36
FIGURE 12: Partial chemical structure of glucomannan and xylan from hardwoods	36
FIGURE 13: Structure of compound 1, syringaresinol	43
FIGURE 14: COSY correlations of compound 1	45
FIGURE 15: NOESY correlations of compound 1	45
FIGURE 16: Structure of compound 2, episyngaresinol	47
FIGURE 17: NOESY correlations of compound 2	49
FIGURE 18: HMBC correlations (C→H) of compound 2	50
FIGURE 19: Structure of compound 3, 3-(4'-hydroxy-3',5'- dimethoxyphenyl)-prop-1-ene	53
FIGURE 20: HMBC correlations (C→H) of compound 3	55
FIGURE 21: COSY correlations of compound 3	55

FIGURE 22: Structure of compound 4, 3-(4'-hydroxy-3',5'- dimethoxyphenyl)-1-hydroxy-propan-2-one displaying keto-enol tautomerism	57
FIGURE 23: HMBC correlations (C→H) of compound 4	59
FIGURE 24: NOESY correlations of compound 4	59
FIGURE 25: Structure of acetylated compound 4	61
FIGURE 26: HMBC correlations (C→H) of the acetylated compound 4	63
FIGURE 27: NOESY correlations of acetylated compound 4	63
FIGURE 28: Structure of compound 5, syringaldehyde	64
FIGURE 29: Structure of compound 6, 2,6-dimethoxy-1,4- benzoquinone	67
FIGURE 30: HMBC correlations (C→H) of compound 6	68
FIGURE 31: Structure of compound 7, vanillin	79
FIGURE 32: Structures of other compounds isolated from the magnesium condensate effluent stream	81
FIGURE 33: Structure of compound 8, β -sitosterol	83
FIGURE 34: Structure of compound 9, hexadecanoic acid	85
FIGURE 35: Structure of syringaldehyde	87
FIGURE 36: Structures of other compounds identified in the E ₂ -stage bleaching effluent	89
FIGURE 37: Structure of compound 10, 9,12-octadecadienoic acid	90

LIST OF SCHEMES

	Page No.
SCHEME 1: Simplified flow chart of a sulphite pulping process	3
SCHEME 2: Reaction scheme for the production of calcium bisulphite	4
SCHEME 3: Reaction of MgO and CaCO ₃ to produce Mg bisulphite and Ca bisulphite	9
SCHEME 4: Shikimate pathway showing the formation of lignin precursors	15
SCHEME 5: Biosynthesis of guaiacylglycerol	16
SCHEME 6: Formation of lignosulphonates	20
SCHEME 7: Typical condensation reactions that compete with sulphonation	20
SCHEME 9: Mechanism of the formation of 24-methylene-cycloartenol from squalene epoxide	25
SCHEME 10: Mechanism showing the alkylation of C-24	26
SCHEME 11: Carboxylation of acetyl-CoA to malonyl-CoA	28
SCHEME 12: Biosynthesis of fatty acids from malonyl-CoA	29
SCHEME 13: Formation of pentoses	32
SCHEME 14: Conversion of ribulose-1,5-diphosphate to glucose	33
SCHEME 15: Formation of lactose from galactose and glucose	34
SCHEME 16: Simplified flow diagram of SAPPI SAICCOR's process	42

LIST OF TABLES

	Page No.
TABLE 1: NMR information of compound 1 (300MHz, CDCl ₃)	46
TABLE 2: NMR information of compound 2 (400MHz, CDCl ₃)	51
TABLE 3: NMR data of compound 3 (400MHz, CDCl ₃)	56
TABLE 4: NMR information of compound 4 (400MHz, CDCl ₃)	60
TABLE 5: NMR information of compound 5 (400MHz, CDCl ₃)	66
TABLE 6: NMR information of compound 6 (400MHz, CDCl ₃)	69
TABLE 7: Results of XRD analysis of residue formed in the calcium – spent liquor	183-184
TABLE 8: Results of XRF analysis of residue formed in the calcium – spent liquor	185
TABLE 9: Data used to calculate the concentration of glucose in the calcium – spent liquor effluent	75
TABLE 10: Data used to calculate the concentration of xylose in the calcium – spent liquor effluent	76
TABLE 11: Results of calcium – spent liquor analysis obtained from SAPPI SAICCOR	221
TABLE 12 : Data for the conductivity titration used to determine the sulphonic acid content of the calcium spent liquor	222-223
TABLE 13: Carbohydrate content of the four streams of effluent	120

ABSTRACT

SAPPI SAICCOR, whose factory is situated south of Durban, South Africa, is one of the few paper and pulp mills that uses the acid sulphite process with calcium and magnesium bases to produce a high-grade cellulose pulp. Four streams of effluent, namely, the calcium - spent liquor stream, the magnesium condensate stream and two streams from the bleaching effluent are produced during this sulphite pulping process and they contain a variety of organic compounds extracted from the wood. Characterisation of the effluent was based on isolation using column chromatography and identification using NMR techniques.

A range of constituents, such as lignans and lignin - type precursors, a triterpenoid and fatty acids were isolated and identified. X-ray diffraction was used to identify an inorganic residue obtained from the calcium - spent liquor stream and gas chromatography/mass spectrometry was used to identify a wax residue, which builds up in the process. In addition to this, the carbohydrate content of the four streams of effluent was determined using UV/visible spectroscopy.

TABLE OF CONTENTS

	Page No
<i>Preface</i>	iii
<i>Acknowledgements</i>	iv-v
<i>List of Abbreviations</i>	vi-vii
<i>List of Figures</i>	viii-ix
<i>List of Schemes</i>	x
<i>List of Tables</i>	xi
<i>Abstract</i>	xii
CHAPTER 1 : INTRODUCTION	
1.1 The aim of the project	1
1.2 A brief overview of the types of sulphite pulping	1-5
1.3 Compounds identified in sulphite pulping effluents	6-7
1.4 A brief description of SAPPI SAICCOR's process	8-11
1.5 References	12
CHAPTER 2 : CLASSES OF COMPOUNDS ISOLATED AND IDENTIFIED FROM SAPPI SAICCOR'S EFFLUENT	
2.1 Lignin	
2.1.1 General	13-14
2.1.2 Biosynthesis of lignins	14-17
2.1.3 The uses of lignins and lignans	17-18
2.2 Lignosulphonates	
2.2.1 General	19
2.2.2 The synthesis of lignosulphonates	19-21
2.2.3 The uses of lignosulphonates	21

2.3 Extractives	
2.3.1 Triterpenoids	
2.3.1.1 General	22-23
2.3.1.2 The biosynthesis of triterpenoids	24-26
2.3.1.3 The uses of sterols	26-27
2.3.2 Fatty Acids	
2.3.2.1 General	28
2.3.2.2 The biosynthesis of fatty acids	28-29
2.3.2.3 The uses of fatty acids	30
2.4 Carbohydrates	
2.4.1 General	31
2.4.2 The biosynthesis of carbohydrates	32-36
2.4.3 The uses of carbohydrates	37
2.5 References	38-40

CHAPTER 3 : RESULTS AND DISCUSSION

3.1 Analysis of the calcium – spent liquor effluent	
3.1.1 Structural elucidation of compound 1	43-46
3.1.2 Structural elucidation of compound 2	47-52
3.1.3 Structural elucidation of compound 3	53-56
3.1.4 Structural elucidation of compound 4	57-60
3.1.4.1 Acetylation of compound 4	61-63
3.1.5 Structural elucidation of compound 5	64-66
3.1.6 Structural elucidation of compound 6	67-69
3.1.7 The extraction of lignosulphonates	70-71
3.1.8 Analysis of the residuc formed in the calcium – spent liquor	72
3.1.9 Carbohydrate content of the calcium – spent liquor	
3.1.9.1 Analysis of hexose	73-75

3.1.9.2 Analysis of pentose	75-76
3.1.10 Analysis of wax balls from calcium – spent liquor evaporates	77-78
3.2 Analysis of the magnesium condensate effluent	
3.2.1 Structural elucidation of compound 7	79-80
3.2.2 Further compounds identified	81
3.2.3 Carbohydrate content of the magnesium condensate	
3.2.3.1 Analysis of hexose	82
3.2.3.2 Analysis of pentose	82
3.3 Analysis of the O ₂ – stage bleaching effluent	
3.3.1 Structural elucidation of compound 8	83-84
3.3.2 Structural elucidation of compound 9	85-86
3.3.3 Other compounds identified in the O ₂ – stage bleaching effluent	87
3.3.4 Carbohydrate content of the O ₂ – stage bleaching effluent	
3.3.4.1 Analysis of hexose	88
3.3.4.2 Analysis of pentose	88
3.4 Analysis of the E ₂ – stage bleaching effluent	
3.4.1 Structural elucidation of compound 10	90
3.4.2 Carbohydrate content of the E ₂ – stage bleaching effluent	
3.4.2.1 Analysis of hexose	91
3.4.2.2 Analysis of pentose	91
3.5 References	92-93

CHAPTER 4 : EXPERIMENTAL

4.1 Foreword to experimental	94-96
4.2 Analysis of the calcium – spent liquor – general sampling and organic extraction procedures	97
4.2.1 Physical data	
4.2.1.1 Compound 1	97-98
4.2.1.2 Compound 2	98
4.2.1.3 Compound 3	98-99
4.2.1.4 Compound 4	99
4.2.1.5 Compound 5	99-100
4.2.1.6 Compound 6	100
4.2.2 Extraction of lignosulphonates from the calcium – spent liquor effluent stream	101-103
4.2.3 Analysis of carbohydrates	
4.2.3.1 Analysis of hexose	103
4.2.3.2 Analysis of pentose	103-104
4.2.4 Analysis of the wax balls	104-105
4.3 Analysis of the magnesium condensate – general sampling and organic extraction procedures	
4.3.1 Physical data	
4.3.1.1 Compound 7	106-107
4.3.1.2 Compound 1	107
4.3.1.3 Compound 2	107-108
4.3.1.4 Compound 3	108
4.3.1.5 Compound 6	108-109
4.4 Analysis of the O₂ – stage bleaching effluent – general sampling and organic extraction procedures	
4.4.1 Physical data	

4.4.1.1 Compound 8	110-111
4.4.1.2 Compound 9	111
4.4.1.3 Compound 5	112
 4.5 Analysis of the E ₂ – stage bleaching effluent – general sampling and organic extraction procedures	
4.5.1 Physical data	
4.5.1.1 Compound 10	113-114
4.5.1.2 Compound 8	114
4.5.1.3 Compound 5	114-115
 4.6 References	116
 CHAPTER 5 : CONCLUSION	117-121
References	122
 APPENDIX A	123-218
 APPENDIX B	219-225

CHAPTER 1: INTRODUCTION

1.1 THE AIM OF THE PROJECT

The aim of this project was to extract and characterise the organic components of SAPPI SAICCOR's effluent. The main effluent is made up of four streams, namely, the calcium - spent liquor, the magnesium condensate, the O₂ - stage bleaching effluent and the E₂ - stage bleaching effluent streams. Attempts, thus far, at reducing the amount of effluent pumped out to sea have been based on a reduction of the calcium – spent liquor and the magnesium effluent streams. Sulphite pulping processes are known to produce lignosulphonates, which have a variety of uses and it is for this reason that Lignotech was built adjacent to the SAPPI SAICCOR factory. At present, approximately 31 % of SAPPI SAICCOR's calcium spent liquor is pumped to Lignotech who remove the lignosulphonates for commercial purposes¹. Future trends could either increase or lower the percentage of effluent that is sent to Lignotech, depending on the capacity and expansion plans of Lignotech¹.

The recently built magnesium – based section recycles its effluent by burning it to produce energy and at the same time producing MgO that is sent back to the digesters to be used as a base. Some analysis had been carried out, over the years, on the effluent but never in great detail. However, recent trends have focussed on the environment and the impact of industrial effluent, which has initiated an investigation into further ways of reducing the effluent. In order to do this, the effluent must be characterised and this has been the basis of this project. Thus, it is SAPPI SAICCOR's intention to identify commercially exploitable compounds that can be extracted and marketed, thus further reducing the impact on the environment.

1.2 A BRIEF OVERVIEW OF THE TYPES OF SULPHITE PULPING

Pulping processes include mechanical pulping, chemi - mechanical and chemi-thermomechanical pulping, semichemical pulping, high yield chemical pulping and full chemical pulping. Full chemical pulping involves alkaline pulping and sulphite pulping, and a brief overview of the various types of sulphite pulping will be given here.

Sulphite processes are characterised by the composition of the cooking liquor, which influences the cooking pH and the choice of the base. They can be grouped into five principle types, that is, acidic sulphite pulping, bisulphite pulping, multi - stage sulphite pulping, neutral sulphite pulping and alkaline sulphite pulping.

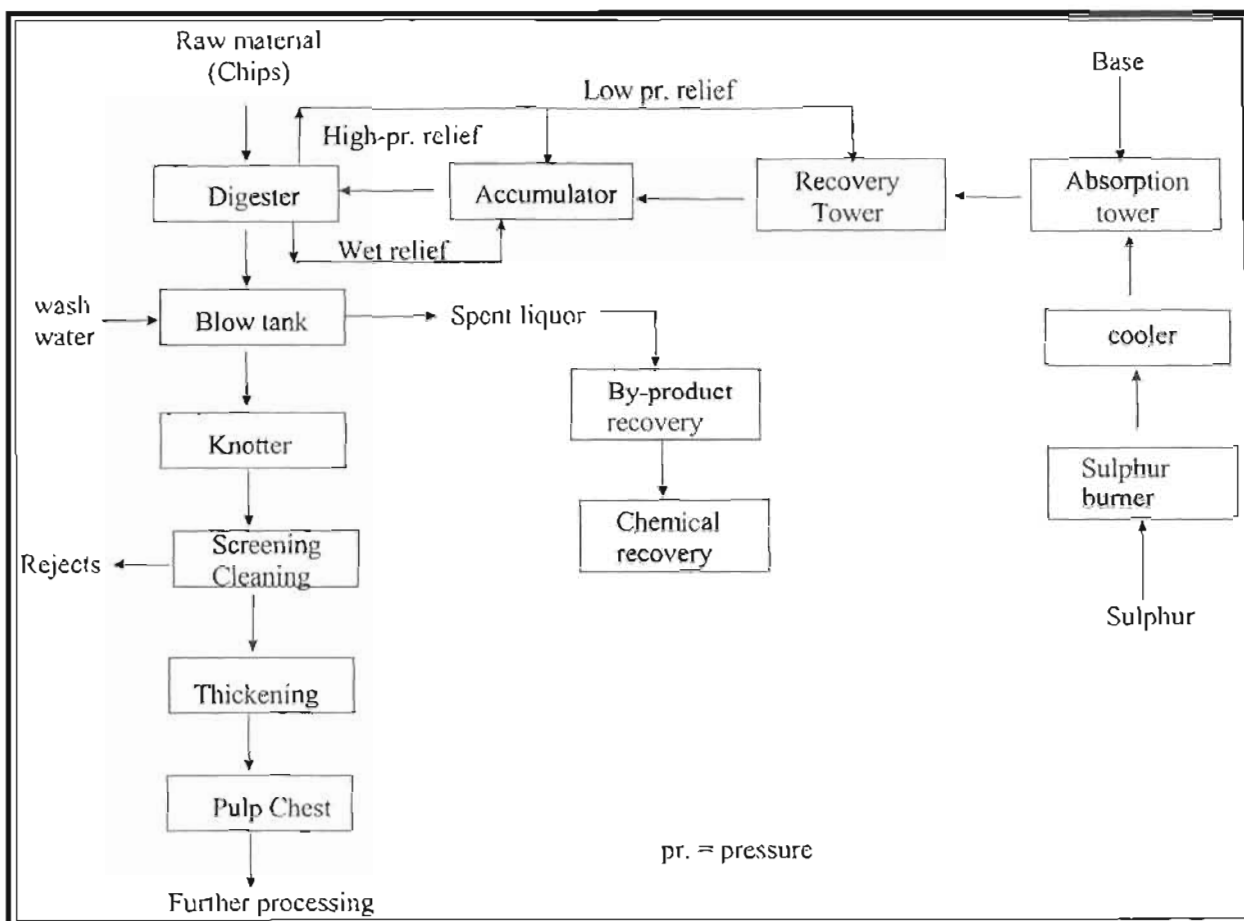
In acidic sulphite pulping, calcium is the classical base and has both advantages and severe disadvantages. The advantages are the low price and the good availability of limestone as the dominant raw material. The disadvantages are the limited solubility of calcium sulphite, scaling problems and the lack of a suitable recovery system². The low solubility of calcium sulphite at elevated temperatures requires an excess of free SO₂ to keep the pH value below 3, preventing the formation of calcium sulphite from calcium hydrogen sulphite.

A much better solubility is obtained with magnesium as a base, covering the pH range up to about 5². The outstanding advantage of magnesium based sulphite pulping is the possibility of combusting the waste liquor to yield magnesium oxide and sulphur dioxide, which may be recycled for producing fresh cooking liquor.

Sulphite pulps have many advantages over Kraft pulps, in that, they have higher yields at a given kappa number resulting in lower wood consumption, higher brightness of unbleached pulps, higher flexibility of bleaching and bleaching without chlorine, lower installation capital costs and higher flexibility in pulp yields and grades^{2,3†}.

A simplified flow diagram of a sulphite pulping process is shown in Scheme 1².

[†] Kappa number refers to the amount of residual lignin present in the pulp and is generally used to determine the grade of pulp produced and its end uses.



SCHEME 1: Simplified flow chart of a sulphite pulping process²

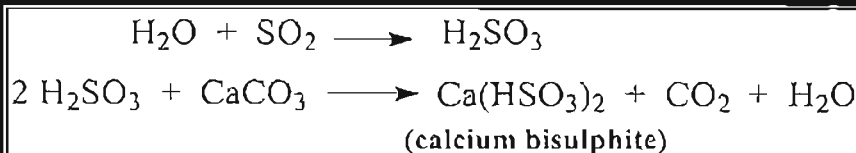
In acidic sulphite pulping the digester is filled with the maximum amount of chips. Generally, the chips are pre - steamed during the filling procedure to remove the air, but evacuation or pressure impregnation can also be effective². This is done to improve the penetration of the cooking liquor into the chips².

Digestion can be carried out continuously or as a batch process, which is the most common form. The liquor is heated by direct steam injection or by indirect heating using a heat exchanger to reach the maximum cooking temperature, which varies between 125 °C and 180° C, depending on the special process and the desired pulp type². The cooking pressure varies between 5 and 7 bar². The cooking temperature is controlled by steam and by reducing the pressure when the cook is finished, the digester content is discharged into the blow - tank at a reduced pressure of about 2 bar. While the spent liquor is being removed, wash water is introduced. The ready

washed pulp is screened and cleaned to remove the rejects, and finally thickened. The unbleached pulp may be further bleached, dried or converted directly into paper depending on the quality and end use of the product. The spent liquor may be used for recovery of by-products or combusted after evaporation to yield heat and to recover the base, if possible.

The classical process, the acidic calcium bisulphite process, applies a cooking liquor of $\text{Ca}(\text{HSO}_3)_2$ with a high excess of free sulphur dioxide, which maintains the pH at approximately 1.2-1.5².

The typical process to prepare the sulphite cooking liquor in acidic calcium bisulphite pulping is to feed sulphur dioxide gas and water through calcium carbonate rocks (limestone) in the absorption tower, in order to have them react according to the equations^{2,4}:



SCHEME 2: Reaction scheme for the production of calcium bisulphite²

As the free highly acidic SO_2 penetrates much more quickly into the wood chips than the liquor, the temperature increase during the heating period must be slow. Otherwise, early lignin condensation reactions will take place, resulting in incomplete delignification^{2,5}. The final cooking temperature is generally kept between 125-135° C for the production of paper pulps, and up to 145° C in dissolving pulp production².

One of the disadvantages of this process is the length of the total cooking cycle, which lasts up to twelve hours. Other disadvantages are scaling problems, the lack of a chemical recovery system and environmental problems. With regard to the wood raw material, no species with a high resin content (e.g. pines and many hardwoods) or chips with considerable amounts of bark can be used, due to condensation reactions of lignin with extractive components preventing a sufficient sulphonation².

The bisulphite processes are characterised by cooking pH values of 3-5 and the use of true bisulphite liquors without excess sulphur dioxide. Sodium and magnesium are used as bases, but in principle, ammonia is also suitable.

The main commercial processes are the Arbiso process using sodium as a base and the magnesium-based Magnefite process². The magnesium bisulphite process offers many advantages, for example, no escape of sulphur dioxide during blowing, continuous pulping, no scaling during evaporation and easy chemical recovery². Additionally, the process is regarded as highly flexible with regard to the wood species used and these pulps have higher brightness values and bleaching advantages².

Numerous multi - stage processes have been suggested to combine the advantages of alkaline and acidic pulping to obtain a higher flexibility of pulp yields and qualities. Only two types using sodium as a base are of commercial importance. The first is the Stora process, starting with a sulphite - bisulphite mixture at a pH between 6 and 8, followed by an acidic step at low pH (1-2) by adding sulphur dioxide and/or acidic liquor⁴. The second type of multi - stage sulphite processes is the Sivola (Rauma) process, which has an initial bisulphite stage (pH 3-5), followed by a cooking stage at pH 6-9⁴. The inclusion of an acidic stage between the bisulphite and alkaline stage is especially suitable for the production of softwood dissolving pulps².

One of the most promising advances in sulphite pulping is the alkaline sulphite process (AS) using sodium sulphite and sodium hydroxide in combination at pH levels up to 13. The process combines the advantages of Kraft pulping with sulphite pulping characteristics such as high yields of bright and well bleachable pulps and fewer or no odour problems².

1.3 COMPOUNDS IDENTIFIED IN SULPHITE PULPING EFFLUENTS

Early studies on the spent liquor of sulphite pulping processes revealed a variety of compounds present in the liquor. Studies based on laboratory sulphite pulped aspen wood using ammonia as the base showed the presence of many different types of compounds ranging from lignans to long chain fatty acids⁶. The compounds isolated and identified were vanillin, syringaldehyde, *p*-hydroxybenzoic acid, vanillic acid, syringic acids and some long chain fatty acids, such as, myristic, palmitic, linoleic and linolenic acids⁷. Isomers of the lignan liriorezinol were also identified as well as some flavonoids⁷.

Thereafter work was carried out on a commercial sulphite liquor sample. Studies by Pearl and Beyer of an ammonia-based aspen spent sulphite liquor involved ether extraction and fractionation into 'neutrals', 'weak acids' and 'strong acids'^{8,9}. The neutrals were found to contain mostly sugars with xylose as the major component. Some lignin - like or phenolic materials were also identified, but only on hydrolysis of this fraction and it was therefore thought that these phenolic materials were complexed with carbohydrates. Some examples of the lignin precursors isolated were vanillin, syringaldehyde and *p*-hydroxybenzoic acid^{8,9}. The 'weak acid' fraction also contained phenolic compounds linked to carbohydrates and on acid hydrolysis, compounds such as vanillic acid, syringic acid and *p*-hydroxybenzoic acid were identified^{8,9}. The 'strong acid' fraction was found to contain similar components on acid and alkaline hydrolysis. This early work was based on paper chromatographic techniques.

More recently research has been carried out on lignosulphonates formed from sulphite pulping of softwood black spruce and hardwood poplar. Studies have shown these lignosulphonates to be either monomeric or disulphonic acids of lignin monomers¹⁰. Examples include, methyl-1-(4'-methoxyphenyl)-2-propene-1-sulphonate, methyl-1-(3',4'-dimethoxyphenyl)-2-propene-1-sulphonate, methyl-(3,4-dimethoxy)-benzoate 1,2-disulphono-methyl-3-(3',4'-dimethoxyphenyl)-prop-2-ene and 1,2-disulphono-methyl-1-(3',4'-dimethoxyphenyl)-propane¹⁰.

Studies on black liquor obtained from a *Eucalyptus globulus* bleached Kraft pulp mill were carried out by separating the liquor into various fractions¹¹. The aromatic acid fraction was found to contain syringaldehyde as the major component and other compounds include syringol, acetosyringone, and aspidinol¹¹. The phenolic compound fraction contained similar compounds as well as syringaresinol, acetovallinone and dehydrodiguaiacol. Syringaresinol was found to be the major component of the ether extract and other compounds identified were 4,4'-dihydroxy-3,3'-dimethoxy-stilbene, 1,1'-disyringyl-ethane, 2-syringyl-ethanol and 3-vanillyl-propanol¹¹. Xylose and galactose were also found to be the major carbohydrate components of this sample of black liquor.

1.4 A BRIEF DESCRIPTION OF SAPPI SAICCOR'S PROCESS

SAICCOR (formerly South African Industrial Cellulose Corporation) is situated approximately 50 km south of Durban near Umkomaas. It was originally set up in 1952 by Courtaulds (UK), Snia Viscosa (Italy) and the Industrial Development Corporation (SA) to supply dissolving pulp to Courtaulds' viscose rayon fibre and cellophane film processes¹². In September 1988, SAICCOR was acquired by SAPPI and is now one of the leading manufacturers of dissolving pulp and the only one on the African continent. It has the capacity to produce 600 000 tons of high grade dissolving pulp per year and almost 100 % of this is exported, their largest customer being the viscose industry.

SAICCOR is one of the few paper and pulp mills that use the acid sulphite process with calcium (Ca) and magnesium (Mg) as bases. The process begins with chipping of the wood (Figure 1), mainly *Eucalyptus grandis* and *Acacia mearnsii* in the ratio 90:10. Approximately 5300 t/day is processed^{1,12}. SAICCOR was also the first company to produce dissolving pulp from *Eucalyptus*¹².

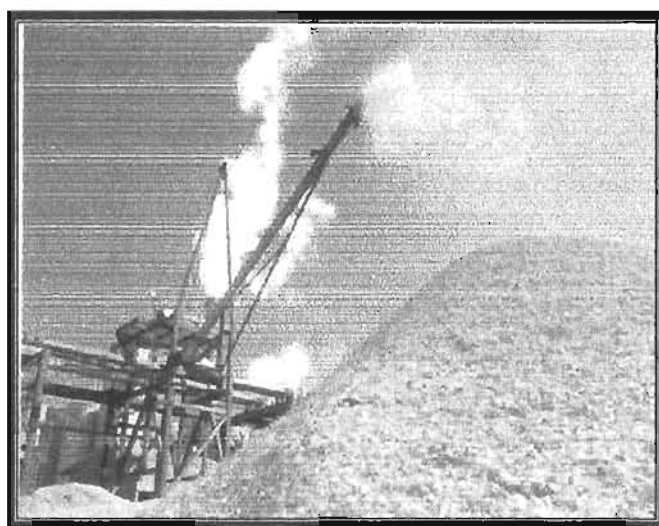
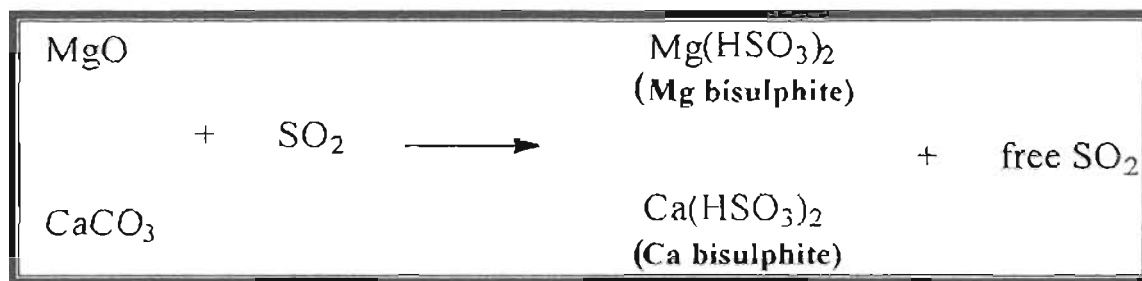


FIGURE 1: Wood chipping
(photograph courtesy of Sappi Saiccor's brochure)

The chips are cooked with calcium bisulphite or magnesium bisulphite (recent plant built with new technology) at 140^o C and 10 bar¹². The calcium bisulphite and

magnesium bisulphite are obtained on site by reacting MgO and CaCO₃ with sulphur dioxide as shown in Scheme 3.



SCHEME 3: Reaction of MgO and CaCO₃ to produce Mg bisulphite and Ca bisulphite

Batch cooking of the wood chips occurs in large digesters (Figure 2), fifteen of which use calcium bisulphite and eight use magnesium bisulphite. The magnesium pulp section operates as a closed cycle where the magnesium effluent is burned to produce energy resulting in the almost complete recovery of magnesium oxide. The only waste going to the effluent stream is the condensate formed during evaporation of the thin liquor.

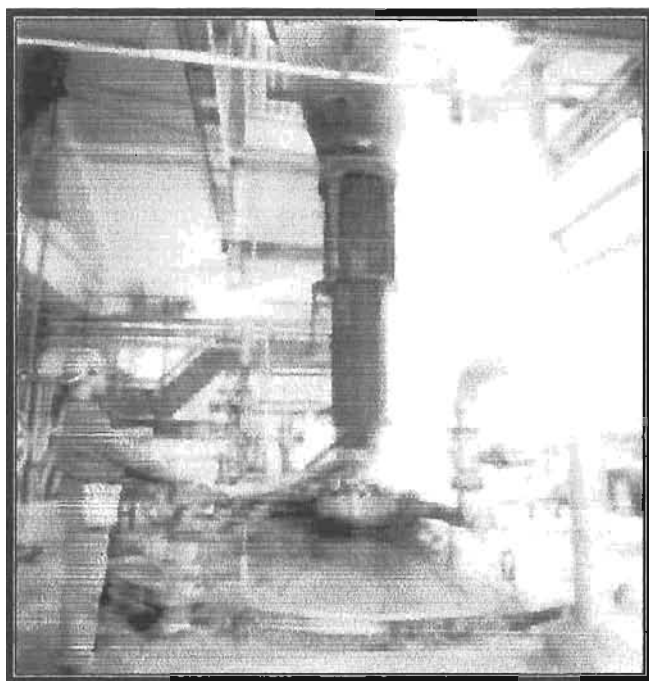


FIGURE 2: Cooking of wood chips in a digester
(photograph courtesy of Sappi Saiccor's brochure)

The calcium - based section produces a large proportion of the total effluent in the form of spent liquor, which contains approximately 16 % total dissolved solids¹. At present approximately 31 % of the calcium - spent liquor is pumped to Lignotech, a subsidiary of SAICCOR, where the lignosulphonates are removed for commercial purposes and the remaining effluent goes to the main effluent drain¹.

The individual calcium and magnesium - based pulps are washed and screened and the two pulps are combined and passed through a five - stage bleaching process, which is elemental chlorine free (ECF). The introduction of ECF bleaching has resulted in reduced levels of resin in the mill's pulp and this has had a significant impact on the downstream manufacturing of products made from SAICCOR's dissolving pulp.

The first stage in bleaching, stage O, uses oxygen and NaOH, which removes some hemicellulose and low molecular weight cellulose. The D₁ stage uses ClO₂ which solubilises the remaining lignin for the next stage. The E stage uses NaOH to dissolve the lignin. The D₂ stage uses ClO₂ to whiten the pulp and break down any remaining lignin residues. The final stage is the H stage, which uses NaOCl to further whiten the pulp and chemically alter the molecular size of the cellulose¹².

The final stage is the only stage that uses pure water – the other stages use water that is recycled counter - current[†]. The O and E stage washings are the remaining two contributors to the final effluent.

After the bleaching stage the pulp is screened to remove any non - cellulose matter and thereafter dried as a continuous sheet, which is cut and baled or reeled. SAICCOR produces approximately 1600 t/day of dissolving pulp, which is converted into various products such as cellophane (Figure 4), acetate, viscose fibres (Figure 3), *etc*¹².

[†] Pure water is defined as fresh water that has been softened.

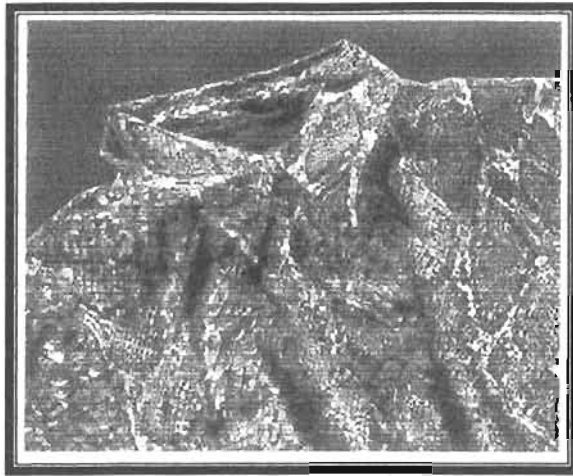


FIGURE 3: Viscose fibres



FIGURE 4: Cellophane wrapping

(photographs courtesy of Sappi Saiccor's brochure)

The four main streams of effluent, that is, the magnesium pulp condensate, the calcium - spent liquor and the O and E stages, combine to form the main effluent. This deep red coloured effluent is accumulated in a holding pond, from where it is pumped out to sea through a 7 km pipeline at an approximate pH of 3.

1.5 REFERENCES

1. Personal Communications – Derek A. Weightman (Technical Director at Sappi Saiccor), John Thubron (Technical Process Manager at Sappi Saiccor) and Tracy Pohl (Chemist at Sappi Saiccor)
2. Fengel, D. and Wegener, G., 1983, *Wood : chemistry, ultrastructure and reactions*, Walter de Gruyter & Co. : Berlin, p454-462
3. Gullichsen, J. and Paulapuro, H., 2000, *Forest Products Chemistry*, Fapet Oy : Helsinki, p78-85
4. Sarkanen, K. V. and Ludwig, C. H., 1971, *Lignins: Occurrence, Formation, Structure and Reactions*, John Wiley and Sons : New York, p598-601
5. Sjostrom, E., 1981, *Wood Chemistry – Fundamentals and Applications*, Academic Press : New York, p13-16(a), 112-114(b), 83-97(c), 49-60(d)
6. Pearl, I. A. and Justman, O., 1961, *Journal of Organic Chemistry*, (26), 3563-3564
7. Pearl, I. A., Beyer, D. L. and Justman, O., 1962, *Tappi*, (45), 107-113
8. Pearl, I. A., Beyer, D. L., 1964, *Tappi*, (47), 458-462
9. Pearl, I. A., Beyer, D. L., 1964, *Tappi*, (47), 779-782
10. Bailski, A. M., Luthe, C. E., Fong, J. L. and Lewis, N. G., 1986, *Canadian Journal of Chemistry*, (64), 1336-1343
11. Neto, C. P., Belino, E., Evtuguin, D. and Silvestre, A. J. D., 1999, *Appita*, (52), 213-217
12. Brochure produced by SAPPI SAICCOR

CHAPTER 2: CLASSES OF COMPOUNDS ISOLATED AND IDENTIFIED FROM SAPPI SAICCOR'S EFFLUENT

A number of compounds belonging to a variety of different classes have been isolated from the four different streams of effluent. Compounds, such as, lignans and lignin precursors, fatty acids, triterpenoids and sugars have been identified and will be reviewed in this chapter.

2.1 LIGNIN

2.1.1 General

The cell wall of wood fibres is made up of a number of layers, namely, the middle lamella (ML), the primary wall (P), the secondary wall (S_1 , 2 and 3) and the inner warty layer (W) (Figure 5)^{1a}. The middle lamella is found between the cells and is essentially the glue that holds the cells together. The primary layer is the first layer that is formed during cell development. It is a thin layer consisting of cellulose, hemicellulose, pectin and protein embedded between lignin^{1a}. The middle lamella together with the primary wall is known as the compound middle lamella and contains a large proportion of lignin. The secondary wall is made up of thin outer (S_1) and inner (S_3) layers and a thick middle layer (S_2), all of which contain lignin and hemicellulose. The inner warty layer is a thin, amorphous layer with wart - like deposits.

The wood cell is mainly made up of cellulose, hemicellulose and lignin. The cellulose is essentially the skeleton, which is surrounded by the hemicellulose matrix and lignin.

The main aim of the acid sulphite process is to remove as much of the lignin as possible leaving only the cellulose. The calcium - spent liquor thus contains a large proportion of lignin and thus lignin deserves further discussion.

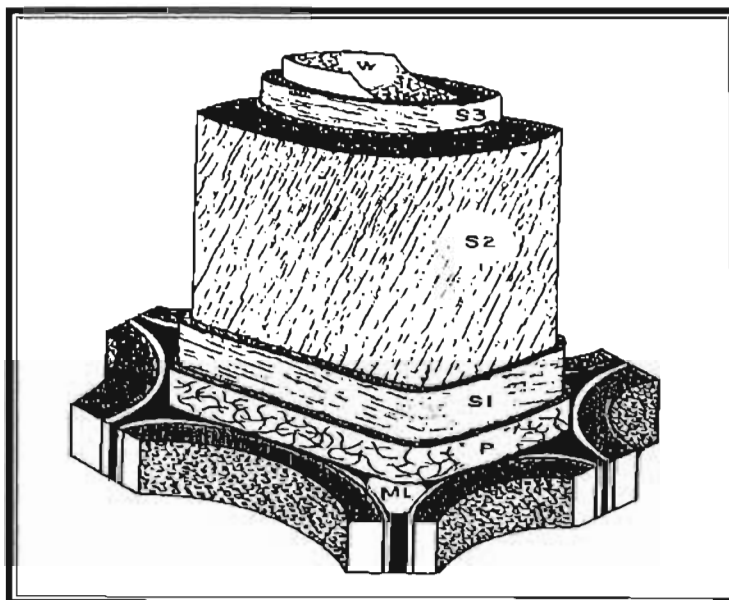


FIGURE 5: Simplified structure of a woody cell^{1a}

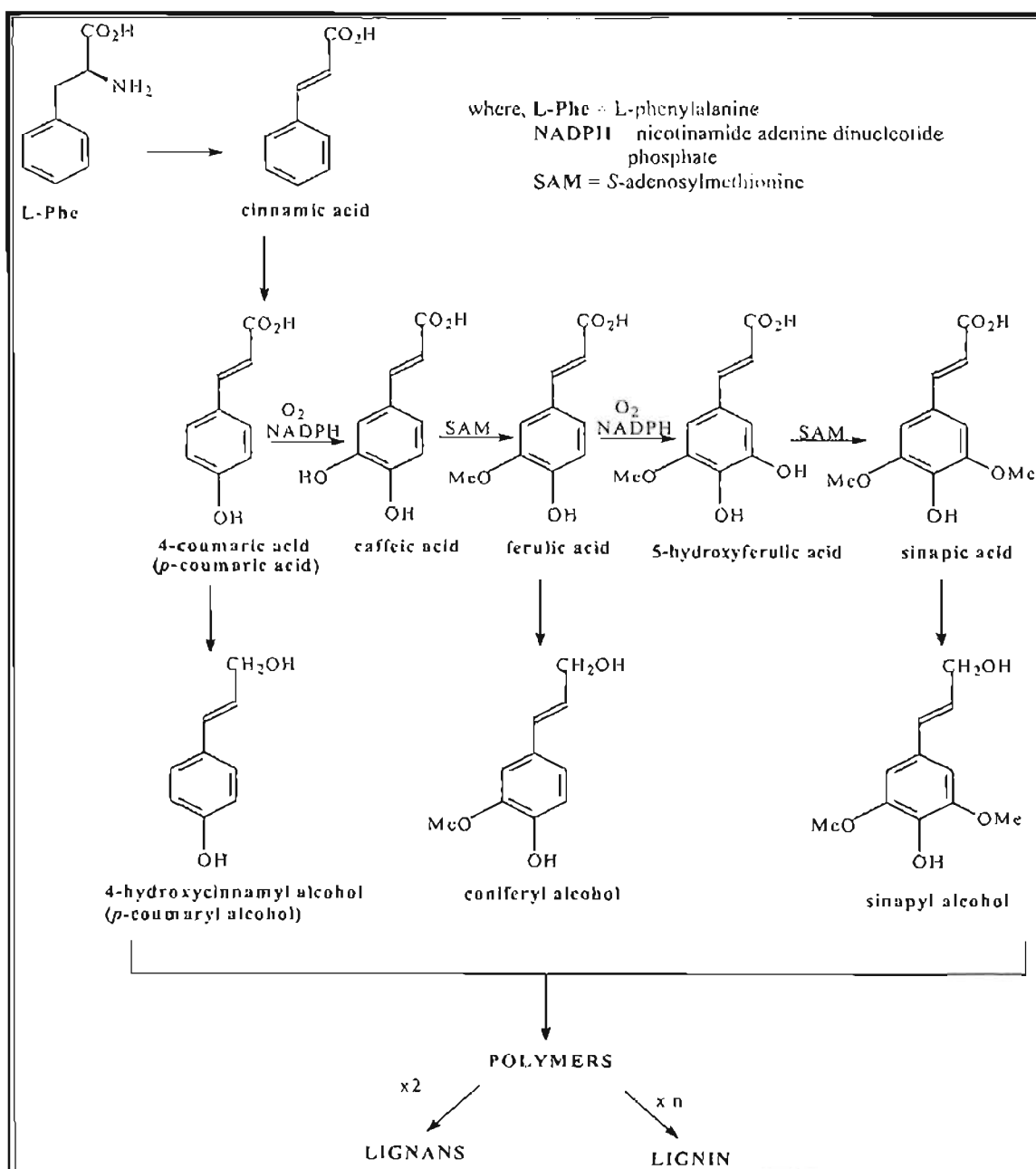
Lignins are an essential component of all plants and trees and make-up about 20 % - 40 % by mass. They are the second most abundant biopolymers in nature, after cellulose, and are one of the most difficult materials to study. The function of lignin is to transport water, nutrients and metabolites to other parts of the plant and to give rigidity to the cell walls by offering permanent bonding between cells resulting in a structure that is resistant towards impact, compression and bending². They also offer resistance to attacks by microorganisms².

2.1.2 Biosynthesis of lignins

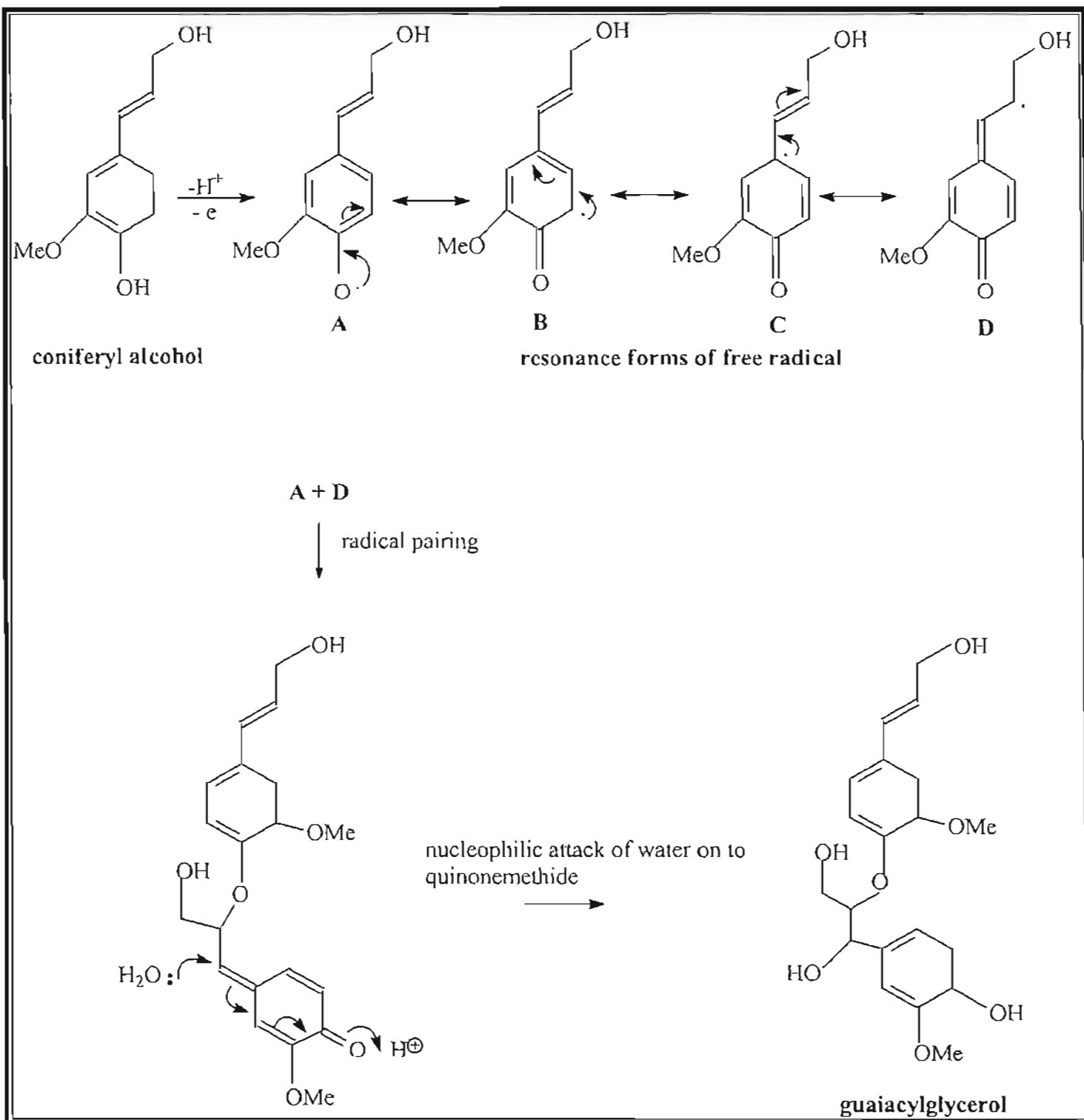
Lignins are polymeric natural products based on C₆ - C₃ building blocks and they arise from primary precursors derived from L - phenylalanine. In plants, the first step is the elimination of ammonia from the side - chain to produce the appropriate *trans* - cinnamic acid^{3a}. This is achieved *via* the enzyme phenylalanine ammonia lyase (PAL). Other forms of cinnamic acid are formed by further hydroxylation and methylation reactions thus building up substitution patterns typical of the shikimate pathway, i.e. an *ortho* oxygenation pattern^{3a} (Scheme 4).

Lignins are able to grow into large and rather complex macromolecules by phenolic oxidative coupling of suitable C₆ - C₃ monomers *via* the formation of phenoxy

radicals. The most important of these monomers are 4-hydroxycinnamyl (*p*-coumaryl) alcohol, coniferyl alcohol and sinapyl alcohol. The phenoxy radicals give various resonance forms and pairing between them produces dimers, such as guaiacylglycerol β -coniferyl ether, dehydrodiconiferyl alcohol and pinoresinol that can undergo further reactions to produce a lignin polymer. Scheme 5 shows the biosynthesis of one possible combination to form guaiacylglycerol.



SCHEME 4: Shikimate pathway showing the formation of lignin precursors^{3a}



SCHEME 5: Biosynthesis of guaiacylglycerol^{3a}

Since the 1950s, it was believed that the coupling between phenoxy radicals was completely random requiring no enzymes or proteins. But in recent years a group of researchers have put forth a new proposal that the process is, in fact, fully controlled

by proteins⁴. Norman G. Lewis, Laurence B. Davin and Simo Sarkanen isolated a protein that had no catalytic activity but has sites that bind either the monomers or the monomer radicals in specific orientations that lead to selective coupling^{5, 6}. They called it a 'dirigent' protein, which means to guide or align. They next proposed that these dirigent proteins are also involved in the specificity observed during lignification. At the start of lignification, lignin precursors move to the furthest ends of the cell wall to precise lignin initiation sites. The dirigent proteins are thought to control which monomer and the type of linkage that will be incorporated into the lignin polymer, by controlling the phenoxy - radical coupling processes^{6, 7}. Once a primary lignin chain has formed, template polymerisation occurs, starting at these sites and working its way back towards the plasma membrane⁷.

However, this new model has received widespread criticism and much more experimental evidence needs to be presented before it is widely accepted⁷.

2.1.3 The uses of lignins and lignans

Lignans have been found to have a variety of uses particularly in human health and are under review for a wide range of properties, including cardioprotective, antiviral, antibacterial, anti fungal and anticancer benefits.

Investigations into the biological activity of lignans have led scientists to believe that lignans interfere with oestrogen metabolism and may have significant use in reducing hormone dependant cancers, such as breast, endometrium and prostate cancers^{6, 8}. This oestrogenic effect of lignans has also been found to prevent bone resorption and promote increased bone density, thus preventing the start of osteoporosis. Podophyllotoxin, a lignan from the mayapple is used to treat venereal warts and is a precursor to the cancer drug etoposide which is used to treat testicular cancer^{4, 6, 8}.

Lignans have also been tested for cardioprotective benefits and the lignan, cinnamophilin, is currently being studied for its ability to reduce platelet aggregation and vasoconstriction^{9, 10}.

Lignans, such as sesamin from the sesame plant have been found to display antioxidant activity.

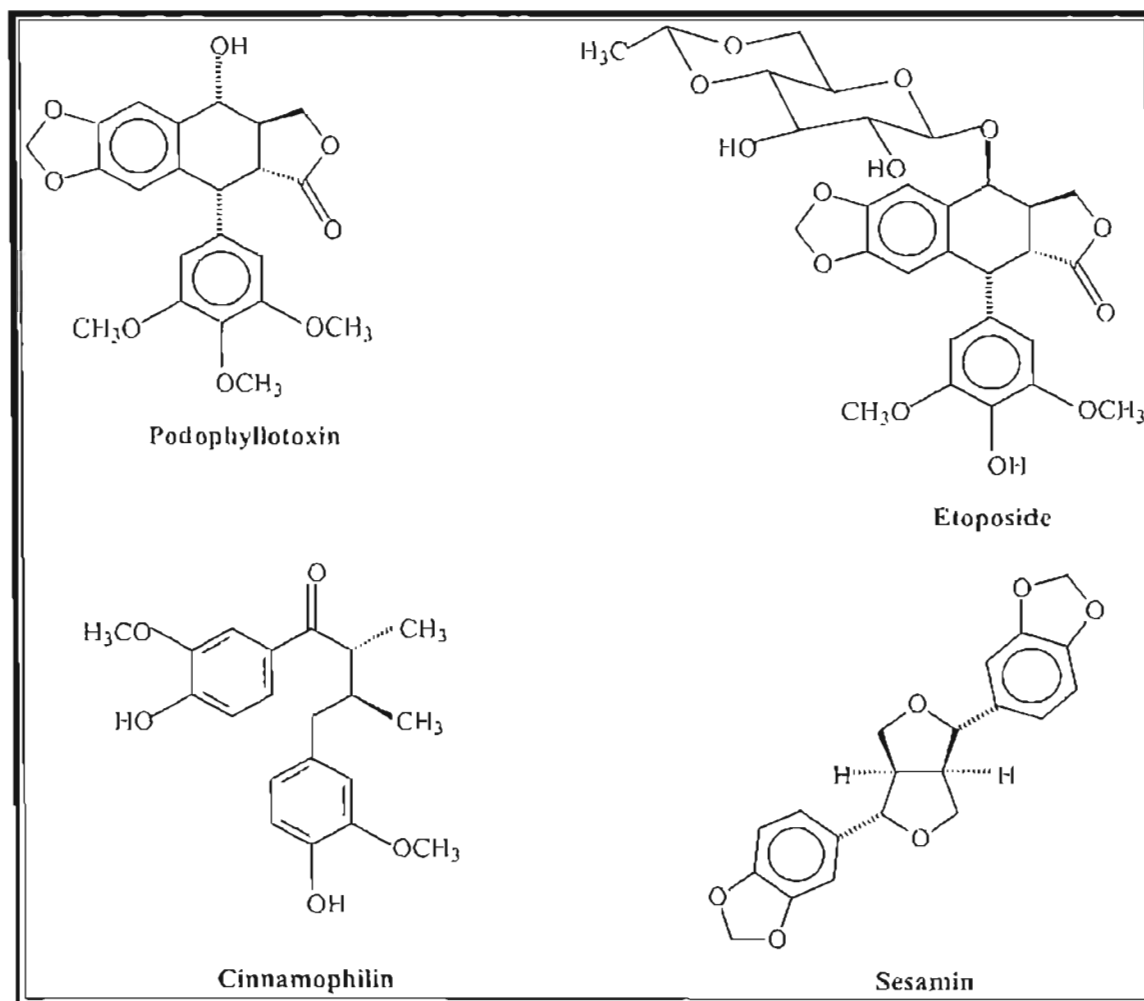


FIGURE 6: Structures of biologically important lignans and the cancer drug etoposide

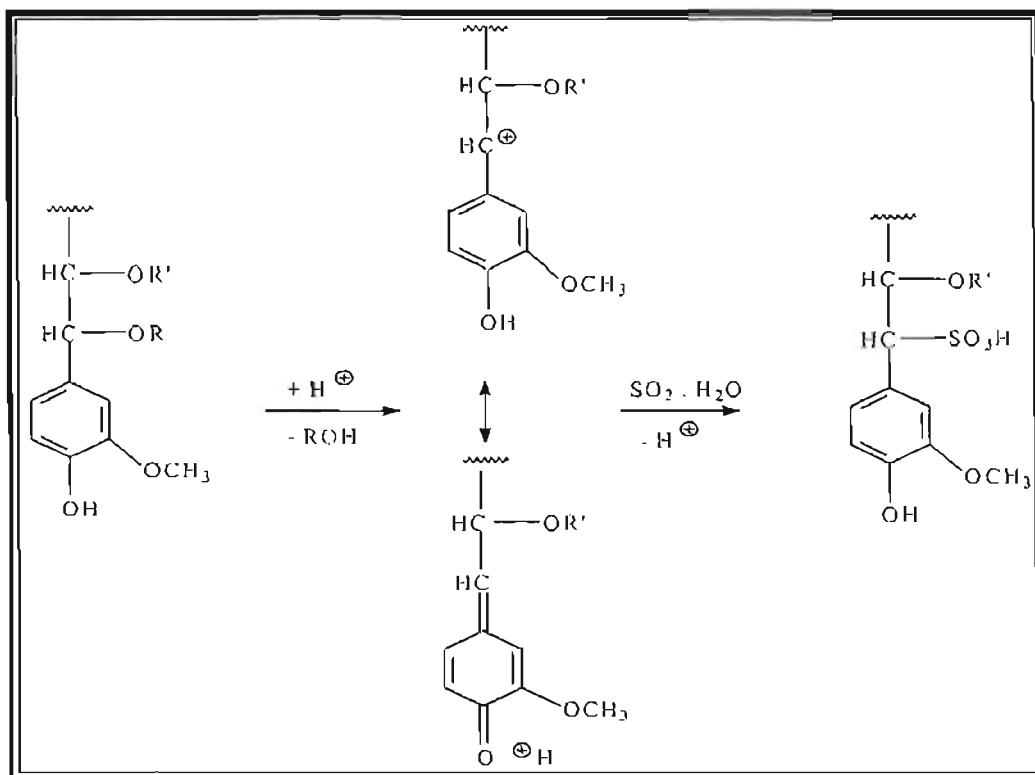
2.2 LIGNOSULPHONATES

2.2.1 General

Natural lignin is hydrophobic (non - wettable) and thus insoluble in water but when it is exposed to the conditions of acid bisulphite pulping it forms lignosulphonates with completely different properties. The introduction of sulphonic acid groups to the phenyl - propane structure converts this inactive compound to a strong anionic ion exchange complex which is now very hydrophilic (wettable)¹¹.

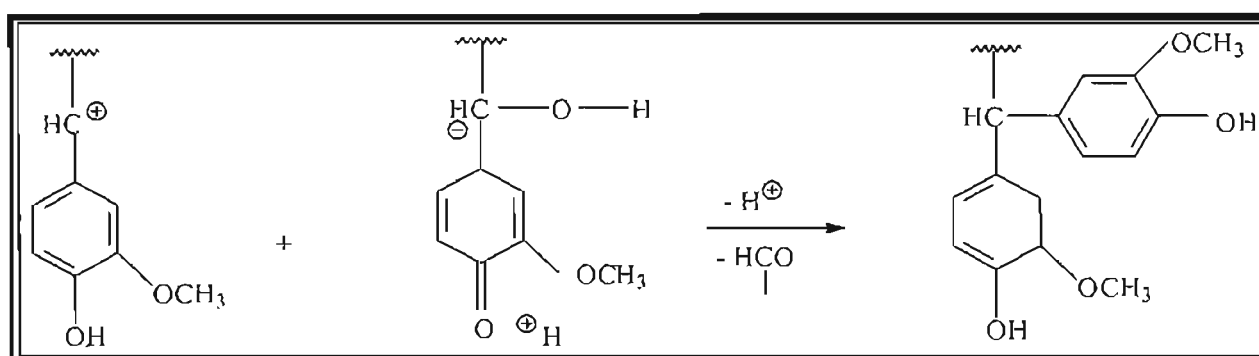
2.2.2 The synthesis of lignosulphonates

During lignin sulphonation, three major reactions proceed, that is, sulphonation, hydrolysis and condensation. The reactive site for the formation of lignosulphonates is the alpha - carbon position in the phenyl propane unit and is rendered active by the formation of quinone methide structures (benzylium ions)¹¹. These structures are sulphonated by attack by hydrated SO_2 or HSO_3^- present in the cooking liquor resulting in lignin that is soluble in the aqueous liquor. The less active beta - carbon position is usually involved in beta - phenolic ether linkages and can be sulphonated after oxygen cleavage in neutral and slightly alkaline media. This type of sulphonation is generally accelerated by sulphonation at the adjacent alpha - carbon position.



SCHEME 6: Formation of lignosulphonates^{1b,12a}

Condensation reactions compete with sulphonation, particularly at low pH values. Scheme 7 shows the carbon - carbon bonds that form between benzylium ions and weakly nucleophilic positions of other phenylpropane units. The resulting compounds have a higher molar mass and a lower solubility in the aqueous liquor^{12a}.



SCHEME 7: Typical condensation reactions that compete with sulphonation^{1b}

Sulphonation can occur over the whole pH range but tends to decrease rapidly towards the strongly alkaline range. The sulphonated complex often carries an equivalent amount of positive base ions with it (for example, Ca^{++} , Mg^{++}) in order to satisfy electroneutrality. When the water is removed from such a structure the positive base ion joins the negative macro ion to form a lignosulphonate salt¹¹.

2.2.3 The uses of lignosulphonates

Lignosulphonates have, for many years, been used in a wide variety of applications. Their early use was in the leather tanning industry where they were used as a tanning agent in combination with chrome tanning agents. They also found their use as an ore binder and as protective colloids for preventing scale formation in steam boiler and feed line systems^{13a}.

The dispersive properties of lignosulphonates have made them suitable for use in oil well - drilling muds where they are able to maintain good flow properties as well as being stable enough to allow drilling at high temperatures. They are used as a dispersant in ceramics, clays, pigments and insecticides.

Lignosulphonates have also been found to be useful as concrete additives when mixing cements. Their use as an additive results in a lower amount of water being required to obtain the desired fluidity of the concrete, thus increasing its compressive strength, density and uniformity^{13a, 14}. They are used as grinding aids for cements where their function is to reduce the agglomeration of the ground particles and to keep the equipment surfaces clean and free.

Since the 1920s, lignosulphonates have been sprayed on roads to produce a hard durable surface and to hold down dust. The dispersing and binding action of the lignosulphonates tend to form an impermeable layer with the natural clays in the soil, keeping the road free of surface water^{2, 14, 15}. In addition, lignosulphonates have also been used as binders, in pellets for animal feed products, coal and charcoal briquettes¹⁴.

2.3 EXTRACTIVES

The term 'extractives' is broadly used to describe compounds either soluble in organic solvents (lipophilic), such as dichloromethane, hexane, toluene, *etc*, or compounds that are soluble in water (hydrophilic). The term "wood resin" generally refers to the lipophilic extractives and are made up of resin acids and diterpenoids present in the resin canals of softwoods and fats and steryl esters present in parenchyma cells that occur in both softwoods and hardwoods^{12b, 16}. The main function of resin acids is to protect the wood against microbiological damage or insect attacks and the fats and steryl esters serve as an energy source for the wood cells' biological functions. The wood resin content differs between species as well as between changes in climates. A large amount of triterpenes has been detected in resins from tropical trees. These together with some steroids may survive the pulping process and are only removed during bleaching^{13b}.

The resin content of trees decreases immediately after they are felled and even more when they are stored as wood chips as compared to logs. This process is initiated by exposure to air, which affects the carbon - carbon double bonds and generates free radicals that are strong oxidants. It is for this reason that the wood is stored as wood chips so as to reduce 'pitch problems' during pulping^{12b, 13b}.

2.3.1 Triterpenoids

2.3.1.1 General

The terpenoids are a large and structurally diverse family of natural products containing C₅ isoprene units joined in a specific orientation. These units form the backbone to monoterpenes (C₁₀), diterpenes (C₂₀), triterpenes (C₃₀) and tetraterpenes (C₄₀) to name a few. Squalene, a C₃₀ molecule, is based on this isoprene unit and is, in fact, a biosynthetic precursor of triterpenes and steroids.

Squalene was first isolated from shark liver and displays a tail – to - tail join in the centre of the molecule as shown in Figure 7.

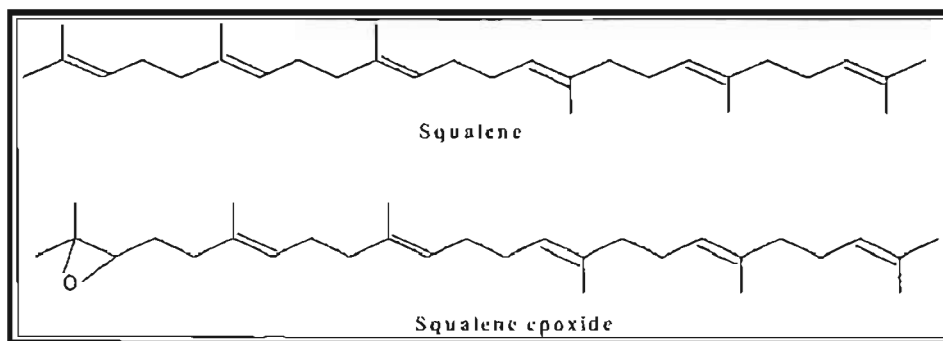


FIGURE 7: Structures of squalene and squalene epoxide

Steroids are modified triterpenoids containing a tetracyclic ring structure. The major animal sterol is cholesterol (C_{27}), which is a precursor for many other steroidal compounds. The major plant sterols are campesterol and sitosterol, shown in Figure 8, which contain respectively 24-methyl and 24-ethyl substituents.

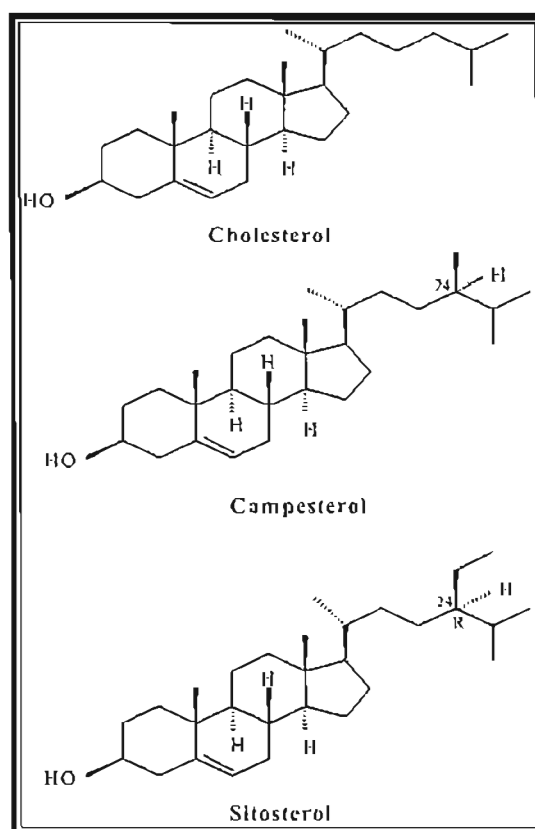
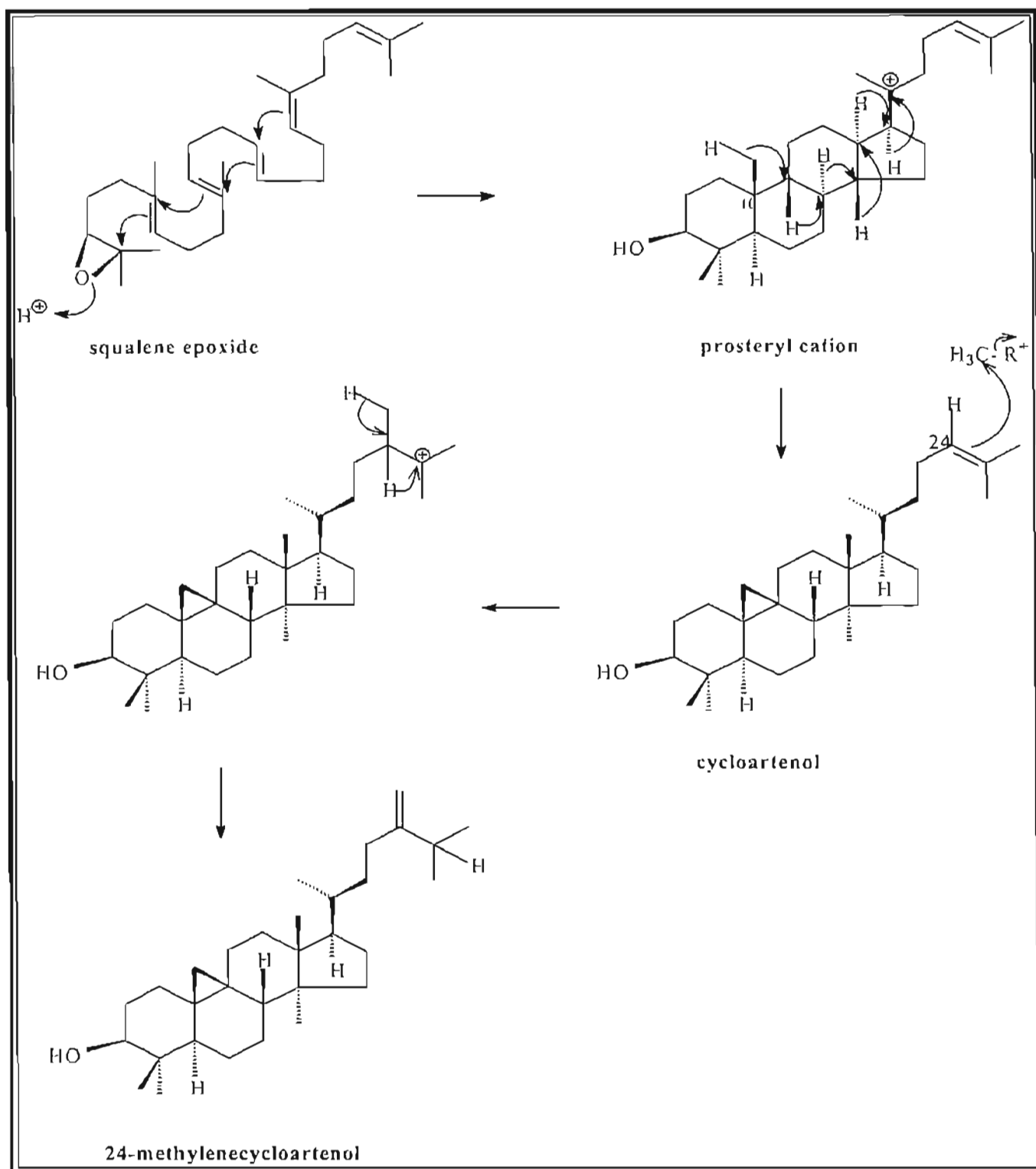


FIGURE 8: Structures of common triterpenoids, eg., cholesterol, campesterol and sitosterol

2.3.1.2 The biosynthesis of triterpenoids

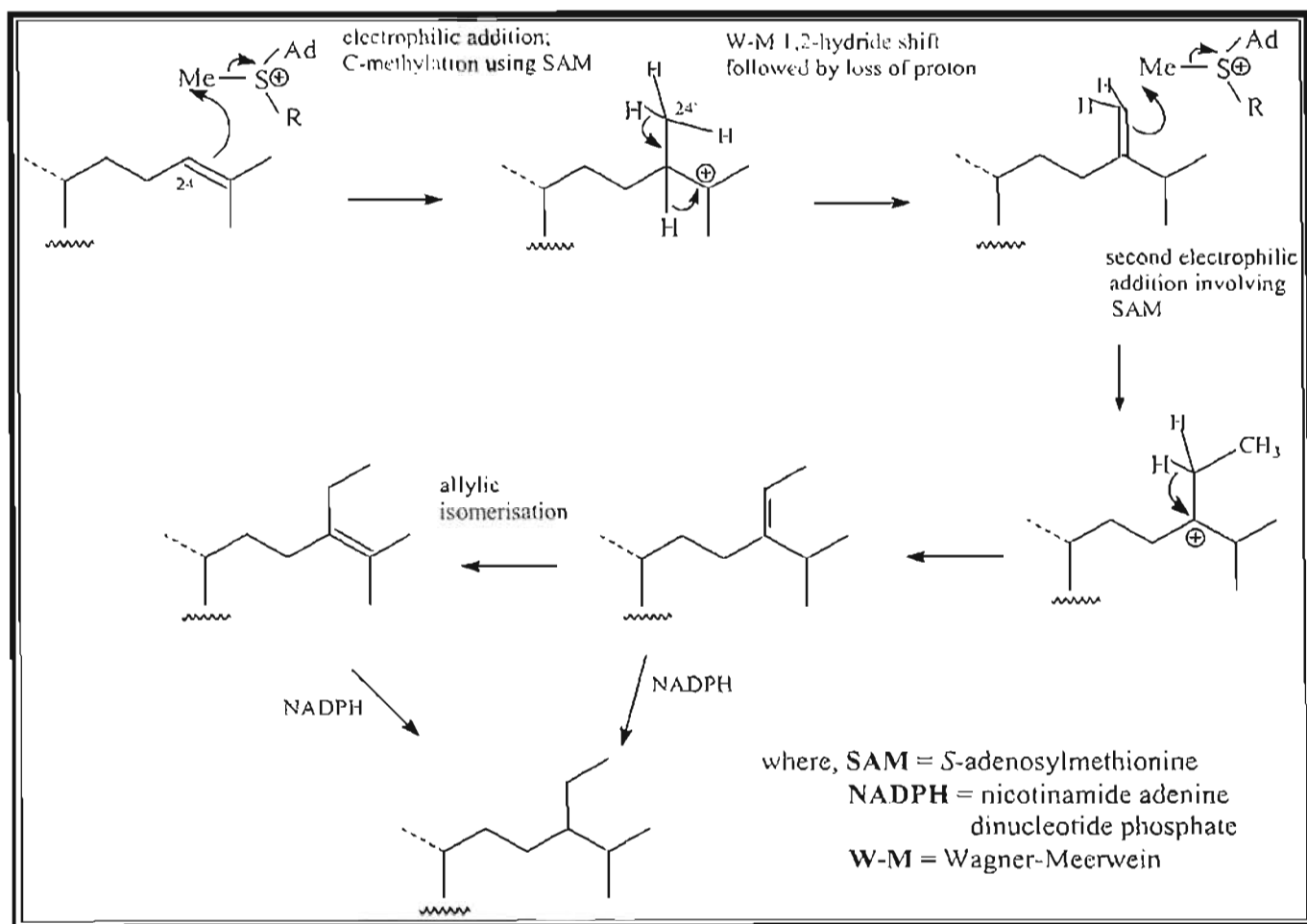
The biosynthesis of triterpenoids begins with the cyclisation of squalene *via* the intermediate squalene epoxide and according to the Biogenic Isoprene Rule, depending on the conformation it takes, forms either the animal triterpenoid, lanosterol or the plant triterpenoid, cycloartenol^{3b, c, 17}.

Protonation of the epoxide group opens the epoxide ring and forms a tertiary carbocation, which then undergoes a series of Wagner-Meerwein 1,2-shifts resulting in the formation of a tertiary protosteryl carbocation. The H-9 proton then migrates to C-8 and the carbocation that forms is quenched by the formation of a cyclopropane ring resulting from the loss of a proton from the methyl group at C-10. This intermediate structure is that of cycloartenol and methylation at C-24 leads to the formation of 24-methylenecycloartenol as shown in Scheme 9.



SCHEME 9: Mechanism of the formation of 24-methylenecycloartenol from squalene epoxide^{17, 18}

As mentioned earlier, sterols contain an additional methyl or ethyl group at C-24, which originates from S-adenosylmethionine (SAM). The double bond on the side chain undergoes methylation to form 24-methylenecycloartenol. A series of carbocation structures form, that eventually undergo allylic isomerisation and together with the simultaneous ring opening of the cyclopropane ring, produce the desired sterols^{3c, 17}. Scheme 10 shows the detailed methylation of the side chain and the migration of the double bond.



SCHEME 10: Mechanism showing the alkylation of C-24^{3c}

2.3.1.3 The uses of sterols

Research into the biological importance of sterols began in the 1930s in Germany and was later studied everywhere. D.W. Petersen from the University of California was the first to show that phytosterols actually block the absorption of cholesterol in

humans¹⁹. Since then, much work has been carried out on sterols with over one hundred published studies all attesting to the benefits of these compounds.

Studies have shown that phytosterols, and in particular β -sitosterol, stigmasterol and campesterol offer protection against high - fat foods by combining with cholesterol in the intestine, forming a crystalline matrix which cannot be absorbed. This matrix is then excreted by the body¹⁹.

In addition, these compounds have been reported to be successful in treating prostate problems (benign prostatic hyperplasia)²⁰. Recent research has also branched out into investigating the effects of phytosterols on other diseases such as tumors in the colon, tuberculosis, some cancers, coronary disease, and even HIV and AIDS.

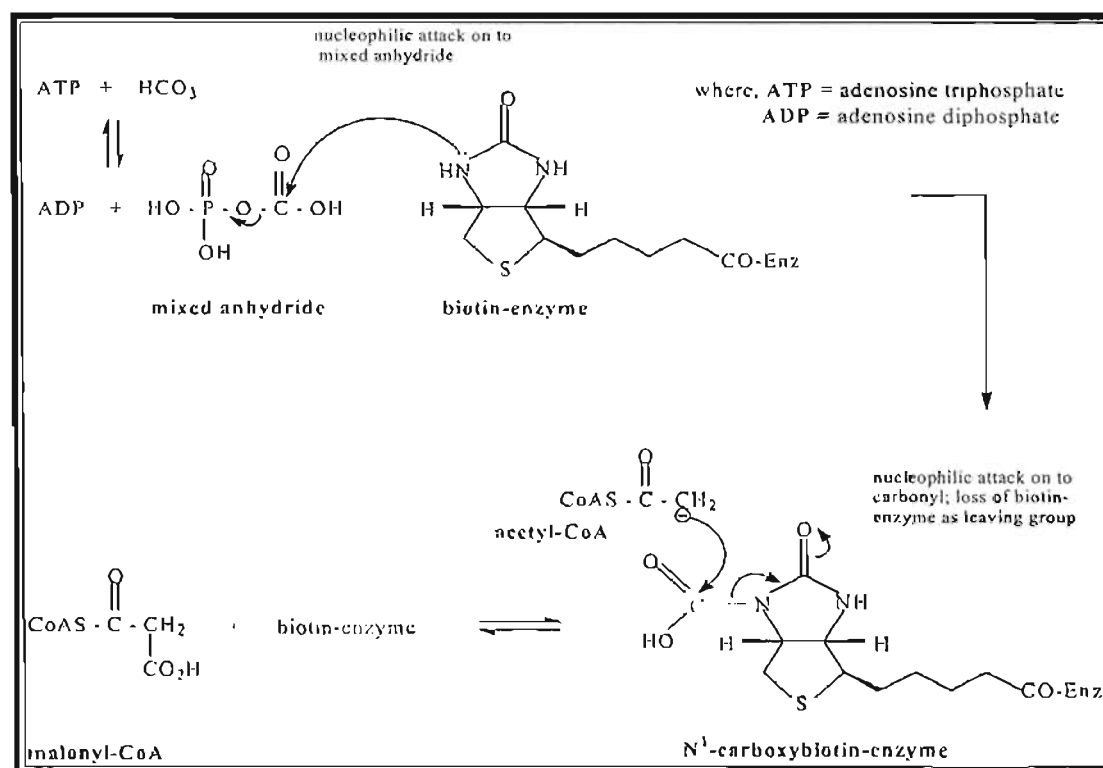
2.3.2 Fatty Acids

2.3.2.1 General

Aliphatic extractives are made up of alkanes, fatty alcohols, fatty acids, fats and waxes. Fatty acids are composed of saturated and unsaturated compounds and a large proportion are found bound to triglycerides^{1c, 12b}. They are generally straight - chain structures containing an even number of carbon atoms though odd numbered straight chain acids are found in nature, particularly in marine organisms and bacteria^{21a}. Branched - chain fatty acids are mainly found in microorganisms.

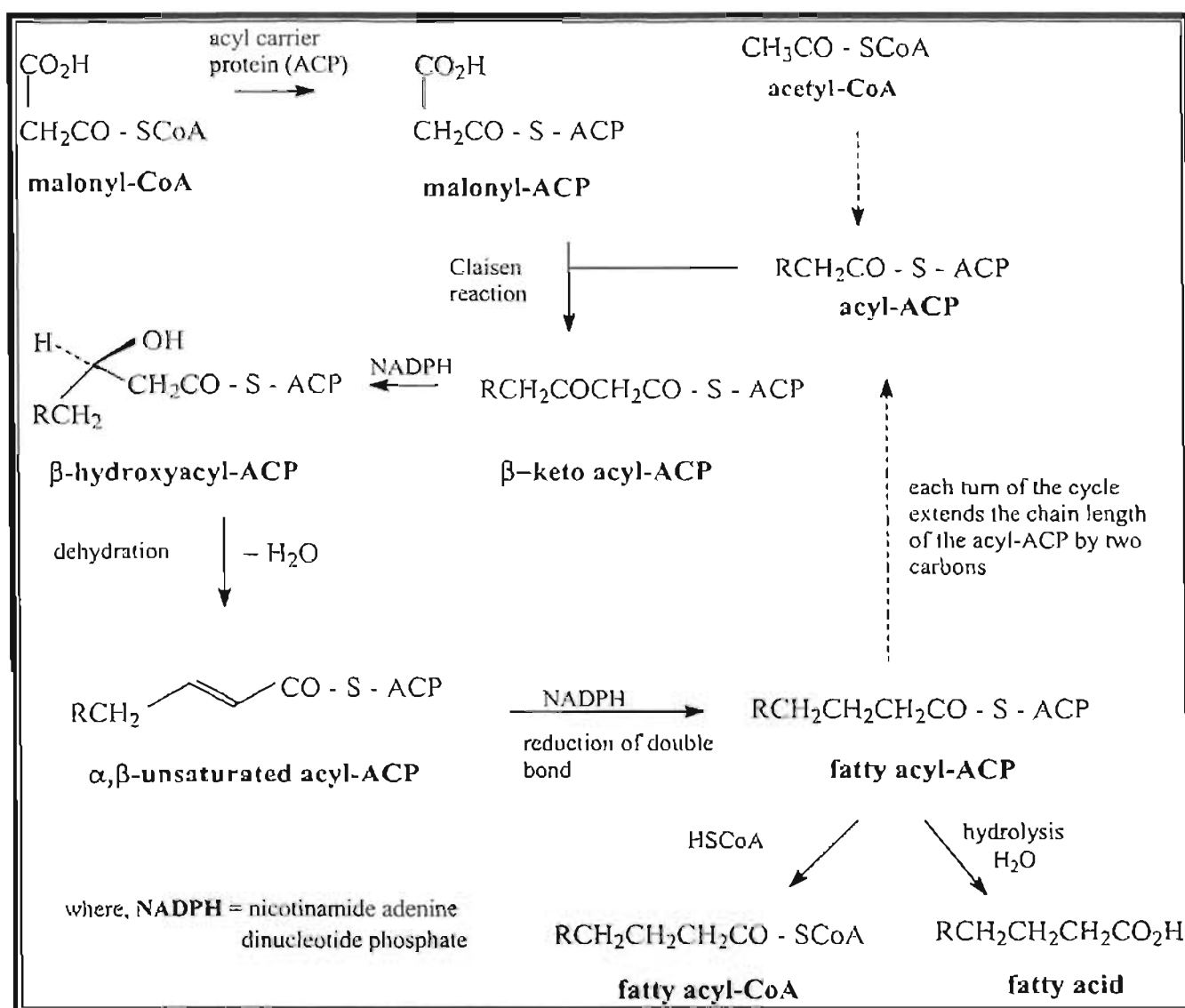
2.3.2.2 The biosynthesis of fatty acids

The fatty acids are part of the group of natural products called polyketides. These compounds were initially thought to form *via* a series of Claisen condensation reactions, the reverse of the β -oxidation reactions involved in the metabolism of fatty acids. However, further studies in this field revealed a more complex system of reactions involving the carboxylation of acetyl-CoA to malonyl using ATP, CO₂ and the coenzyme, biotin^{3d} (Scheme 11).



SCHEME 11: Carboxylation of acetyl-CoA to malonyl-CoA^{3d}

Plants and bacteria use a number of separate enzymes during the biosynthesis of fatty acids. Acetyl-CoA and malonyl-CoA are first converted into thiol esters with an attached acyl carrier protein (ACP). The Claisen reaction converts the ester into an acetoacetyl-ACP, which is then reduced to the corresponding β -hydroxy ester using NADPH. Water is eliminated to give the E (*trans*)- α,β -unsaturated ester and the double bond is thereafter reduced to give a saturated acyl-ACP which has two additional carbons compared to the starting material. The fatty acyl-ACP can then go back into the reaction sequence and repeat the series of reductions and dehydrations, adding on two carbons per cycle until the required length has been reached^{3d, 21a}.



SCHEME 12: Biosynthesis of fatty acids from malonyl-CoA^{3d, 21a}

2.3.2.3 The uses of fatty acids

Fatty acids have found a wide variety of uses ranging from an additive in the paint and printing inks industry to a starting material in the soap industry. In alkaline pulping factories the fatty acids and resins are extracted from the waste liquor as crude tall oil by adding sulphuric acid^{13a}. This crude tall oil can be fractionated into a number of useful products, namely, light oil, fatty acids, rosin and pitch residue. Light oils are used as rust protection or for combustion. Fatty acids are used in paints, soaps, lubricants and as a flotation agent. Rosin is used in alkyd resins, printing inks, adhesives and emulsifiers, and pitch residue is used in oil - well drilling muds, in printing ink pitch and as an asphalt additive. Many of the fatty acids, such as, myristic acid, palmitic acid and lauric acid have also found applications in the cosmetic industry in creams and lotions.

In addition, it has been reported that complexing palmitic acid with insulin, extends the time action of human insulin on diabetic dogs²². These favourable results have shown that the insulin - palmitic acid complex can be used to increase safety during intensive insulin therapy, but more clinical trials involving humans need to be carried out.

2.4 CARBOHYDRATES

2.4.1 General

Carbohydrates are an important group of natural products and are extremely abundant in plants. They give structure to plants, flowers, vegetables and trees but in addition to this, they function as energy - storage systems which can be broken down into water, carbon dioxide and heat or other energy²³. They also serve as the building blocks for fats and nucleic acids. The term 'carbohydrate' originated from the molecular formulae of the simple sugars $C_n(H_2O)_n$, which suggests the 'hydrate of carbon'^{21b}.

Monosaccharides are the simplest type of carbohydrates and an example is glucose, which is one saccharide unit. The most common monosaccharides found in nature are the six - carbon sugars (hexoses) and the five - carbon sugars (pentoses). Linking a few monosaccharide units (typically two - five monomers) together forms an oligosaccharide. An example is maltose, a disaccharide formed by linking two saccharide molecules together. Long polymers of monosaccharides are called polysaccharides. An example is the starch amylose.

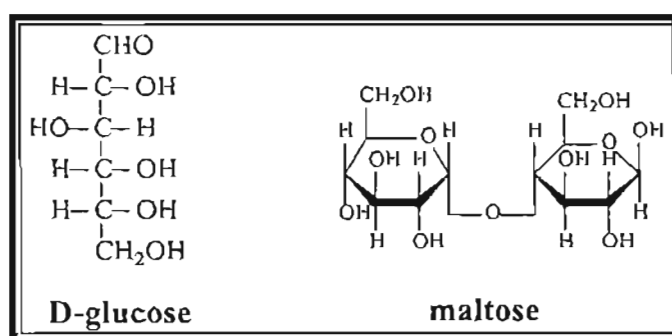
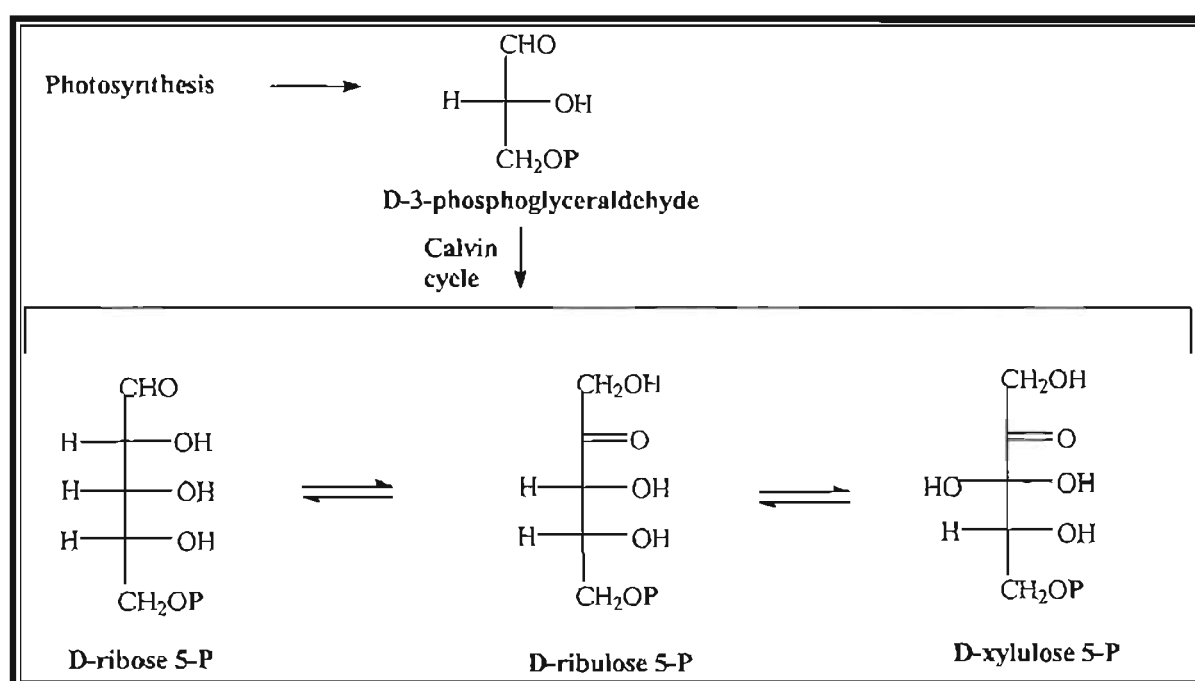


FIGURE 9: Structures of a common monosaccharide and disaccharide

2.4.2 The biosynthesis of carbohydrates

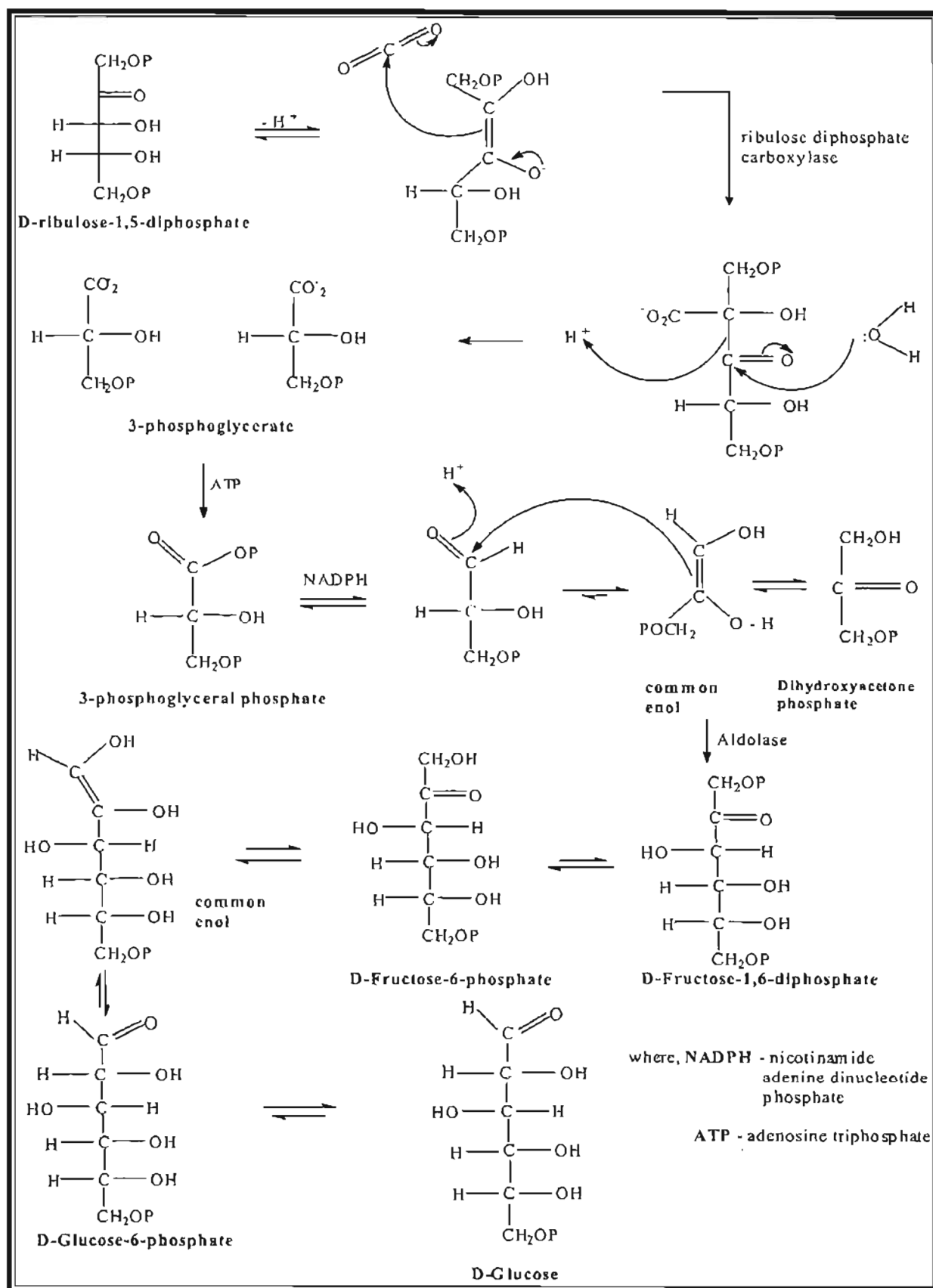
Carbohydrates are the first products formed during photosynthesis and are used by the plant to synthesise its own food reserves as well as other chemical constituents. This thereafter becomes a source of food for other organisms.

Initially the three carbon sugar 3-phosphoglyceraldehyde forms and follows through the Calvin cycle to produce the pentoses, namely, D-ribose 5-phosphate, D-ribulose 5-phosphate and D-xylulose 5-phosphate^{3c} (Scheme 13).



SCHEME 13: Formation of pentoses³

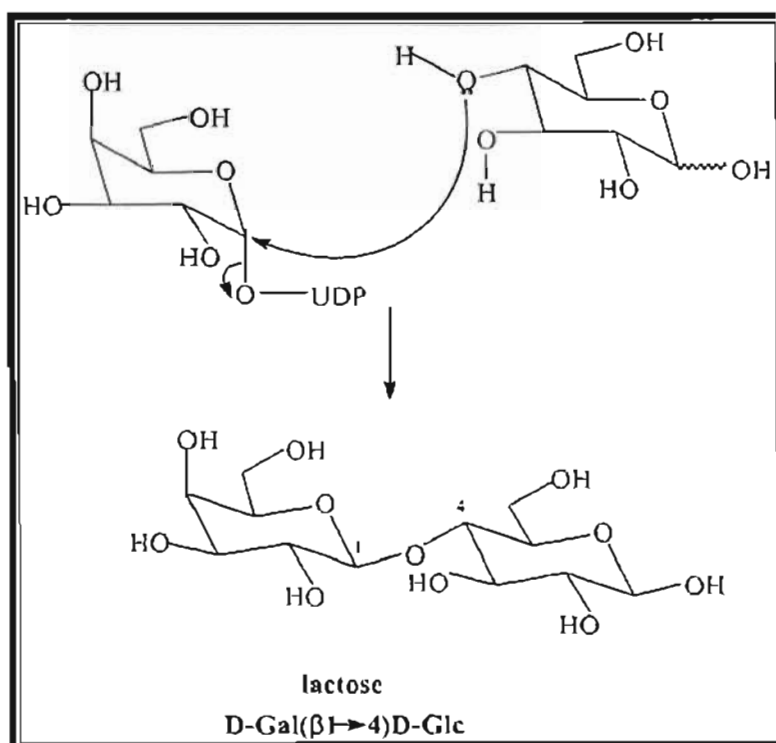
Ribulose-1,5-diphosphate is converted into glucose *via* a series of steps involving the formation of an intermediate which converts into two molecules of 3-phosphoglycerate. Phosphorylation with ATP converts this to 3-phosphoglyceryl phosphate and reduction with NADPH yields the aldehyde. Rearrangement and an aldol condensation produces D-fructose-1,6-diphosphate. A further series of phosphate hydrolyses produces D-glucose^{3c, 21b}. This is represented in Scheme 14 on page 33.



SCHEME 14: Conversion of ribulose-1,5-diphosphate to glucose^{21b}

Glucose formed from D-ribulose-1,5-diphosphate is used to form other hexoses. Glucose and ribose are the most important simple sugars with glucose being the monomeric unit in many polysaccharides, for example, cellulose, starch and glycogen.

Oligosaccharides are formed by first binding a nucleoside diphosphate, such as, uridine diphosphate (UDP) to a monomer^{3e, 21b}. Nucleophilic displacement of the UDP leaving group by another sugar molecule results in the formation of a disaccharide. A typical example is the formation of lactose from galactose and glucose.



SCHEME 15: Formation of lactose from galactose and glucose^{3e, 21b}

Polysaccharides are made up of many monomer units and those that are naturally occurring, are joined by hemiacetal linkages. The biosynthesis is similar to that described for the formation of oligosaccharides. Polysaccharides may be linear, such as amylose, which can contain up to two thousand glucopyranose units, or linear with branches, such as amylopectin which has $\alpha 1 \rightarrow 6$ linkages at about every 20 units in addition to the usual $\alpha 1 \rightarrow 4$ linkages^{3e}.

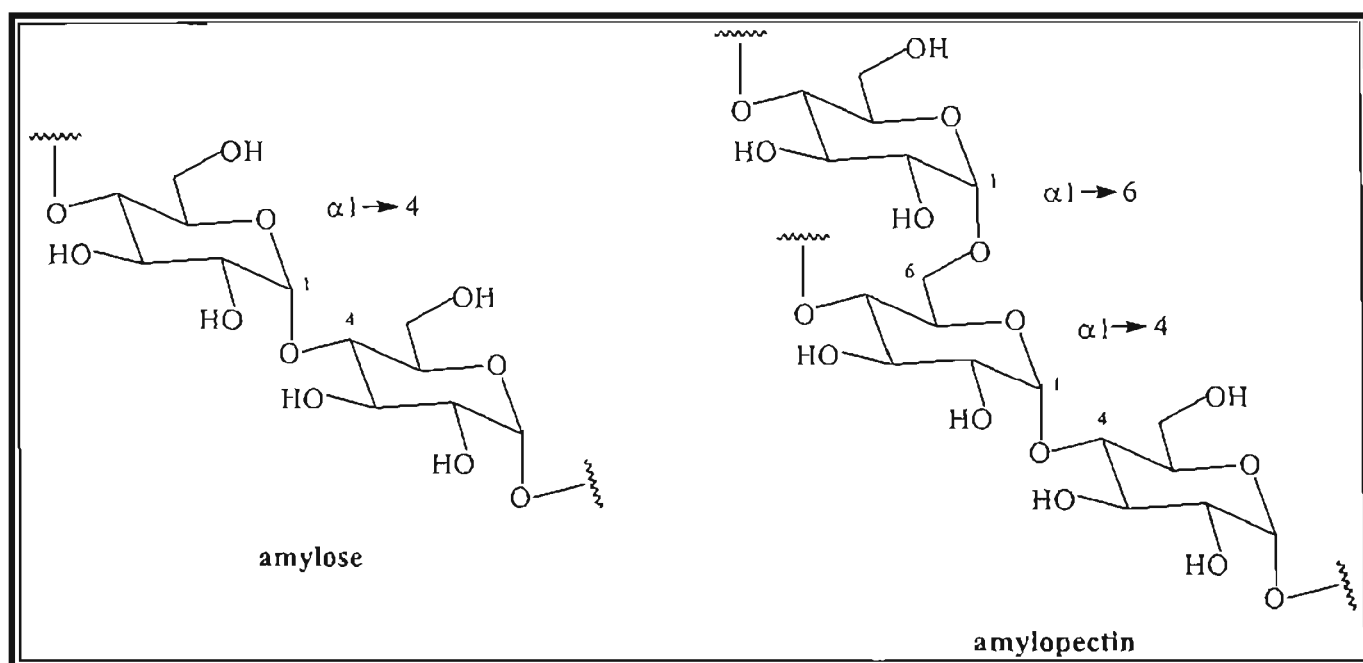


FIGURE 10: Structures of linear and branched polysaccharides

One of the most widespread occurrences of polysaccharides in animals is in chitin found in crustaceans. The strength and rigidity of the hard shell is derived from hydrogen bonds between adjacent molecules^{3c}. Bacterial cell walls also contain a type of polysaccharide that is cross - linked with polypeptides and many antibiotics contain carbohydrate moieties that play an important role in optimising their antibacterial activity²⁴.

However, cellulose is by far the most abundant organic material on earth and is the main structural constituent in plants. It may contain up to eight thousand glucopyranose units linked $\beta 1 \rightarrow 4$ in a linear chain joined together with glycosidic bonds^{3c}. Cellulose has very strong fibres resulting from intra - and intermolecular hydrogen bonds between adjacent molecules^{1d, 12b}. It is these bonds that are responsible for the properties of cellulose, such as high tensile strength and insolubility in most solvents.

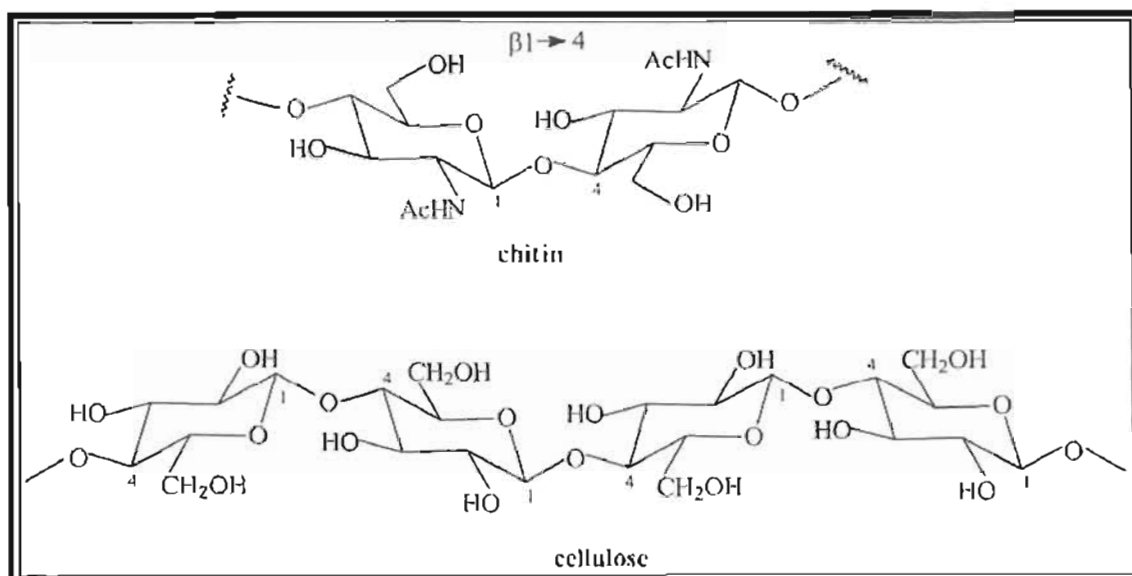


FIGURE 11: Structures of some common naturally occurring polysaccharides

In addition to cellulose, another important polysaccharide is hemicellulose. It differs from cellulose in that it contains shorter molecular chains and different branching of the chain molecules^{13c}. The main constituents of hemicellulose are glucomannan and xylan shown in Figure 12 and its percentage composition differs between softwoods and hardwoods^{12b}. Softwoods have a high proportion of mannose, in the form of galacto-glucomannan units, and more galactose units than hardwoods^{13c}. Hardwoods contain a larger amount of xylose units (glucuronoxylan) and acetyl groups than softwoods^{13c}.

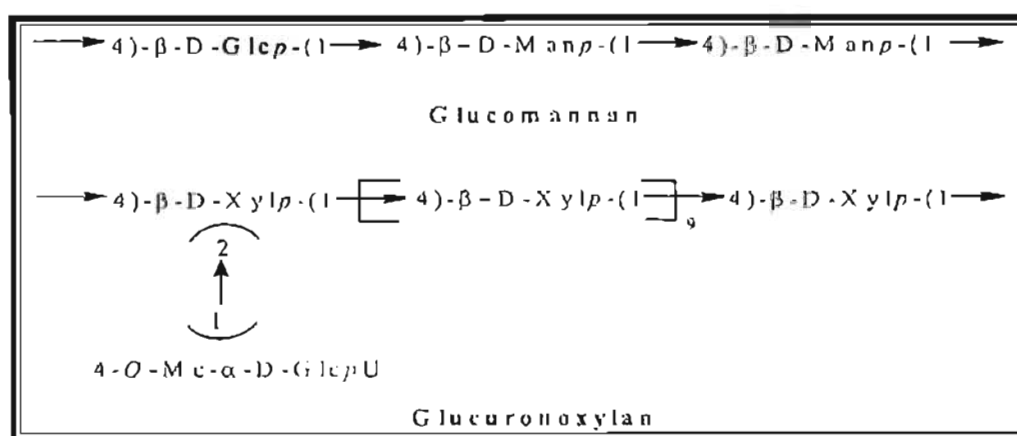


FIGURE 12: Partial chemical structure of glucomannan and xylan from hardwoods

2.4.3 The uses of carbohydrates

Carbohydrates are used in a variety of applications. In the monosaccharide group, glucose is the most common molecule and is used as a nutrient. D-fructose and D-sorbitol are used as food sweeteners by diabetic patients^{3e, 23}. Many pulping mills further utilise glucose from their spent liquors to produce ethanol, fodder yeast, organic acids, alcohols and acetone by a fermentation process. It has been reported that hexoses are suitable for industrial scale fermentation into ethanol and both hexoses and pentoses, can be used to produce yeast and protein respectively^{13a}. Furfural can also be produced from xylose *via* hydrolysis and acid catalysed dehydrogenation^{13a}.

Sucrose, a disaccharide, is used as a sweetening agent for foods and drug preparations and lactose is used as a diluent in tablets^{3e}.

Polysaccharides are widely used in the medicinal and pharmaceutical fields. Starch is used extensively in the food industry and its absorbent properties make it ideal for use as dusting powders. However, cellulose and its derivatives are the most widely used polysaccharides. A large proportion of SAICCOR's cellulose is exported, and then used to manufacture viscose fibres, cellophane, acetates, *etc*²⁵. The cellulose derivatives also find their use in the pharmaceutical industry. Hemicellulose found in spent liquor may be hydrolysed to its monomeric unit, glucose, which can thereafter be fermented to produce the products mentioned above.

2.5 REFERENCES

1. Sjöström, E., 1981, *Wood Chemistry – Fundamentals and Applications*, Academic Press : New York, p13-16(a), 112-114(b), 83-97(c), 49-60(d)
2. Sarkanen, K.V. and C.H. Ludwig, 1971, *Lignins – Occurrence, Formation, Structure and Reactions*, Wiley-Interscience : New York, p1-3
3. Dewick, P.M., 1997, *Medicinal Natural Products*, John Wiley and Sons Ltd : West Sussex, p119-122(a), 152-154(b), 194-238(c), 15-42(d), 427-438(e)
4. Rouhi, A. M., 2000, *Chemical and Engineering News*, (78), 29-32
5. Davin, L. B., Wang, H. B., Crowell, A. L., Bedgar, D. L., Martin, D. M., Sarkanen, S. and Lewis, N. G., 1997, *Science*, (275), 362-366
6. Davin, L. B. and Lewis, N. G., 2000, *Plant Physiology*, (123), 453-461
7. Rouhi, A. M., 2001, *Chemical and Engineering News*, (79), 52-56
8. MacRae, W. D. and Towers, G. H. N., 1984, *Phytochemistry*, (23), 1207-1220
9. Wu, T-S., Leu, Y-L., Chan, Y-Y., Yu, S-M., Teng, C-M and Su, J-D., 1994, *Phytochemistry*, (36), 785-788
10. http://www.wholehealthmd.com/refshelf/substances_view
11. Ingruber, O. V., Kocurek, M. J. and Wong, A., 1985, *Pulp and Paper Manufacture : Vol. 4 Sulphite Science and Technology*, Joint Textbook Committee of the Paper Industry : Montreal, p31-34

12. Gullichsen, J. and Paulapuro, H., 2000, *Forest Products Chemistry*, Fapet Oy : Helsinki, p81-83(ii). 34-52(b)
13. Fengel, D. and Wegener, G., 1983, *Wood : chemistry, ultrastructure and reactions*, Walter de Gruyter & Co. : Berlin, p536-560(a), 182-214(b), 106-131(c)
14. <http://www.fraserpapersparkfalls.com/>
15. <http://www.assnhq.com>
16. Sjostrom, E. and Alen, R., 1999, *Analytical Methods in Wood Chemistry, Pulping and Papermaking*. Springer : Berlin, p125-127
17. Templeton, W., 1969, *The Terpenoids. in An introduction to the chemistry of the terpenoids and steroids*, Butterworths and Co. Ltd. : London, p129-135
18. Lenton, J. R., Goad, L. J. and Goodwin, T. W., 1975, *Phytochemistry*, (14), 1523-1528
19. <http://www.naturleaf.com>
20. <http://www.cochrane.org>
21. Mann, J., Davidson, R. S., Hobbs, J. B., Bantlorpe, D. V. and Harborne, J. B., 1994, *Natural Products : Their chemistry and biological significance*, Longman Scientific and Technical : Marlow, Essex, p240-246(a), 7-25(b)
22. Meyers, S. R., Yakuba-Madus, F. E., Johnson, W. T., Baker, J. E., Cusick, T. S., Williams, V. K., Tinsley, F. C., Kriauciunas, A., Manetta, J. and Chen, V. J., 1997, *Diabetes*, (46), 637-642

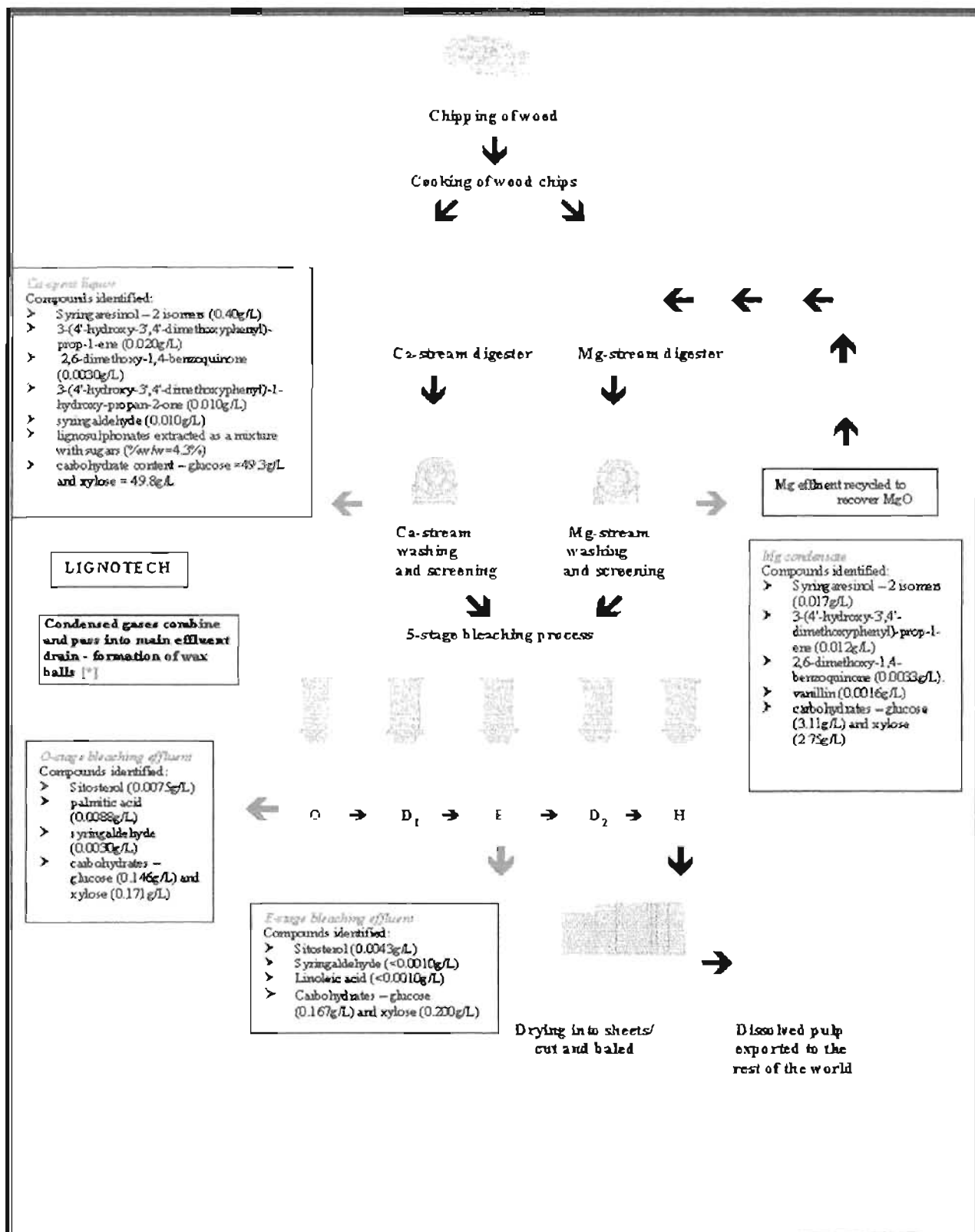
23. Vollhardt, K. P. C. and Schore, N. E., 1994, *Organic Chemistry*, W. H. Freeman and Company : New York, p942-975
24. Hanessian, S. and Haskell, T. M., 1970, *The Carbohydrates : Chemistry and Biochemistry*, Academic Press : New York, p139
25. Personal Communications –Derek A. Weightman (Technical Director at Sappi Saiccor) and John Thubron (Technical Process Manager at Sappi Saiccor)

CHAPTER 3: RESULTS AND DISCUSSION

The four streams of effluent, namely, calcium - spent liquor, magnesium condensate, O₂ - stage bleaching stream and E₂ - stage bleaching stream were individually subjected to chloroform extraction to remove the organic components. Only the calcium - spent liquor and magnesium condensate organic extracts were neutralised with a sodium bicarbonate solution and thereafter the organic extracts from all four effluent streams were passed through individual silica gel gravity columns. Varying combinations of solvents in a stepwise gradient were used to elute a variety of compounds and NMR, infrared spectroscopy and gas chromatography/mass spectrometry (GC/MS) were used to determine the structures of these compounds, which will be discussed in this chapter.

3.1 ANALYSIS OF THE CALCIUM-SPENT LIQUOR EFFLUENT

The following compounds were isolated and identified from the organic extract of the calcium - spent liquor: - two isomers of syringaresinol; 3-(4'-hydroxy-3',5'-dimethoxyphenyl)-prop-1-ene; 2,6-dimethoxy-1,4-benzoquinone; 3-(4'-hydroxy-3',5'-dimethoxyphenyl)-1-hydroxy-propan-2-one and syringaldehyde. A residue was filtered off from the calcium - spent liquor and identified using X - ray diffraction and a lignosulphonate extraction was attempted. A waxy substance was obtained from the gases that collect from the evaporation process and identified as a mixture of fatty acids and their derivatives using GC/MS analysis. The carbohydrate content was also determined using UV/visible spectroscopy.



SCHEME 16: Simplified flow diagram of SAPPI SAICCOR's process and compounds isolated during this study

3.1.1 Structural elucidation of compound 1, *meso* - syringaresinol

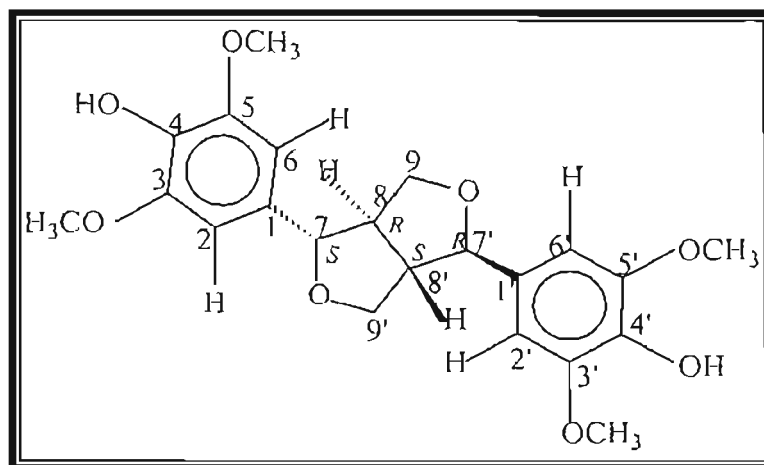


FIGURE 13: Structure of compound 1, syringaresinol

The infrared spectrum of compound 1 (Spectrum 1) shows a broad band at 3420 cm^{-1} indicative of a hydroxyl substituent. The sharp peaks at 2932 cm^{-1} and 2851 cm^{-1} are typical of C-H stretching, the sharp peak at 1116 cm^{-1} is typical of C-O stretching and the peaks at 1624 cm^{-1} and 1518 cm^{-1} correspond to C=C stretching in an aromatic ring. The peak between 1350 cm^{-1} and 1300 cm^{-1} indicates syringyl breathing¹.

Analysis of the mass spectrum (Spectrum 2), shows a molecular ion peak at m/z 418, which is, in fact, twice that of a lignin monomer and thus confirms a dimeric structure, namely, a lignan. The peak at m/z 210 corresponds to the splitting of the dimer and the base peak at m/z 181 suggests the fragmentation of an ethylene group from the propane side chain resulting in the formation of syringaldehyde².

The ^1H and ^{13}C NMR spectra show only one half of the resonances expected and, therefore, the structure must be symmetrical. Thus the assignments of the structure of one half of the molecule based on NMR data will first be discussed, then the joining of the two parts of the molecule will follow.

The ^1H NMR spectrum (Spectrum 3) shows single strong peaks at δ 6.56 ppm (2H, H-2, H-6) and δ 3.88 ppm (6H, 2 x OCH_3) which are typical of aromatic and methoxy proton

resonances respectively and indicative of a symmetrical aromatic ring. The peak at δ 3.07 ppm is due to the methine group proton at position 8 and the peaks at δ 4.26 ppm and δ 3.86 ppm are due to the methylene group protons at position 9. The doublet at δ 4.71 ppm ($J = 4.03$ Hz) corresponds to the methine proton at position 7. The resonances at δ 3.86 ppm, δ 4.26 ppm and δ 4.71 ppm occur downfield due to the deshielding effect of the electronegative oxygen atom attached to both groups. The peak at δ 5.48 ppm is due to the phenolic proton.

The ^{13}C NMR spectrum (Spectrum 4) shows an intense peak at δ 56.4 ppm, which is characteristic of a methoxy group carbon resonance. The peak at δ 54.4 ppm corresponds to the methine carbon at position 8. The oxygenated methine and methylene group carbons at positions 7 and 9 are depicted by the peaks at δ 86.1 ppm and δ 71.9 ppm respectively. These peaks again occur downfield due to the attached electronegative oxygen atom. The other sharp, distinct peak at δ 102.7 ppm is characteristic of the two protonated carbons (C-2, C-6) of the aromatic ring. The remaining peaks in the aromatic region of the spectrum are due to the fully substituted carbons on the aromatic ring.

The HMBC NMR spectrum (Spectrum 5) was used to confirm the above assignments and to assign the carbon resonances of the aromatic ring. The carbon peak at δ 147.2 ppm shows strong correlations to the methoxy and aromatic protons and can therefore be assigned to C-3 and C-5 where the methoxy groups are attached. The carbon peak at δ 134.3 ppm shows a strong 3J correlation to the aromatic protons and can be ascribed to C-4. A weak correlation, resulting from a weak 2J correlation, is seen from the carbon at δ 132.1 ppm to the proton at C-7 and can thus be assigned to C-1.

The COSY spectrum (Spectrum 6) shows a correlation from the aromatic protons to the protons of the methoxy groups. This confirms that the aromatic protons are adjacent to the methoxy groups on the aromatic ring as shown in Figure 14. The COSY spectrum also shows a strong correlation from the methine proton at position 8 to the protons of both the oxygenated methine (H-7) and methylene groups (2H-9). This confirms that the

methine group at position 8 is, in fact, between the methine and methylene groups at positions 7 and 9 respectively. There is also a COSY correlation between the two non-equivalent methylene protons at C-9. Figure 14 shows the relevant COSY correlations.

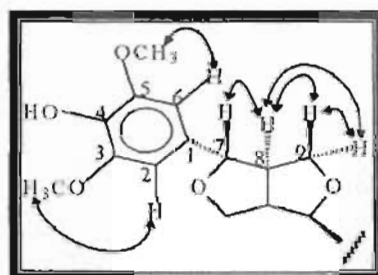


FIGURE 14: COSY correlations of compound 1

The relative stereochemistry of this half of the molecule could be determined from the NOESY spectrum (Figure 15) (Spectrum 7), which shows strong correlations between the aromatic protons (H-2, H-6) and H-7, H-8 and one of the methylene protons. A strong correlation is seen between H-7 and one of the methylene group protons (H-9 β) and is given a relative stereochemistry of β . A weak correlation is seen between H-7 and the proton at C-8. This suggests that H-8 is *trans* to H-7 β and is given the relative stereochemistry of α . The other methylene proton (δ 4.26 ppm), shows correlations to the proton at C-8 and the first methylene proton, and could therefore be placed at H-9 α . The H-9 β resonance shows a strong NOESY correlation to H-9 α and H-7. Thus H-7 is assigned the β stereochemistry and H-8 is in the α position.

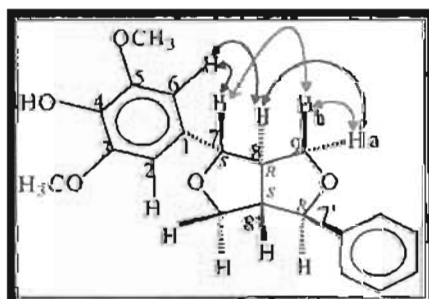


FIGURE 15: NOESY correlations of compound 1

From this, the stereochemistry at C-7 can be assigned as *S* and at C-8 as *R*. As the molecule is symmetrical, a second identical half was attached to form the complete molecule. The optical rotation was very small (almost zero) suggesting the presence of a *meso* - compound. In comparison, the optical rotation for (+) syringaresinol is + 62.2° and (-) syringaresinol is - 5.2°³. Thus the stereochemistry at C-7' was assigned a stereochemistry of *R* (the opposite of C-7) and C-8' was assigned a stereochemistry of *S* (the opposite of C-8).

Compound 1 is one of the major components of the calcium - spent liquor and has been identified as a lignan with a symmetrical structure known as *meso* – syringaresinol, which has not been reported previously. Although syringaresinol has been reported to occur in sulphite pulping effluent streams, the exact stereoisomers isolated have not been specified. This isomer having $[\alpha]_D = 0$ is not given in the Dictionary of Natural Products although (+) and (-) syringaresinol have been reported³.

TABLE 1: NMR data for compound 1 (300MHz, CDCl₃)

Position	¹ H	¹³ C	HMBC (C→H)	COSY	NOESY
1		132.1	H-7(² J), H-2/6(² J)		
2	6.56	102.7	H-7, H-6	OCH ₃	H-7, H-8
3		147.2	OCH ₃ , H-2(² J)		
4		134.3	H-2/6		
5		147.2	OCH ₃ , H-6(² J)		
6	7.24	102.7	H-7, H-2	OCH ₃	H-7, H-8
7	4.71 d (<i>J</i> =4.03Hz)	86.1	H-9, H-8(² J), H-2/6	H-8	H-9β, H-2/6, H-8
8	3.07 m	54.4	H-9, (² J), H-7(² J)	H-7, H-9α/β	H-2/6, H-7, H-9α
9α	4.26 m	71.8	H-7	H-8, H-9β	H-9β, H-8
9β	3.88	71.8	H-7	H-9α, H-8	H-9α, H-7
OCH ₃	3.88	56.4		H-2, H-6	
OH	5.48				

Note: All HMBC correlations are ³*J* correlations unless otherwise stated.

3.1.2 Structural elucidation of compound 2, episyringaresinol

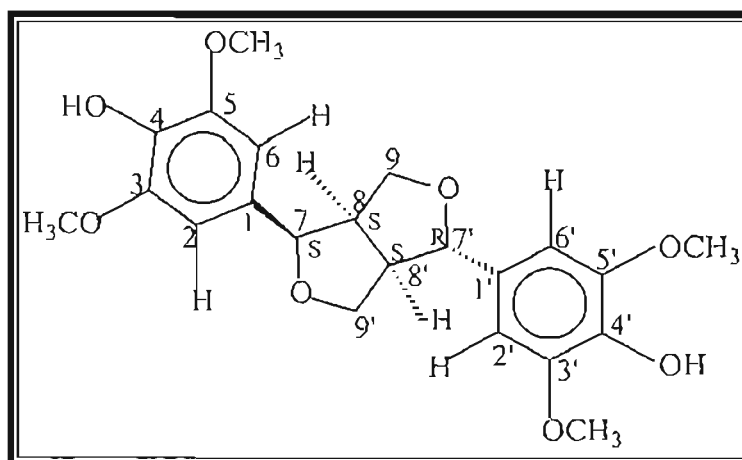


FIGURE 16: Structure of compound 2, episyringaresinol

Compound 2 is a stereoisomer of compound 1 in that it has the same molecular formula and structure but it has a different stereochemistry at the chiral centres. It was isolated as a mixture with syringaresinol (compound 1) and it was not possible to obtain a pure sample of the compound. However, its structure was fully elucidated by the process of subtraction of the peaks of the known compound 1, syringaresinol.

The mass spectrum of compound 2 (Spectrum 8) shows a molecular ion peak at m/z 418, which is the same as that of syringaresinol and indicates that compound 2 is a structural isomer. Here again, the fragmentation pattern is similar to that of syringaresinol with the splitting of the dimer to form a monomer and the loss of an ethylene group to give the base peak at m/z 181².

However, the ¹H and ¹³C NMR spectra display more peaks than that shown for compound 1 and this indicates that this compound is not symmetrical.

The ¹³C NMR spectrum (Spectrum 9) shows two methine carbon resonances at δ 50.4 ppm and δ 54.9 ppm, two oxygenated methylene group carbons at δ 69.7 ppm and δ 71.0 ppm and two oxygenated methine group carbons at δ 82.2 ppm and δ 88.0 ppm. Here

again, the oxygenated carbon resonances occur downfield due to the electronegative oxygen atoms and the effect of the aromatic ring. The two strong, sharp peaks at δ 102.3 ppm and δ 102.8 ppm are due to the protonated carbons on the aromatic rings. The intense peak at δ 56.6 ppm is characteristic of methoxy group carbon resonances. Both aromatic rings are symmetrical resulting in fewer carbons than expected in the ^{13}C NMR spectrum. The fully substituted carbons of the aromatic ring are shown between δ 129 ppm to δ 147 ppm and are in the same positions as shown for compound one. This suggests that the aromatic rings for compound 2 are the same as those of syringaresinol.

The ^1H NMR spectrum of compound 2 (Spectrum 10) shows the typical strong peak at δ 6.59 ppm for the aromatic proton resonances. The strong sharp peak at δ 3.89 ppm is typical of methoxy group protons. The doublets at δ 4.84 ppm ($J = 5.13$ Hz) and δ 4.40 ppm ($J = 7.14$ Hz) correspond to oxygenated methine group protons that have shifted downfield due to the deshielding effect of the electronegative oxygen atom and the aromatic ring and maybe ascribed to H-7 and H-7' respectively. The peaks at δ 2.89 ppm and δ 3.32 ppm correspond to H-8' and H-8 respectively. The peak at δ 4.13 ppm is due to one of the oxygenated methylene protons at C-9', that has shifted downfield. The coupling constant of 9.52 Hz indicates geminal coupling between the two methylene protons at C-9'. Two methylene proton resonances, due to one of the protons at C-9 and C-9' occur at δ 3.85 ppm, hidden beneath the methoxy group proton resonance and the fourth methylene proton resonance is found at δ 3.31 ppm, hidden beneath the resonance of H-8.

The relative stereochemistry of the two tetrahydrofuran rings could be determined from the NOESY NMR spectrum (Spectrum 11), which shows correlations between the aromatic protons and the benzylic protons at positions 7 and 7' as well as the protons of the methine groups at positions 8 and 8'. Weak correlations to the protons of the methylene groups can also be observed. NOESY correlations are seen between the methine proton at C-7, assigned the relative stereochemistry of α , and one of the methylene protons at C-9' as well as the methine proton at C-8. This suggests that one of

the protons at C-9' is on the same side of the molecule as H-7 α , and can therefore be placed at position C-9' α . A coupling constant of 5.13 Hz also suggests a *cis* configuration between the protons on C-7 and C-8. The methine proton at C-7' is seen to correlate to the methylene protons at H-9' β and H-9 β suggesting that these protons are on the same side of the molecule. The C-7' proton does not show any correlations to any protons in the α position, which confirms that it is in the β position. Figure 17 shows the relevant correlations as observed in the NOESY NMR spectrum and the stereochemistry could be assigned as 7*S*, 7'*R*, 8*S*, 8'*S*.

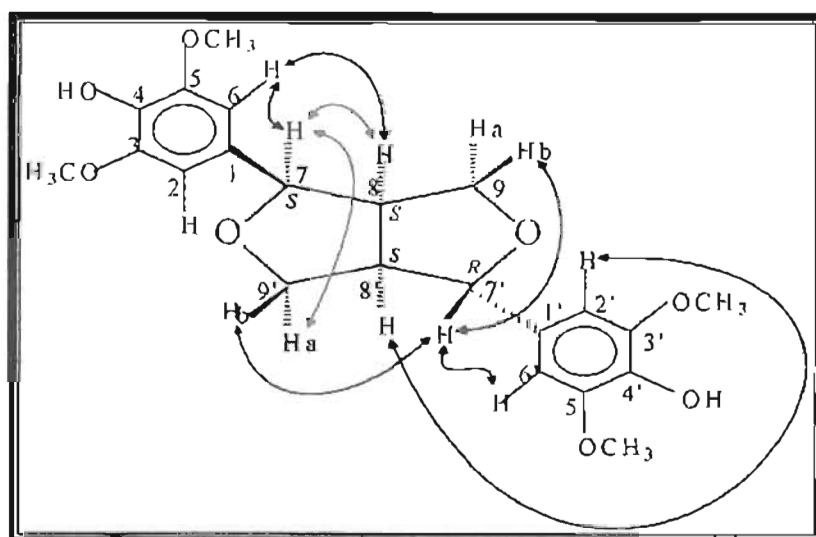


FIGURE 17: NOESY correlations of compound 2

The HMBC NMR spectrum (Spectrum 12) confirmed the structure of compound 2. Strong 3J correlations are observed between C-4, C-2, C-6, and C-7 and the aromatic protons (H-2 and H-6) as well as between C-4', C-2' C-6', and C-7' and the aromatic protons (H-2 and H-6). Coupling (2J) can also be seen from C-3 and C-5 to the adjacent aromatic protons and from C-3' and C-5' to its adjacent aromatic protons. Weak coupling can be seen from C-1 and C-1' to the adjacent aromatic protons. Figure 18 shows the HMBC correlations of compound 2. The correlations of the different systems are shown in different colours, that is, the correlations within the aromatic rings, within the tetrahydrofuran rings and between the aromatic rings and the tetrahydrofuran rings.

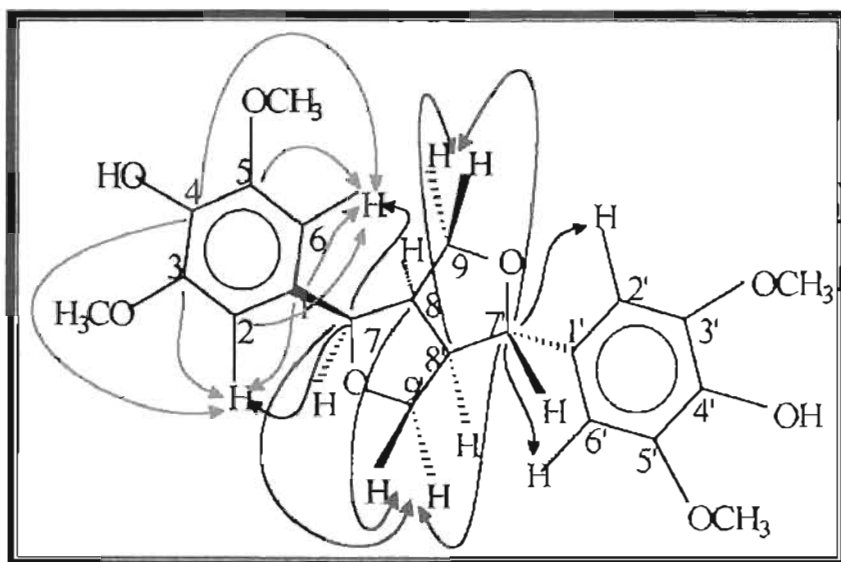


FIGURE 18: HMBC correlations (C→H) of compound 2

Further strong 3J coupling is observed between the carbons at position 7' and 8' and the methylene protons at position 9 as shown in the figure below as well as between the C-7', C-7 and C-8 and the protons at C-9'. Table 2 contains the full set of HMBC correlations.

The infrared spectrum (Spectrum 13) shows a broad band at 3420 cm^{-1} , which is characteristic of the hydroxy substituent and the strong bands at 1221 cm^{-1} and 1116 cm^{-1} correspond to the C-O stretching. The peaks at approximately 1500 cm^{-1} and 1600 cm^{-1} correspond to C=C stretching of the aromatic ring and the peaks at 2947 cm^{-1} and 2846 cm^{-1} are due to C-H stretching.

TABLE 2: NMR data for compound 2 (400MHz, CDCl₃)

Position	¹ H	¹³ C	HMBC (C→H)	NOESY
1		129.6	H-7 (² J), H-2/6 (² J)	
2	6.58	102.5	H-7, H-2/6	H-7, H-8, H-9α/β
3		147.1	OCH ₃ , H-2/6 (² J)	
4		133.8	H-2/6	
5		147.1	OCH ₃ , H-2/6 (² J)	
6	6.58	102.5	H-7, H-2/6	H-7, H-8, H-9α/β
7	4.84 d (J=5.13Hz)	82.4	H-9, H-9', H-2/6	H-9α, H-9'α, H-8, H-2/6
8	3.32	50.4	H-9'	H-2/6, H-7, H-9α, H-9'α, H-8'
9α	3.85	70.0	H-7	H-7, H-9β, H-8, H-8', H-2/6
9β	3.31	70.0	H-7	H-9α, H-7', H-2/6
1'		132.3	H-2'/6' (² J)	
2'	6.58	103.0	H-7', H-2/6	H-7, H-8', H-9'α/β
3'		147.1	OCH ₃ , H-2/6 (² J)	
4'	5.48	134.5	H-2/6	
5'		147.1	OCH ₃ , H-2/6 (² J)	
6'	6.58	103.0	H-7', H-2/6	H-7', H-8', H-9'α/β
7'	4.40 d (J=7.14Hz)*	88.2	H-9, H-9', H-2/6	H-9β, H-9'β, H-2'/6'
8'	2.89	54.9	H-9	H-8, H-9α, H-9'α, H-2'/6'
9'α	3.85	71.2	H-7'	H-8', H-8, H-9'β, H-7, H-2'/6'
9'β	4.13 d (J=9.52Hz)	71.2	H-7'	H-9'α, H-7', H-2'/6'
OCH ₃	3.89	56.6		
OH	5.48			

Note: All HMBC correlations are ³J correlations unless otherwise stated.

*A model of compound 2 together with the dihedral angle calculated using Karplus equation showed that this value is predictable.

Much research has been carried out on the stereochemistry of lignans and it has been found that the coupling constants cannot exclusively be used to determine the stereochemistry⁴. Thus the advent of NOESY NMR spectroscopy has proved invaluable in the determination of relative stereochemistry. Previous studies have incorrectly assigned the low field benzylic proton as axial⁵. However, further studies based on

various independent methods have shown that the benzylic proton in the high field region is, in fact, axial^{4, 6}. Compound 2 agrees with this, showing that the benzylic proton at C-7' is further up field and thus the aromatic ring attached at C-7' is axial. In addition the difference between the carbon resonances at C-1 and C-1' is δ 2.7 ppm and this suggests that compound 2 is an epi-lignan⁶. The difference in carbon resonances between C-7 and C-7' is 5.8 ppm and is further evidence that suggests an epi-lignan structure as was indicated by the NOESY correlations⁴.

Thus, compound 2 has been identified as episyringaresinol, which has been previously isolated from *Liriodendron tulipifera* and is a degradation product of birch lignin⁷. It is the other major compound in the calcium - spent liquor effluent. The mixture of the two isomers has a combined approximate concentration of 0.400 g/L in the calcium - spent liquor effluent.

3.1.3 Structural elucidation of compound 3, 3-(4'-hydroxy-3',5'-dimethoxyphenyl)-prop-1-ene

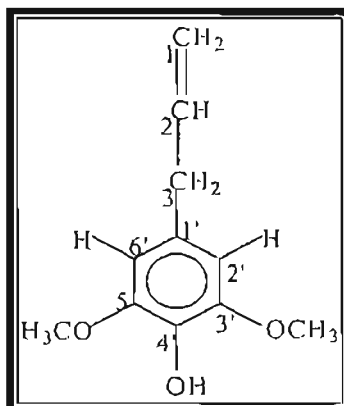


FIGURE 19: Structure of compound 3, 3-(4'-hydroxy-3',5'-dimethoxyphenyl)-prop-1-ene

The low - resolution mass spectrum of compound 3 (Spectrum 14) gave a molecular ion peak at m/z 194, which corresponds to the molecular formula of $C_{11}H_{14}O_3$. Fragmentation between C-3 and C-2 results in the loss of 27 mass units and gives a peak at m/z 167, which corresponds to the hydroxy-dimethoxytropylium ion.

The infrared spectrum (Spectrum 15) shows a distinct broad band at 3427 cm^{-1} , which indicates the presence of a hydroxyl substituent. There are also strong bands at 2923 cm^{-1} and 2859 cm^{-1} that correspond to C-H stretching of methine and methylene groups. The peak between 1680 cm^{-1} and 1600 cm^{-1} shows C=C stretching, which is not part of an aromatic ring. The distinct sharp peak at 1126 cm^{-1} is again characteristic of C-O stretching.

The ^1H NMR spectrum (Spectrum 16) shows a single sharp peak at δ 6.39 ppm, integrating to two protons, indicating two equivalent aromatic proton resonances. The other strong peak at δ 3.86 ppm, integrating to six protons, is characteristic of protons of two equivalent methoxy groups. The ^1H NMR peaks integrate to 2:1:2:6:1 and suggests a

symmetrical aromatic ring in the molecule. The doublet at δ 3.30 ppm is indicative of methylene protons and the multiplet peaks at δ 5.92 ppm and δ 5.07 ppm correspond to methine and methylene protons respectively, which are attached to double bonds.

The carbon spectrum (Spectrum 17) shows the strong characteristic peak of a methoxy carbon resonance at δ 56.2 ppm and the protonated aromatic carbon resonance at δ 105.1 ppm. The peaks between δ 110 ppm and δ 150 ppm correspond to carbons of the aromatic ring or carbons attached to the double bond and these were assigned based on HMBC correlations. The peak at δ 40.3 ppm corresponds to the C-3 carbon of the methylene group.

The HMBC NMR spectrum (Spectrum 18) shows a strong correlation between the carbon at δ 146.9 ppm and the protons of the methoxy group and would thus allow assignment of that carbon to C-3' and C-5'. There is also a weak 2J correlation to the aromatic protons. A strong correlation is observed from a carbon resonance hidden at δ 132.9 ppm (not clearly observed on the ^{13}C NMR spectrum) to the aromatic protons and corresponds to C-4'. The protonated aromatic carbons (C-2', C-6') at δ 105.1 ppm show 3J correlations to the methylene protons at C-3. The carbon resonances at δ 137.6 ppm and δ 131.1 ppm show correlations to the methylene protons and could either be the C-1' and C-2 or *vice versa*. However, the resonance at δ 137.6 ppm is stronger than that at δ 131.1 ppm and is probably due to the protonated carbon at position 2. Therefore the resonance at δ 131.1 ppm is assigned to C-1'. Figure 20 shows the relevant HMBC correlations with the strong or 3J correlations in red.

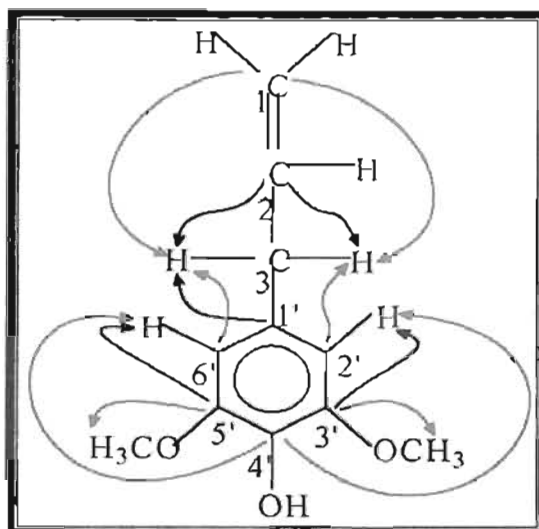


FIGURE 20: HMBC correlations (C→H) of compound 3

The COSY NMR spectrum (Spectrum 19) confirms this structure by showing correlations from the aromatic protons to the methoxy group protons. The methine proton at position 2 shows correlations to the methylene group protons at positions 1 and 3, confirming the structure of the side chain.

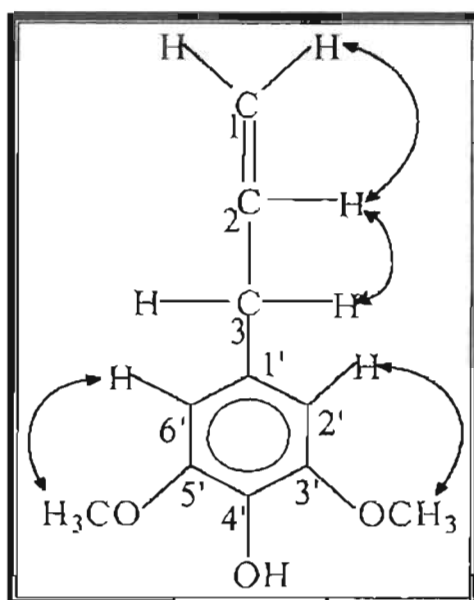


FIGURE 21: COSY correlations of compound 3

Compound 3 was subsequently identified as a 3-(4'-hydroxy-3',5'-dimethoxyphenyl)-prop-1-ene from the GC/MS library. It is a common compound found in wood products and its concentration is approximately 0.020 g/L in the calcium - spent liquor effluent.

TABLE 3: NMR data for compound 3 (400MHz, CDCl₃)

Position	¹ H	¹³ C	HMBC (C→H)
1'		131.1	H-3'
2'	6.39	105.1	H-3, H-6'
3'		146.9	OCH ₃ , H-2'
4'		132.9	H-2'/6'
5'		146.9	OCH ₃ , H-6'
6'	6.39	105.1	H-3, H-2'
3	3.30 d (2H)	40.3	H-2'/6'
2	5.92 m (1H)	137.6	H-3
1	5.06 m (2H)	115.7	H-3
OCH ₃	3.86	56.2	

3.1.4 Structural elucidation of compound 4, 3-(4'-hydroxy-3',5'-dimethoxyphenyl)-1-hydroxy-propan-2-one

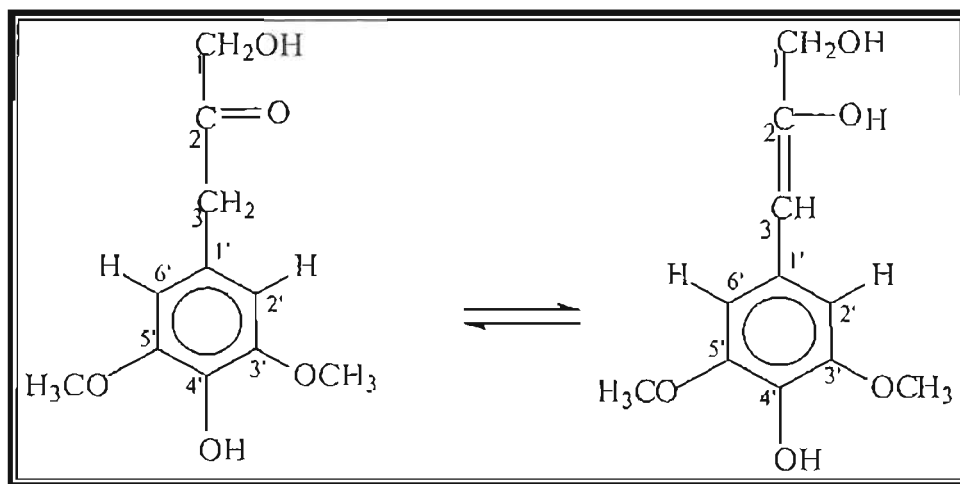


FIGURE 22: Structure of compound 4, 3-(4'-hydroxy-3',5'-dimethoxyphenyl)-1-hydroxy-propan-2-one displaying keto-enol tautomerism

The mass spectrum, Spectrum 20, shows a molecular ion peak at m/z 226 indicating a molecular formula of $C_{11}H_{14}O_5$ for the compound. α -Cleavage between positions 3 and 2 yields the corresponding substituted tropylium ion indicated by the base peak at m/z 167. The loss of 59 mass units to give the peak at m/z 167 corresponds to the loss of the carbonyl attached to the hydroxy methylene substituent.

The infrared spectrum (Spectrum 21) shows a broad band between 3400 cm^{-1} and 3600 cm^{-1} , which is ascribed to the hydroxyl group and a characteristic carbonyl peak at 1721 cm^{-1} , which is ascribed to the carbonyl group at position 2 on the molecule.

The proton NMR spectrum, Spectrum 22, shown on page 152, shows a peak at δ 6.41 ppm (2H) characteristic of an aromatic ring proton or alkene proton and is assigned H-2' and H-6'. The strong peak at δ 3.87 ppm (3H) is characteristic of a methoxy group proton resonance and the peak at δ 3.63 ppm is due to a methylene group proton attached to an electronegative group, such as, a carbonyl group. The peak at δ 4.28 ppm is that of a

methylene group proton attached to an electronegative atom, such as oxygen, that has shifted it downfield. The methylene group proton resonance at δ 4.28 ppm (2H) is more downfield than the methylene group at δ 3.63 ppm and could be ascribed to the 2H-1 resonance attached to a hydroxyl group. The integration of the aromatic substituents is 2:6 confirming a symmetrical aromatic ring structure. Thus the peak at δ 6.41 ppm corresponds to H-2' and H-6' and there are two methoxy groups, which are attached to C-3' and C-5' on the molecule.

Spectrum 24, the HSQC NMR spectrum, confirms that the peaks at δ 4.28 ppm and δ 3.62 ppm are, in fact, due to methylene group protons and that they correspond to the peaks at δ 67.7 ppm and δ 46.1 ppm respectively in the carbon NMR spectrum (Spectrum 23). The peak at δ 6.41 ppm, due to the two aromatic protons, corresponds to the same carbon peak at δ 106.1 ppm. The carbon peak resonance at δ 56.6 ppm corresponds to methoxy group carbons.

The HMBC spectrum, Spectrum 25, shows carbon to proton correlations as shown in Table 4. A peak at δ 207 ppm characteristic of a carbonyl group was not clearly shown on the carbon spectrum. Ketone carbonyl peaks are sometimes difficult to see as they are weak resonances. However, the carbon of the ketone was seen to correlate to the protons of both methylene groups in the HMBC NMR spectrum and is therefore positioned between the two methylene groups. The carbon peak at δ 147.5 ppm shows correlations to the protons of the methoxy groups as well as the protons at δ 6.41 ppm (H-2' and H-6'). The peak at δ 134.4 ppm shows a correlation only to the peak at δ 6.41 ppm. It does not show any correlations to the methoxy group protons, which would be a 4J correlation and this is generally not seen. Therefore this carbon resonance could be assigned to C-4'. The carbon peak at δ 123.8 ppm is ascribed to carbon position 1' on the molecule and correlates to the protons on the methylene group at δ 3.63 ppm (H-7') and to the protons on the aromatic ring (H-2' and H-6'). The carbons, at positions 2' and 6', correlate to the protons on the methylene group at position 3. The C-1 resonance of the methylene group occurs at δ 67.7 ppm and shows a correlation to the protons of the other methylene group

(2H-3). The C-3 resonance of the methylene group at δ 46.1 ppm shows a correlation to the protons at δ 6.41 ppm (H -2' and H -6'). Figure 23 and Table 4 show the full set of HMBC correlations.

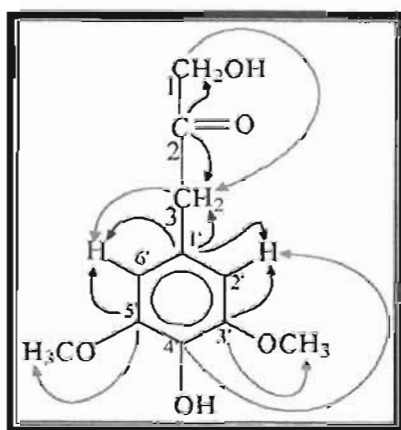


FIGURE 23: HMBC correlations (C→H) of compound 4

The NOESY NMR spectrum, Spectrum 26, shows a correlation between the protons at δ 6.41 ppm and the protons of the methylene group at δ 3.63 ppm. The spectrum also shows a correlation between the protons of the two methylene groups (Figure 24).

A COSY correlation is seen between the aromatic protons and the methoxy group protons (Spectrum 27).

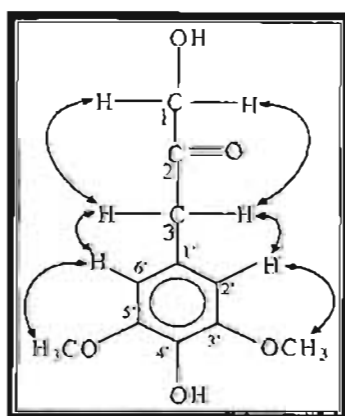


FIGURE 24: NOESY correlations of compound 4

TABLE 4: NMR data for compound 4 (400MHz, CDCl₃)

Position	¹ H	Acetylated ¹ H	¹³ C	HMBC (C→H)	NOESY
1'			123.78	H-3(² J), H-2' & H-6'(² J)	
2'	6.41	6.68	106.14	H-3(³ J)	H-3, OCH ₃
3'			147.49	OCH ₃ (³ J), H-2'(² J)	
4'			134.37	H-2' & H-6'(³ J)	
5'			147.49	OCH ₃ (³ J), H-6'(² J)	
6'	6.41	6.68	106.14	H-3(³ J)	H-3, OCH ₃
3	3.63 s (2H)	6.24	46.14	H-2'(³ J), H-6'(³ J)	H-1, H-2' & H-6'
2			207	H-3(² J), H-1(² J)	
1	4.28 s (2H)	4.77	67.67	H-3(³ J)	H-3
OCH ₃	3.87 (6H)	3.79	56.6		H-2', H-6'

Compound 4 was identified as 3-(4'-hydroxy-3',5'-dimethoxyphenyl)-1-hydroxy-propan-2-one, having an approximate concentration of 0.010 g/L in the calcium - spent liquor effluent.

3.1.4.1 Acetylation of compound 4

Compound 4 was acetylated to confirm the positioning of the hydroxyl groups. This was carried out using pyridine and acetic anhydride. The details of the acetylation procedure are given in the experimental section, page 96.

Structural elucidation of the acetylated compound 4

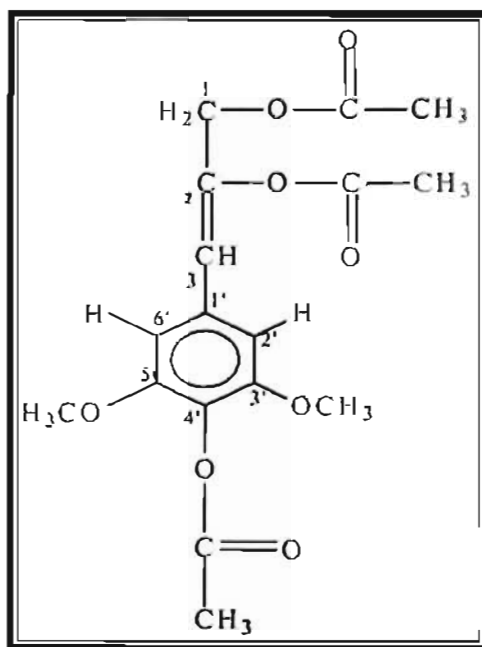


FIGURE 25: Structure of acetylated compound 4

The ¹H NMR spectrum (Spectrum 28) shows that the acetylated product is a triacetate and not a diacetate, as one would have expected. The acetylation at carbon position 2 occurred because keto-enol tautomerism results in the formation of the enol form as shown in Figure 22. The double bond between carbons 3 and 2 results in a conjugated structure with the aromatic ring, affording greater stability to the molecule.

The mass spectrum (Spectrum 29) gives a molecular ion peak at *m/z* 352, which corresponds to the addition of three acetate groups (3 x 42 = 126) to the original

compound (m/z 226). The mass spectrum shows fragmentation ions at m/z 310, 268 and 226 resulting from the loss of three $\text{O}=\text{CCH}_3$ fragments.

The infrared spectrum (Spectrum 30) shows a distinct, strong carbonyl band at 1762 cm^{-1} due to the presence of three acetate carbonyl groups. There is no evidence of a hydroxyl substituent.

The three acetate group proton resonances occur at δ 2.31 ppm, δ 2.20 ppm and δ 2.10 ppm (each 3H) in the proton NMR spectrum, Spectrum 28. The acetylation of the hydroxyl group at carbon position 1 has caused a downfield shift of the 2H-1 protons from δ 4.28 ppm to δ 4.77 ppm. The proton NMR spectrum also shows the disappearance of the methylene group at position 3 and the presence of a new methine peak at δ 6.24 ppm corresponding to the formation of the double bond in conjugation with the aromatic ring. The HSQC spectrum (Spectrum 31) further confirms the presence of only one methylene group at δ 4.77 ppm corresponding to the carbon at δ 64.2 ppm (C-1).

The HMBC NMR spectrum (Spectrum 32) of the acetylated compound shows the same correlations as seen for the original unacetylated compound 4. In addition, correlations can be seen between the carbons of the carbonyl groups of the acetate substituents and the protons of the acetate methyl groups. A correlation can be observed between the carbonyl of the acetate group at C-1 and the protons at C-1. The carbon at position 2 (δ 143.7 ppm) is correlated to the protons on the methylene group at C-1 and the proton on the methine group at position 3.

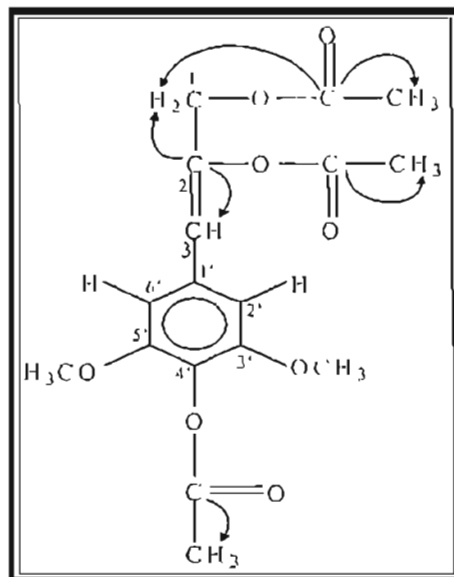


FIGURE 26: HMBC correlations (C→H) of the acetylated compound 4

The NOESY NMR spectrum (Spectrum 33) shows correlations between the aromatic protons and the methine proton at C-3 and the protons of the acetate group at C-2. A correlation is also observed between the protons of the methoxy group and the acetate substituent at position 4' on the aromatic ring.

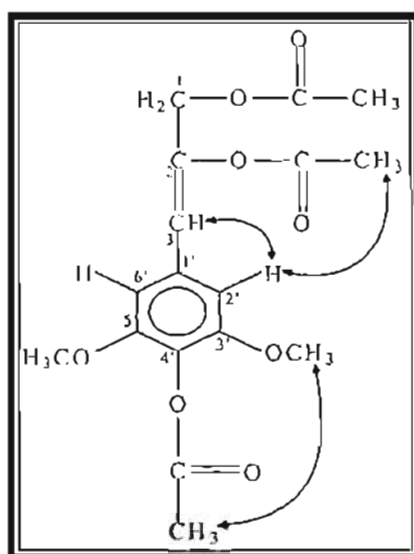


FIGURE 27: NOESY correlations of acetylated compound 4

3.1.5 Structural elucidation of compound 5, 4-hydroxy-3,5-dimethoxybenzaldehyde (commonly known as syringaldehyde)

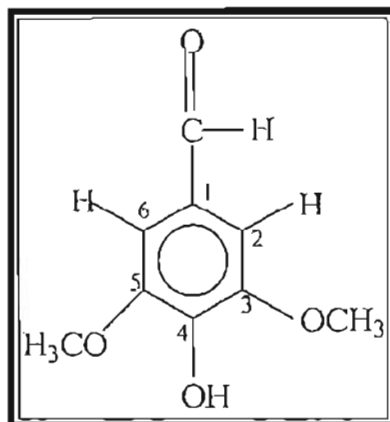


FIGURE 28: Structure of compound 5, syringaldehyde

The mass spectrum, Spectrum 34, shows a molecular ion peak at m/z 182, confirming that compound 6 has a molecular formula of $C_9H_{10}O_4$. The distinct peak at $M-1$ corresponds to the loss of a hydrogen, which is characteristic of an aldehyde. A loss of 17 mass units ($182-165$) shows the loss of a hydroxyl group.

The infrared spectrum (Spectrum 35) shows a broad band between 3200 cm^{-1} and 3400 cm^{-1} characteristic of a hydroxyl substituent. The sharp peak at 1671 cm^{-1} is characteristic of carbonyl stretching in conjugation with the aromatic ring and can be ascribed to the aldehyde group. The two peaks between 2800 cm^{-1} and 3000 cm^{-1} are characteristic of C-H stretching of the aldehyde group. The peaks at 1607 cm^{-1} and 1512 cm^{-1} are ascribed to aromatic ring vibrations and the distinct peak between 1300 cm^{-1} and 1350 cm^{-1} is characteristic of syringyl ring breathing¹.

The proton NMR spectrum of this compound (Spectrum 36) shows only four peaks in the ^1H NMR spectrum, which suggests that the compound is symmetrical. The spectrum shows a singlet at δ 9.80 ppm characteristic of an aldehyde proton. The peak at δ 7.13 ppm (2H) is characteristic of aromatic protons and the strong peak at δ 3.96 ppm (6H)

corresponds to the protons of a methoxy group. The integration of the peaks from left to right is 1:2:1:6, confirming a symmetrical aromatic ring with two aromatic protons, H-2 and H-6, occurring at δ 7.13 ppm and two methoxy group proton resonances for the groups at C-3 and C-5, at δ 3.96 ppm. The peak at δ 6.06 ppm integrates to 1 proton and corresponds to the phenolic proton of the substituent at C-4. The presence of this proton was further confirmed by the disappearance of this peak when a proton NMR spectrum was run using deuterated water as the solvent, Spectrum 37.

The HSQC NMR spectrum (Spectrum 39) shows that the proton of the aldehyde group corresponds to the carbon resonance at δ 190.9 ppm, the aromatic protons correlate with the carbon resonance at δ 106.9 ppm and the methoxy group proton resonance corresponds to the carbon resonance at δ 56.7 ppm. The remaining three carbon resonances are due to fully substituted carbons.

The HMBC NMR spectrum (Spectrum 40) shows that the carbon atom of the aldehyde group correlates to the protons of the aromatic ring (H-2 and H-6). The carbon atoms at positions 3 and 5 (δ 147.6 ppm) are seen to correlate to the protons of the methoxy substituents, the phenolic proton at C-4 and the protons of the aromatic ring. The C-4 resonance correlates to the phenolic proton and the protons of the aromatic ring. The C-1 resonance (δ 128.6 ppm) correlates to the protons of the aromatic ring and the aldehyde proton. The C-2 and C-6 resonances show an HMBC correlation to the aromatic protons as well as to the proton of the aldehyde group.

The NOESY NMR spectrum (Spectrum 41) shows proton correlations between the aldehyde proton and the H-2 and H-6 resonances. The spectrum also shows proton correlations between the aromatic protons and the methoxy group protons. These correlations confirm the positioning of the aldehyde group, methoxy groups and the aromatic protons.

This compound was identified as syringaldehyde and occurs at a concentration of approximately 0.010 g/L in the calcium - spent liquor. Syringaldehyde is another

commonly occurring compound in sulphite liquors and its structure was confirmed from literature spectra.

TABLE 5: NMR data for compound 5 (400MHz, CDCl₃)

Position	¹ H	¹³ C	HMBC (C→H)	NOESY
1		128.61	H-2(² J), CHO(² J)	
2	7.13	106.89	H-6(³ J), CHO(³ J)	CHO, OCH ₃
3		147.55	H-2(² J), OH(³ J), OCH ₃ (³ J)	
4		141.00	H-2(³ J), H-6(³ J), OH(² J)	
5		147.55	OH(³ J), H-6(² J), OCH ₃ (³ J)	
6	7.13	106.89	H-2(³ J), CHO(³ J)	CHO, OCH ₃
CHO	9.80	190.99	H-2, H-6(³ J)	H-2, H-6
OCH ₃	3.96	56.69		H-2, H-6
OH	6.06			

3.1.6 Structural elucidation of compound 6, 2,6-dimethoxy-1,4-benzoquinone

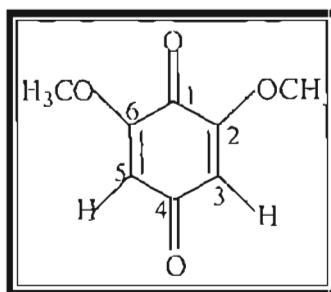


FIGURE 29: Structure of compound 6, 2,6-dimethoxy-1,4-benzoquinone

Compound 6 was isolated as a mixture with compound 5, syringaldehyde. The t.l.c plate showed one clean spot but on running the GC/MS, two compounds having an approximate ratio of 2:1 was seen with compound 6 present in almost half the quantity of compound 5, Spectrum 42.

The mass spectrum (Spectrum 43) shows a molecular ion peak at m/z 168, which corresponds to a molecular formula of $C_8H_8O_4$. The GC/MS library immediately identified this compound as 2,6-dimethoxy-1,4-benzoquinone with an 86 % certainty.

The 1H NMR spectrum (Spectrum 44) shows the peaks due to syringaldehyde, as described in the previous section. In addition to this, the spectrum shows another proton resonance at δ 5.84 ppm, which can be ascribed to the protons attached to the double bond (H-3 and H-5) and the peak at δ 3.80 ppm is due to the methoxy group proton resonance.

The ^{13}C NMR spectrum (Spectrum 45) shows carbon resonances for both compounds. The peaks for syringaldehyde were subtracted and the remaining resonances were found to correspond to compound 6. These were a strong peak at δ 107.4 ppm, which corresponds to the protonated carbon resonances at C-3 and C-5 and the peak at δ 157.3 ppm, which corresponds to C-2 and C-6 to which the methoxy groups are attached.

Analysis of the HMBC correlations shows a small hidden carbon resonance in the downfield region, at approximately δ 176 ppm (Spectrum 46). This shows a strong correlation to H-3 and H-5 and can be assigned to C-1 attached to an oxygen atom. Carbonyl resonances are generally weak and are often not clearly seen. The HMBC NMR spectrum further confirms the assignment of C-2 and C-6 by showing a strong 3J correlation from those carbons at δ 157.3 ppm to the protons of their methoxy groups. The HMBC correlations for syringaldehyde are discussed in the previous section.

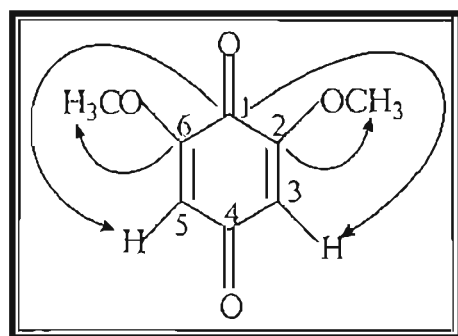


FIGURE 30: HMBC correlations (C→H) of compound 6

The NOESY NMR spectrum (Spectrum 47) confirms the presence of a mixture of the two compounds by showing proton correlations from each compound's aromatic protons to their respective methoxy group protons.

The above spectra clearly confirms the GC/MS library's identification of compound 6 as 2,6-dimethoxy-1,4-benzoquinone. It is present in minor quantities in the effluent with an estimated concentration of approximately 0.0030 g/L.

TABLE 6: NMR data for compound 6 (400MHz, CDCl₃)

Position	¹ H	¹³ C	HMBC
1		~ 178 *	H-3, H-5
2		157.3	OCH ₃
3	5.84	107.4	
4		~ 175-180 *	
5	5.84	107.4	
6		157.3	OCH ₃
OCH ₃	3.80	56.5	

* These carbon resonances for the carbonyl groups are approximate values as carbonyl resonances are weak and are often not clearly seen. They were detected using the HMBC NMR spectrum.

3.1.7 The extraction of lignosulphonates

An extraction of the lignosulphonates was attempted using the method described by Konturri and Sundholm^{8,9}. This method involved first complexing the lignosulphonates with a long-chain alkyl amine, which was then extracted into an organic solvent. The lignosulphonates were thereafter regenerated by the addition of an alkali such as NaOH. Section 4.2.2 in the experimental chapter contains the details of the extraction procedure.

A cream - coloured precipitate (w/w % = 4.2 %), from the extraction of the aqueous portion of the calcium - spent liquor effluent stream, was obtained and was subjected to a variety of tests. The precipitate was found to be insoluble in dichloromethane (MeCl_2) and methanol (MeOH) but soluble in water. On air evaporation of a water solution of the sample, white square - like crystals were obtained resembling sugar. An ignition test was carried out on the sample, which gave off a candy floss aroma. The sample did not ignite or give off smoke but charred to a black residue.

A ^1H NMR spectrum (Spectrum 48, page 178) of the precipitate showed peaks between δ 3 ppm- δ 5 ppm and a few peaks in the aromatic region. This suggested a mixture of aromatic compounds with sugar molecules. The ^{13}C NMR spectrum (Spectrum 49) showed peaks between δ 60 ppm- δ 90 ppm, which are indicative of sugars. The sample was then spotted on a t.l.c. plate and developed in 100% MeOH but poor separation was obtained. Separation on a preparative t.l.c. plate was also unsuccessful.

A sodium fusion test gave a positive test for the presence of sulphur.

An infrared analysis, Spectrum 50 in Appendix A, showed a broad distinct band between 3600 cm^{-1} and 3000 cm^{-1} characteristic of O-H stretching. The other distinct bands at 1603 cm^{-1} and 1402 cm^{-1} are indicative of C=C stretching of an aromatic ring. The shoulder peak at 1208 cm^{-1} can be ascribed to sulphonic acid groups and the broad band

between 1100 cm^{-1} and 1000 cm^{-1} indicates the presence of sugar or polysaccharide moieties^{10a}.

An ultraviolet scan, Spectrum 51, of the sample showed a high absorption maximum at approximately 210 nm and a smaller absorption at approximately 280 nm, which compares favourably with UV spectra shown for lignosulphonates from spruce, beech and pine wood^{10a}

Based on the above analysis carried out on the sample, it was concluded that the lignosulphonate extract obtained from the extraction of the calcium - spent liquor effluent, includes a mixture of lignosulphonates with sugars. It has not been possible to isolate and identify pure lignosulphonate compounds during the course of this project. The isolation and identification of pure lignosulphonates would require considerable time and the use of other techniques, such as, HPLC or ion exchange chromatography to separate such compounds and was considered beyond the scope of this project. The equipment necessary for the use of these techniques was also presently unavailable.

3.1.8 Analysis of the residue formed in the calcium - spent liquor

The calcium - spent liquor produced a residue on cooling and standing having a concentration of approximately 0.72 g/L. It was initially thought that the light, fibrous - like residue contained calcium oxalate, which contributed to the scaling problems in the pipeline. An X - ray diffraction analysis revealed that there was no calcium oxalate present in this particular sample but there was, in fact, two forms of calcium sulphate present, gypsum ($\text{CaSO}_4 \cdot 2\text{H}_2\text{O}$) and the hemihydrate form more commonly known as Plaster of Paris ($\text{CaSO}_4 \cdot 0.5\text{H}_2\text{O}$). These two components were identified by matching the d-spacings obtained for this sample with those found in a library, starting with the peak of highest relative intensity. Spectrum 52 shows the two compounds with the identified peaks coloured but there is a third component present in minor quantities that was not identified.

An elemental composition of the sample was obtained by subjecting it to X - ray fluorescence analysis (Table 8). The sample preparation involved fusing it with $\text{Li}(\text{BO}_4)_4$ in a muffle furnace at 1000°C and thereafter cooling it to form a pellet. The XRF analysis revealed that the sample contained mostly calcium (82.8 %) and a significant amount of sulphur, whose percentage could not accurately be determined. The sample also contained silica (5.9 %) and sodium (1.3 %) and other elements such as aluminium, magnesium, phosphorous and chromium were present in trace amounts, that is $<0.3\%$. The sample had a large organic content, which was lost during ashing, shown by a loss on ignition of 80.4 %. Sulphates could also have been lost during the ashing process. The high calcium content suggests that the organic component could have calcium cations complexed with it.

3.1.9 Carbohydrate content of the calcium - spent liquor effluent

Carbohydrates make up a major proportion of the calcium - spent liquor and generally originate from hemicelluloses^{11a}. Hemicelluloses are subdivided into hexoses, pentoses and deoxyhexoses^{11b}. There may be a small portion of polysaccharides present in the spent liquor but the pulping process through which the wood chips pass usually converts almost all the polysaccharides to monosaccharides^{11a}. The carbohydrate content in the form of hexose based on glucose and pentose based on xylose was determined using UV spectroscopy and the experimental details can be read in section 4.2.3. This technique is useful for a rapid estimation of the quantity of soluble carbohydrates present in the effluent^{12a}.

In order for a compound to absorb in the visible region, it must generally be coloured, therefore the samples were treated with colour reagents that allowed absorption of visible wavelengths at approximately 490 nm for glucose and 660 nm for xylose^{12a}. The colour reagents most commonly used are phenol, anthrone and orcinol. In this analysis, phenol was complexed with glucose and orcinol was complexed with xylose¹³. The use of concentrated acids ensured complete hydrolysis of any polysaccharides that may have been present, to monosaccharides.

3.1.9.1 Analysis of hexoses¹³

Three glucose standards were prepared having the following concentrations, 0.10 mg/ml, 0.25 mg/ml and 0.35 mg/ml. These standards were subjected to the same preparation procedures as the sample and their absorbances were determined, Spectrum 53. These results were then used to calculate their absorptivities using Beer's Law. The calculations are as follows:

Beer's Law equation:

$$A = alc$$

Where A = absorbance

a = absorptivity

l = path length of the cell which is 1cm

c = concentration

Using the data in Table 9.

Standard solution of 0.10 mg/ml

$$\begin{aligned} a &= A/(l \times c) \\ &= 0.463 / (1 \times 0.10) \\ &= 4.630 \end{aligned}$$

Similarly, the absorptivities for the other standards were calculated (Table 9) and the average absorptivity was calculated to be 4.633. Using this absorptivity, the concentration of glucose in the calcium - spent liquor sample was calculated as follows.

$$\begin{aligned} c &= A/al \\ &= 0.571 / (4.633 \times 1) \\ &= 0.123 \text{ mg/ml} \end{aligned}$$

Taking into account the dilution factor, the concentration of glucose in the calcium - spent liquor effluent stream is 49.3 g/L. This value (weight % = 4.9 %) compares favourably with that obtained from SAICCOR (3.3 % by weight) (Table 11 in Appendix B).

TABLE 9: Data used to calculate the concentration of glucose in the calcium - spent liquor effluent

Sample	Absorbance (A)	Absorptivity (a)	Concentration (c) (mg/ml)
Std 0.10 mg/ml	0.436	4.630	0.10
0.25 mg/ml	1.139	4.556	0.25
0.35 mg/ml	1.650	4.714	0.35
Ca-spent liquor	0.571	4.633	0.123

3.1.9.2 Analysis of pentoses¹³

Various xylose standards were prepared ranging from 0.05 mg/ml to 0.35 mg/ml. The absorbance for each standard was determined (Spectrum 55) and used to calculate their absorptivities using Beer's Law as shown for hexose:

For example, the absorptivity for a standard 0.10 mg/ml solution was calculated as follows:

$$\begin{aligned}
 A &= alc \\
 a &= A / (c \times l) \\
 &= 0.258 / (0.10 \times 1) \\
 &= 2.58
 \end{aligned}$$

Similarly, the absorptivities of the other standards (Table 10) were calculated and the average absorptivity was determined as 2.49. This value was then used to calculate the concentration of xylose in the sample.

$$\begin{aligned}
 c &= A/a \\
 &= 0.620 / (2.49 \times 1) \\
 &= 0.249 \text{ mg/ml}
 \end{aligned}$$

Taking into account the dilution factor, the xylose concentration in the calcium - spent liquor effluent was determined to be 49.8 g/L. Converting this value to weight % = 5.0 %, it is in agreement with that obtained from SAICCOR (3.3 % by weight) for the calcium - spent liquor stream (Table 11 in Appendix B).

TABLE 10: Data used to calculate the concentration of xylose in the calcium - spent liquor effluent

Sample	Absorbance (A)	Absorptivity (a)	Concentration (c) (mg/ml)
Std 0.05 mg/ml	0.123	2.46	0.05
0.10 mg/ml	0.258	2.58	0.10
0.15 mg/ml	0.400	2.67	0.15
0.20 mg/ml	0.527	2.64	0.20
0.25 mg/ml	0.598	2.39	0.25
0.30 mg/ml	0.706	2.35	0.30
0.35 mg/ml	0.807	2.31	0.35
Ca-spent liquor	0.620	2.49	0.249

3.1.10 Analysis of wax balls from calcium - spent liquor evaporates

A very distinct smelling sample made up of yellow and cream - coloured wax balls was found to build-up in both the calcium and magnesium sections. The sample analysed in this work was obtained from the calcium - section at the stage where the condensed gases combine from an evaporation process in the spent sulphite liquor stream. Marked as [*] on Scheme 16, page 42.

The build - up of this waxy substance is generally a rare occurrence, but is, in fact, dependant on plant operating conditions, such as temperature and pH. Discussions with plant operating personnel revealed that these wax balls only formed if the temperature of the condensing gases, from an evaporation process, cools to below approximately 60⁰ C¹⁴. At temperatures above 60⁰ C, the waxy substances remain in solution, which combines with the rest of the calcium - spent liquor effluent stream and is carried to the main effluent pipeline out to sea. Furthermore, an increase in pH to approximately 5.5-6.0 also encourages the solidification of these wax balls out of the condensing gases¹⁴. However, none of these compounds were identified in the organic extracts of both the calcium and magnesium effluent streams, which is probably due to operating conditions at the time the samples were collected and possibly because they are present in minor quantities.

The wax balls were analysed using GC/MS and they were identified as a combination of fatty acids and their derivatives. The major constituent was found to be palmitic acid, which makes up approximately 65 % of the sample. It has been reported that the major fatty acid found in *Eucalyptus globulus* is linoleic acid followed by palmitic acid^{10b}. Other constituents present in minor quantities include pentadecanoic acid (5.6 %), 2-hydroxy-cyclopentadecanone (4.1 %), the methyl ester of palmitic acid (3.2 %), myristic acid (2.6 %) and 1,2,3,4-tetrahydro-1,6-dimethyl-4-(1-methylethyl)-naphthalene (1.9 %). A few trace constituents present include dodecanoic acid, hexadecanoic acid and derivatives of octadecadienoic acid and naphthalene. Spectrum 57 in Appendix A shows the gas chromatogram and spectra 58 to 67 shows the mass spectra identifying the various constituents.

Fatty acids have a variety of uses ranging from applications in the pharmaceutical and cosmetic industry to the soaps and detergent industry. The details of their biosynthesis and uses can be read in section 2.3.2. If commercially viable markets could be found for these compounds, they could be extracted from the effluent stream before it is pumped out to sea, thus reducing the impact of the effluent on the environment. A possible means of extracting these fatty acids would be in the same manner described above, that is, by adjusting the pH and reducing the temperature.

However, a future study would need to be undertaken to determine accurately the quantities of these substances available from this source.

3.2. ANALYSIS OF THE MAGNESIUM CONDENSATE EFFLUENT

The following compounds were identified in the organic extract of the magnesium condensate – two isomers of syringaresinol; 3-(4'-hydroxy-3',5'-dimethoxyphenyl)-prop-1-ene; 2,6-dimethoxy-1,4-benzoquinone and vanillin. Only vanillin will be discussed here as the other compounds have been previously isolated from the calcium – spent liquor effluent stream and their detailed structural elucidations can be read in section 3.1. The carbohydrate content in the form of hexose and pentose was also determined using UV/visible spectroscopy.

3.2.1 Structural elucidation of compound 7, vanillin

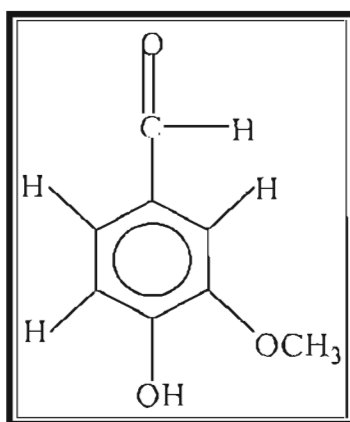


FIGURE 31: Structure of compound 7, vanillin

The infrared spectrum (Spectrum 68) shows a broad band between 3600 cm^{-1} and 3200 cm^{-1} , which indicates the presence of a hydroxyl group and the weak bands at 2860 cm^{-1} and 2734 cm^{-1} correspond to C-H stretching of the aldehyde group. The sharp peak at 1671 cm^{-1} is characteristic of carbonyl stretching and the peaks at 1591 cm^{-1} and 1517 cm^{-1} can be ascribed to aromatic ring vibrations. The peak between 1250 cm^{-1} and 1050 cm^{-1} indicates C-O stretching of the methoxy group.

The ^1H NMR spectrum (Spectrum 69) shows a distinct strong peak at $\delta\ 3.93\text{ ppm}$ (3H), which is characteristic of a methoxy group proton resonance. A peak at $\delta\ 9.82\text{ ppm}$ (1H)

is characteristic of an aldehyde proton resonance. Peaks at δ 6.97 ppm and δ 7.56 ppm correspond to aromatic proton resonances and are due to one proton and two protons respectively. The broad peak at δ 6.21 ppm can be ascribed to a phenolic proton. The integration suggests only one methoxy substituent present.

A literature search identified this compound as vanillin, a characteristic compound found in pulping liquors¹⁴. The infrared library identified compound 7 as vanillin and ^1H NMR spectra matched those found in literature. No further spectra were run on this compound, as it is a simple, well-known compound. It also gave off the characteristic smell of vanillin. The concentration of vanillin in the magnesium condensate effluent was found to be approximately 0.0016 g/L.

3.2.2 Further compounds identified

Four additional compounds were isolated and identified from the magnesium condensate effluent stream. These were also isolated from the calcium - spent liquor stream and were identified as the two lignans, syringaresinol and episyringaresinol; 3-(4'-hydroxy-3',5'-dimethoxyphenyl)-prop-1-ene (~0.012 g/l); and 2,6-dimethoxy-1,4-benzoquinone (~0.0033 g/l). The two syringaresinol compounds were isolated as a mixture and were found to be the major organic components present in this stream of effluent having an approximate concentration of 0.017 g/L.

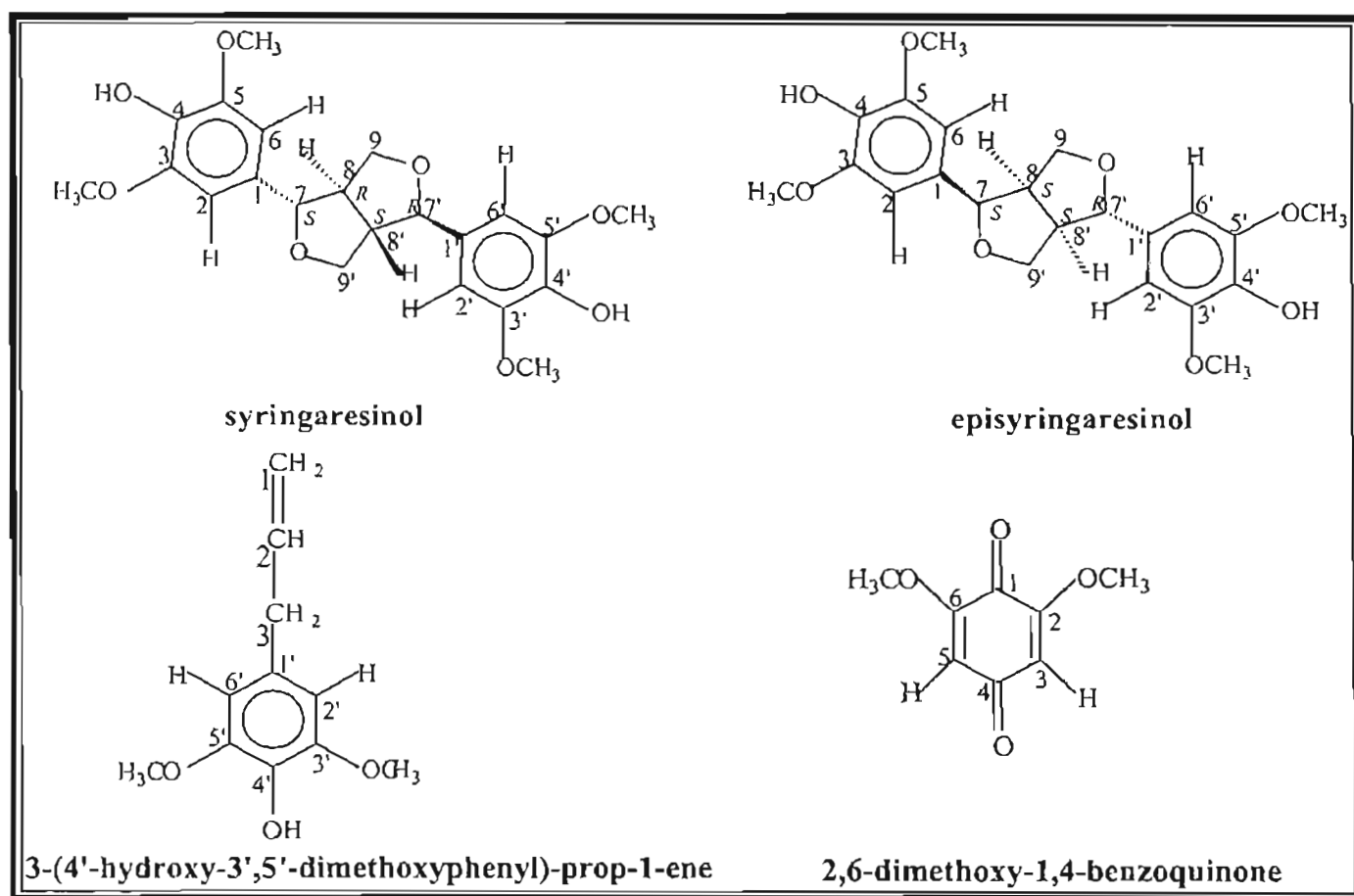


FIGURE 32: Structures of other compounds isolated from the magnesium condensate effluent stream

The structural elucidation of these four compounds will not be discussed in this section but can be referred to in sections 3.1.1, 3.1.2, 3.1.3 and 3.1.6.

3.2.3 Carbohydrate content of the magnesium condensate

The magnesium condensate was analysed for hexoses based on the glucose content (Spectrum 70) and pentoses based on the xylose content (Spectrum 71) using the UV spectrophotometer¹³. The sample was prepared in the same manner as previously described in section 3.1.9.

3.2.4.1 Analysis of hexoses¹³

Using the average absorptivity calculated previously, the concentration of glucose in the magnesium condensate sample was calculated as follows.

$$\begin{aligned}c &= A/a \\&= 0.721 / (4.633 \times 1) \\&= 0.156 \text{ mg/ml}\end{aligned}$$

Taking into account the dilution factor, the concentration of glucose in the magnesium condensate effluent stream is 3.11 g/L.

3.2.4.2 Analysis of pentoses¹³

Using the average absorptivity calculated previously, the concentration of xylose was determined as follows:

$$\begin{aligned}c &= A/(a \times l) \\&= 0.683 / (2.49 \times 1) \\&= 0.275 \text{ mg/ml}\end{aligned}$$

Taking into account the dilution factor, the concentration of xylose in the magnesium condensate effluent is 2.75 g/L. No analysis for comparison was available from SAICCOR.

3.3 ANALYSIS OF THE O₂ – STAGE BLEACHING EFFLUENT

A sample of the O₂ - stage bleaching effluent was subjected to chloroform extraction to remove the organic components. The sample of effluent had a neutral pH and therefore the organic extract did not need to be neutralised as was the case with the previous effluent samples. The organic extract was then passed through a gravity column with varying solvent mixtures. The following compounds were isolated and identified in the organic extract of the O₂ - stage bleaching effluent – sitosterol; syringaldehyde and palmitic acid. The carbohydrate content of the effluent was determined in the same manner as previously discussed.

3.3.1 Structural elucidation of compound 8, β -sitosterol

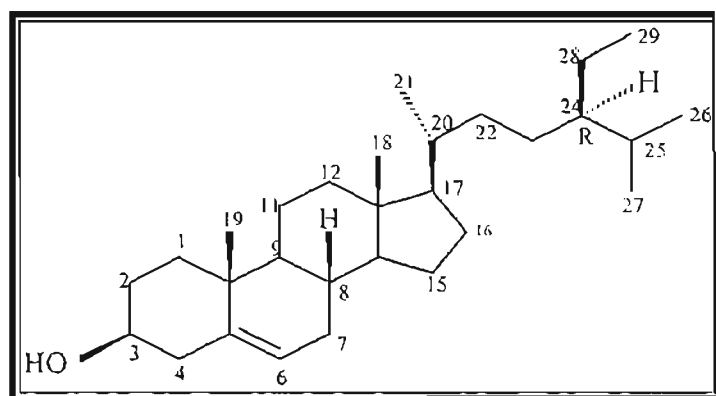


FIGURE 33: Structure of compound 8, β -sitosterol

Compound 8 was isolated as a white crystalline substance. It is a common triterpenoid, and occurs widely in many plants and has previously been isolated and identified in bleaching effluent^{11b}.

The strong bands that stand out in the infrared spectrum (Spectrum 72) are found at 2932 cm⁻¹ and 2863 cm⁻¹ and are indicative of C-H stretching. There is also a broad band at 3379 cm⁻¹, which indicates the presence of a hydroxyl substituent.

The ^1H NMR spectrum (Spectrum 73) shows a peak at in the double bond region at δ 5.32 ppm, which corresponds to the methine proton at C-6. The peak at δ 3.50 ppm can be ascribed to the methine proton at C-3 and has shifted downfield because of the electronegative hydroxyl group.

The carbon resonances at δ 140.9 ppm and δ 121.9 ppm, in the ^{13}C NMR spectrum (Spectrum 74), are found in the double bond region and can be ascribed to the fully substituted carbon at C-5 and the methine carbon at C-6 respectively. The peak at δ 72.0 ppm is indicative of a methine proton that has shifted downfield due to the electronegative effect of the attached hydroxyl substituent. This peak can therefore be ascribed to the proton at C-3.

On comparison of the spectra for compound 8 with library spectra, it was identified as β -sitosterol¹⁵. The concentration of this compound in the O_2 - stage bleaching effluent was found to be approximately 0.0075 g/L.

3.3.2 Structural elucidation of compound 9, hexadecanoic acid (commonly known as palmitic acid)



FIGURE 34: Structure of compound 9, hexadecanoic acid

Compound 9 has a simple, long-chain aliphatic structure and is also commonly found in plants and in the bleaching effluent of paper and pulp mills.

The mass spectrum of compound 9 (Spectrum 75) shows a molecular ion peak at m/z 256, suggesting a molecular formula of $C_{16}H_{32}O_2$. The peak at m/z 213 results from the loss of 43 mass units and corresponds to the loss of a propyl fragment ($-CH_2-CH_2-CH_3$) resulting from fragmentation between C-13 and C-14. The next three peaks show losses of 28 mass units each and correspond to fragmentation of ethyl groups. The peak at m/z 73 is ascribed to the remaining fragment of propanoic acid. The GC/MS library identified compound 9 as palmitic acid.

The characteristic bands in the infrared spectrum (Spectrum 76) further confirm the structure of compound 9. The strong bands at 2923 cm^{-1} and 2847 cm^{-1} are typical of an acid group. The infrared spectrum also shows a strong sharp band at 1712 cm^{-1} that is characteristic of carbonyl stretching of the $-COOH$ functional group. The infrared spectrum compares favourably with that in the literature and confirms the absence of the band at approximately $3600\text{ cm}^{-1} - 3000\text{ cm}^{-1}$ due to O-H stretching¹⁶.

The ^1H NMR spectrum (Spectrum 77) only shows peaks in the upfield region of the spectrum indicative of an aliphatic compound. The peak at δ 2.32 ppm corresponds to the methylene protons at C-2 that have shifted slightly downfield due to the attached acid substituent. The peak at δ 1.61 ppm can be ascribed to the methylene protons at C-15 and

the strong sharp peak at δ 1.23 ppm is ascribed to the protons of the twelve equivalent methylene groups in the centre of the structure. The last peak, a triplet at δ 0.86 ppm, corresponds to the end methyl group protons.

The ^{13}C NMR spectrum (Spectrum 78) shows a carbon resonance at δ 179.3 ppm, which is indicative of an acid carbon substituent. The other carbon resonances are found in the upfield region of the spectrum, typical of an aliphatic compound. The end methyl carbon is seen at δ 14.1 ppm and the other peaks are due to the methylene carbons.

The NMR spectra confirmed the structure of compound 9, which has been identified as hexadecanoic acid or more commonly known as palmitic acid with an approximate concentration of 0.0088 g/L.

3.3.3 Other compounds identified in the O₂ - stage bleaching effluent

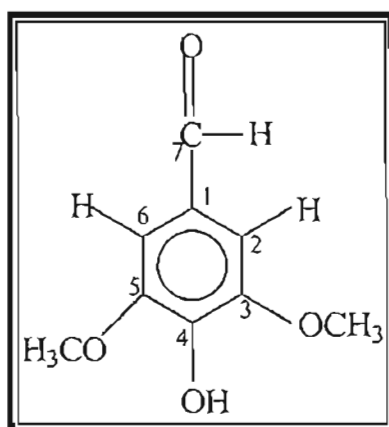


FIGURE 35: Structure of syringaldehyde

Syringaldehyde is another compound isolated from the bleaching effluent. This compound is commonly found in wood products and has been previously isolated from the calcium - spent liquor stream of effluent. The concentration of syringaldehyde in this effluent stream is approximately 0.0030 g/L and a detailed structural elucidation can be read in section 3.1.5.

3.3.4 Carbohydrate content of the O₂ - stage bleaching effluent

The absorptivities, previously obtained for the standards, were used to calculate the concentration of hexose based on glucose (Spectrum 79) and pentose based on xylose (Spectrum 80) in the O₂ - stage bleaching effluent¹³.

3.3.4.1 Analysis of hexose¹³:

$$A = alc$$

$$c = A / (a \times l)$$

$$= 0.678 / (4.633 \times 1)$$

$$= 0.146 \text{ mg/ml}$$

3.3.4.2 Analysis of pentose¹³:

$$A = alc$$

$$c = A / (a \times l)$$

$$= 0.426 / (2.49 \times 1)$$

$$= 0.171 \text{ mg/ml}$$

Thus the O₂ - stage bleaching effluent contains 0.146 g/L hexose in the form of glucose and 0.171 g/L of pentose in the form of xylose.

3.4 ANALYSIS OF THE E₂ - STAGE BLEACHING EFFLUENT

I also helped supervise a honours student's project based on the E₂ - stage bleaching effluent stream. As was expected sitosterol and syringaldehyde (Figure 36), which had been isolated from the O₂ - stage bleaching effluent, were isolated as well. Another compound linoleic (9,12-octadecadienoic acid) acid was also isolated from this stream of effluent, which had not been isolated from the O₂ - stage bleaching effluent.

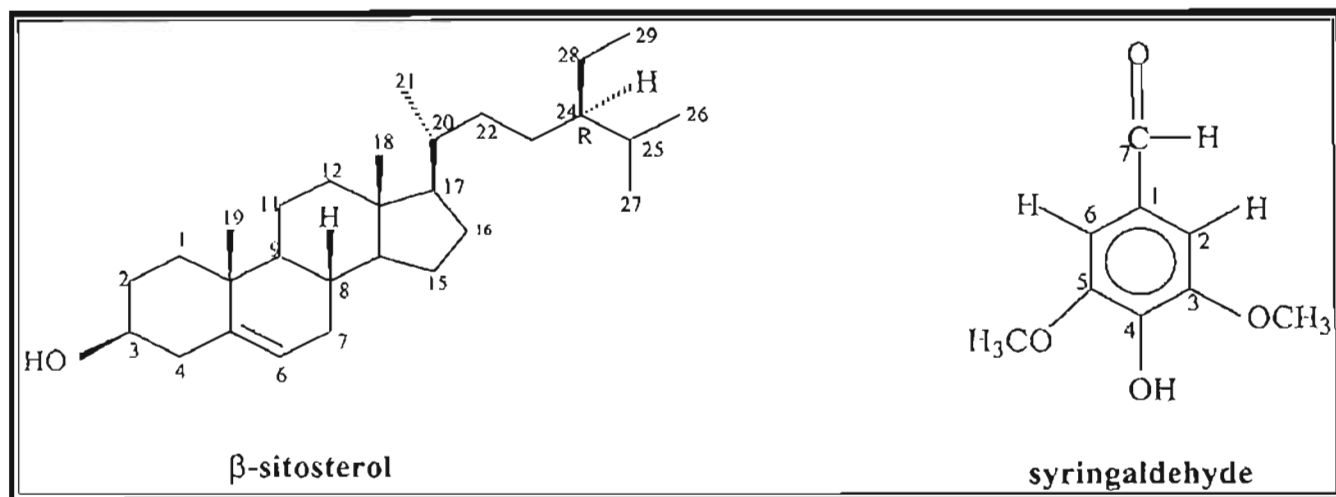


FIGURE 36: Structures of other compounds identified in the E₂ - stage bleaching effluent

The effluent sample was treated in the same manner as the O₂ - stage bleaching effluent sample to remove the organic constituents, which also did not require neutralisation. The compounds isolated were sitosterol (0.0043 g/L), syringaldehyde (<0.0010 g/L) and linoleic acid (<0.0010 g/L). The carbohydrate content of the effluent was determined using UV/visible spectrometry.

3.4.1 Structural elucidation of compound 10, 9,12-octadecadienoic acid (more commonly known as linoleic acid)

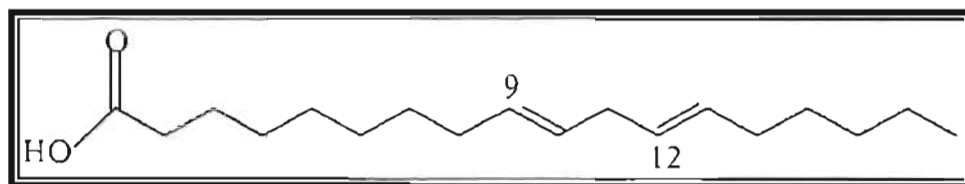


FIGURE 37: Structure of compound 10, 9,12-octadecadienoic acid

Compound 10 is another simple aliphatic compound that is commonly found in the Plant Kingdom. It has a structure very similar to that of palmitic acid but is unsaturated with double bonds at positions 9 and 12 and two additional methylene groups.

The mass spectrum (Spectrum 81) shows a molecular ion peak at m/z 280, corresponding to a molecular formula of $C_{18}H_{32}O_2$. The loss of 18 mass units to give the peak at m/z 262 corresponds to the loss of water. Compound 10 was immediately identified as linoleic acid from the MS library.

The 1H NMR spectrum (Spectrum 82) is similar to that of palmitic acid showing the characteristic peaks of the methylene protons in the upfield region indicative of an aliphatic structure. The major difference is the peak at δ 5.39 ppm, integrating to four hydrogens, in the double bond region, which corresponds to the protons of the methine carbons of the double bonds.

3.4.2 Carbohydrate content of E₂ - stage bleaching effluent

The sample was treated as previously described and the hexose (Spectrum 83) and pentose (Spectrum 84) concentration was determined using UV/visible spectrometry¹³.

3.3.4.1 Analysis of hexose¹³:

$$\begin{aligned} A &= alc \\ c &= A / (a \times l) \\ &= 0.775 / (4.633 \times 1) \\ &= 0.167 \text{ mg/ml} \end{aligned}$$

3.3.4.2 Analysis of pentose¹³:

$$\begin{aligned} A &= alc \\ c &= A / (a \times l) \\ &= 0.497 / (2.49 \times 1) \\ &= 0.200 \text{ mg/ml} \end{aligned}$$

Thus the E₂ - stage bleaching effluent contains 0.167 g/L hexose in the form of glucose and 0.200 g/L of pentose in the form of xylose.

3.5 REFERENCES

1. Sarkanen, K. V. and Ludwig, C. H., 1971, *Lignins: Occurrence, Formation, Structure and Reactions*, John Wiley and Sons : New York, p267-293
2. Pelter, A., 1967, *Journal of Chemical Society (C)*, 376-1380
3. Dictionary of Natural Products (DNP) on CD-ROM, version 9:1, 1982-2000, Chapman and Hall Electronic Publishing Division : London
4. Pelter, A. and Ward, R. S., 1976, *Tetrahedron*, (32), 2783-2788
5. Ludwig, C. H., Nist, B. J. and McCarthy, J. L., 1964, *Journal of American Chemical Society*, (86), 1186-1196
6. Pelter, A. and Ward, R. S., 1977, *Tetrahedron Letters*, (47), 4137-4140
7. Briggs, L. H., Cambie, R. C., and Couch, R. A. F., 1968, *Journal of Chemical Society (C)*, 3042-3045
8. Konturri, A. K. and Sundholm, G., 1986, *Acta Chemica Scandinavica*, (A 40), 121-125
9. Lin, S. Y. and Dence, C. W., 1992, *Methods in Lignin Chemistry*, Springer-Verlag : Berlin, p75-80
10. Fengel, D. and Wegener, G., 1983, *Wood : chemistry, ultrastructure and reactions*, Walter de Gruyter & Co. : Berlin, p157-164(a), 200-205(b)
11. Gullichsen, J. and Paulapuro, H., 2000, *Forest Products Chemistry*, Fapet Oy : Helsinki, p81-86(a), 35-39(b), 100-102(c)

12. Sjostrom, E. and Alen, R., 1999, *Analytical Methods in Wood Chemistry, Pulping and Papermaking*, Springer : Berlin, p46-48(a), 240-252(b)
13. Chaplin, M. F. and Kennedy, J. F., 1986, *Carbohydrate Analysis – a practical approach*, IRL Press Limited : England, p2-4
14. Personal Communication – John Thuhron (Technical Process Manager at Sappi Saiccor)
15. *Aldrich Library of ^{13}C and ^1H FT NMR Spectra*, 1993, (2) 959A, (3), 569A
16. *Aldrich Library of FT-IR Spectra 1st edition*, 1986, (1), 1448B

CHAPTER 4: EXPERIMENTAL

4.1 FOREWORD TO EXPERIMENTAL

Nuclear Magnetic Resonance Spectroscopy (NMR Spectroscopy)

Nuclear magnetic resonance spectroscopy was carried out on a 300 MHz Varian Gemini spectrophotometer and a 400 MHz Varian UNITY-INOVA spectrophotometer. The spectra for all compounds were recorded at room temperature in deuterated chloroform (CDCl_3) or deuterated water (D_2O). The chemical shifts were all recorded in ppm relative to TMS. The spectra were referenced against the central line of the CDCl_3 signal at $\delta_{\text{C}} = 77.2$ ppm and $\delta_{\text{H}} = 7.24$ ppm and for the D_2O signal at $\delta_{\text{H}} = 4.61$ ppm.

Infrared Spectroscopy (I.R. Spectroscopy)

The infrared spectra were recorded using a Nicolet Impact 400D Fourier-Transform Infrared (FT-IR) spectrometer, which was calibrated against an air background. The compounds were analysed using a NaCl window with dichloromethane as the solvent and the lignosulphonate mixture was analysed using a KBr disc.

Gas Chromatography/Mass Spectroscopy (GC/MS)

All samples were introduced using a 1 μL auto injection system onto a HP5-MS column in the GC/MS with 1 : 75 split. The starting temperature was 50°C , the sample was held for two minutes, the temperature was ramped at 20°C per minute until it reached 300°C and thereafter the sample was held for another two minutes. Low - resolution mass spectrometry was carried out on an Agilent 5973 mass spectrometer connected to a 6890 GC.

X-Ray Diffraction (XRD)

The aqueous extract was filtered and a residue of mass 0.72 g was obtained. No special sample preparation was required for the XRD analysis, which was simply packed onto a sample holder and introduced into the instrument.

X-Ray Fluorescence (XRF)

Approximately 0.2 g of spectroflux 105, $(\text{Li}(\text{BO}_4)_4$, was heated in a 5 % gold in platinum crucible in a muffle furnace at 1000°C for half an hour. Approximately 0.53 g of sample was added to this spectroflux melt and further heated at 1000°C for one hour. The sample ignited on entering the furnace and the organics were burnt off. The fused material was then cooled and reweighed. The melt was reheated until it was a liquid and cooled into a pellet. The pellet was placed in a sample holder and introduced into the instrument for analysis.

General Chromatography

All compounds from the organic extract were isolated using gravity column chromatography and thin layer chromatographic techniques. 1 cm and 2 cm in diameter gravity columns were used depending on the amount of sample available and final purifications were generally carried out on open 0.75 cm pasteur-pipette columns. All columns were packed with Merck Art. 9385 silica gel. The mobile phase for both column and thin layer chromatography were varying ratios of dichloromethane, hexane, ethyl acetate and methanol. Thin layer chromatography was carried out on 0.2 mm silica-gel, aluminium-backed plates (Merck Art. 5554). The plates were visualised with a mixture of anisaldehyde : conc. H_2SO_4 : methanol (1:2:97) spray reagent. They were first analysed under UV (336 nm) and then by heating.

Preparative Thin Layer Chromatography (PTLC)

Some compounds were purified using preparative thin layer chromatography. The extract was loaded as a line, 15 mm from the bottom, onto the plate by dipping a capillary tube in the extract dissolved in minimum solvent (dichloromethane) and allowing it to run onto the silica - gel by touching it to the plate. The plates were developed in a chromatography tank and the compound of interest was marked under UV. The marked bands were cut off the plate, dissolved in methanol and thereafter the solvent evaporated.

Acetylation

Compound 4 (7 mg) was dissolved in pyridine (1 ml) and acetic anhydride (2 ml) and left to react over 48 hours in a round-bottom flask connected to a drying tube (CaCl_2). The acetic anhydride and pyridine were removed with methanol and toluene, *in vacuo*. The acetylated mixture was spotted on a t.l.c. plate to see if the reaction had gone to completion and to see if it needed to be purified. The acetylated product was passed through a column to separate the product from the impurities. The pure acetylated compound eluted with 100 % dichloromethane.

Optical Rotation

Optical rotations were measured at room temperature in chloroform using a Perkin Elmer 241 Polarimeter with tube 10 cm in length or Optical Activity AA-5 Polarimeter together with a series A2 stainless steel (4 x 200 mm) unjacketed flow tube, 20 cm in length.

4.2 ANALYSIS OF THE CALCIUM-SPENT LIQUOR - GENERAL SAMPLING AND ORGANIC EXTRACTION PROCEDURES

The calcium – spent liquor was collected from a sampling spigot after the washing and screening stage as the waste spent liquor goes to the effluent drain but before it is pumped to Lignotech. During pumping the sample is generally under pressure to maintain a continuous flow through the pipeline, which results in a high velocity and ensures the homogeneity of the sample. The sample container was first rinsed with the sample to be taken and thereafter the container was filled. The temperature of the sample was between 85 and 100⁰ C and had a pH of 1.8.

A litre of the cooled calcium – spent liquor sample was extracted with 3 x 1 L portions of chloroform using a 6 L separating flask. The organic extract was neutralised with a saturated solution of NaHCO₃ using universal indicator paper. The neutralised organic portions were evaporated using a BUCHI Rotavapor.

4.2.1 PHYSICAL DATA

Mass of organic extract = 2.609 g

4.2.1.1 Physical data for compound 1, *meso*-syringaresinol

Name: *meso*-syringaresinol

Yield: 10 mg

Physical Description: pale yellow to brown amorphous substance

$[\alpha]_D^{25} = 0$

Eluted with 20 % ethyl acetate in dichloromethane.

Mass spectrum : LRMS : $[M^+]$ at m/z 418, C₂₂H₂₆O₈ requires 418.40 g/mol

EIMS : m/z : 418, 235, 210, 181, 167, 161, 154, 140, 123, 105, 77

I.R Data : ν_{\max} [NaCl](cm^{-1}) : 3420 (O-H stretching), 2932, 2851 (aliphatic C-H stretching), 1624, 1518 (C=C stretching of the aromatic ring), 1332 (syringyl breathing), 1116 (C-O stretching)

^1H and ^{13}C NMR data are presented in Table I in chapter 3

4.2.1.2 Physical data for compound 2, episyringaresinol

Name : episyringaresinol

Yield : 10 mg

Physical description : yellow to brown amorphous substance

$[\alpha]_{\text{D}}^{25} = +107^{\circ}$: lit. $+127^{\circ}$

Mixture of syringaresinol isomers eluted with 10 % ethyl acetate in dichloromethane

Mass spectrum : LRMS : $[\text{M}^+]$ at m/z 418, $\text{C}_{22}\text{H}_{26}\text{O}_8$ requires 418.40 g/mol

EIMS : m/z : 418, 251, 210, 181, 167, 161, 154, 123, 93

I.R Data : ν_{\max} [NaCl](cm^{-1}) : 3420 (O-H stretching), 2947, 2846 (aliphatic C-H stretching), 1619, 1528 (C=C stretching of the aromatic ring), 1332 (syringyl breathing), 1221, 1116 (C-O stretching)

The ^1H and ^{13}C data are presented in Table 2 in chapter 3

4.2.1.3 Physical data for compound 3, 3-(4'-hydroxy-3',5'-dimethoxyphenyl)-prop-1-ene

Name : 3-(4'-hydroxy-3',5'-dimethoxyphenyl)-prop-1-ene

Yield : 4 mg

Physical Description : yellow to brown amorphous substance

Eluted with 60 % dichloromethane in hexane

Mass spectrum : LRMS : $[M^+]$ at m/z 194, $C_{11}H_{14}O_3$ requires 194.22 g/mol
EIMS : m/z : 194, 179, 167, 147, 131, 119, 91, 77, 65, 53, 39

I.R Data : $\nu_{\max}[\text{NaCl}](\text{cm}^{-1})$: 3427 (O-H stretching), 2923, 2859 (C-H aliphatic stretching), 1674 (unsaturated C=C stretching), 1596 (C=C stretching of the aromatic ring), 1336 (syringyl breathing), 1219, 1126 (C-O stretching)

The ^1H and ^{13}C NMR data are presented in Table 3 in chapter 3

4.2.1.4 Physical data for compound 4, 3-(4'-hydroxy-3',5'-dimethoxyphenyl)-1-hydroxy-propan-2-one

Name : 3-(4'-hydroxy-3',5'-dimethoxyphenyl)-1-hydroxy-propan-2-one

Yield : 3 mg

Physical Description : yellow amorphous substance

Eluted with 30 % ethyl acetate in dichloromethane

Mass spectrum : LRMS : $[M^+]$ at m/z 226, $C_{11}H_{14}O_5$ requires 226.20 g/mol
EIMS : m/z : 226, 167, 151, 123, 106, 78, 66, 53, 39

I.R Data : $\nu_{\max}[\text{NaCl}](\text{cm}^{-1})$: 3434 (O-H stretching), 2921, 2849 (aliphatic C-H stretching), 1721 (C=O stretching), 1613, 1525 (C=C stretching of an aromatic ring), 1335 (syringyl breathing), 1223, 1115 (C-O stretching)

The ^1H and ^{13}C NMR data are presented in Table 4 in chapter 4

4.2.1.5 Physical data for compound 5, syringaldehyde

Name : 4-hydroxy-3,5-dimethoxybenzaldehyde (commonly known as syringaldehyde)

Yield : 5 mg

Physical Description : yellow crystalline solid

Melting point : 108-110⁰ C : lit. 113-114⁰ C²

Eluted with 100 % dichloromethane

Mass spectrum : LRMS : [M⁺] at *m/z* 182, C₉H₁₀O₄ requires 182.15 g/mol

EIMS : *m/z* : 182, 181, 167, 153, 139, 123, 111, 96, 79, 65, 51, 39

I.R Data : ν_{\max} [NaCl](cm⁻¹) : 3286 (O-H stretching), 2939, 2837 (C-H stretching of the aldehyde group), 1671 (C=O stretching), 1608, 1513 (C=C stretching of the aromatic ring), 1214, 1113 (C-O stretching)

The ¹H and ¹³C NMR data are presented in Table 5 in chapter 3

4.2.1.6 Physical data for compound 6, 2,6-dimethoxy-1,4-benzoquinone

Name : 2,6-dimethoxy-1,4-benzoquinone

Yield : 2 mg

The mixture of this compound with syringaldehyde eluted with 75 % dichloromethane in hexane

Mass spectrum : LRMS : [M⁺] at *m/z* 168, C₈H₈O₄ requires 168.12 g/mol

EIMS : *m/z* : 168, 138, 125, 112, 97, 81, 69, 53, 41

The ¹H and ¹³C data are presented in Table 6 in chapter 3

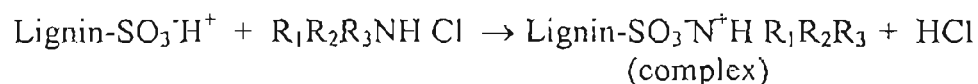
4.2.2 EXTRACTION OF LIGNOSULPHONATES FROM THE CALCIUM - SPENT LIQUOR EFFLUENT STREAM

A sample of calcium - spent liquor was extracted with chloroform to remove the organic components. A conductometric titration was carried out on the aqueous portion to determine the concentration of sulphonic acid groups³. This was carried out using a Microprocessor Conductivity meter LF 320 at room temperature with a TetraCon 325 conductivity electrode having a cell constant of 1.000 cm⁻¹. The instrument was calibrated with the standard provided which had a conductivity of 3.15 mS/cm at a cell constant of 1.000 cm⁻¹. The conductivity of deionised water was determined as 0.00 mS/cm at a cell constant of 1.000 cm⁻¹.

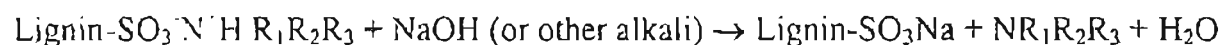
The conductivity titration was carried out on a sample (mass = 50.04 g) with a 0.1 mol/dm³ solution of NaOH³. The results were plotted on a graph shown in Graph 1 in Appendix B, Page 224, and the sulphonic acid content was determined to be 3.997 x 10⁻⁵ mol/g. The relevant calculations are shown in Appendix B, Page 225. This value was used to determine the equivalent number of moles of dodecylamine to be used.

Extraction procedure^{4,5}:

An ion exchanger was prepared by mixing 1 M HCl with a solution of dodecyl amine made up in butanol. The top layer of the ion exchanger (mass = 100.24g) was mixed with the spent liquor (actual mass = 78.21 g) for 30 minutes with continuous stirring at a temperature of 50 - 58⁰ C. The sample was allowed to separate in a separating flask for 2 hours at this temperature and thereafter the organic layer was removed.



The organic layer was adjusted to pH 9 using a 1M solution of NaOH and universal indicator paper and allowed to separate over 24 hours whilst the temperature was maintained at 50 - 60⁰ C.



Where R₁, R₂, R₃ are hydrogen or alkyl groups

The aqueous layer (bottom layer) was washed twice with butanol to remove as much of the amine as possible. The aqueous layer was evaporated on a BUCHI Rotavapor, which gave a creamy coloured precipitate (mass = 3.286 g).

Sodium fusion test to test for the presence of sulphur⁶:

A small portion of the precipitate (~40 mg) was introduced into a short hard-glass test-tube and a small piece of metallic sodium was added to it. The contents of the test-tube were carefully heated over a bunsen flame until the product was fully roasted. The hot glass tube was then immediately plunged into another larger test-tube containing about 10 ml of deionised water, maintaining it at a 45⁰ angle position at all times. The vigorous reaction causes the inner glass tube to fracture and the excess sodium to react with the water. The contents of the larger test-tube were filtered and the filtrate tested for the presence of sulphur. This was done by dissolving a few crystals of sodium nitroprusside, Na₂[Fe(CN)₅NO].2H₂O, in water and adding it to the filtrate. The filtrate turned a purple colour indicative of the presence of sulphur. A control sample of aniline sulphate was used as a check for the correct purple colour.

I.R Data : ν_{max} [NaCl](cm⁻¹) : 3394 (O-H stretching), 1603, 1402 (C=C stretching of the aromatic ring), 1208 (sulphonic acid groups), 1111, 1043 (presence of sugar or polysaccharide moieties)

UV : λ_{max} (nm) [water]: 210, 280

All other analyses were carried out as described in the foreword to the experimental.

4.2.3 ANALYSIS OF CARBOHYDRATES

The ultra-violet adsorption spectra were obtained on a Varian Cary 1E double beam UV-visible spectrophotometer, serial number 95071136. All spectra were run in water using matched glass cuvettes. The instrument was zeroed using the blanks prepared.

4.2.3.1 Analysis of hexose⁷

Three glucose standards having concentrations of 0.10 mg/ml 0.25 mg/ml and 0.35 mg/ml were prepared in deionised water. A 1 ml sample from each of the aqueous portions of the effluent streams (calcium and magnesium stream samples were diluted 400 x and 20 x respectively and the bleaching streams were not diluted) were transferred to individual flasks. Each sample was mixed with 1 ml of phenol solution (5 % w/v). Concentrated sulphuric acid (5 ml) was rapidly added directly to each of the samples without touching the sides of the glass. The samples were left undisturbed for 10 minutes and thereafter vigorously shaken. The absorbances of the samples were determined at 490 nm after 30 minutes. The standards were subjected to the same preparation procedures and a blank was prepared using the same preparation procedure with 1 ml of deionised water in place of the volume of the sample.

4.2.3.2 Analysis of pentose⁷

A range of xylose standards from 0.05 mg/ml to 0.35 mg/ml were prepared in deionised water. A 1 ml volume of samples from the aqueous portions of the different effluent streams (calcium and magnesium stream samples were diluted 200 x and 10 x respectively and the bleaching streams were not diluted) were transferred to individual flasks. The samples were mixed with 1 ml of trichloroacetic acid solution in water (10 % w/v) and heated at 100⁰ C for fifteen minutes. The samples were rapidly cooled in a water-bath and 6 ml of a solution of ferric ammonium sulphate (1.15 % w/v) and orcinol

(0.2 % w/v) made up in 9.6 M of HCl, were added to each sample. The samples were thoroughly shaken and reheated at 100⁰ C for 20 minutes. The absorbances of the samples were determined at 660 nm once they had cooled to room temperature. The standards and a blank were prepared in the same manner described above with the blank containing 1 ml of deionised water in place of the sample.

4.2.4 ANALYSIS OF THE WAX BALLS

A small quantity of the wax balls (~50 mg) was dissolved in dichloromethane and filtered under gravity to remove any dust particles and insoluble materials. The solution was then auto injected onto a HP5-MS column in the GC/MS. The sample was introduced using a 1 uL auto injection system with 1 : 75 split. The starting temperature was 50⁰ C held for two minutes, then the temperature was increased at 20⁰ C per minute to 300⁰ C held for two minutes. Low - resolution mass spectrometry was carried out on an Agilent 5973 mass spectrometer connected to a 6890 GC.

Palmitic acid : major component (65 %)

Mass spectrum : LRMS : [M⁺] at *m/z* 256, C₁₆H₃₂O₂ requires 256.46 g/mol
EIMS : *m/z* : 256, 213, 185, 157, 129, 97, 73, 60, 43

Pentadecanoic acid : (5.62 %)

Mass spectrum : LRMS : [M⁺] at *m/z* 242, C₁₅H₃₀O₂ requires 242.43 g/mol
EIMS : *m/z* : 242, 199, 185, 171, 157, 143, 129, 115, 97, 73, 60, 43

2-hydroxy-cyclopentadecanone : (4.09 %)

Mass spectrum : LRMS : [M⁺] at *m/z* 240, C₁₅H₂₈O₂ requires 240.41 g/mol
EIMS : *m/z* : 240, 222, 180, 151, 138, 123, 110, 97, 83, 69, 55, 41

Palmitic acid methyl ester : (3.24 %)

Mass spectrum : LRMS : [M⁺] at *m/z* 270, C₁₇H₃₄O₂ requires 270.49 g/mol
EIMS : *m/z* : 270, 239, 227, 199, 185, 171, 143, 129, 87, 74, 43

Myristic acid : (2.63 %)

Mass spectrum : LRMS : $[M^+]$ at m/z 228, $C_{14}H_{28}O_2$ requires 228.40 g/mol

EIMS : m/z : 228, 185, 171, 157, 143, 129, 115, 97, 83, 73, 60, 43

1,2,3,4-tetrahydro-1,6-dimethyl-4-(1-methylethyl)-naphthalene : (1.89 %)

Mass spectrum : LRMS : $[M^+]$ at m/z 202, $C_{15}H_{22}$ requires 202.37 g/mol

EIMS : m/z : 202, 159, 144, 129, 10577, 41

Dodecanoic acid : (trace amounts)

Mass spectrum : LRMS : $[M^+]$ at m/z 200, $C_{12}H_{24}O_2$ requires 200.34 g/mol

EIMS : m/z : 200, 183, 157, 143, 129, 115, 101, 73, 60, 43

n-hexadecanoic acid : (trace amounts)

Mass spectrum : LRMS : $[M^+]$ at m/z 256, $C_{16}H_{32}O_2$ requires 256.46 g/mol

EIMS : m/z : 256, 227, 213, 185, 171, 157, 129, 95, 81, 73, 55, 40

7,10-octadecadienoic acid, methyl ester (trace amounts)

Mass spectrum : LRMS : $[M^+]$ at m/z 294, $C_{19}H_{34}O_2$ requires 294.51 g/mol

EIMS : m/z : 294, 263, 220, 178, 164, 150, 136, 123, 109, 95, 81, 67, 55, 41

1,6-dimethyl-4-(1-methylethyl)-naphthalene : (1.03 %)

Mass spectrum : LRMS : $[M^+]$ at m/z 198, $C_{15}H_{18}$ requires 198.33 g/mol

EIMS : m/z : 198, 183, 188, 153, 141, 128, 115, 83, 63,

4.3 ANALYSIS OF THE MAGNESIUM CONDENSATE - GENERAL SAMPLING AND ORGANIC EXTRACTION PROCEDURES

The magnesium effluent is burned to recover the MgO but during the burning process, some of the gases condense to form a colourless magnesium condensate, which goes to the effluent drain. Some of this condensate is used as wash water during the washing and screening stage giving it a reddish – brown colour. A sample of the magnesium condensate, which had been used during washing, was collected in the same manner as described for sampling of the calcium – spent liquor. The temperature of the sample was between 85^o C and 100^o C and had an acid pH.

A three litre sample of the cooled magnesium condensate sample was extracted with 7.5 L of chloroform, in portions, using a 6 L separating flask. The organic extract was neutralised with a saturated solution of NaHCO₃ using universal indicator paper. The neutralised organic portions were evaporated using a BUCHI Rotavapor.

4.3.1 PHYSICAL DATA

Mass of organic extract = 0.530 g

4.3.1.1 Physical data for compound 7, vanillin

Name : 4-hydroxy-3-methoxybenzaldehyde (commonly known as vanillin)

Yield : 4 mg

Physical data : white amorphous substance with a characteristic vanillin smell

Separation was achieved using a preparative plate as discussed in the foreword to the experimental. The preparative plate was developed in 5 % methanol in dichloromethane.

I.R Data : $\nu_{\text{max}}[\text{NaCl}](\text{cm}^{-1})$: 3215 (O-H stretching), 2860, 2734 (C-H stretching of the aldehyde group), 1671 (C=O stretching), 1591, 1517 (C=C stretching of the aromatic ring), 1156 (C-O stretching)

^1H NMR data : δ_{H} (ppm) (CDCl_3 , 300 MHz)

9.82 (1H, s, CHO), 7.56 (2H, m, H-2, H-6), 6.97 (1H, d, H-5), 6.21 (1H, s, OH), 3.93 (3H, s, OCH_3)

4.3.1.2 Physical data for compound 1, *meso* – syringaresinol

Name: *meso* – syringaresinol

Yield : lignan mixture = 18 mg

Physical Description: pale yellow to brown amorphous substance

$[\alpha]_{\text{D}}^{25} = 0$

Eluted as a mixture of isomers with 10% ethyl acetate in dichloromethane.

Mass spectrum : LRMS : $[\text{M}^+]$ at m/z 418, $\text{C}_{22}\text{H}_{26}\text{O}_8$ requires 418.40 g/mol

EIMS: m/z : 418, 235, 210, 181, 167, 161, 154, 140, 123, 105, 77

I.R Data : $\nu_{\text{max}}[\text{NaCl}](\text{cm}^{-1})$: 3420 (O-H stretching), 2932, 2851 (aliphatic C-H stretching), 1624, 1518 (C=C stretching of the aromatic ring), 1332 (syringyl breathing), 1116 (C-O stretching)

^1H and ^{13}C NMR data are presented in Table 1 in chapter 3

4.3.1.3 Physical data for compound 2, *episyngaresinol*

Name : *episyngaresinol*

Yield : lignan mixture = 18 mg

Physical description : yellow to brown amorphous substance

$[\alpha]_{\text{D}}^{25} = +107^{\circ}$; lit. $+127^{\circ}$

Mixture of syringaresinol isomers eluted with 10 % ethyl acetate in dichloromethane

Mass spectrum : LRMS : $[\text{M}^+]$ at m/z 418, $\text{C}_{22}\text{H}_{26}\text{O}_8$ requires 418.40 g/mol

EIMS : m/z : 418, 251, 210, 181, 167, 161, 154, 123, 93

I.R Data : $\nu_{\max}[\text{NaCl}](\text{cm}^{-1})$: 3420 (O-H stretching), 2947, 2846 (aliphatic C-H stretching), 1619, 1528 (C=C stretching of the aromatic ring), 1332 (syringyl breathing), 1221, 1116 (C-O stretching)

The ^1H and ^{13}C data are presented in Table 2 in chapter 3

4.3.1.4 Physical data for compound 3, 3-(4'-hydroxy-3',5'-dimethoxyphenyl)-prop-1-ene

Name : 3-(4'-hydroxy-3',5'-dimethoxyphenyl)-prop-1-ene

Yield : 25 mg

Physical Description : yellow to brown amorphous substance

Separation was achieved using a preparative plate as discussed in the foreword to the experimental. The preparative plate was developed in a three solvent system made up of 56 % hexane, 38 % dichloromethane and 6 % methanol.

Mass spectrum : LRMS : $[\text{M}^+]$ at m/z 194, $\text{C}_{11}\text{H}_{14}\text{O}_3$ requires 194.22 g/mol

EIMS : m/z : 194, 179, 167, 147, 131, 119, 91, 77, 65, 53, 39

I.R Data : $\nu_{\max}[\text{NaCl}](\text{cm}^{-1})$: 3427 (O-H stretching), 2923, 2859 (C-H aliphatic stretching), 1674 (unsaturated C=C stretching), 1596 (C=C stretching of the aromatic ring), 1336 (syringyl breathing), 1219, 1126 (C-O stretching)

The ^1H and ^{13}C NMR data are presented in Table 3 in chapter 3

4.3.1.5 Physical data for compound 6, 2,6-dimethoxy-1,4-benzoquinone

Name : 2,6-dimethoxy-1,4-benzoquinone

Yield : 2 mg

The mixture of this compound with syringaldehyde eluted with 100 % dichloromethane.

Mass spectrum : LRMS : $[M^+]$ at m/z 168, $C_8H_8O_4$ requires 168.12 g/mol

EIMS : m/z : 168, 138, 125, 112, 97, 81, 69, 53, 41

The 1H and ^{13}C data are presented in Table 6 in chapter 3

4.4 ANALYSIS OF THE O₂ - STAGE BLEACHING EFFLUENT - GENERAL SAMPLING AND ORGANIC EXTRACTION PROCEDURES

A five litre sample of the O₂ - stage bleaching effluent was taken from the waste liquor going to the effluent drain after the pulp had been filtered. The sampling container was first rinsed with the sample to be taken and thereafter the container was filled. The sample had a much lighter colour than the calcium and magnesium samples and had a neutral pH. Its temperature was between 75⁰ C and 90⁰ C.

A four litre sample of the cooled O₂ – stage bleaching effluent was extracted with approximately twelve litres of chloroform, in portions, using a 6L separating flask. The organic extract did not require neutralisation as it had a neutral pH. The organic extract was evaporated using a BUCHI Rotavapor.

4.4.1 PHYSICAL DATA

Mass of organic extract = 0.397 g

4.4.1.1 Physical data for compound 8, β -sitosterol

Name : β -sitosterol

Yield : 22 mg

Physical Description : white crystalline material

Melting Point : 137-140⁰ C : lit. 141⁰ C⁷

Eluted with 50 % dichloromethane in hexane

I.R Data : ν_{\max} [NaCl](cm⁻¹) : 3379 (O-H stretching), 2932, 2863 (aliphatic C-H stretching), 1474, 1385 (CH₂ and CH₃ bending), 1051 (C-O stretching)

^1H NMR data : δ_{H} (ppm) (CDCl_3 , 300 MHz)

5.32 (1H, H-6), 3.50 (1H, m, H-3), 0.99 (3H, s, H-19), 0.91 (3H, d, $J = 6.4\text{Hz}$, H-21), 0.82 (3H, t, $J = 7.2\text{Hz}$, H-29), 0.80 (3H, d, $J = 7.9\text{Hz}$, H-26), 0.78 (3H, d, $J = 7.1\text{Hz}$, H-27), 0.66 (3H, s, H-18)

^{13}C NMR data : δ_{C} (ppm) (CDCl_3 , 300MHz)

140.9 (C-5), 121.9 (C-6), 72.0 (C-3), 56.9 (C-14), 56.2 (C-17), 50.3 (C-9), 46.0 (C-24), 42.7 (C-4), 42.5 (C-13), 39.9 (C-12), 37.4 (C-1), 36.7 (C-10), 36.3 (C-20), 34.1 (C-22), 32.1 (C-8), 31.8 (C-2), 29.9 (C-7), 29.3 (C-25), 28.4 (C-16), 26.2 (C-23), 24.5 (C-15), 23.2 (C-28), 21.3 (C-11), 20.0 (C-26), 19.6 (C-19), 19.2 (C-27), 18.9 (C-21), 12.2 (C-29), 12.0 (C-18)

4.4.1.2 Physical data for compound 9, hexadecanoic acid

Name : Hexadecanoic acid (commonly known as palmitic acid)

Yield : 15 mg

Physical Description : pale yellow amorphous substance with a wax-like appearance

Eluted with 30 % ethyl acetate in dichloromethane

Mass spectrum : LRMS : $[\text{M}^+]$ at m/z 256, $\text{C}_{16}\text{H}_{32}\text{O}_2$ requires 256.46 g/mol

EIMS : m/z : 256, 213, 185, 157, 129, 101, 73, 43

I.R Data : $\nu_{\text{max}}[\text{NaCl}](\text{cm}^{-1})$: 2923, 2847 (aliphatic C-H stretching), 1712 (C=O stretching), 1470 (CH_2 bending)

^1H NMR data : δ_{H} (ppm) (CDCl_3 , 300 MHz)

2.32 (2H, t, H-2), 1.61 (2H, m, H-15), 1.23 (12H, 12 x CH_2), 0.86 (3H, t, H-16)

^{13}C NMR data : δ_{C} (ppm) (CDCl_3 , 300MHz)

179.3 (COOH), 33.9 (C-2), 32.5 (CH_2), 31.9 (CH_2), 29.7 (3 x CH_2), 29.6, 29.4, 29.4, 29.3, 29.1, 29.0, 24.7 (7 x CH_2), 22.7 (C-15), 14.1 (CH_3)

4.4.1.3 Physical data for compound 5, syringaldehyde

Name : 4-hydroxy-3,5-dimethoxybenzaldehyde (commonly known as syringaldehyde)

Yield : 10 mg

Physical Description : yellow crystalline solid

Melting point : 108-110⁰ C : lit. 113-114⁰ C²

Eluted with 100 % dichloromethane

Mass spectrum : LRMS : [M⁺] at *m/z* 182, C₉H₁₀O₄ requires 182.15 g/mol

EIMS : *m/z* : 182, 181, 167, 153, 139, 123, 111, 96, 79, 65, 51, 39

I.R Data : ν_{\max} [NaCl](cm⁻¹) : 3286 (O-H stretching), 2939, 2837 (C-H stretching of the aldehyde group), 1671 (C=O stretching), 1608, 1513 (C=C stretching of the aromatic ring), 1214, 1113 (C-O stretching)

The ¹H and ¹³C NMR data are presented in Table 5 in chapter 3

4.5 ANALYSIS OF THE E₂ - STAGE BLEACHING EFFLUENT - GENERAL SAMPLING AND ORGANIC EXTRACTION PROCEDURES

A five litre sample of the E₂ - stage bleaching effluent was taken from the waste liquor going to the effluent drain after the pulp had been filtered. The sampling procedure was carried out in the same manner as described for the sampling of the O₂ – stage bleaching effluent. This sample was very much lighter in colour than the O₂ – stage bleaching effluent as most of the unwanted materials had been removed in the previous bleaching and washing stages. The sample had a neutral pH and a temperature between 75^o C and 90^o C.

A four litre sample of the cooled E₂ – stage bleaching effluent was extracted with approximately twelve litres of chloroform, in portions, using a 6 L separating flask. The organic extract did not require neutralisation as it had a neutral pH. The organic extract was evaporated using a BUCHI Rotavapor.

4.5.1 PHYSICAL DATA

Mass of organic extract = 1.145 g

4.5.1.1 Physical data of compound 10, 9,12-octadecadienoic acid

Name : 9,12-Octadecadienoic acid (commonly known as linoleic acid)

Yield : 2 mg

Physical Description : pale yellow amorphous substance

Compound 10 eluted with 20 % ethyl acetate made up in dichloromethane

Mass spectrum : LRMS : [M⁺] at *m/z* 280, C₁₈H₃₂O₂ requires 280.48 g/mol

EIMS : *m/z* : 280, 262, 178, 150, 123, 110, 95, 81, 67, 55, 41

¹H NMR data : δ_H (ppm) (CDCl₃, 300 MHz)

5.39 (4H, m, H-9, H-10, H-12, H-13), 2.32 (2H, m, H-2), 1.58 (2H, m, H-17), 1.25 (14H, H-3-7, H-15, H-16), 0.85 (3H, m, H-18)

4.5.1.2 Physical data for compound 8, sitosterol

Name : β -sitosterol

Yield : 17 mg

Physical Description : white crystalline material

Melting Point : 137-140⁰ C : lit. 141⁰ C⁷

Eluted with 50 % dichloromethane in hexane

I.R Data : ν_{\max} [NaCl](cm⁻¹) : 3379 (O-H stretching), 2932, 2863 (aliphatic C-H stretching), 1474, 1385 (CH₂ and CH₃ bending), 1051 (C-O stretching)

¹H NMR data : δ_H (ppm) (CDCl₃, 300 MHz)

5.32 (1H, H-6), 3.50 (1H, m, H-3), 0.99 (3H, s, H-19), 0.91 (3H, d, $J = 6.4$ Hz, H-21), 0.82 (3H, t, $J = 7.2$ Hz, H-29), 0.80 (3H, d, $J = 7.9$ Hz, H-26), 0.78 (3H, d, $J = 7.1$ Hz, H-27), 0.66 (3H, s, H-18)

¹³C NMR data : δ_C (ppm) (CDCl₃, 300MHz)

140.9 (C-5), 121.9 (C-6), 72.0 (C-3), 56.9 (C-14), 56.2 (C-17), 50.3 (C-9), 46.0 (C-24), 42.7 (C-4), 42.5 (C-13), 39.9 (C-12), 37.4 (C-1), 36.7 (C-10), 36.3 (C-20), 34.1 (C-22), 32.1 (C-8), 31.8 (C-2), 29.9 (C-7), 29.3 (C-25), 28.4 (C-16), 26.2 (C-23), 24.5 (C-15), 23.2 (C-28), 21.3 (C-11), 20.0 (C-26), 19.6 (C-19), 19.2 (C-27), 18.9 (C-21), 12.2 (C-29), 12.0 (C-18)

4.5.1.3 Physical data for compound 5, syringaldehyde

Name : 4-hydroxy-3,5-dimethoxybenzaldehyde (commonly known as syringaldehyde)

Yield : < 2 mg

Physical Description : yellow crystalline solid

Melting point : 108-110⁰ C : lit. 113-114⁰ C²

Eluted with 100 % dichloromethane

Mass spectrum : LRMS : [M⁺] at *m/z* 182, C₉H₁₀O₄ requires 182.15 g/mol

EIMS : *m/z* : 182, 181, 167, 153, 139, 123, 111, 96, 79, 65, 51, 39

I.R Data : ν_{\max} [NaCl](cm⁻¹) : 3286 (O-H stretching), 2939, 2837 (C-H stretching of the aldehyde group), 1671 (C=O stretching), 1608, 1513 (C=C stretching of the aromatic ring), 1214, 1113 (C-O stretching)

The ¹H and ¹³C NMR data are presented in Table 5 in chapter 3

4.6 REFERENCES

1. Briggs, L. H., Cambie, R. C. and Couch, R. A. F., 1968, *Journal of Chemical Society (C)*, 3042-3045
2. Dictionary of Natural Products (DNP) on CD-ROM, version 9:1, 1982-2000, Chapman and Hall Electronic Publishing Division, London
3. Lin, S. Y. and Dence, C. W., 1992, *Methods in Lignin Chemistry*, Springer-Verlag, Berlin, p474-477
4. Sjostrom, E. and Alen, R., 1999, *Analytical Methods in Wood Chemistry. Pulping and Papermaking*, Springer, Berlin, p46-48(a), 240-252(b)
5. Konturri, A. K. and Sundholm, G., 1986, *Acta Chemica Scandinavica*, (A 40), 121-125
6. Mann, F. G. and Saunders, B. C., 1973, *Practical Organic Chemistry : New Impression*, Longman Group Limited, England, p321-326
7. Chaplin, M. F. and Kennedy, J. F., 1986, *Carbohydrate Analysis – a practical approach*, IRL Press Limited, England, p2-4
8. *Aldrich Library of ^{13}C and ^1H FT NMR Spectra*, 1993, (2) 959A, (3), 569A, (1) 756B

CHAPTER 5: CONCLUSION

The four streams of effluent, namely, the calcium - spent liquor, magnesium condensate, O₂ - stage bleaching stream and the E₂ - stage bleaching stream were analysed individually using various techniques. The organic components were extracted and subjected to column chromatography resulting in the isolation and identification of the major components. These make up approximately 20 % of the compounds present in each of the effluent streams and account for the bulk of the mass. The remaining organic extract was found to contain a large number of minor constituents that had broken down during the pulping process and were difficult to isolate in appreciable quantities.

The organic extract of the calcium - spent liquor was found to contain lignans and lignin precursors. The major constituents were two isomers of the lignan, syringaresinol (0.400 g/L). Other compounds identified were 3-(4'-hydroxy-3',5'-dimethoxyphenyl)-prop-1-ene (0.020 g/L), 2,6-dimethoxy-1,4-benzoquinone (0.0030 g/L), 3-(4'-hydroxy-3',5'-dimethoxyphenyl)-1-hydroxy-propane-2-one (0.010 g/L) and syringaldehyde (0.010 g/L). All the compounds isolated are found to be widespread in wood and pulp liquors, for example, sulphite liquor and are common degradation products of lignin.

Syringaldehyde has a reported LD₅₀ of 1000 mg/kg¹. 2,6-Dimethoxy-1,4-benzoquinone has also been found to cause dermatitis and has mutagenic properties¹.

An attempt was made to extract the lignosulphonates from the aqueous phase. However, the extraction of pure lignosulphonates proved difficult and a mixture including sugars was obtained (w/w% = 4.2 %). NMR, infrared and UV spectroscopy were used to confirm the crude product extracted. Isolation of pure lignosulphonates will require more time and the use of techniques such as HPLC and ion exchange chromatography.

The calcium - spent liquor contained a residue concentrate of approximately 0.72 g/L. X-ray diffraction studies carried out on the sample revealed two forms of calcium sulphate,

that of gypsum ($\text{CaSO}_4 \cdot 2\text{H}_2\text{O}$) and the hemihydrate form more commonly known as Plaster of Paris ($\text{CaSO}_4 \cdot 0.5\text{H}_2\text{O}$).

A sample of wax balls was obtained from the calcium - spent liquor at the point where the condensed gases from an evaporation process collect. An analysis using gas chromatography/mass spectrometry showed that the sample contained a mixture of fatty acids and their derivatives. The major constituent was palmitic acid (65 %). These wax balls are also found in the magnesium - pulping section and would probably have a similar composition, however, none were available for analysis during the project.

The magnesium condensate organic extract was found to contain lignans and lignin precursors. Here again, the major constituents were the two syringaresinol isomers (0.017 g/L). The lignin precursors identified were 3-(4'-hydroxy-3',5'-dimethoxyphenyl)-prop-1-ene (0.012 g/L) and 2,6-dimethoxy-1,4-benzoquinone (0.0033 g/L). In addition to this, a minor amount of vanillin (0.0016 g/L) was isolated, which had not been isolated from the calcium - spent liquor. In terms of hazard and toxicity of the compounds isolated, vanillin is reported to have a LD_{50} of 1580 mg/kg in rats and has reproductive effects¹.

The two bleaching stages contained similar types of compounds. The organic extract of the O_2 - stage was found to contain sitosterol (0.0075 g/L) and palmitic acid (0.0088 g/L) as its major constituent as well as syringaldehyde (0.0030 g/L). The reported LD_{50} of palmitic acid is 57 mg/kg and behaves as a skin irritant¹.

The E_2 - stage organic extract was also found to contain sitosterol (0.0043 g/L) as its major constituent as well as syringaldehyde (<0.0010 g/L) and linoleic acid (<0.0010 g/L). Linoleic acid is also reported to behave as a skin irritant and causes gastrointestinal effects if ingested¹.

Based on average plant effluent flowrates obtained from plant personnel, the quantity of these compounds passing out to the effluent holding site was determined:

Ca - spent liquor – flowrate² ~75 m³/hour[†]

Syringaresinol mixture ~ 30 kg/hour[†]

3-(4'-hydroxy-3',5'-dimethoxyphenyl)-prop-1-ene ~ 1.50 kg/hour

2,6-dimethoxy-1,4-benzoquinone ~ 0.23 kg/hour

3-(4'-hydroxy-3',5'-dimethoxyphenyl)-1-hydroxy-propane-2-one ~ 0.75 kg/hour

syringaldehyde ~ 0.75 kg/hour

Mg condensate – flowrate² ~ 170 m³/hour

Syringaresinol mixture ~ 2.83 kg/hour

3-(4'-hydroxy-3',5'-dimethoxyphenyl)-prop-1-ene ~ 1.98 kg/hour

2,6-dimethoxy-1,4-benzoquinone ~ 0.567 kg/hour

vanillin ~ 0.283 kg/hour

O₂ - stage bleaching effluent – flowrate² ~ 160 m³/hour

Sitosterol ~ 1.20 kg/hour

Palmitic acid ~ 1.40 kg/hour

Syringaldehyde ~ 0.480 kg/hour

E₂ - stage bleaching effluent – flowrate² ~ 160 m³/hour

Sitosterol ~ 0.680 kg/hour

Linoleic acid ~ 0.080 kg/hour

Syringaldehyde ~ 0.080 kg/hour

[†] The flowrate quoted above is, at present, the remaining 60 % of the effluent that is pumped to the main effluent drain. It is still much lower than the magnesium section as it is presently not functioning at its maximum capacity. The flowrates have been confirmed by John Thubron from SAPPI SAICCOR.

[†] This value appears very high. Further quantification of this over a period of time is needed to confirm the amount of lignan mixture being sent to the effluent holding site.

The carbohydrate content was determined for all four streams of effluent and the results are shown in Table 13. The samples were analysed for hexose based on glucose and pentose based on xylose³. The calcium – spent liquor has the highest concentration of hexose and pentose and the O₂ – stage bleaching effluent has the lowest concentration of hexose and pentose. The quantities of hexose and pentose going to the effluent holding site are based on the flowrates given on page 119.

TABLE 13: Carbohydrate content of the four streams of effluent

Effluent stream	Concentration of hexose (g/l)	Quantity of hexose going to effluent holding site (kg/hr) ¹	Concentration of pentose (g/l)	Quantity of pentose going to effluent holding site (kg/hr) ²
Ca - spent liquor	49.3	3697.5	49.8	3735
Mg condensate	3.11	528.7	2.75	467.5
O ₂ - stage bleaching effluent	0.146	23.4	0.171	27.4
E ₂ - stage bleaching effluent	0.167	26.7	0.200	32.0

The aim of this project was to characterise SAPPI SAICCOR's effluent with the intention of extracting the commercially viable components, so as, to reduce the amount of effluent being pumped out to sea. This project has focussed on the neutral organic components present in the effluent and more specifically those extractable with chloroform. The complete characterisation of the effluent has therefore, by no means been fully achieved as there are many more aspects to be studied, which was considered beyond the scope of this thesis. Further studies based on other solvent extractions as well as extractions at different pH values should be carried out in order to obtain a more complete characterisation of the total organic content. A more in - depth study is also required of the water - soluble components.

¹ At present, the plant produces 40 t/hr of pulp from 140 t/hr of wood². Thus, 100 t/hr of effluent is produced. The combined percentage of hexose from all the streams of effluent is 4.3 %, which is realistic based on the present capacity and flowrates of the plant.

² Similarly, the combined percentage of pentose in the effluent is also 4.3 %.

The investigations presented in this thesis should also be repeated over a period of time to determine a more accurate quantification of the components present. This is important if the commercially viable components are to be extracted. Furthermore, an investigation of the possible commercial uses of the major components found should be undertaken together with a financial study. In particular, the commercial uses for syringaresinol should be undertaken as it is the major constituent of both the calcium and magnesium streams. A study of the commercial uses of carbohydrates is also advisable as it makes up a large proportion of the effluent.

A study of possible extraction procedures of the major components should be carried out in collaboration with chemical engineering personnel. Pilot studies on a laboratory scale should first be attempted before plant trials are undertaken to fully establish the feasibility of the extraction procedures.

REFERENCES

1. Dictionary of Natural Products (DNP) on CD-ROM, version 9:1, 1982-2000, Chapman and Hall Electronic Publishing Division : London
2. Personal Communication – John Thubron (Technical Process Manager at Sappi Saiccor)
3. Chaplin, M. F. and Kennedy, J. F., 1986, *Carbohydrate Analysis – a practical approach*, IRL Press Limited, England, p2-4

APPENDIX A

LIST OF SPECTRA AND TABLES IN APPENDIX A

	Page No.
SPECTRUM 1 : Infrared spectrum of compound 1, syringaresinol	131
SPECTRUM 2 : Mass spectrum of compound 1, syringaresinol	132
SPECTRUM 3 : ¹ H NMR spectrum of compound 1, syringaresinol, in CDCl ₃	133
SPECTRUM 4 : ¹³ C NMR spectrum of compound 1, syringaresinol, in CDCl ₃	134
SPECTRUM 5 : HMBC NMR spectrum of compound 1, syringaresinol, in CDCl ₃	135
SPECTRUM 6 : COSY NMR spectrum of compound 1, syringaresinol, in CDCl ₃	136
SPECTRUM 7 : NOESY NMR spectrum of compound 1, syringaresinol, in CDCl ₃	137
SPECTRUM 8 : Mass spectrum of compound 2, episyngaresinol	138
SPECTRUM 9 : ¹³ C NMR spectrum of compound 2, episyngaresinol, in CDCl ₃	139
SPECTRUM 10 : ¹ H NMR spectrum of compound 2, episyngaresinol, in CDCl ₃	140
SPECTRUM 11 : NOESY NMR spectrum of compound 2, episyngaresinol, in CDCl ₃	141
SPECTRUM 12 : HMBC NMR spectrum of compound 2, episyngaresinol, in CDCl ₃	142
SPECTRUM 13 : Infrared spectrum of compound 2, episyngaresinol	143

SPECTRUM 14 : Mass spectrum of compound 3, 3-(4'-hydroxy-3',5'-dimethoxyphenyl)-prop-1-ene	144
SPECTRUM 15 : Infrared spectrum of compound 3, 3-(4'-hydroxy-3',5'-dimethoxyphenyl)-prop-1-ene	145
SPECTRUM 16 : ¹ H NMR spectrum of compound 3, 3-(4'-hydroxy-3',5'-dimethoxyphenyl)-prop-1-ene, in CDCl ₃	146
SPECTRUM 17 : ¹³ C NMR spectrum of compound 3, 3-(4'-hydroxy-3',5'-dimethoxyphenyl)-prop-1-ene, in CDCl ₃	147
SPECTRUM 18 : HMBC NMR spectrum of compound 3, 3-(4'-hydroxy-3',5'-dimethoxyphenyl)-prop-1-ene, in CDCl ₃	148
SPECTRUM 19 : COSY NMR spectrum of compound 3, 3-(4'-hydroxy-3',5'-dimethoxyphenyl)-prop-1-ene, in CDCl ₃	149
SPECTRUM 20 : Mass spectrum of compound 4, 3-(4'-hydroxy-3',5'-dimethoxyphenyl)-1-hydroxy-propan-2-one	150
SPECTRUM 21 : Infrared spectrum of compound 4, 3-(4'-hydroxy-3',5'-dimethoxyphenyl)-1-hydroxy-propan-2-one	151
SPECTRUM 22 : ¹ H NMR spectrum of compound 4, 3-(4'-hydroxy-3',5'-dimethoxyphenyl)-1-hydroxy-propan-2-one, in CDCl ₃	152
SPECTRUM 23 : ¹³ C NMR spectrum of compound 4, 3-(4'-hydroxy-3',5'-dimethoxyphenyl)-1-hydroxy-propan-2-one, in CDCl ₃	153
SPECTRUM 24 : HSQC NMR spectrum of compound 4, 3-(4'-hydroxy-3',5'-dimethoxyphenyl)-1-hydroxy-propan-2-one, in CDCl ₃	154
SPECTRUM 25 : HMBC NMR spectrum of compound 4, 3-(4'-hydroxy-3',5'-dimethoxyphenyl)-1-hydroxy-propan-2-one, in CDCl ₃	155
SPECTRUM 26 : NOESY NMR spectrum of compound 4, 3-(4'-	

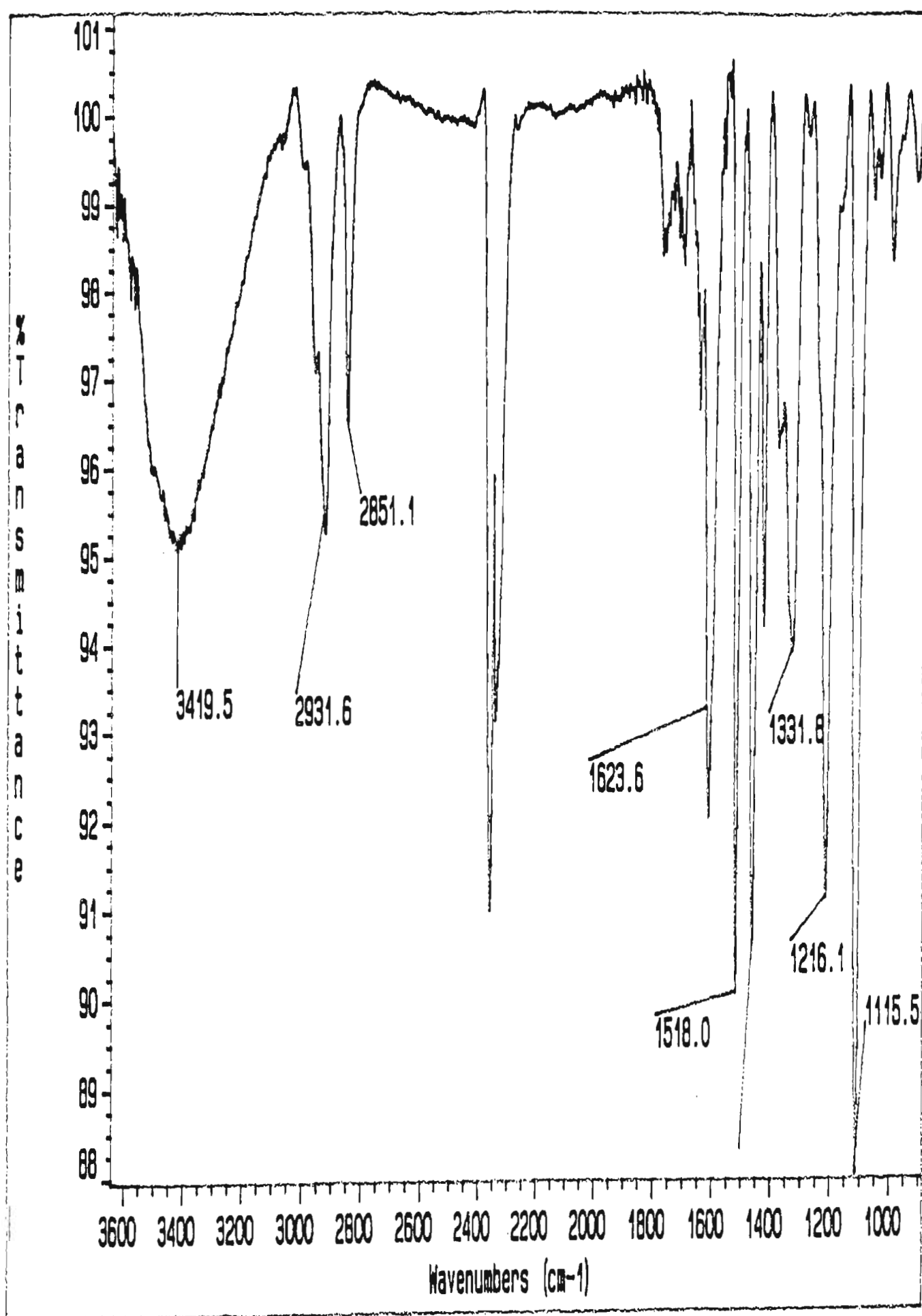
hydroxy-3',5'-dimethoxyphenyl)-1-hydroxy- propan-2-one, in CDCl ₃	156
SPECTRUM 27 : COSY NMR spectrum of compound 4, 3-(4'- hydroxy-3',5'-dimethoxyphenyl)-1-hydroxy- propan-2-one, in CDCl ₃	157
SPECTRUM 28 : ¹ H NMR spectrum of acetylated compound 4, in CDCl ₃	158
SPECTRUM 29 : Mass spectrum of acetylated compound 4	159
SPECTRUM 30 : Infrared spectrum of acetylated compound 4	160
SPECTRUM 31 : HSQC NMR spectrum of acetylated compound 4, in CDCl ₃	161
SPECTRUM 32 : HMBC NMR spectrum of acetylated compound 4, in CDCl ₃	162
SPECTRUM 33 : NOESY NMR spectrum of acetylated compound 4, in CDCl ₃	163
SPECTRUM 34 : Mass spectrum of compound 5, syringaldehyde	164
SPECTRUM 35 : Infrared spectrum of compound 5, syringaldehyde	165
SPECTRUM 36 : ¹ H NMR spectrum of compound 5, syringaldehyde, in CDCl ₃	166
SPECTRUM 37 : ¹ H NMR spectrum of compound 5, syringaldehyde, in D ₂ O	167
SPECTRUM 38 : ¹³ C NMR spectrum of compound 5, syringaldehyde, in CDCl ₃	168
SPECTRUM 39 : HSQC NMR spectrum of compound 5, syringaldehyde, in CDCl ₃	169
SPECTRUM 40 : HMBC NMR spectrum of compound 5, syringaldehyde, in CDCl ₃	170
SPECTRUM 41 : NOESY NMR spectrum of compound 5,	

syringaldehyde, in CDCl ₃	171
SPECTRUM 42 : Gas chromatogram of compound 6, 2,6-dimethoxy-1,4-benzoquinone	172
SPECTRUM 43 : Mass spectrum of compound 6, 2,6-dimethoxy- 1,4-benzoquinone	173
SPECTRUM 44 : ¹ H NMR spectrum of compound 6, 2,6-dimethoxy-1,4-benzoquinone, in CDCl ₃	174
SPECTRUM 45 : ¹³ C NMR spectrum of compound 6, 2,6-dimethoxy-1,4-benzoquinone, in CDCl ₃	175
SPECTRUM 46 : HMBC NMR spectrum of compound 6, 2,6- dimethoxy-1,4-benzoquinone, in CDCl ₃	176
SPECTRUM 47 : NOESY NMR spectrum of compound 6, 2,6- dimethoxy-1,4-benzoquinone, in CDCl ₃	177
SPECTRUM 48 : ¹ H NMR spectrum of crude lignosulphonate mixture, in D ₂ O	178
SPECTRUM 49 : ¹³ C NMR spectrum of crude lignosulphonate mixture, in D ₂ O	179
SPECTRUM 50 : Infrared spectrum of crude lignosulphonate mixture	180
SPECTRUM 51 : UV spectrum of crude lignosulphonate mixture, in H ₂ O	181
SPECTRUM 52 : XRD spectrum of residue formed from calcium – spent liquor	182
SPECTRUM 53 : UV spectra of the glucose standards used for the determination of hexose	186
SPECTRUM 54 : UV spectra of the calcium – spent liquor and glucose standards used for the determination of hexose	187

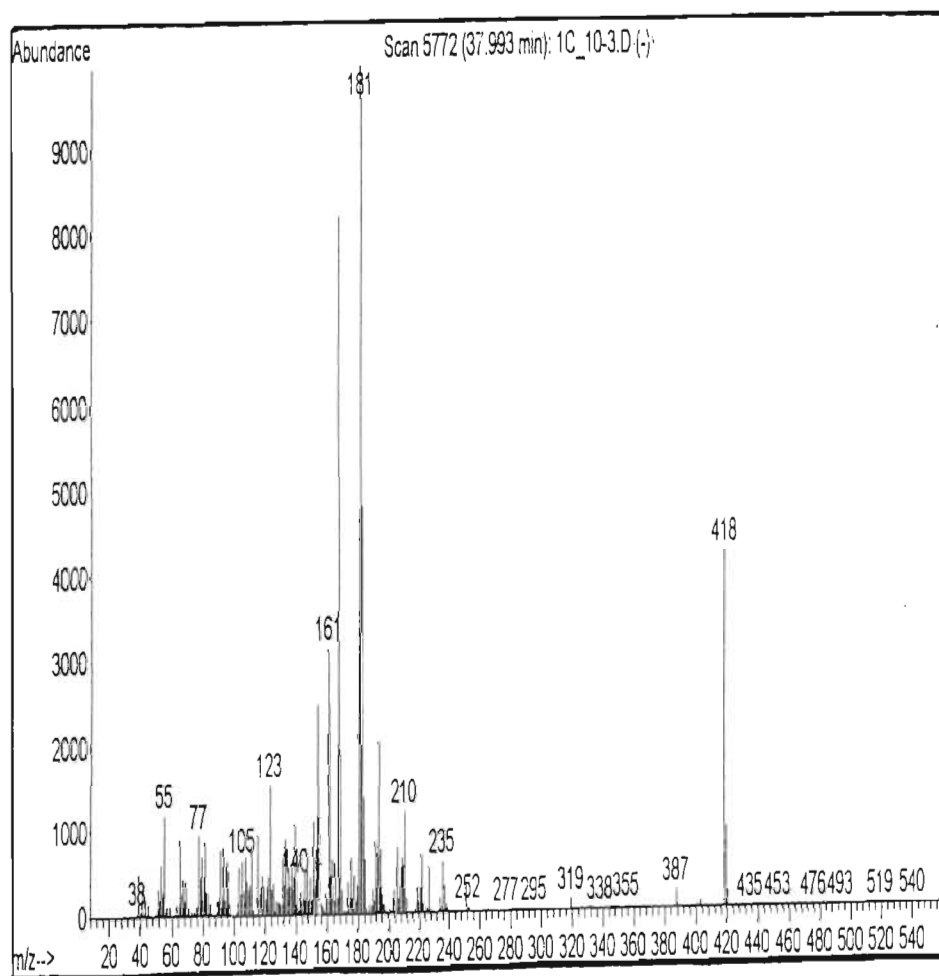
SPECTRUM 55 : UV spectra of the xylose standards used for the determination of pentose	188
SPECTRUM 56 : UV spectra of the calcium – spent liquor and xylose standards used for the determination of pentose	189
SPECTRUM 57 : Gas chromatogram of the wax balls from the calcium – spent liquor evaporates	190
SPECTRUM 58 : Mass spectrum of 1,2,3,4-tetrahydro-1,6- dimethyl-4-(1-methylethyl)-naphthalene	191
SPECTRUM 59 : Mass spectrum of dodecanoic acid	192
SPECTRUM 60 : Mass spectrum of 1,6-dimethyl-4-(1-methylethyl)- Naphthalene	193
SPECTRUM 61 : Mass spectrum of myristic acid	194
SPECTRUM 62 : Mass spectrum of 2-hydroxy-cyclopentadecanone	195
SPECTRUM 63 : Mass spectrum of pentadecanoic acid	196
SPECTRUM 64 : Mass spectrum of palmitic acid methyl ester	197
SPECTRUM 65 : Mass spectrum of palmitic acid	198
SPECTRUM 66 : Mass spectrum of hexadecanoic acid	199
SPECTRUM 67 : Mass spectrum of 7,10-octadecadienoic acid, methyl ester	200
SPECTRUM 68 : Infrared spectrum of compound 7, vanillin	202
SPECTRUM 69 : ¹ H NMR spectrum of compound 7, vanillin, in CDCl ₃	203
SPECTRUM 70 : UV spectra of the magnesium condensate and glucose standards used for the determination of hexose	204
SPECTRUM 71 : UV spectra of the magnesium condensate and xylose standards used for the determination	

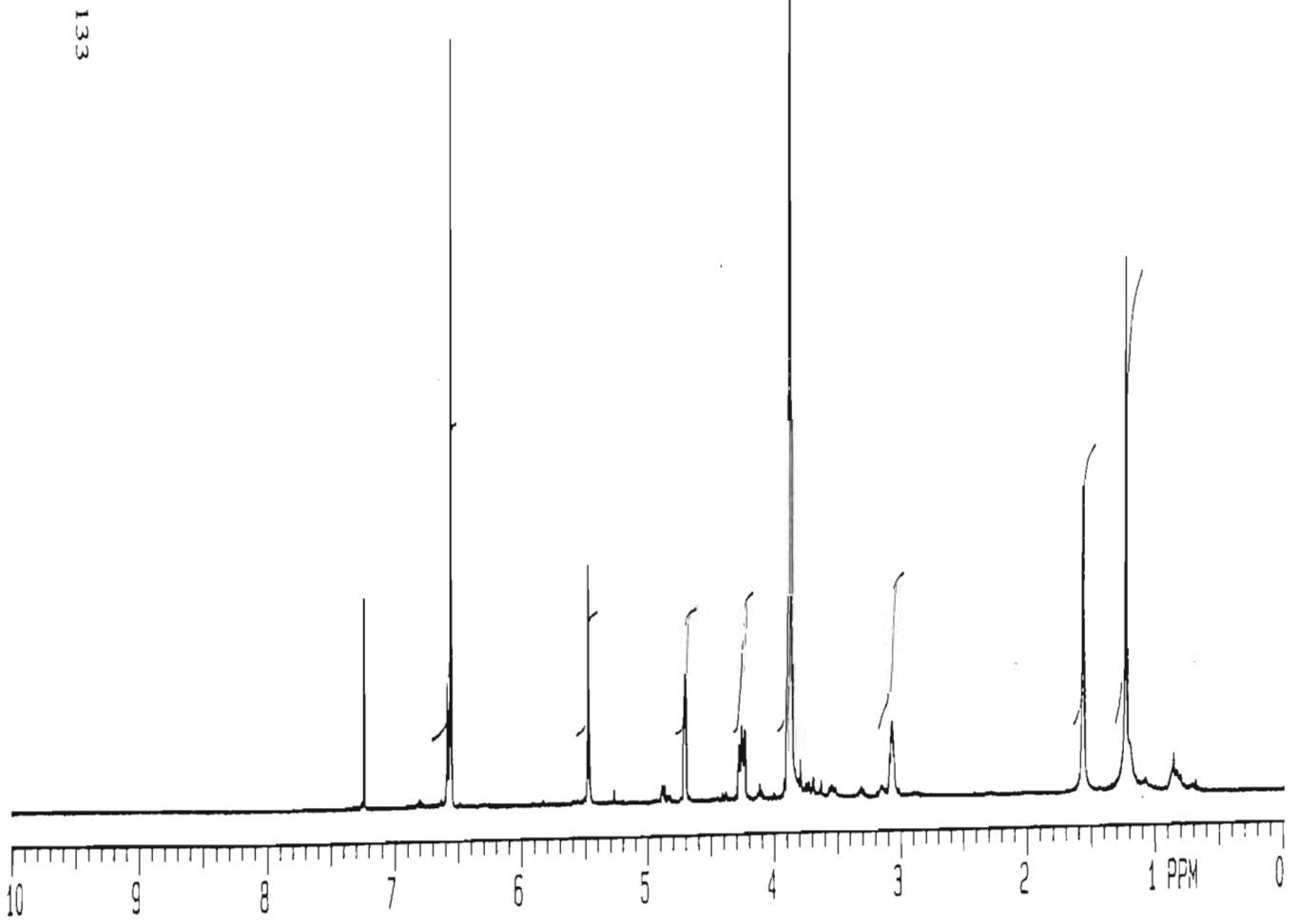
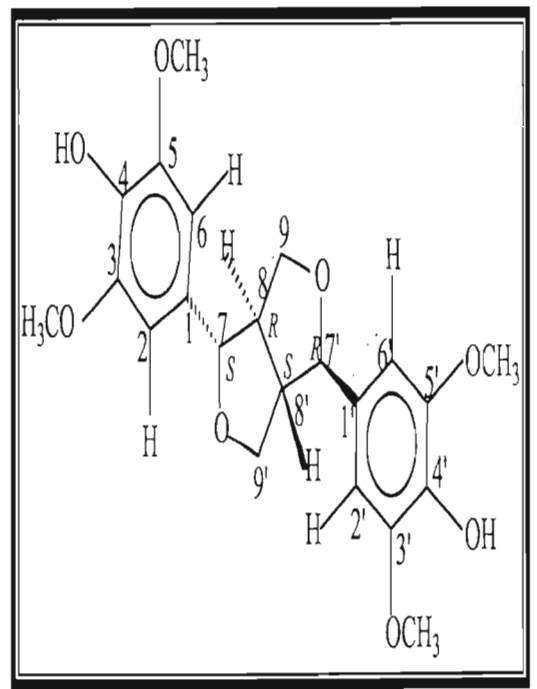
of pentose	205
SPECTRUM 72 : Infrared spectrum of compound 8, β -sitosterol	206
SPECTRUM 73 : ^1H NMR spectrum of compound 8, β -sitosterol, in CDCl_3	207
SPECTRUM 74 : ^{13}C NMR spectrum of compound 8, β -sitosterol, in CDCl_3	208
SPECTRUM 75 : Mass spectrum of compound 9, hexadecanoic acid	209
SPECTRUM 76 : Infrared spectrum of compound 9, hexadecanoic acid	210
SPECTRUM 77 : ^1H NMR spectrum of compound 9, hexadecanoic acid, in CDCl_3	211
SPECTRUM 78 : ^{13}C NMR spectrum of compound 9, hexadecanoic acid, in CDCl_3	212
SPECTRUM 79 : UV spectra of the O_2 – stage bleaching effluent and glucose standards used for the determination of hexose	213
SPECTRUM 80 : UV spectra of the O_2 – stage bleaching effluent and xylose standards used for the determination of pentose	214
SPECTRUM 81 : Mass spectrum of compound 10, 9,12-octadecadienoic acid	215
SPECTRUM 82 : ^1H NMR spectrum of compound 10, 9,12-octadecadienoic acid, in CDCl_3	216
SPECTRUM 83 : UV spectra of the E_2 – stage bleaching effluent and glucose standards used for the determination	

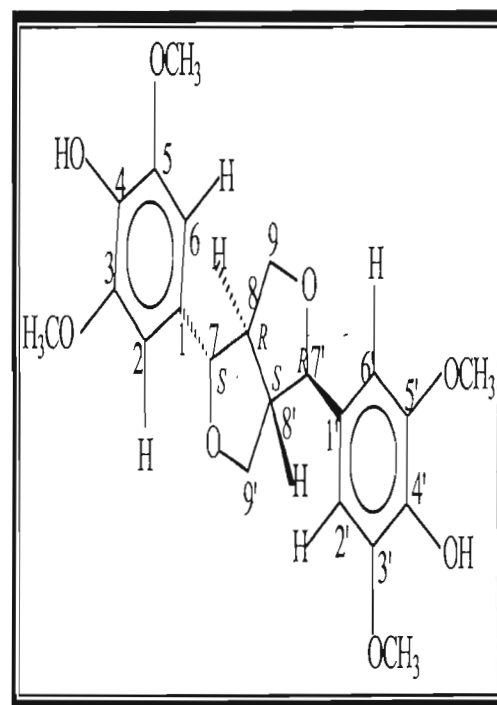
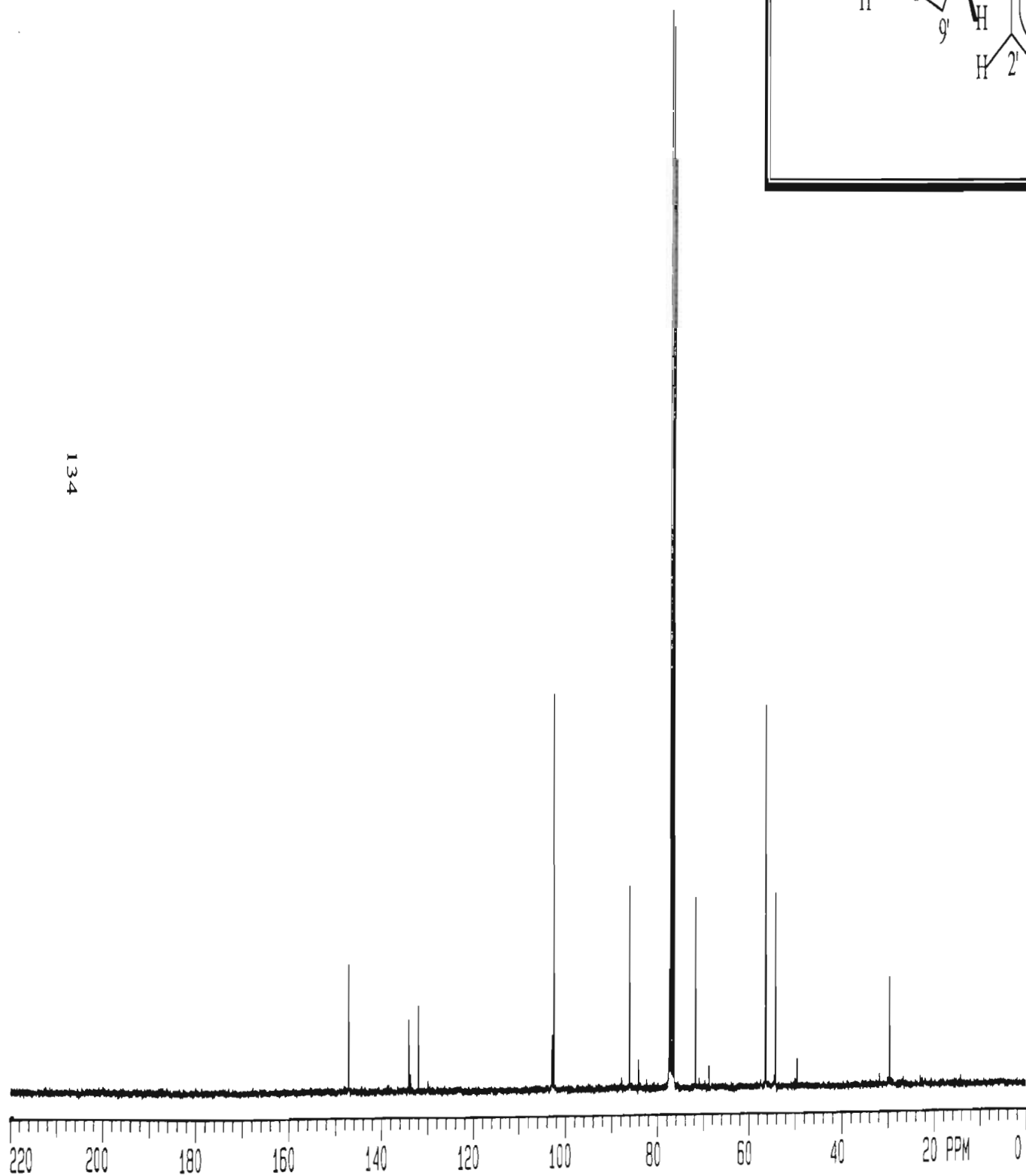
of hexose	217
SPECTRUM 84 : UV spectra of the E₂ – stage bleaching effluent and xylose standards used for the determination of pentose	218
TABLE 7 : Results of XRD analysis of residue formed in the calcium – spent liquor	183-184
TABLE 8 : Results of XRF analysis of residue formed in the calcium – spent liquor	185
Area percent report of the GC/MS analysis of the wax balls	201



SPECTRUM 1 : Infrared spectrum of compound 1, syringaresinol



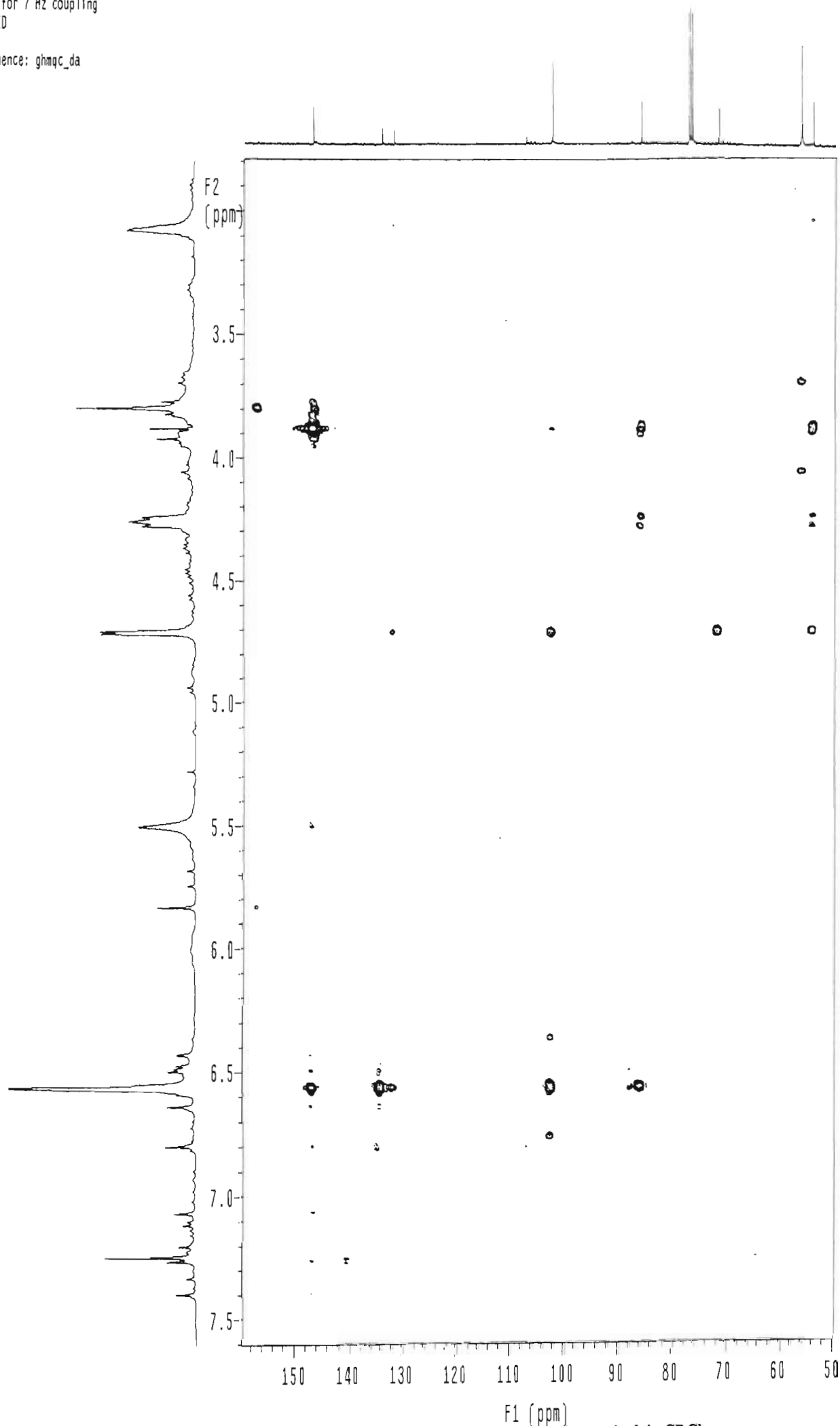




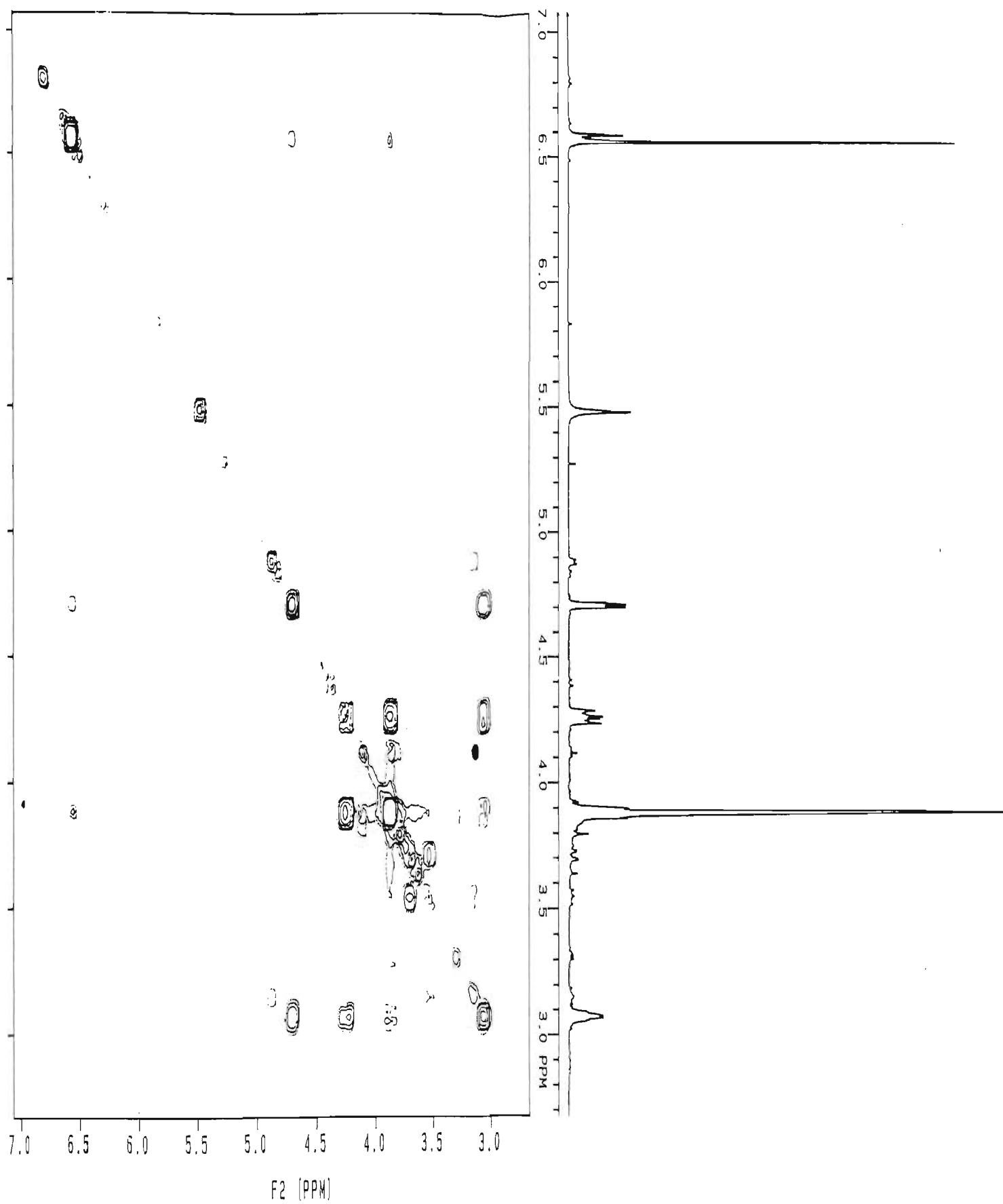
HBsse20.sse 1c/10-20 in cdc13
Gradient HMBC expt.
optimized for 7 Hz coupling
probe=3mmID

Pulse Sequence: ghmqc_da

135



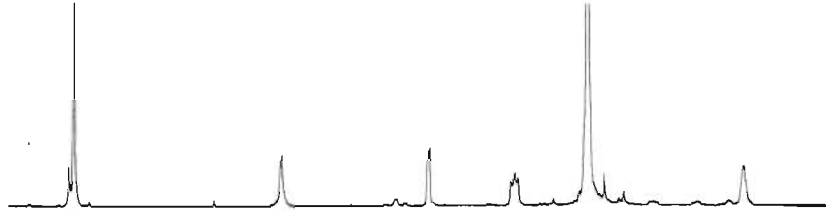
SPECTRUM 5 : HMBC NMR spectrum of compound 1, syringaresinol, in CDCl₃



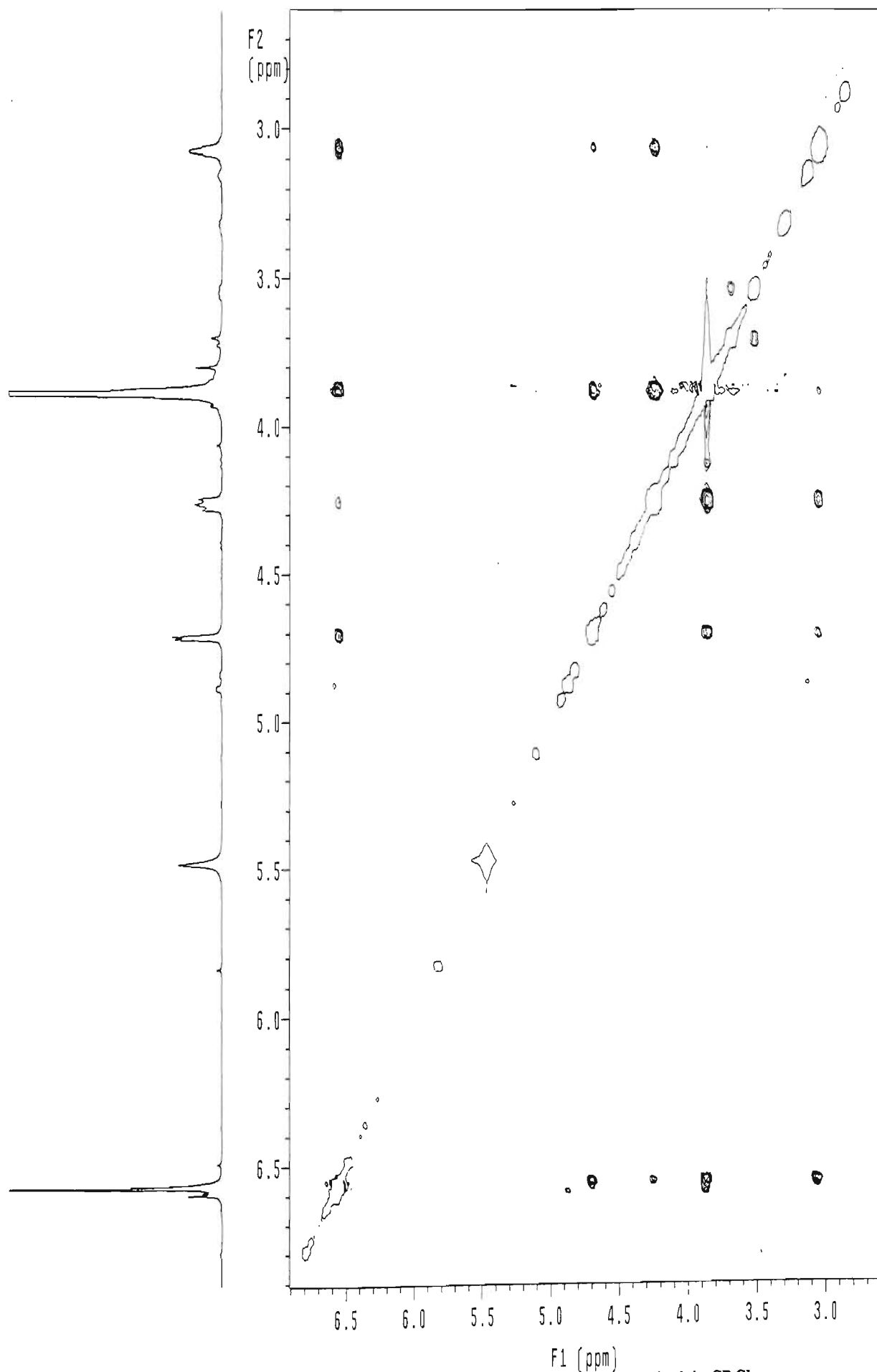
SPECTRUM 6 : COSY NMR spectrum of compound 1, syringaresinol, in CDCl₃

NOSSelc.sse-1c/10-20 in cdc13
Gradient NOESY expt.
mix=1sec
probe=5mmASW

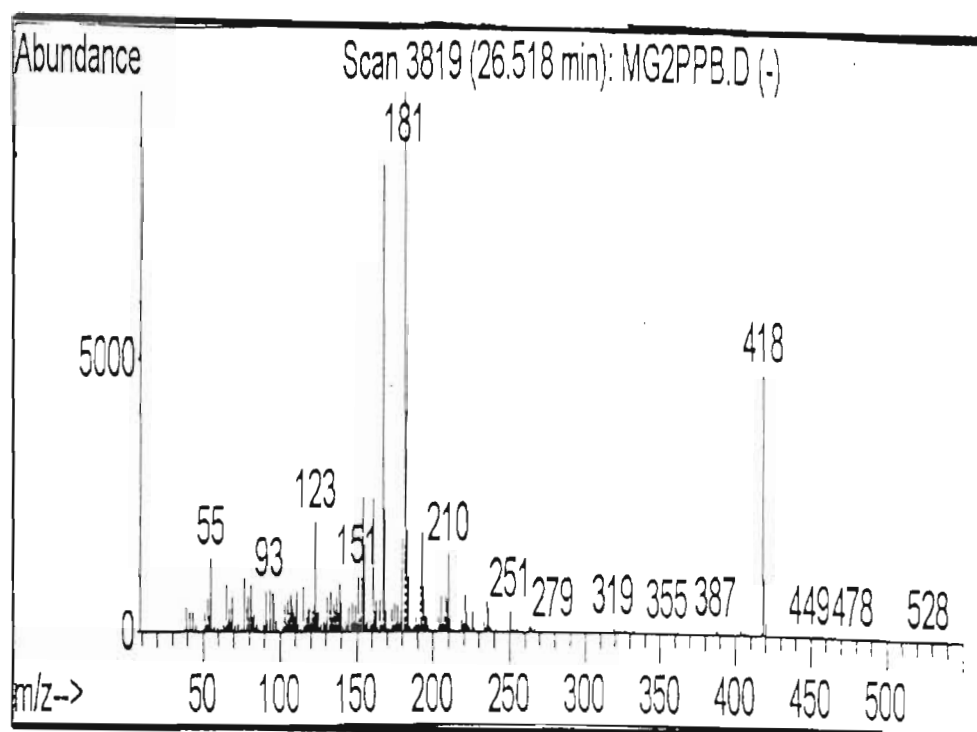
Pulse Sequence: noesy_da



137

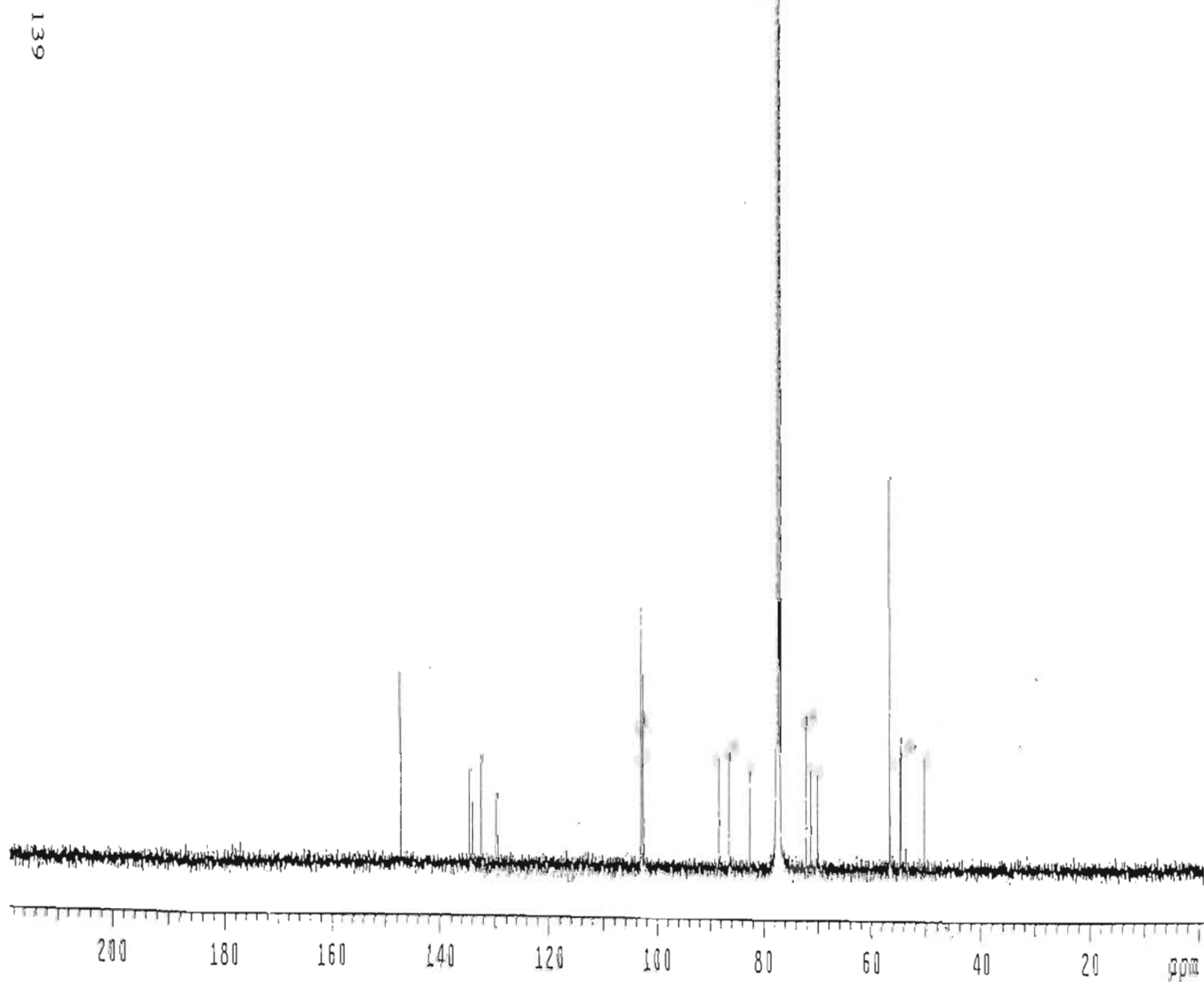


SPECTRUM 7 : NOESY NMR spectrum of compound 1, syringaresinol, in CDCl₃



— compound 2

1	14810.284	147.268	18.5
2	14795.024	147.116	14.0
3	13524.691	134.484	6.9
4	13517.062	134.408	9.3
5	13456.025	133.801	6.0
6	13306.484	132.314	6.4
7	13298.854	132.239	10.6
8	13033.343	129.598	6.9
9	10353.818	102.954	20.1
10	10343.137	102.848	25.1
11	10305.752	102.476	18.8
12	8866.041	88.160	10.7
13	8679.115	86.302	11.3
14	8291.530	82.448	9.5
15	7800.945	77.570	737.2
16	7789.501	77.456	26.2
17	7768.901	77.251	750.0
18	7736.856	76.932	718.7
19	7246.271	72.054	14.9
20	7163.871	71.235	9.7
21	7034.930	69.953	9.2
22	5696.694	56.646	38.0
23	5516.635	54.855	10.9
24	5493.746	54.628	12.9
25	5065.724	50.372	10.8

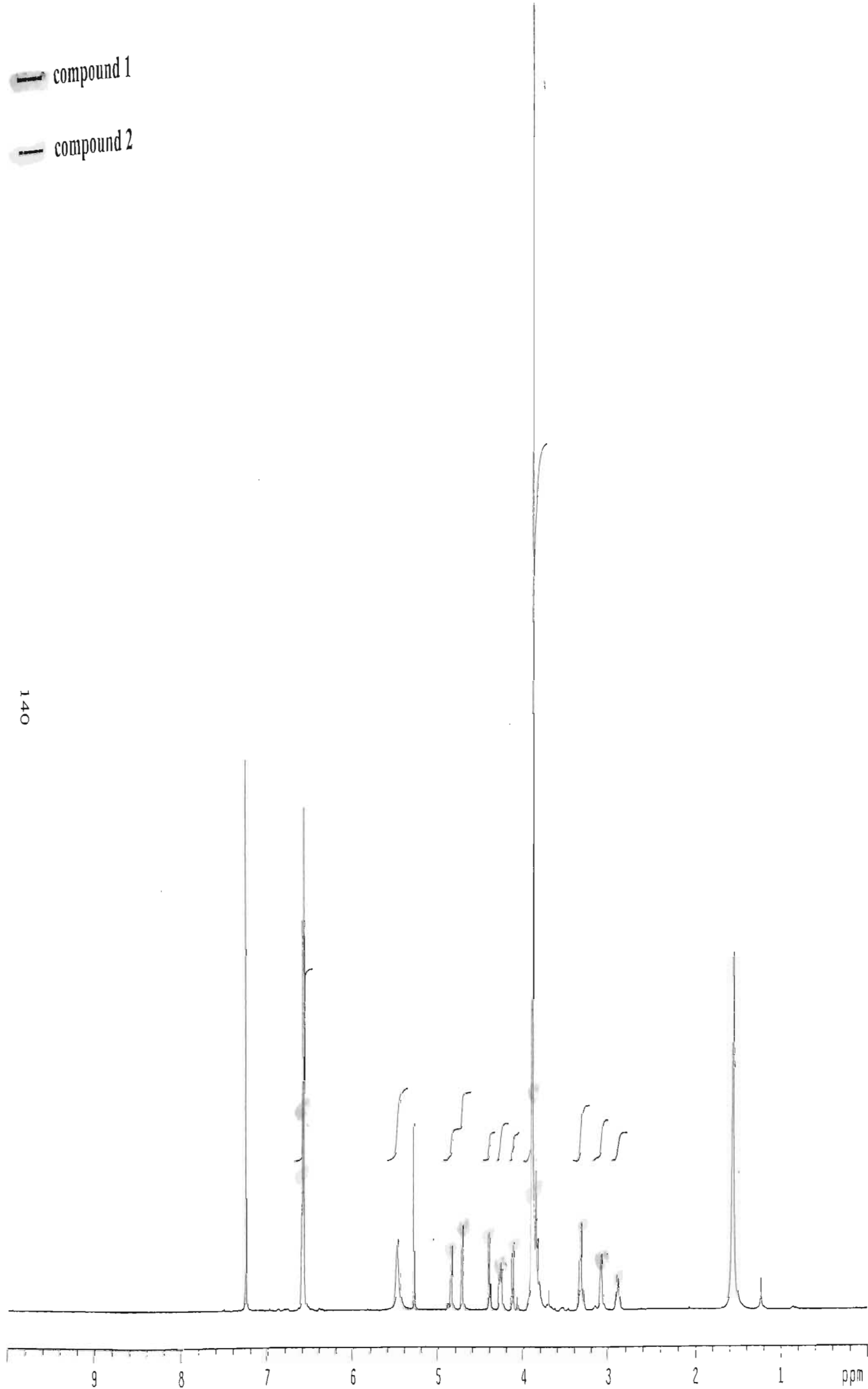


SPECTRUM 9: ^{13}C NMR spectrum of compound 2, episyringaresinol, in CDCl_3

— compound 1

— compound 2

140

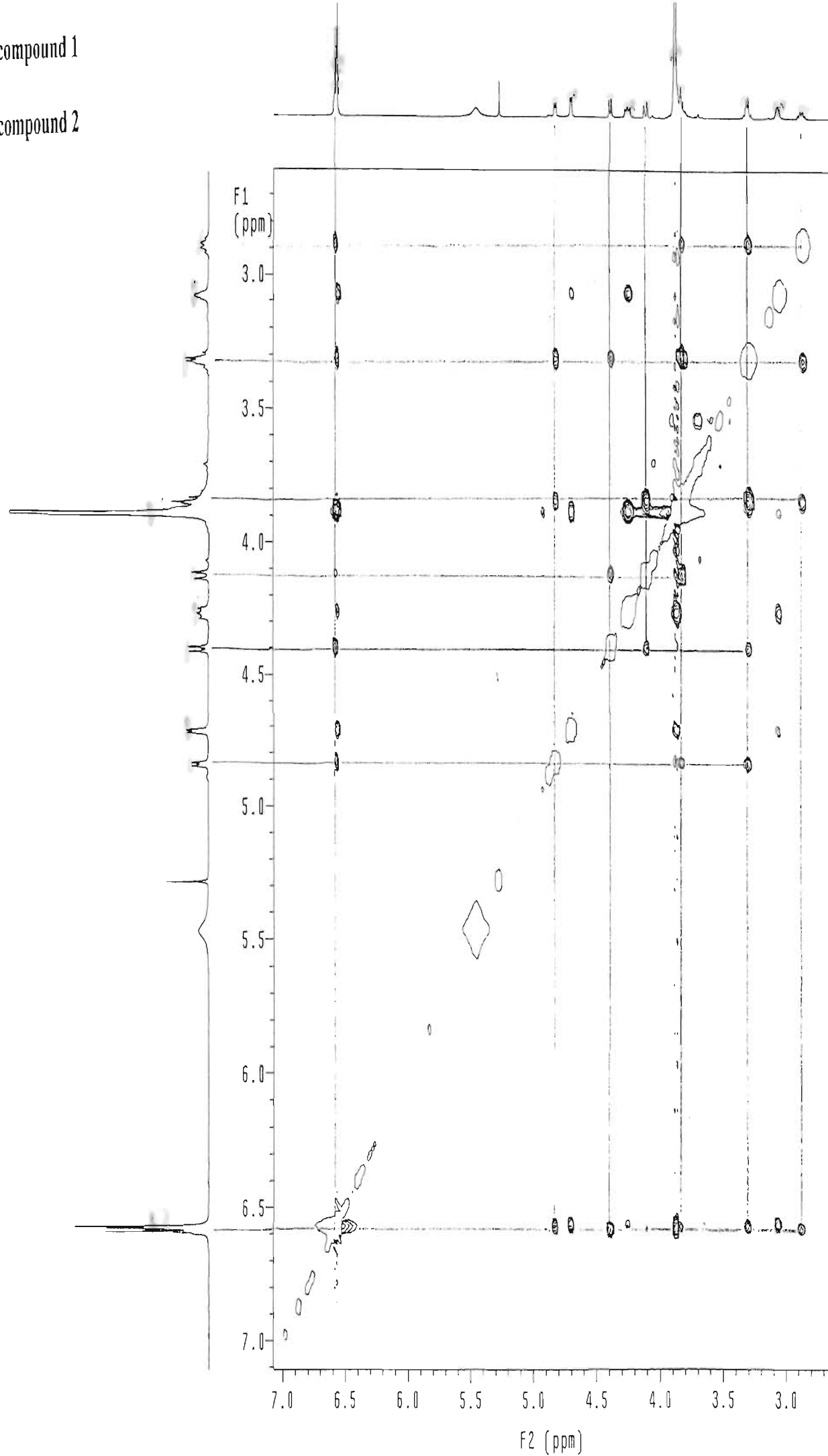


SPECTRUM 10. ^1H NMR spectrum of compound 2 enicuringresinol in CDCl_3 .

— compound 1

- - - compound 2

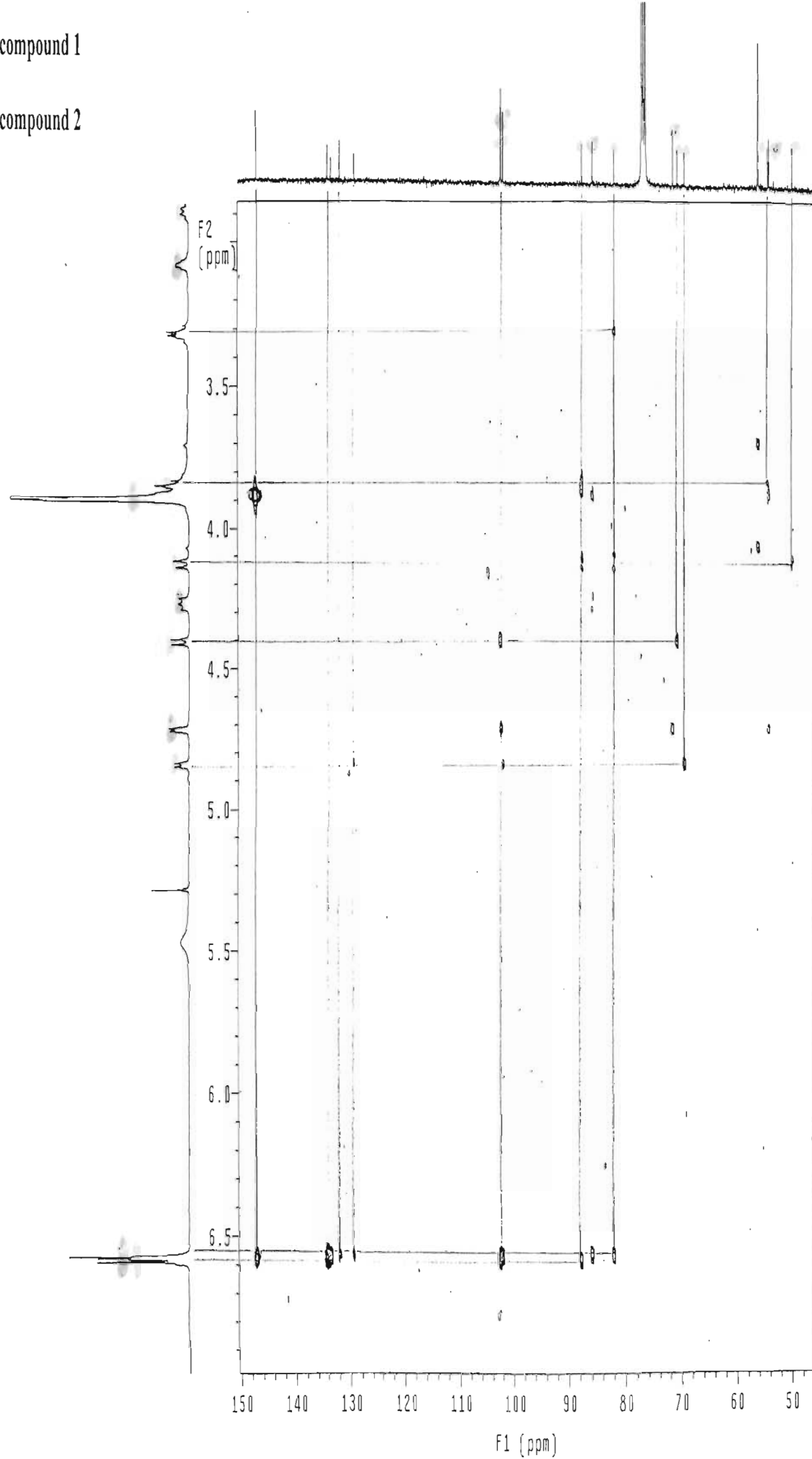
141

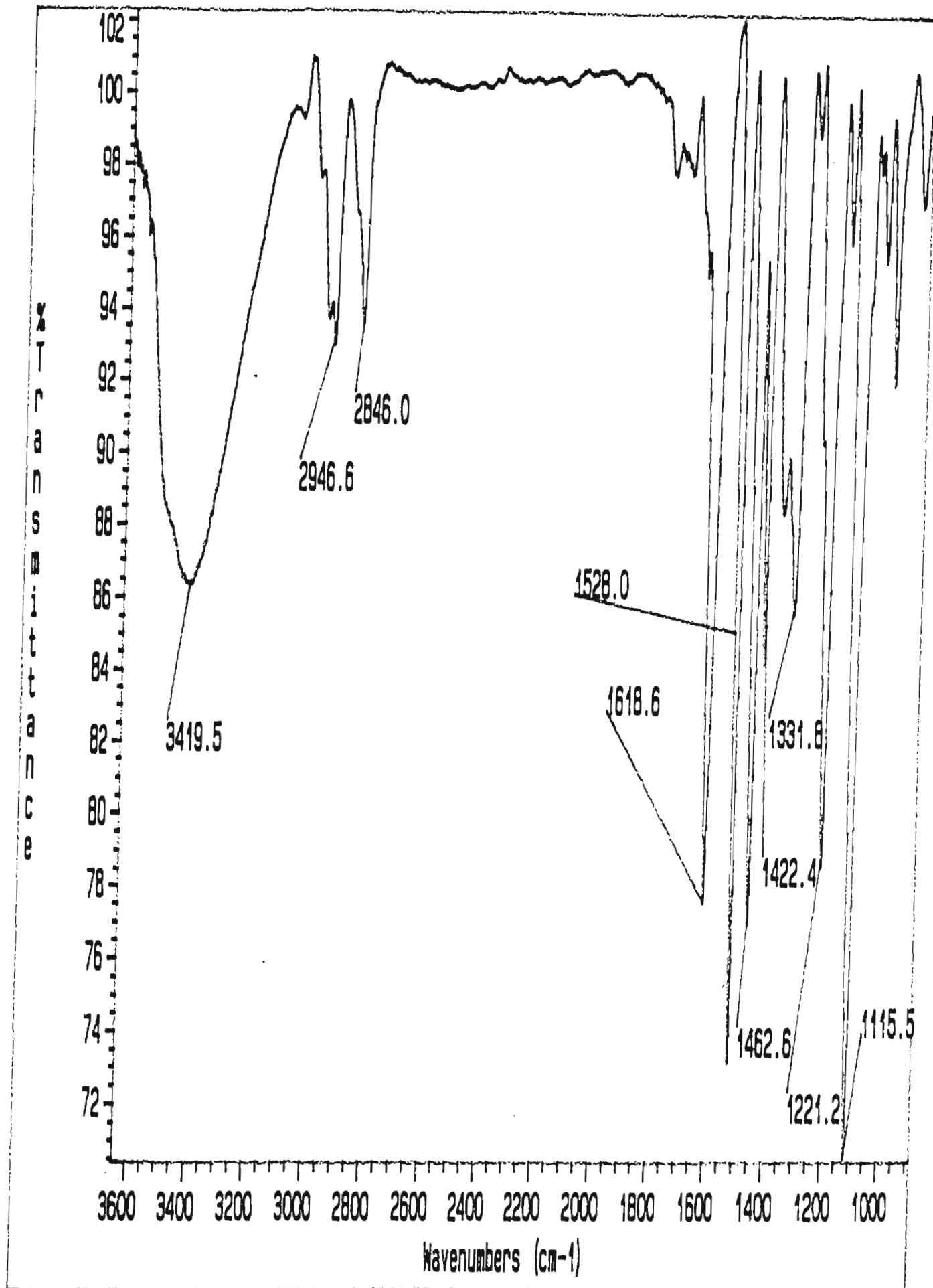


SPECTRUM 11 : NOESY NMR spectrum of compound 2, enisvringaresinol, in CDCl₃

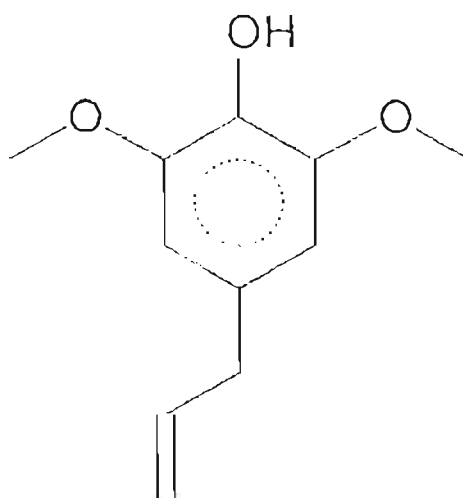
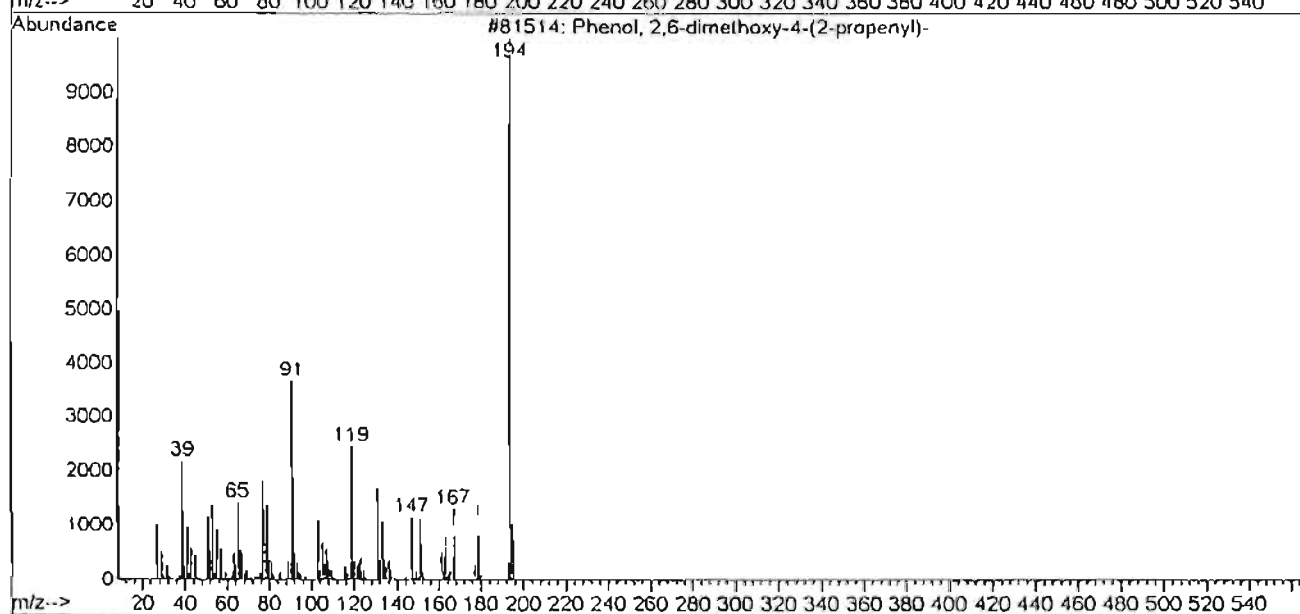
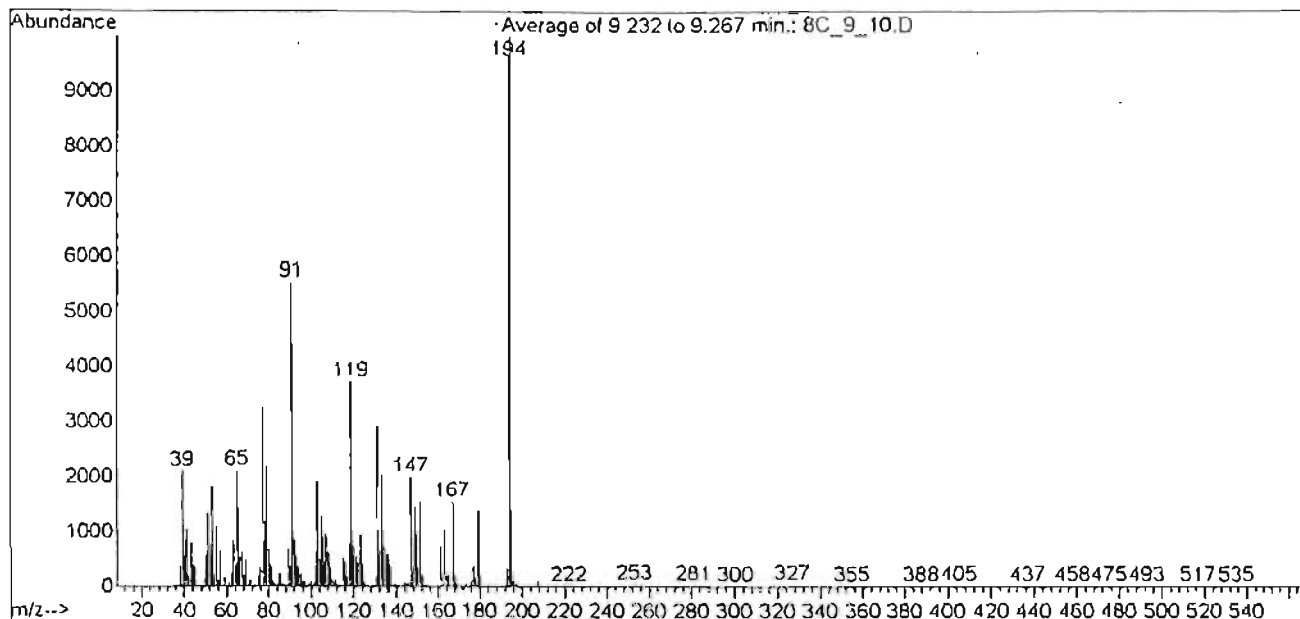
— compound 1

— compound 2

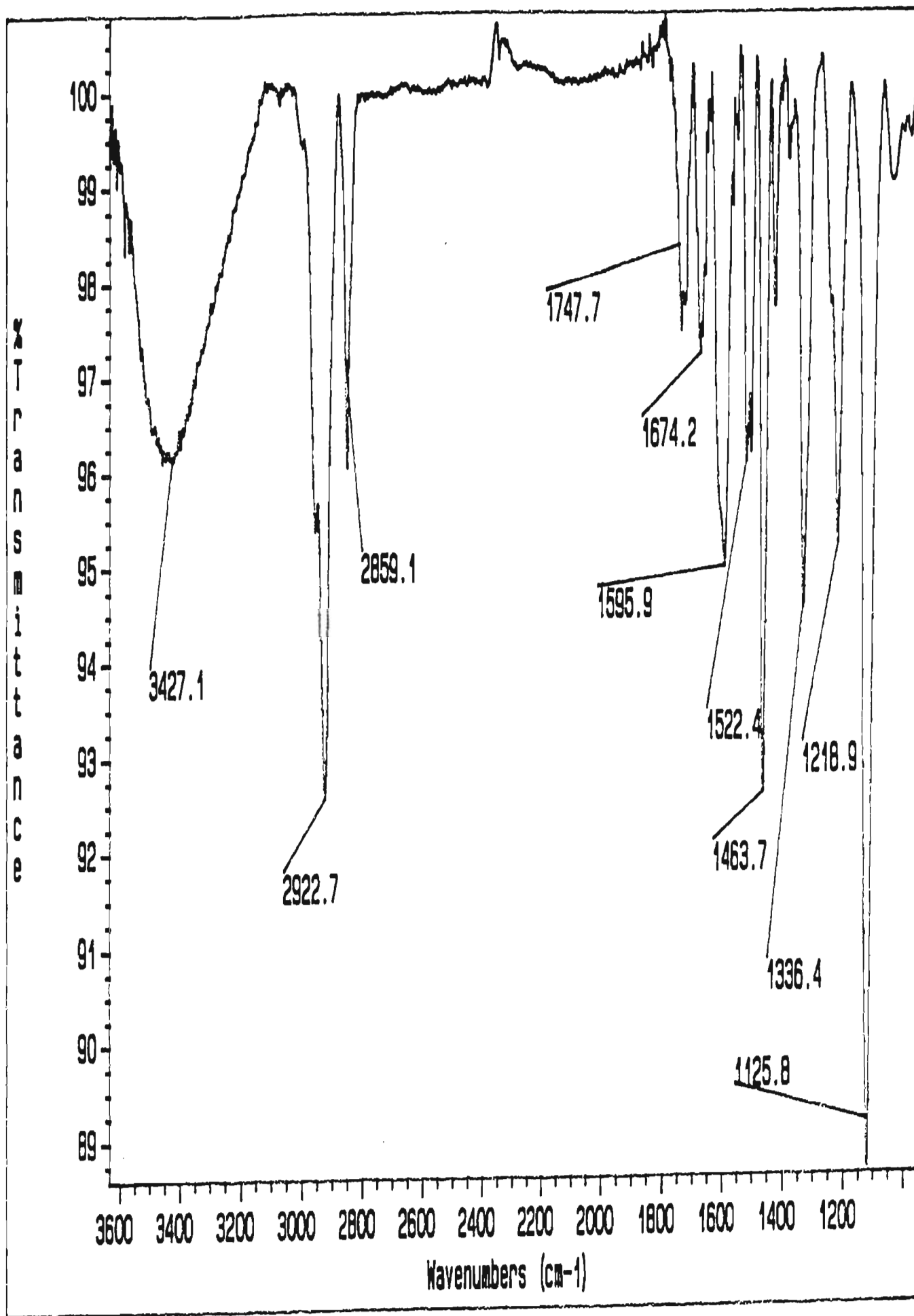




Library Searched : C:\Database\Nist98.1
Quality : 96
ID : Phenol, 2,6-dimethoxy-4-(2-propenyl)-

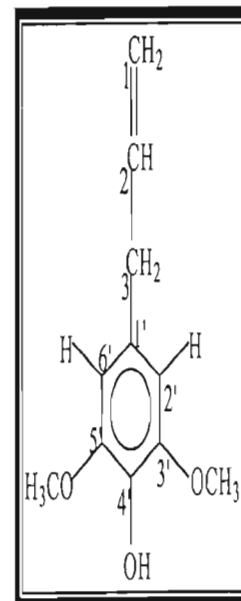


SPECTRUM 14 : Mass spectrum of compound 3, 3-(4'-hydroxy-3',5'-dimethoxyphenyl)-prop-1-ene



hsae8c.sse-8c/9-10 in cdc13
probe=5mmASW

Pulse Sequence: s2pul

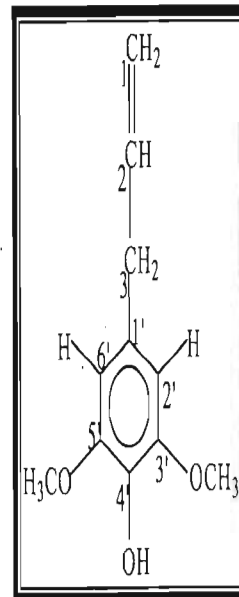


Chemical structure: (1E)-1-(4-hydroxy-3,5-dimethoxyphenyl)prop-1-ene in CDCl₃

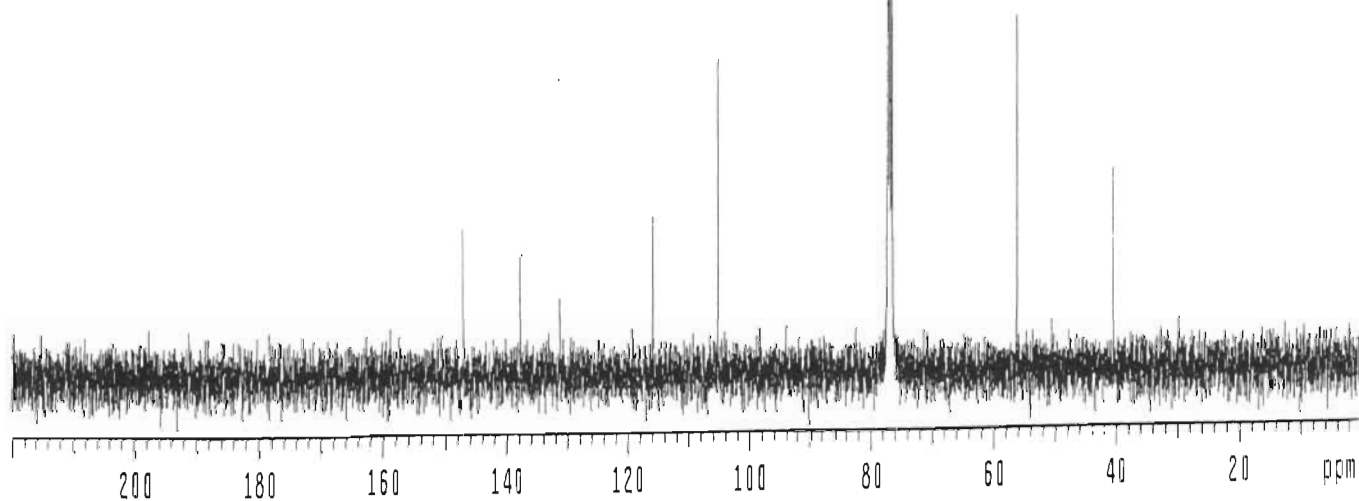
csse8c.sse-8c/9-10 In cdc13
probe=5mmASW

Pulse Sequence: s2pul

INDEX	FREQUENCY	PPM	HEIGHT
1	14777.951	146.948	12.9
2	13835.313	137.575	10.6
3	13181.889	131.077	6.9
4	11637.733	115.723	13.8
5	10568.195	105.087	27.2
6	7775.694	77.320	959.0
7	7764.158	77.205	58.3
8	7743.559	77.000	1000.0
9	7711.423	76.680	964.9
10	5654.745	56.229	30.7
11	4055.382	40.326	17.6



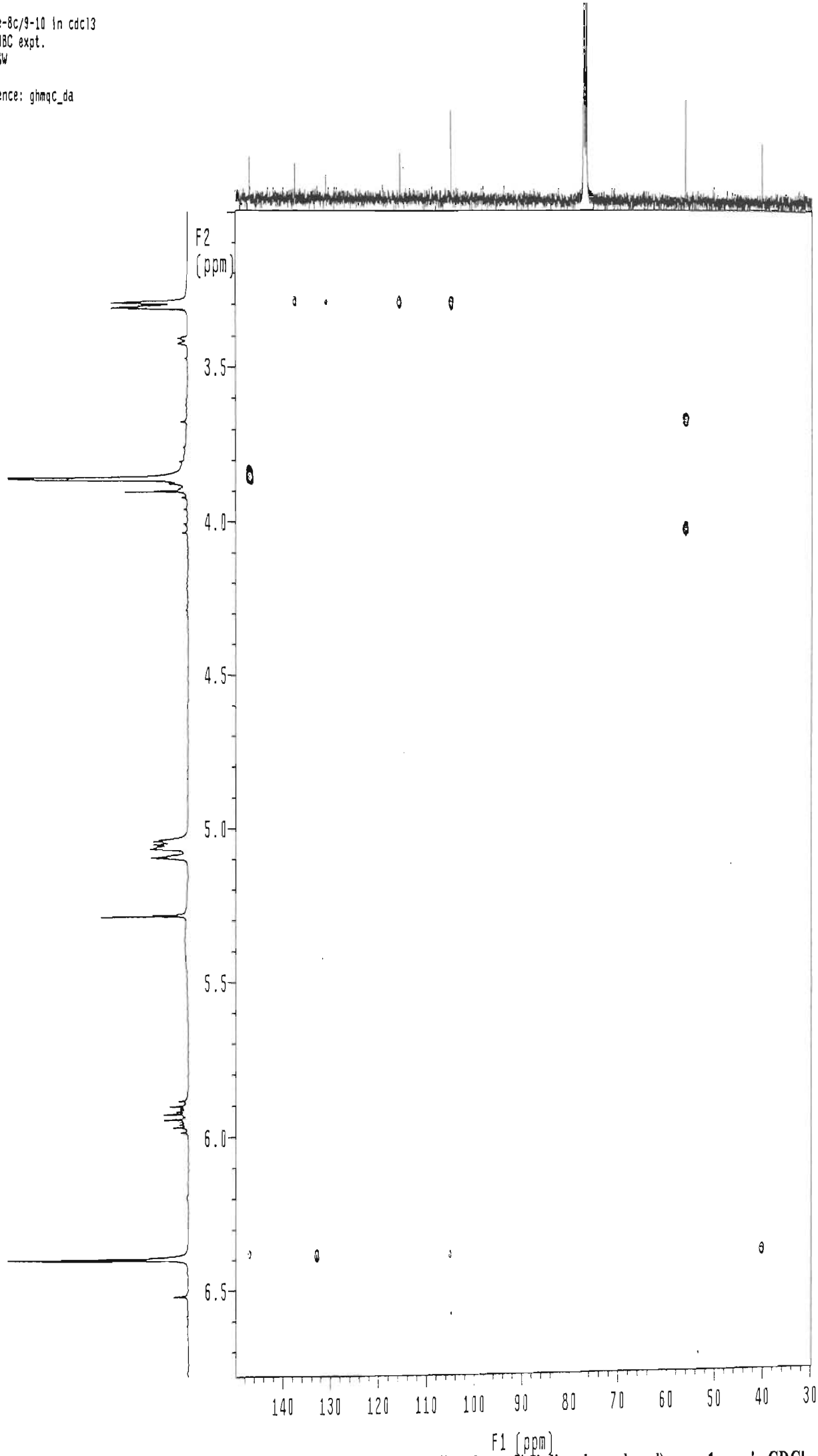
147



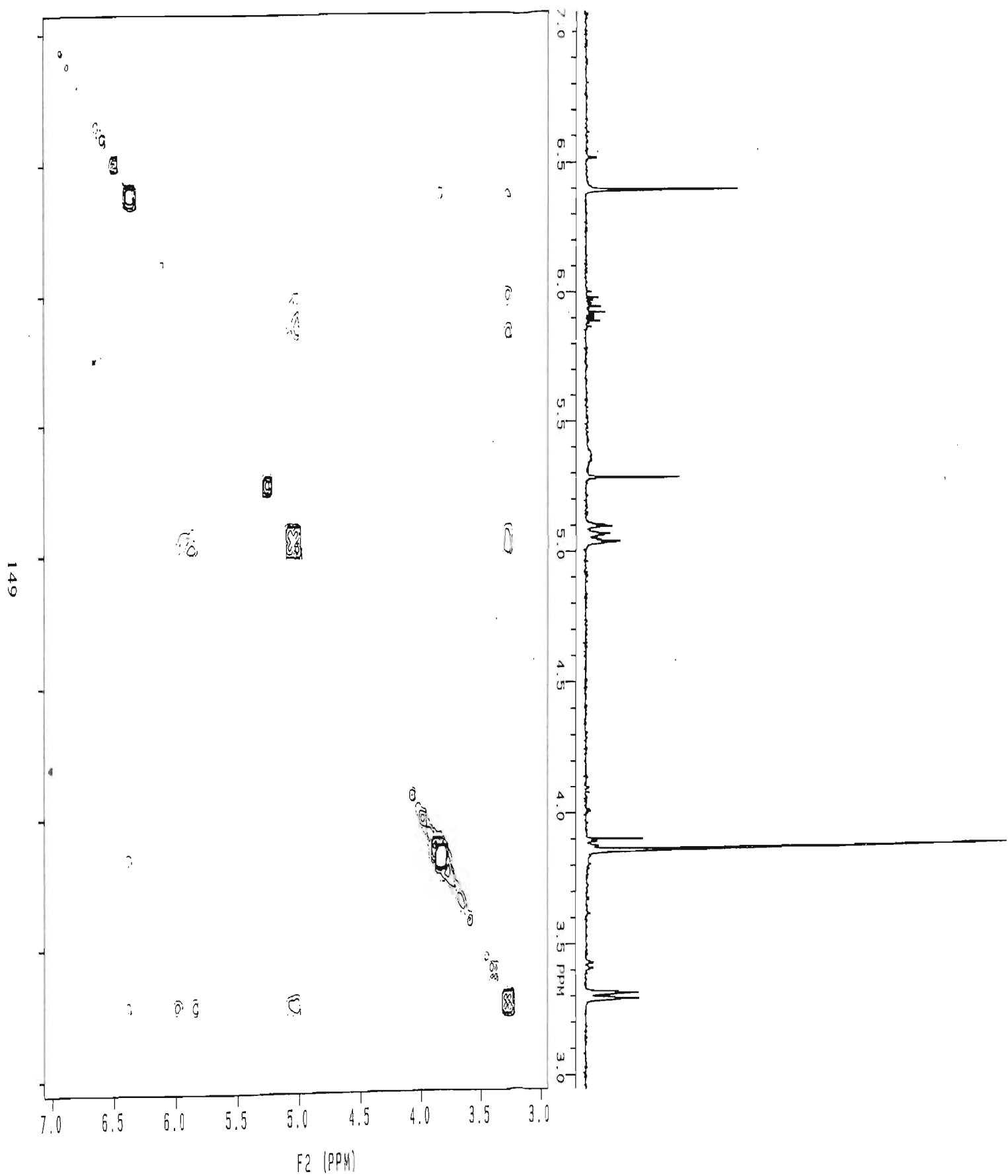
H8sse8c.sse-8c/9-10 in cdc13
Gradient HMBc expt.
probe=5mmASW

Pulse Sequence: ghmqc_da

148

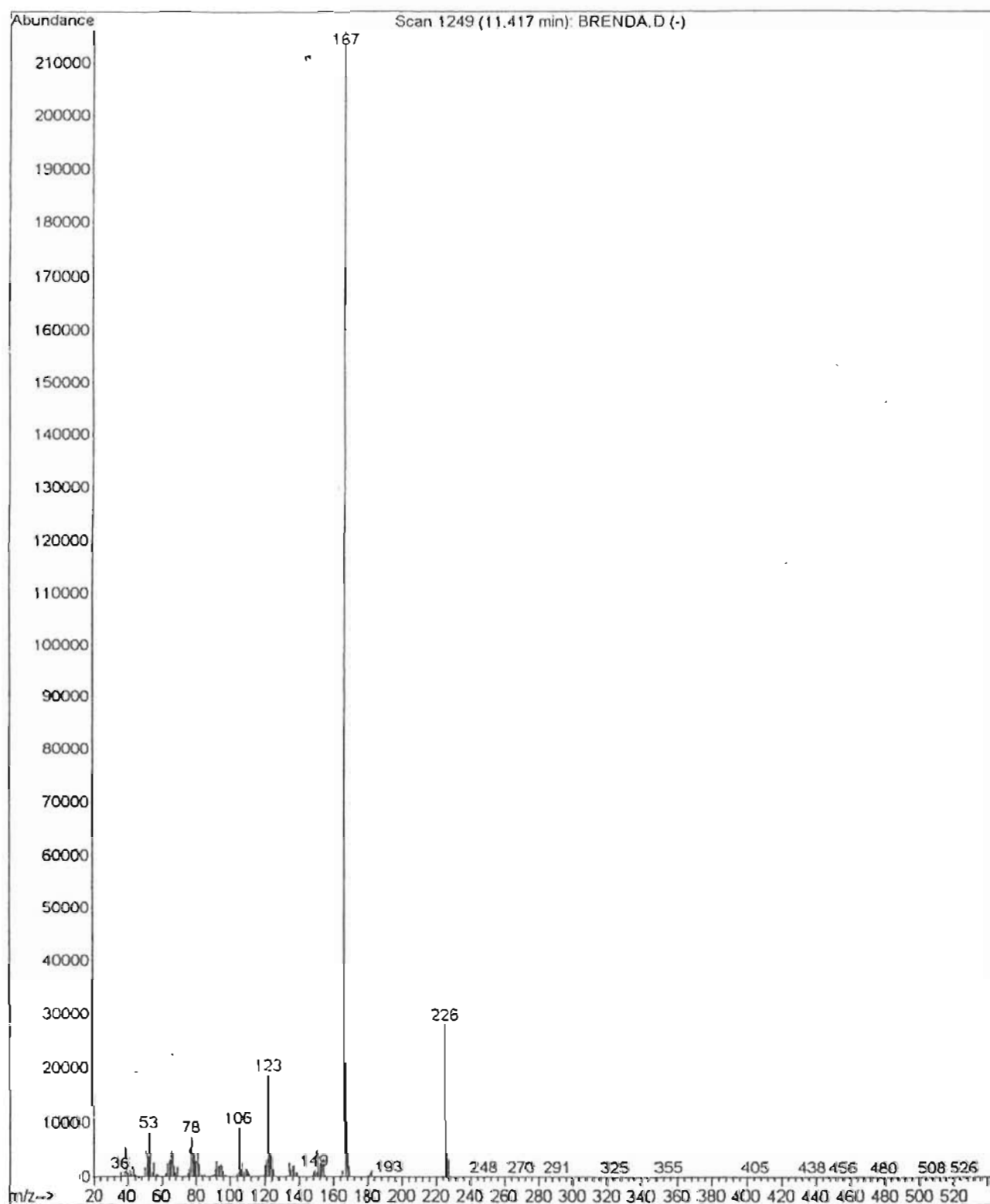


SPECTRUM 18 : HMBC NMR spectrum of compound 3, 3-(4'-hydroxy-3',5'-dimethoxyphenyl)-prop-1-ene, in CDCl₃

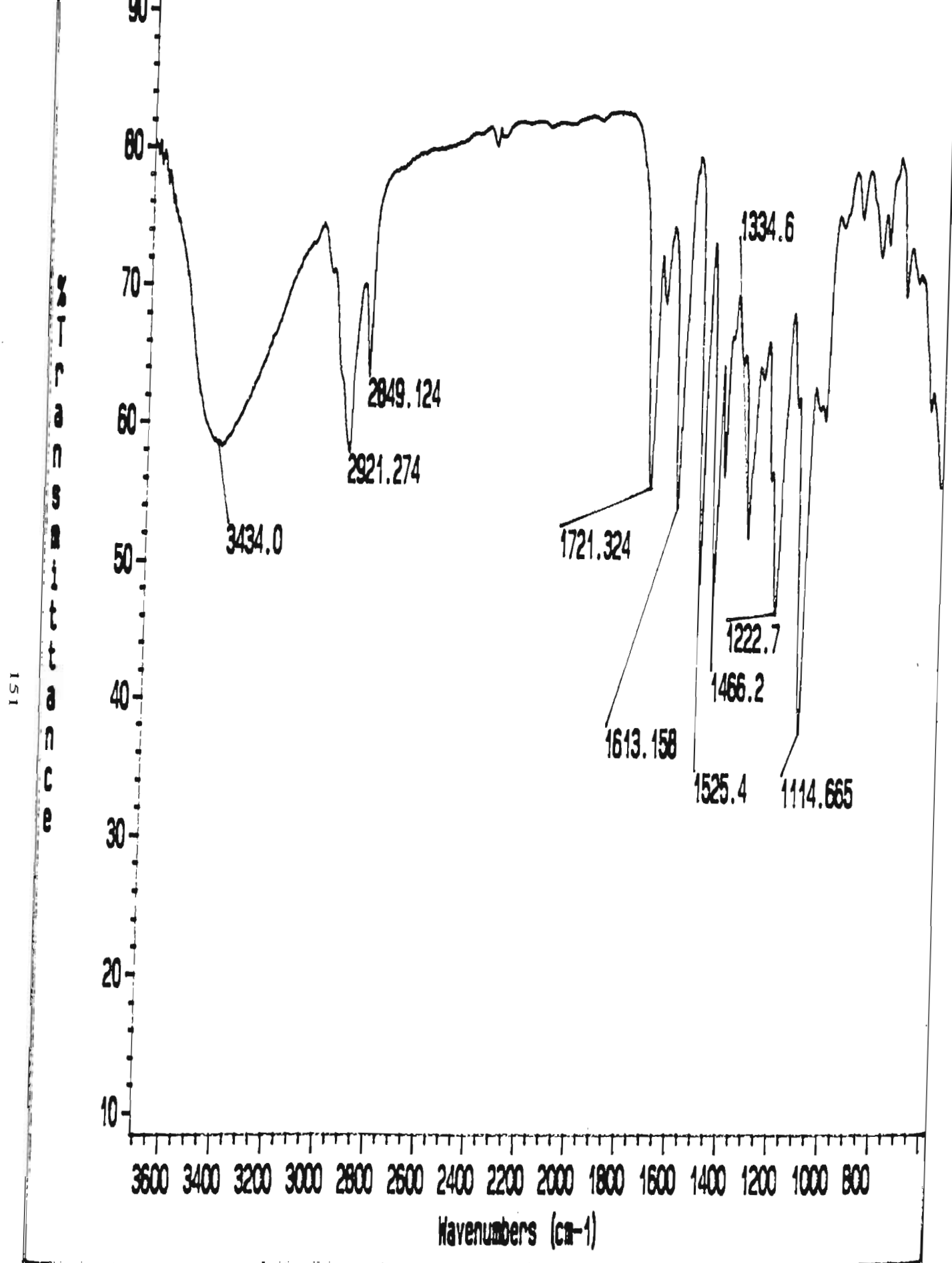


SPECTRUM 19 : COSY NMR spectrum of compound 3, 3-(4'-hydroxy-3',5'-dimethoxyphenyl)-prop-1-ene, in CDCl₃

Instrument : Instrumen
Sample Name: Brenda
Misc Info : splitl 50:1, 1ul injection in dichloromethane
Vial Number: 10



PECTRUM 20 : Mass spectrum of compound 4, 3-(4'-hydroxy-3',5'-dimethoxyphenyl)-1-hydroxy-propan-2-one

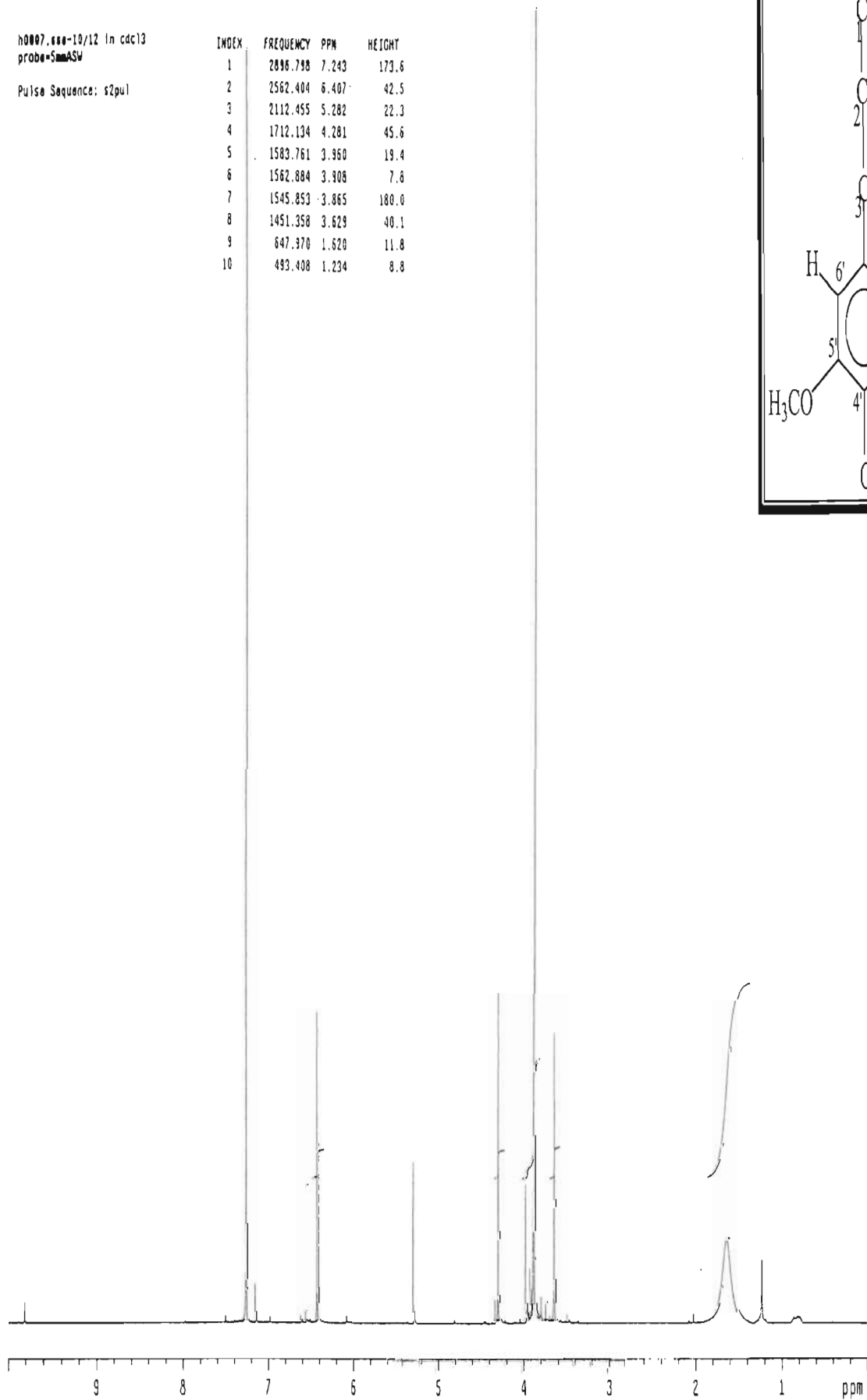
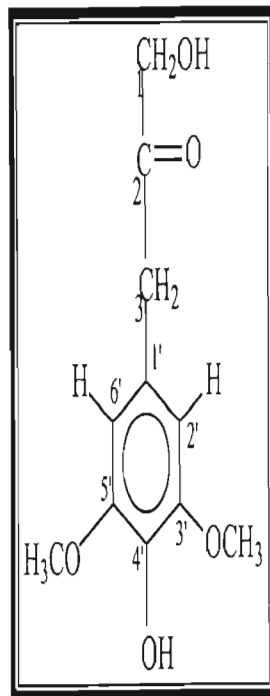


SPECTRUM 21 : Infrared spectrum of compound 4, 3-(4'-hydroxy-3',5'-dimethoxyphenyl)-1-hydroxy-propan-2-one

h0007.000-10/12 in cdc13
probe=5mmASW

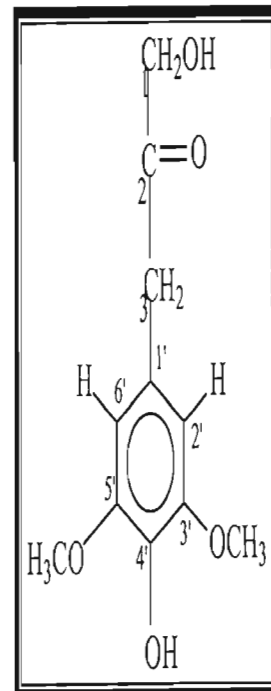
Pulse Sequence: zgpg30

INDEX	FREQUENCY	PPM	HEIGHT
1	2896.798	7.243	173.6
2	2562.404	6.407	42.5
3	2112.455	5.282	22.3
4	1712.134	4.281	45.6
5	1583.761	3.960	19.4
6	1562.884	3.908	7.8
7	1545.853	3.865	180.0
8	1451.358	3.629	40.1
9	647.370	1.620	11.8
10	493.408	1.234	8.8

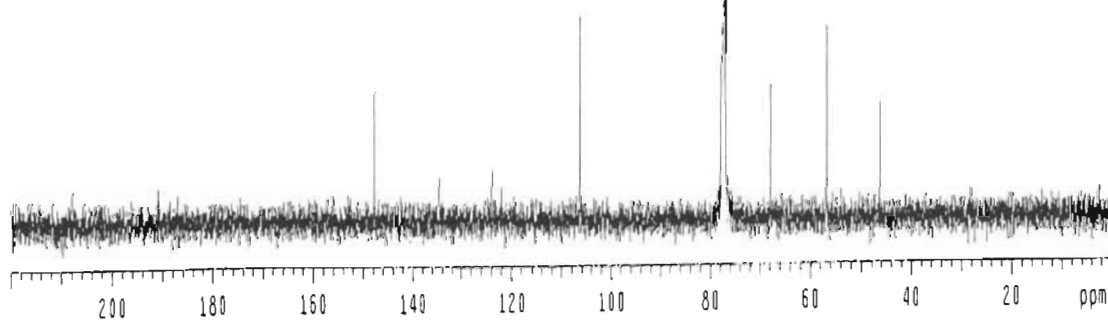


cd007.ssa-10/12 in cdcl3
 probe=5mmASW
 Pulse Sequence: s2pul

INDEX	FREQUENCY	PPM	HEIGHT
1	14832.784	147.491	14.1
2	13513.331	134.371	5.0
3	12448.063	123.779	5.6
4	10674.534	106.143	22.1
5	7717.897	77.539	1179.5
6	7786.381	77.425	49.7
7	7765.816	77.220	1200.0
8	7733.734	76.901	1149.8
9	6805.018	67.666	14.6
10	5688.748	56.567	20.6
11	4639.931	46.138	13.0



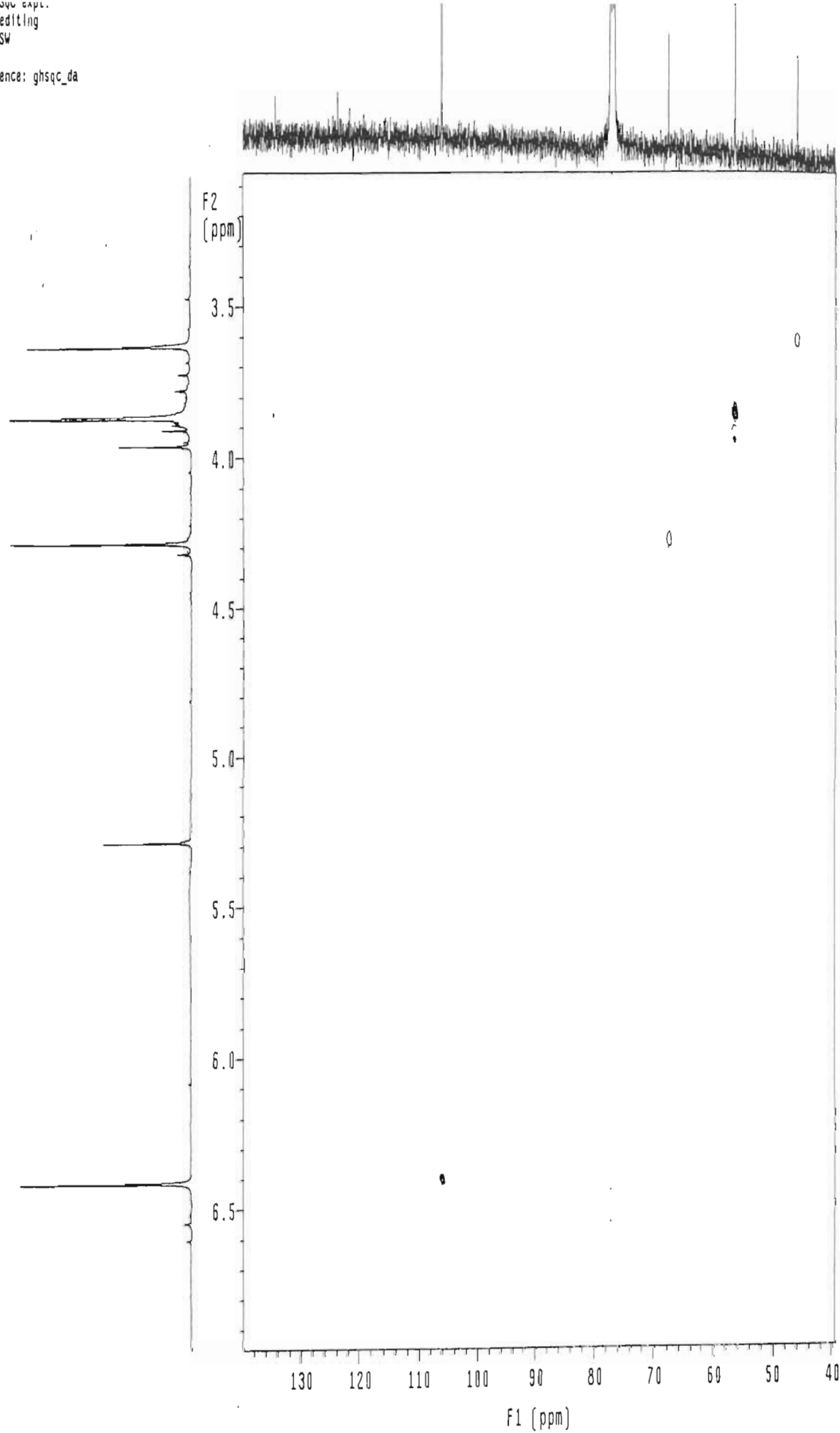
153



gradient hsqc expt.
with mult.editing
probe=5mmASW

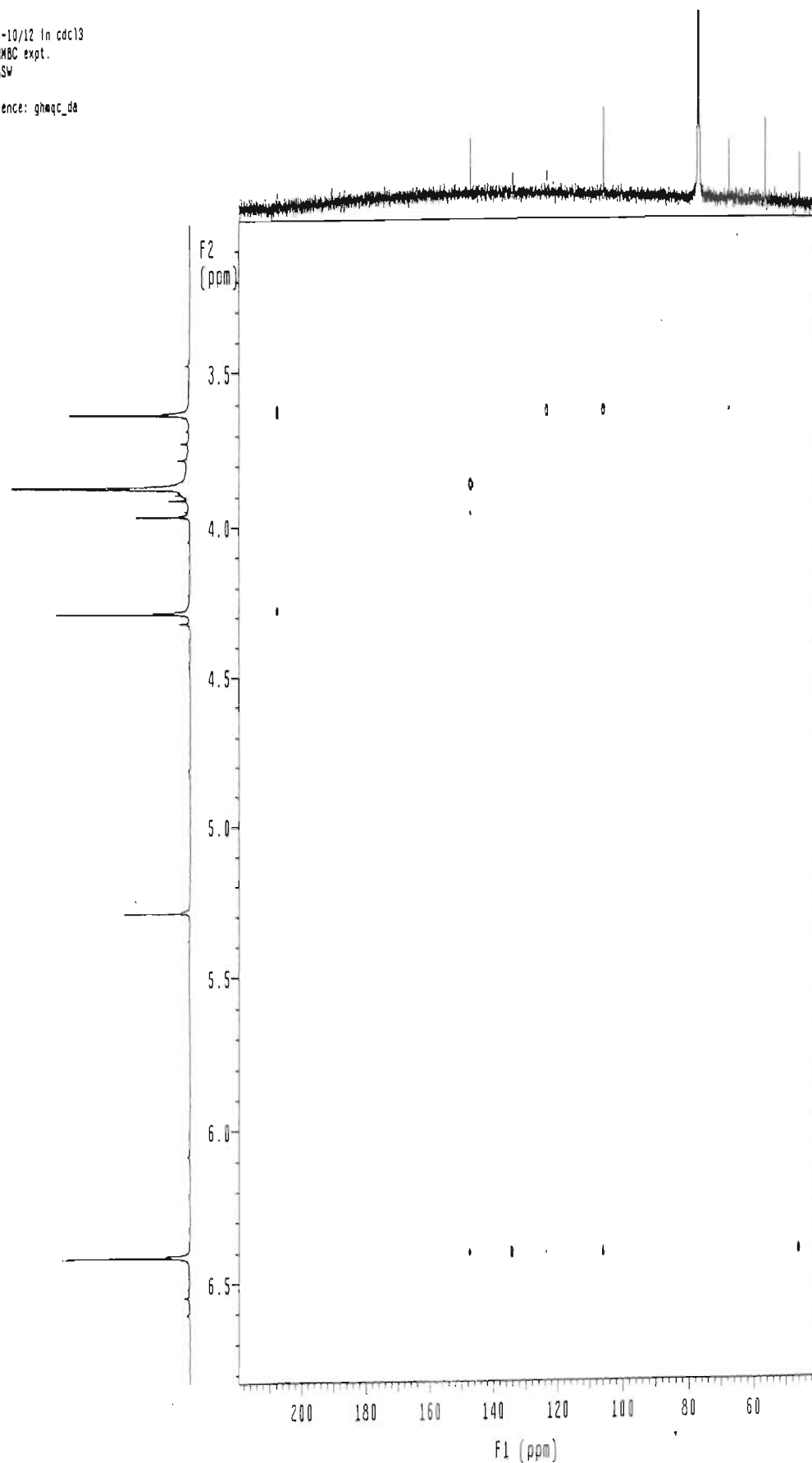
Pulse Sequence: ghsqc_da

154



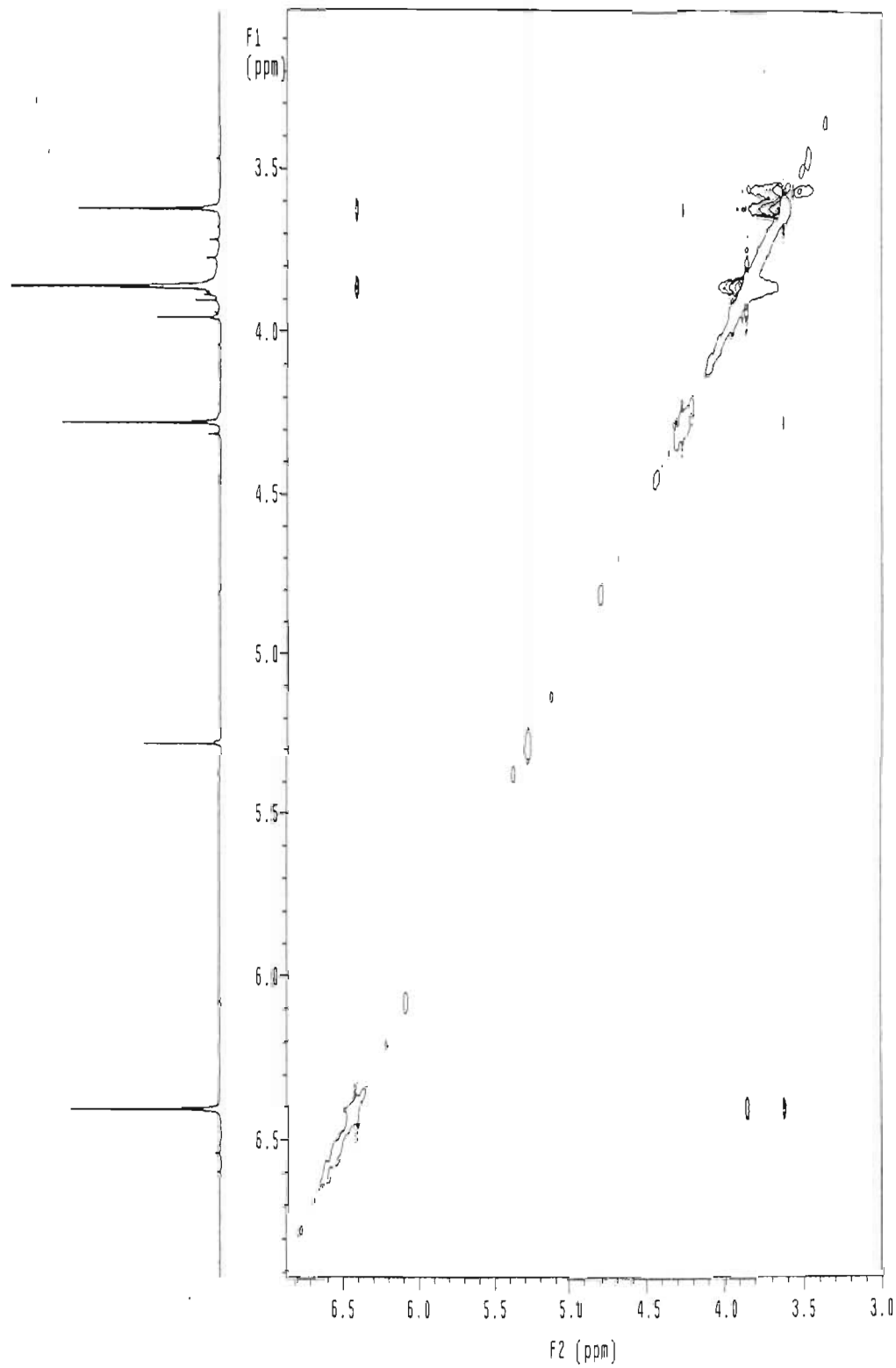
HB0007.sse-10/12 in cdcl3
Gradient HMBC expt.
probe=5mmASW
Pulse Sequence: ghmqc_de

155



NO0007.558-14/12 in cdcl3
Gradient NOESY expt.
mix=1sec
probe=5mmASW
Pulse Sequence: noesy_da

156

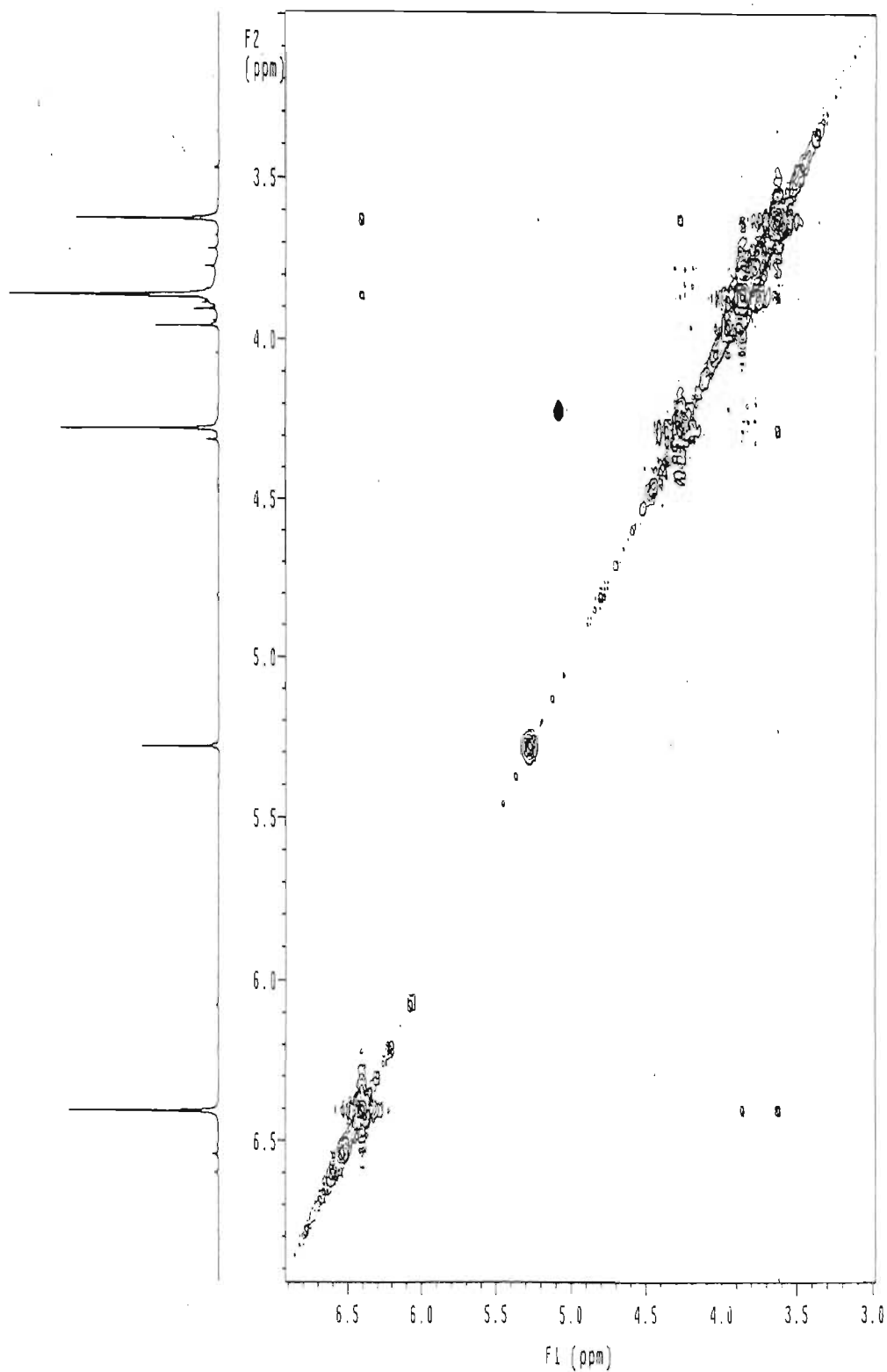


SPECTRUM 26 : NOESY NMR spectrum of compound 4, 3-(4'-hydroxy-3',5'-dimethoxyphenyl)-1-hydroxy-propan-2-one, in CDCl₃

cy0007.ssa-10/12 in cdcl3
1H Cosy-90
probe=5mmBBO

Pulse Sequence: relayh

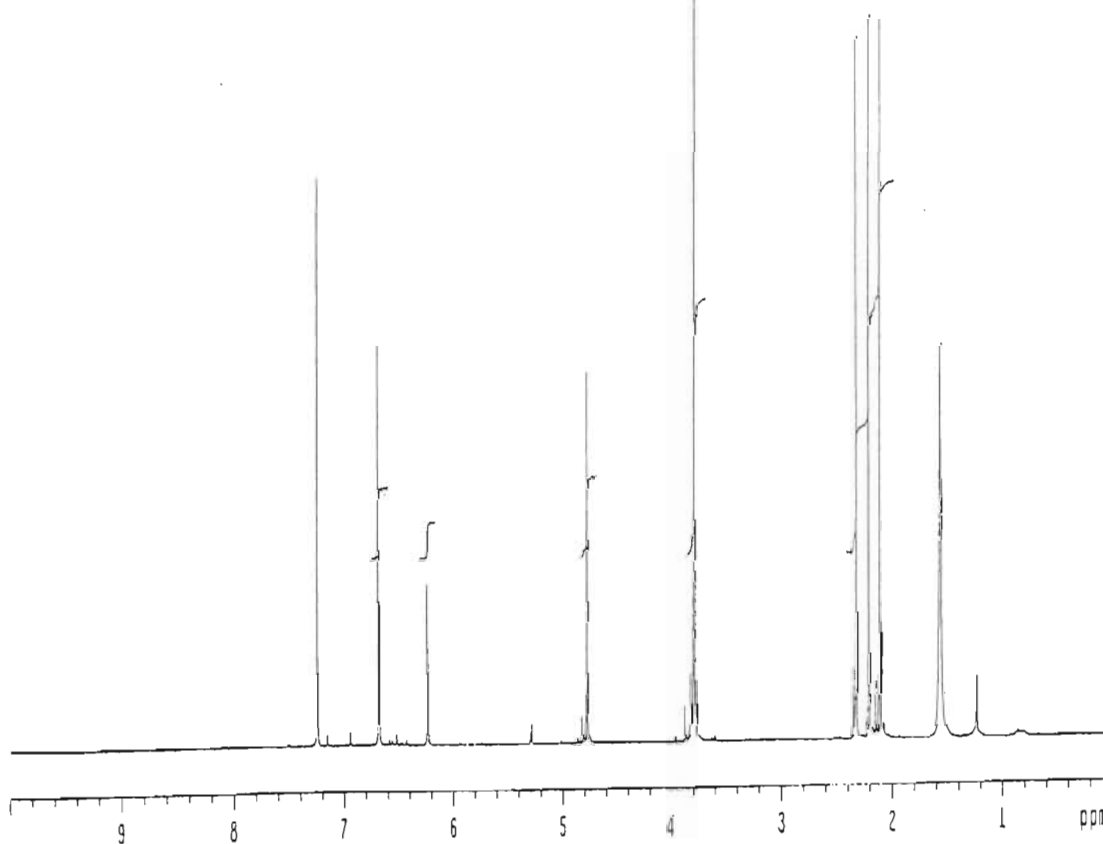
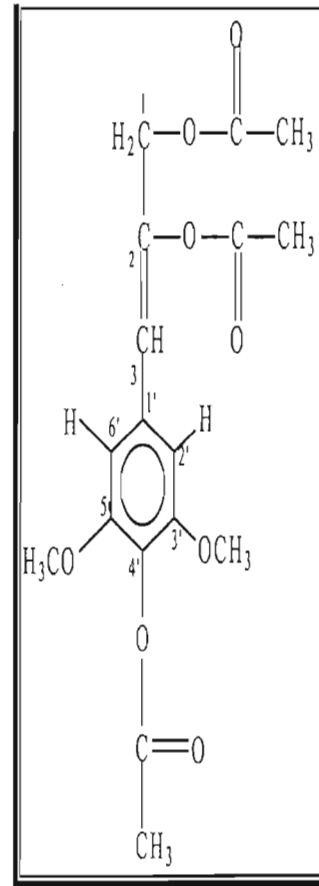
157



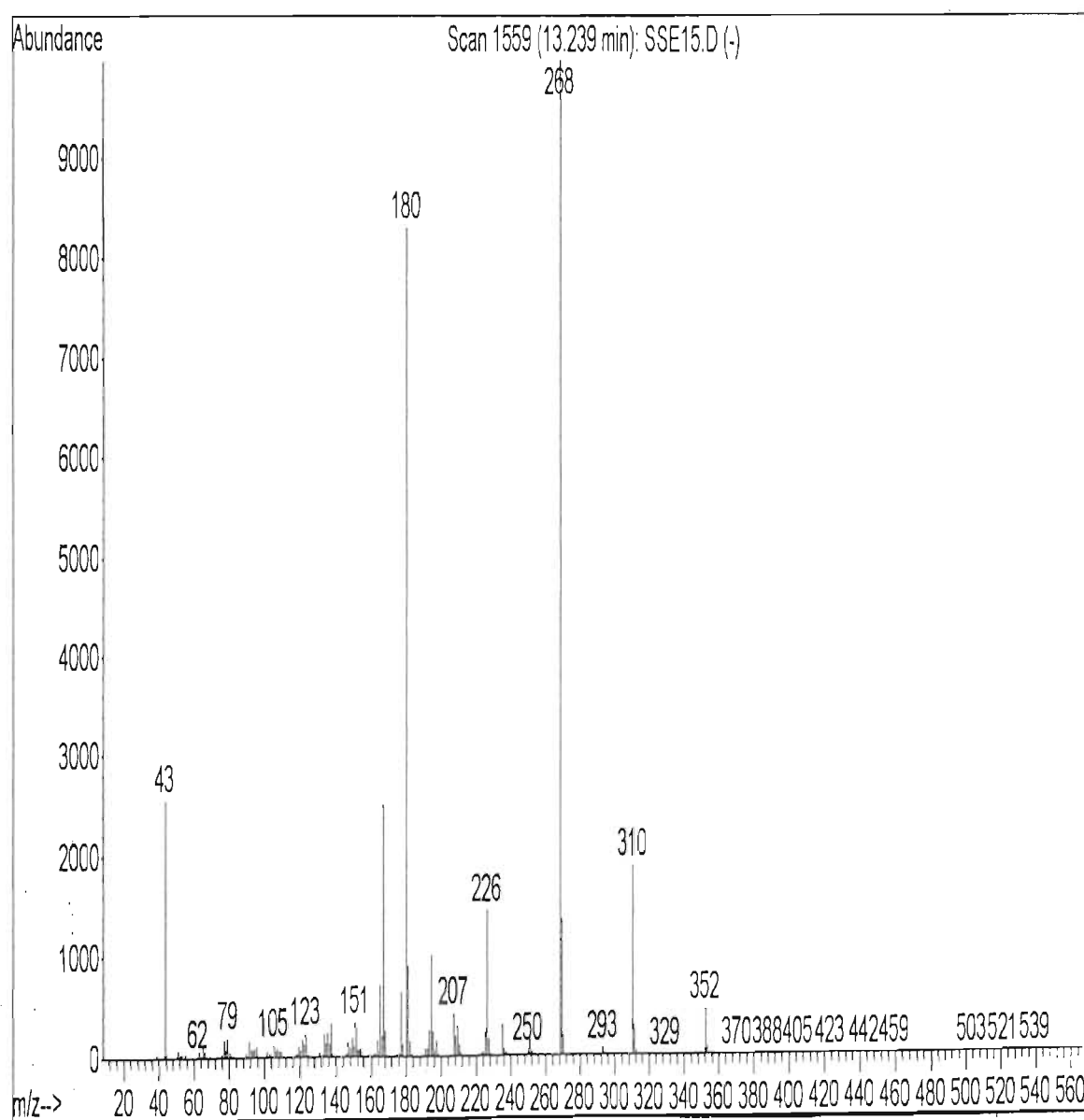
SPECTRUM 27 : COSY NMR spectrum of compound 4, 3-(4'-hydroxy-3',5'-dimethoxyphenyl)-1-hydroxy-propan-2-one, in CDCl₃

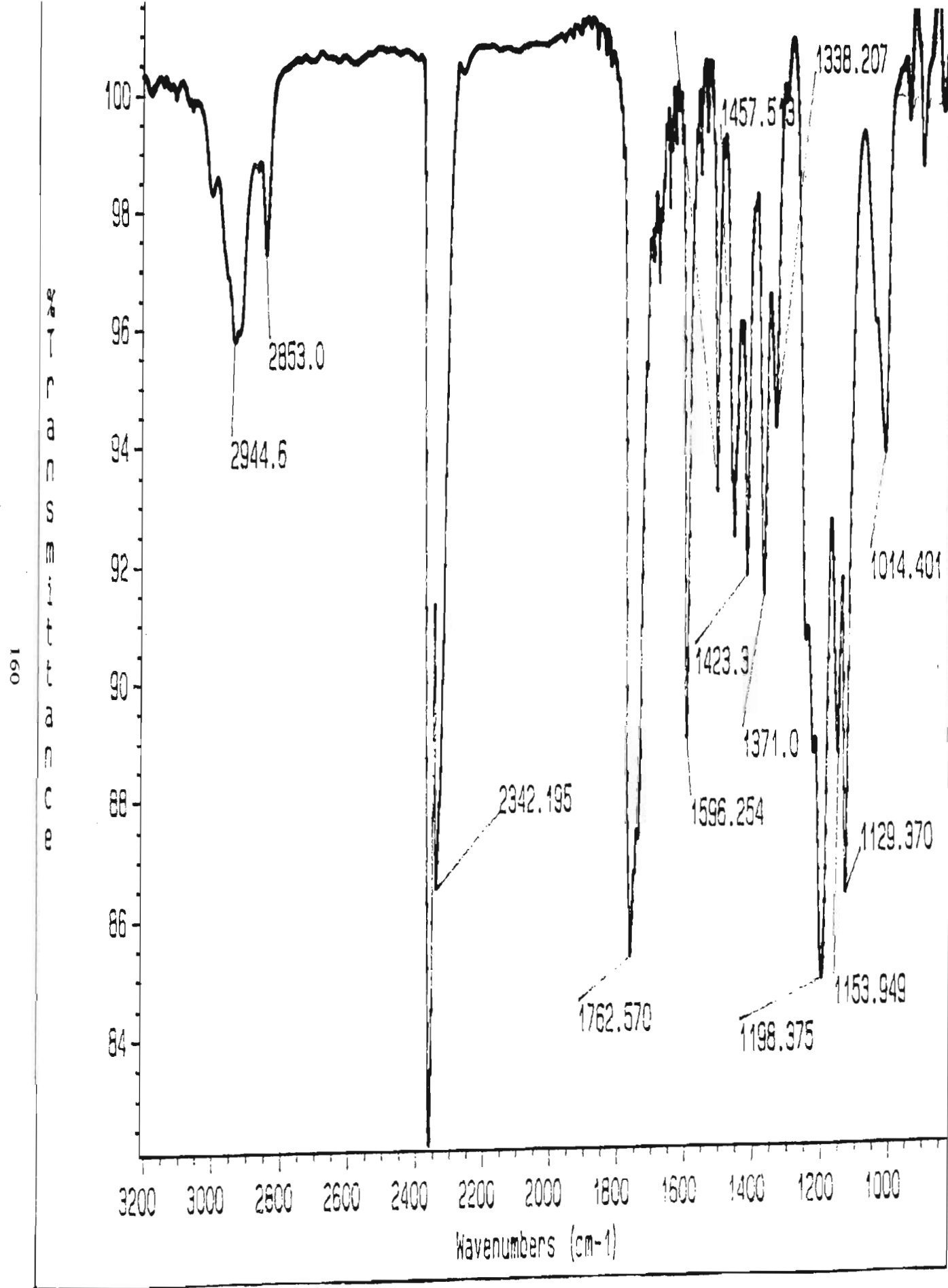
h0008.ssa-15/21-28 in cdcl3
 probe=5mmASW
 Pulse Sequence: s2pul

INDEX	FREQUENCY	PPM	HEIGHT
1	2898.615	7.242	60.5
2	2671.915	6.681	42.6
3	2493.547	6.235	17.6
4	1907.350	4.769	39.8
5	1513.988	3.785	150.0
6	925.044	2.313	75.1
7	879.628	2.199	77.5
8	839.523	2.099	77.1
9	621.416	1.554	42.0



SPECTRUM 28 : ^1H NMR spectrum of acetylated compound 4, in CDCl_3

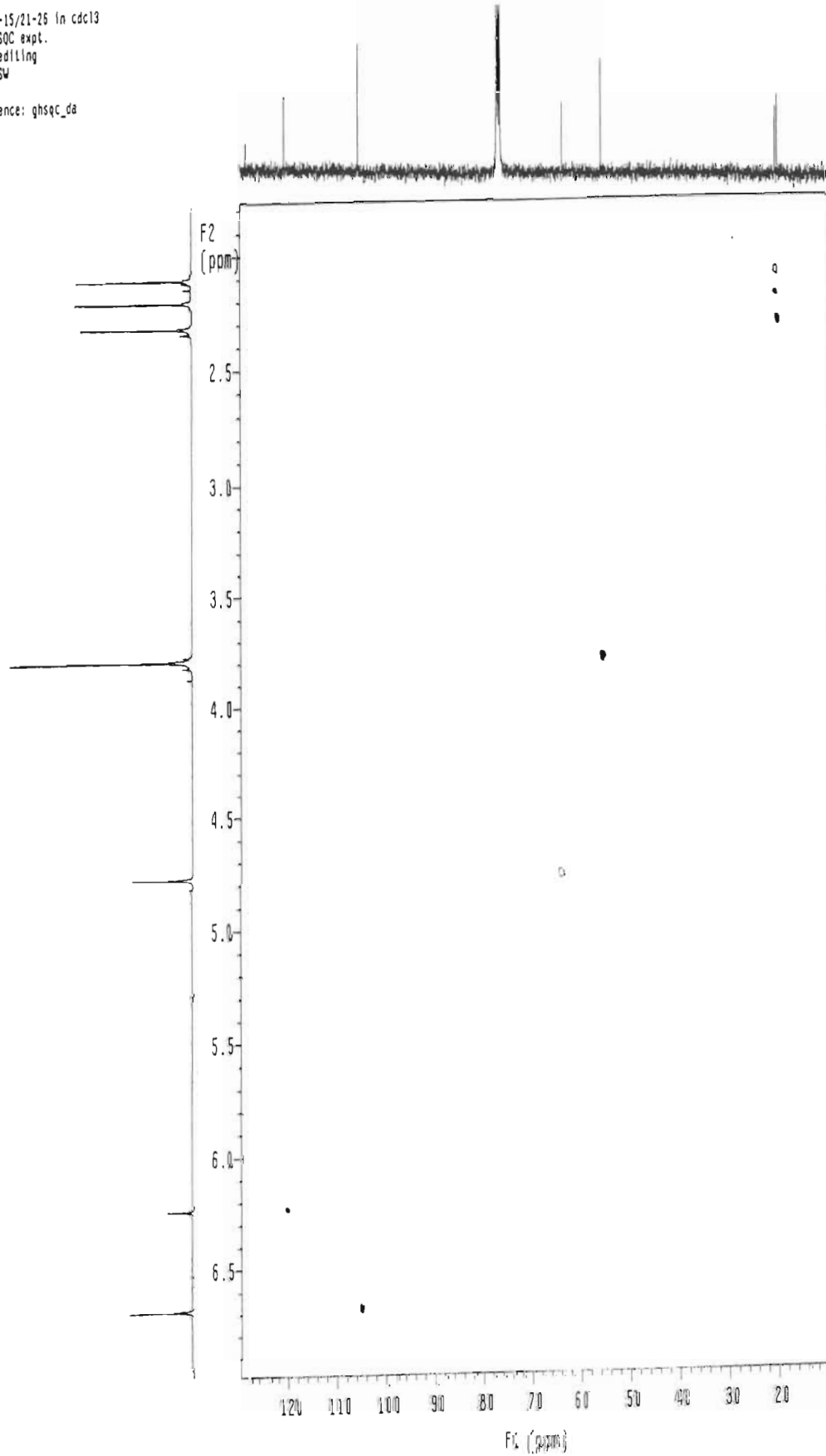




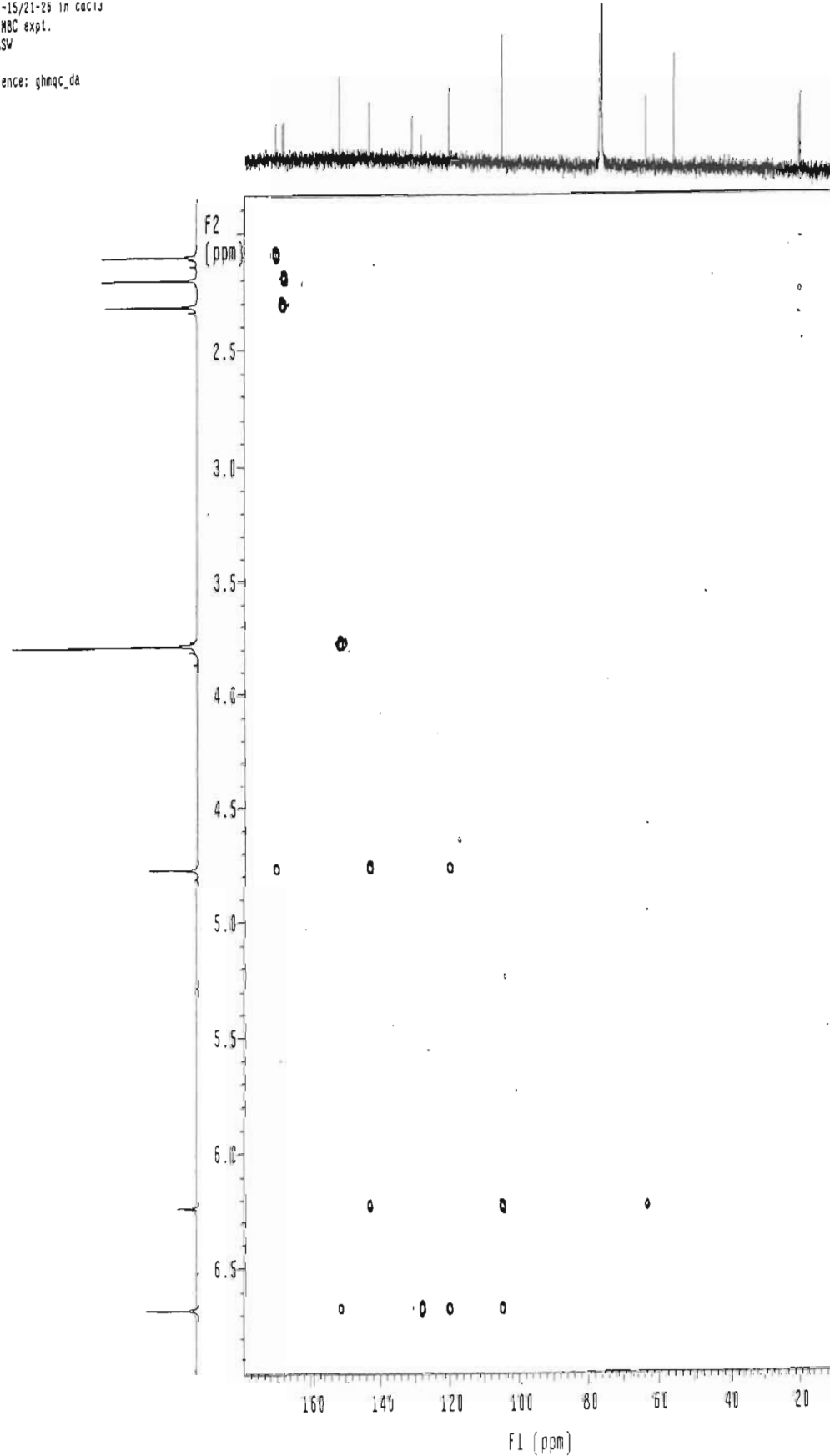
SPECTRUM 30 : Infrared spectrum of acetylated compound 4

HQ0008.sse-15/21-26 in cdcl3
Gradient HSQC expt.
with mult.editing
probe=5mmASW
Pulse Sequence: ghsqc_da

191



162

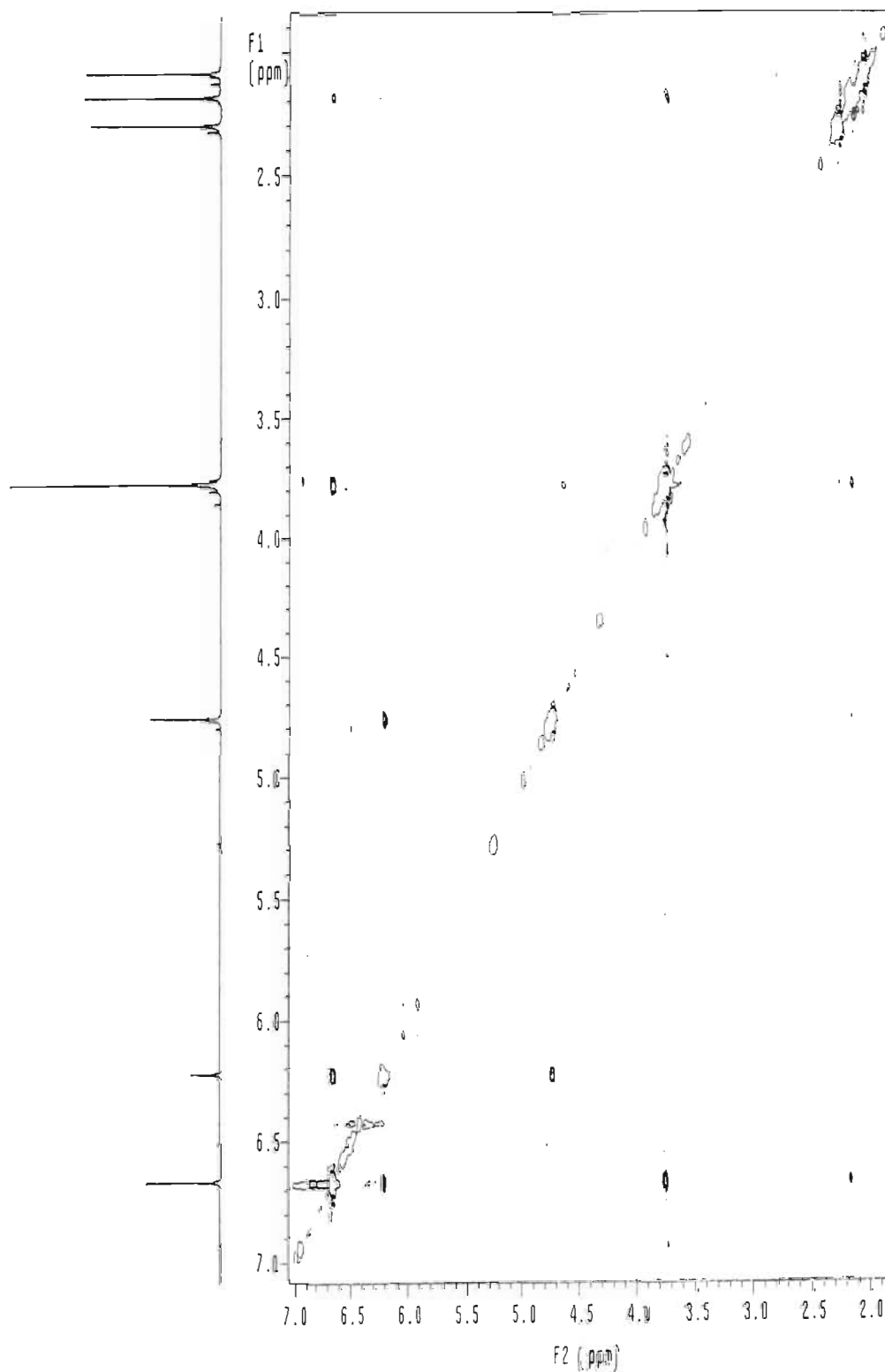


SPECTRUM 32 : HMBC NMR spectrum of acetylated compound 4, in CDCl_3

NO0008.sse-15/21-26 in cdc13
Gradient NOESY expt.
mix=1sec
probe=5mmASW
Pulse Sequence: noesy_da

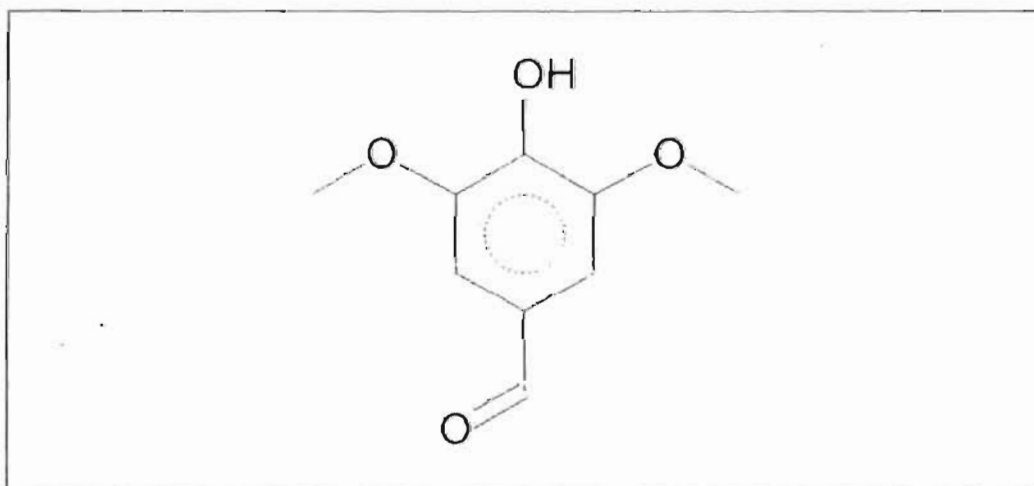
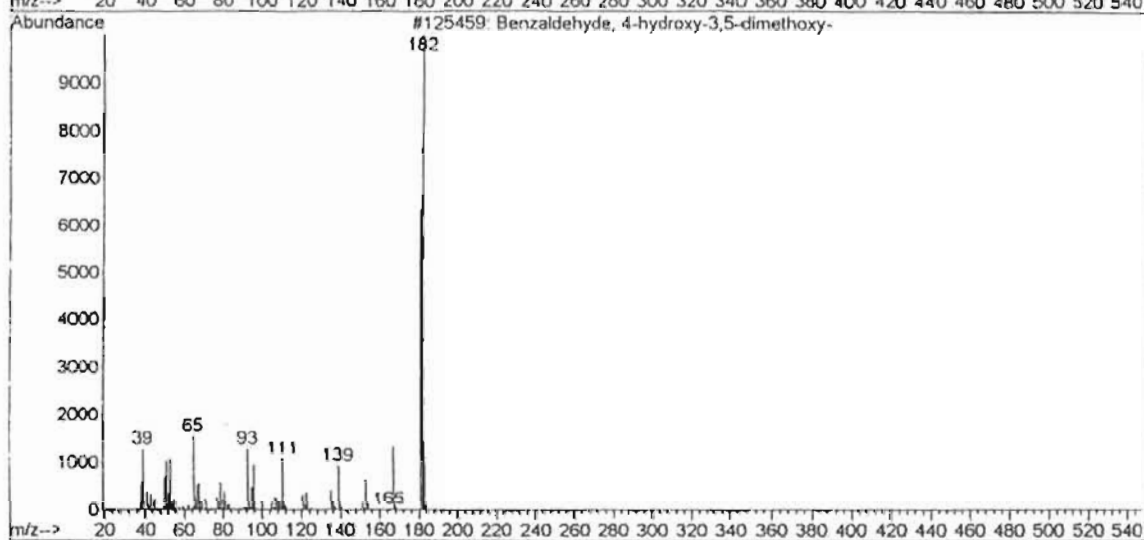
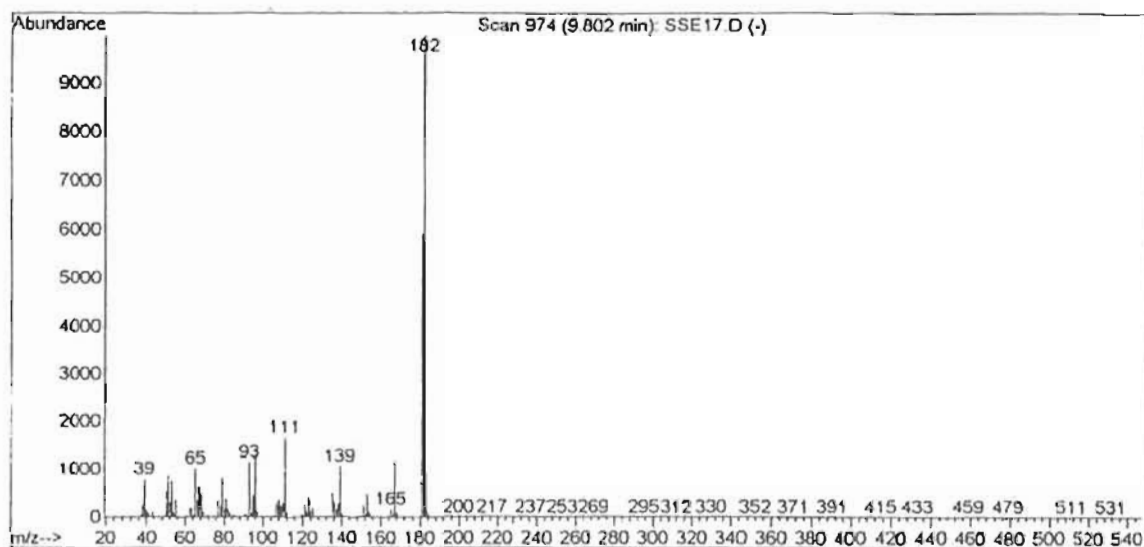


163



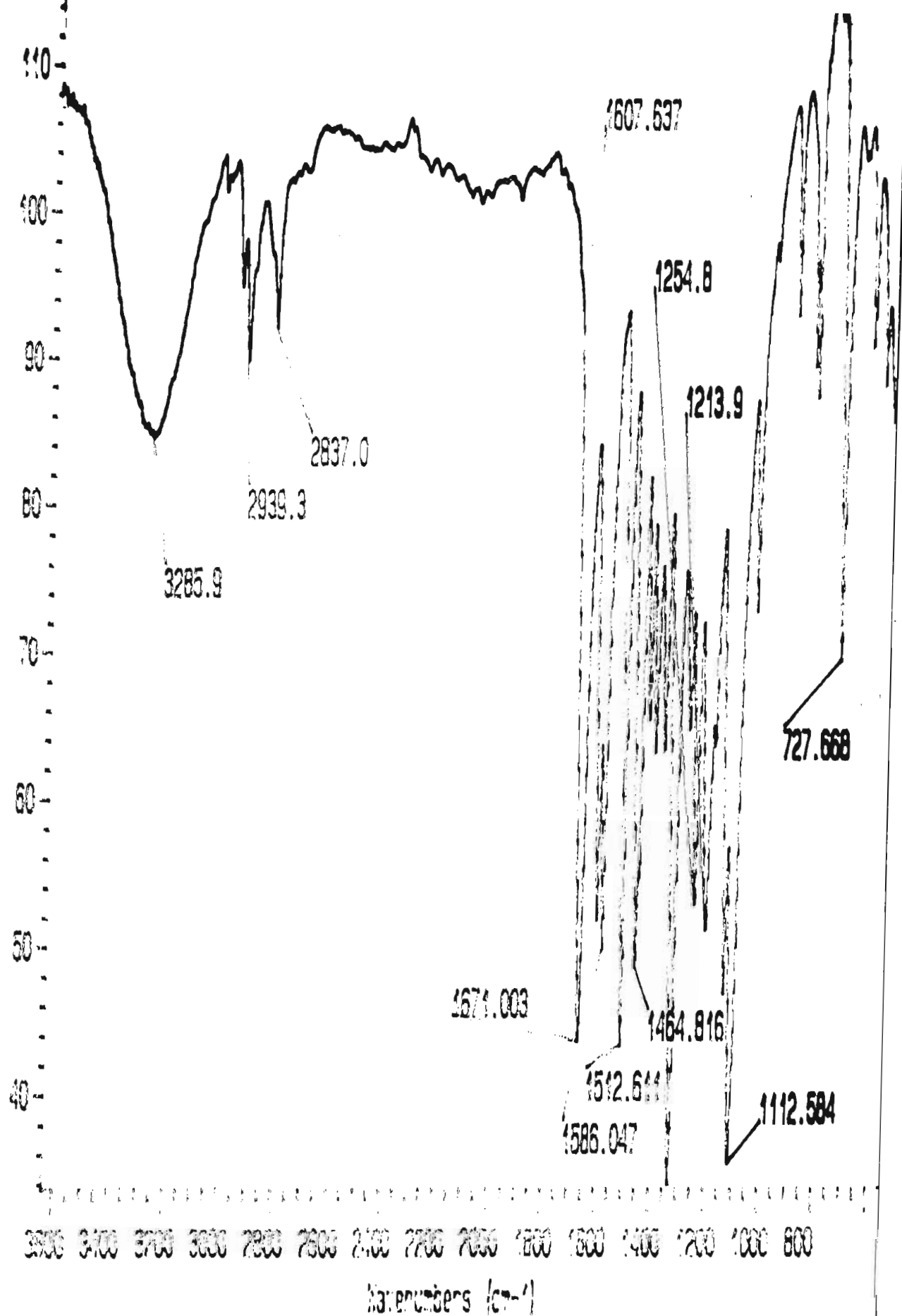
SPECTRUM 33 : NOESY NMR spectrum of acetylated compound 4, in CDCl_3

Library Searched : C:\Database\Nist98.1
Quality : 94
ID : Benzaldehyde, 4-hydroxy-3,5-dimethoxy-



SPECTRUM 34 : Mass spectrum of compound 5, syringaldehyde

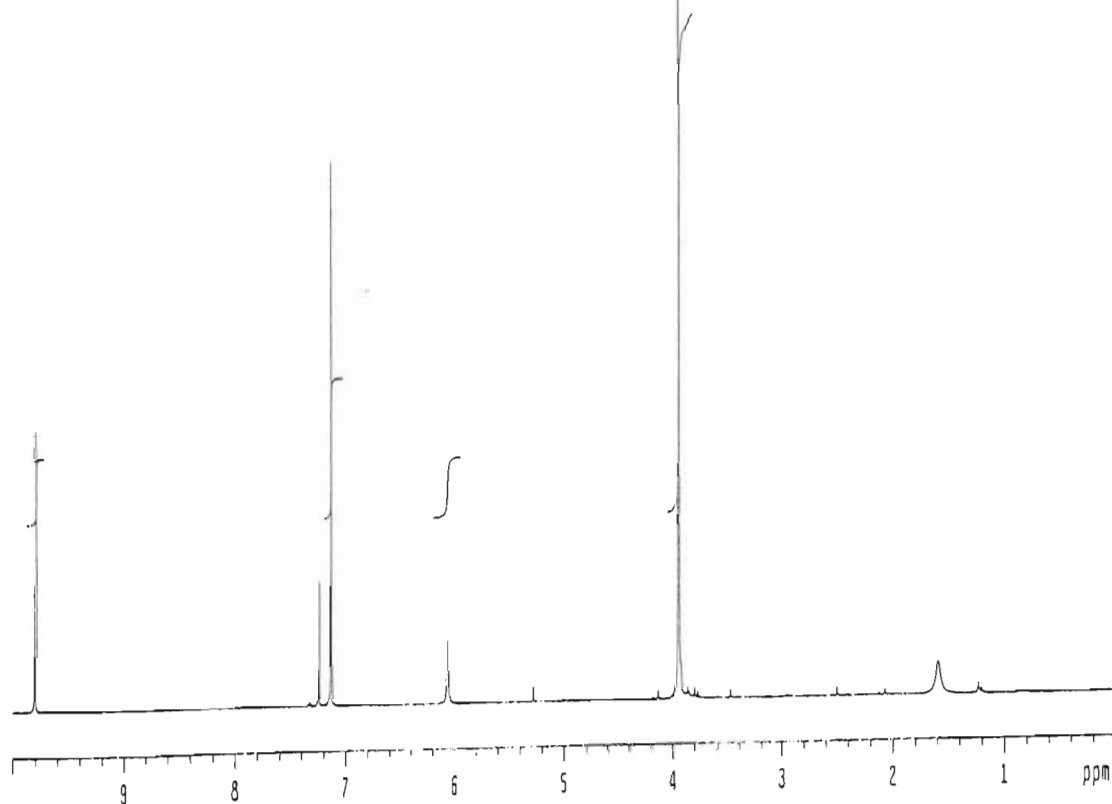
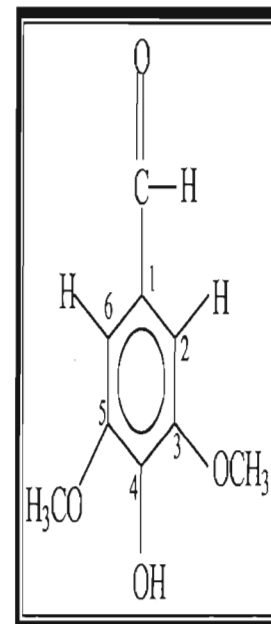
TRANSMITTANCE



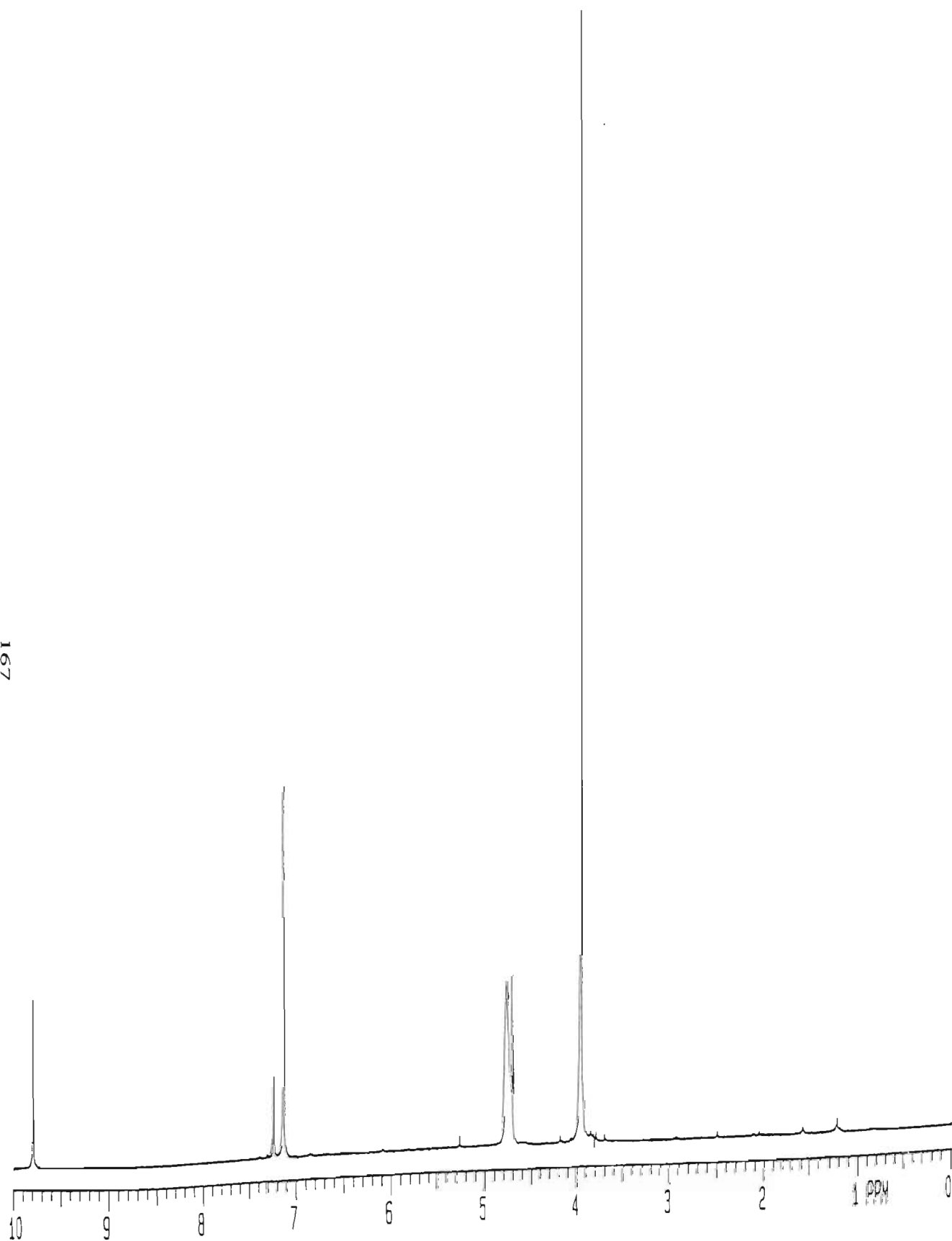
h0009.666-17/11-20 In cdc13
probe=5mmASW

Pulse Sequence: s2pul

INDEX	FREQUENCY	PPM	HEIGHT
1	3919.942	9.801	29.8
2	2896.798	7.243	13.3
3	2853.397	7.134	57.7
4	2424.874	6.063	6.9
5	1581.929	3.955	200.0
6	1573.689	3.935	5.1



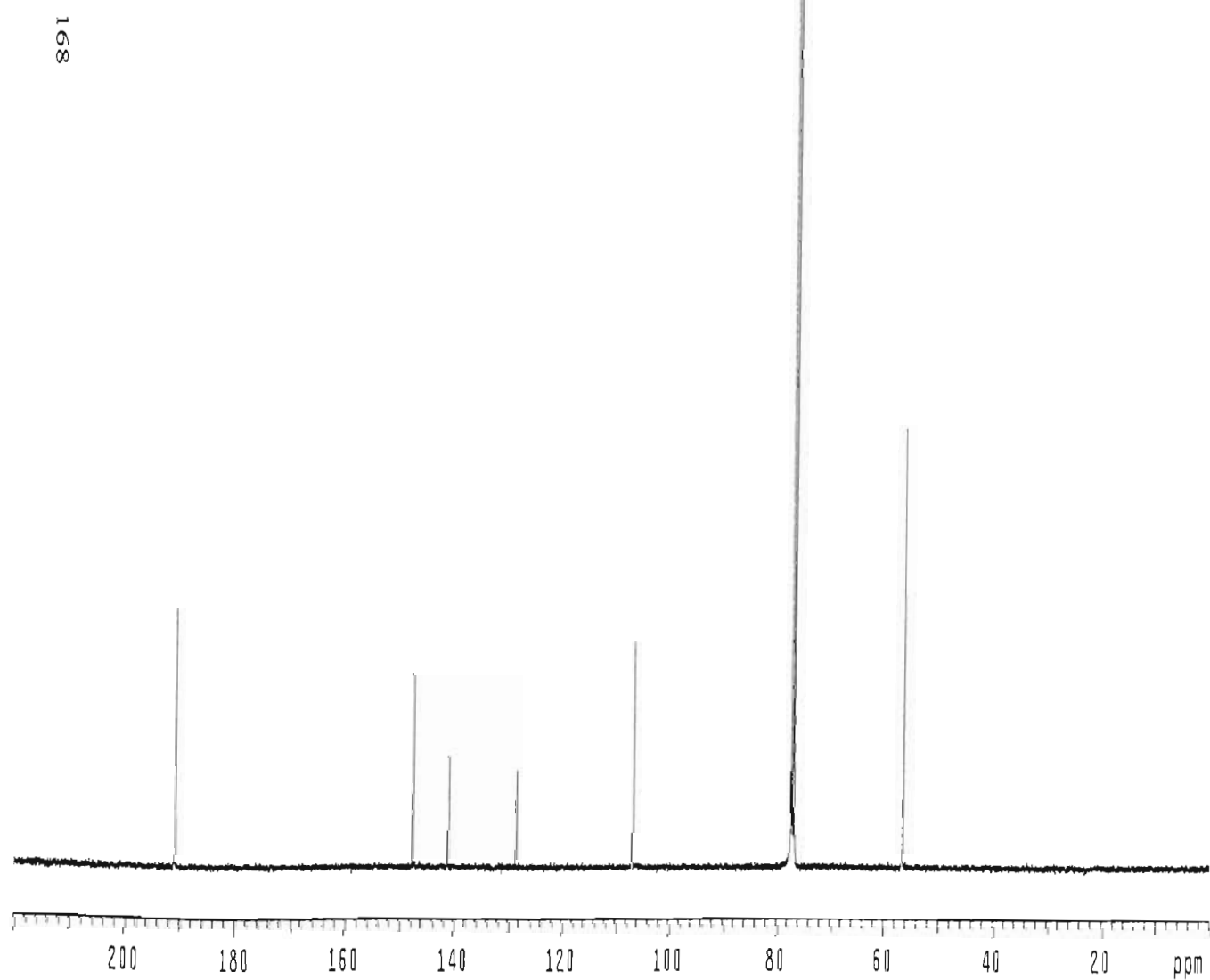
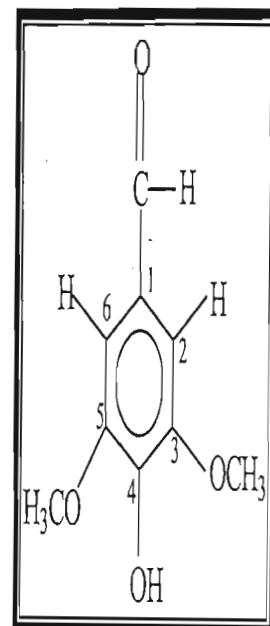
SPECTRUM 36 : ¹H NMR spectrum of compound 5, syringaldehyde, in CDCl₃

SPECTRUM 27. ^1H NMR spectrum of compound 5, cuningaldehyde, in D_2O .

c0009.ssa-17/11-20 in cdc13
probe=5mmASW

Pulse Sequence: s2pu1

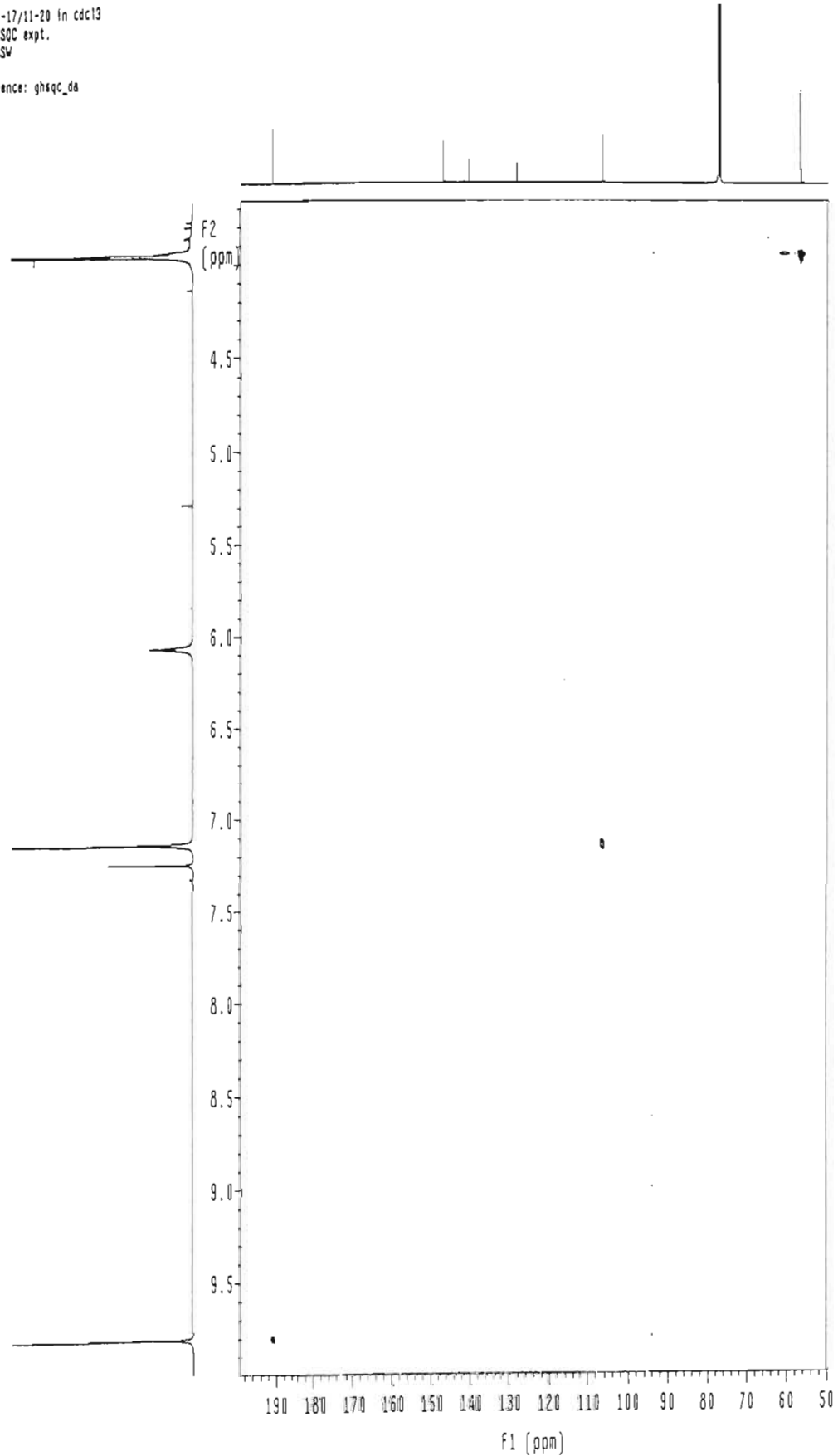
INDEX	FREQUENCY	PPM	HEIGHT
1	19207.378	190.991	25.0
2	14838.542	147.549	18.8
3	14179.639	140.997	10.8
4	12933.398	128.605	9.4
5	10749.391	106.888	22.0
6	7798.720	77.547	195.9
7	7766.639	77.228	200.0
8	7734.557	76.909	193.2
9	5701.087	56.689	42.6



SPECTRUM 38: ¹³C NMR spectrum of compound 5, syringaldehyde, in CDCl₃

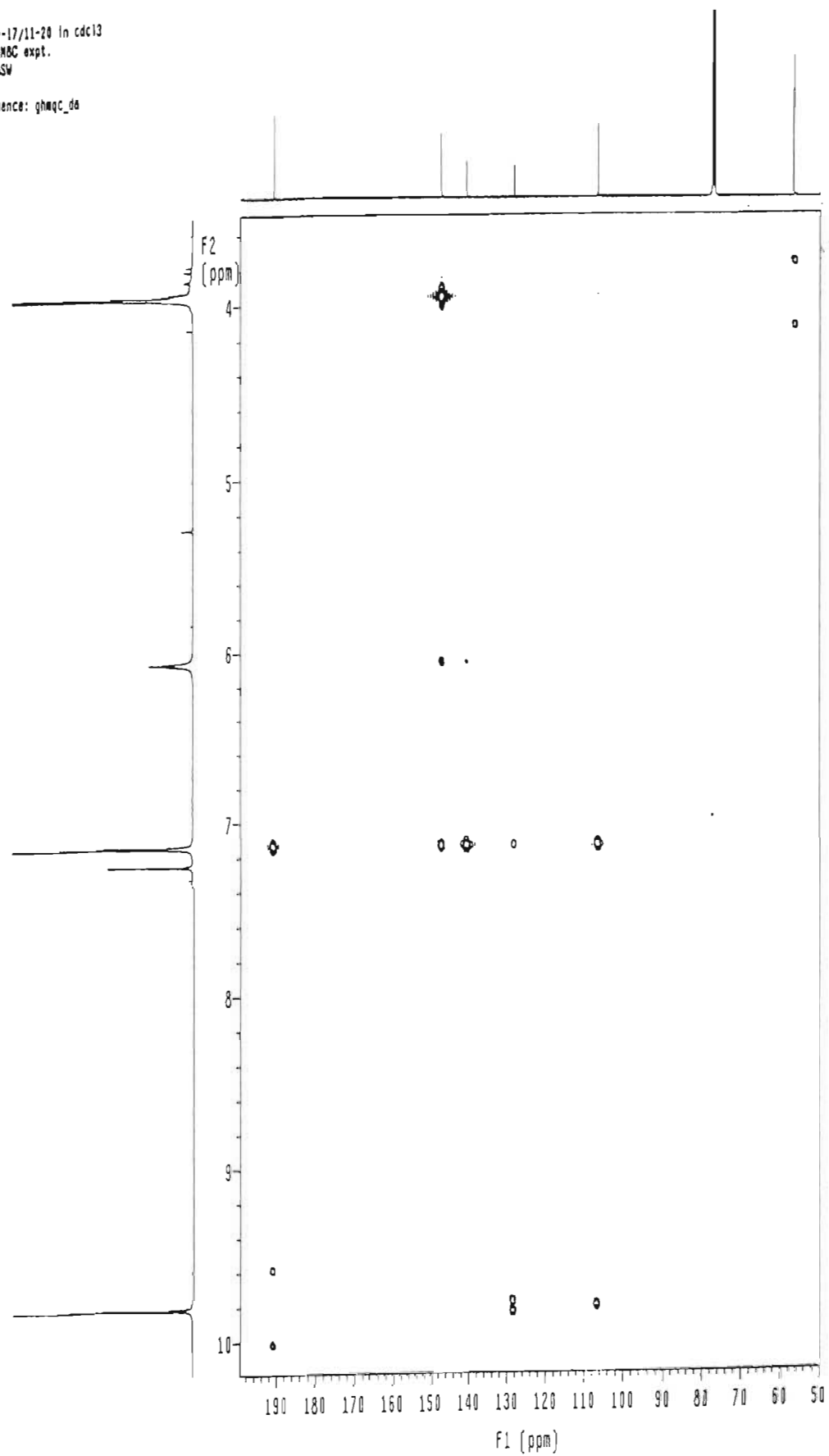
HQ0009.ssa-17/11-20 in cdcl3
Gradient HSQC expt.
probe=5mmASW
Pulse Sequence: ghsqc_da

169



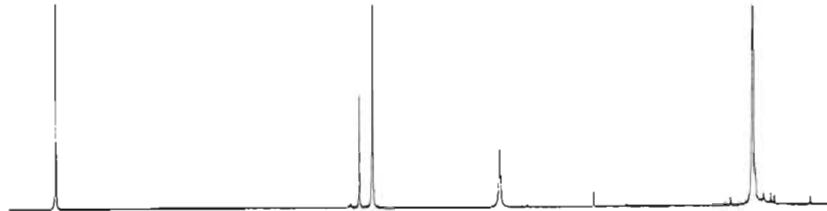
HS0009.sv-17/11-20 in cdc13
Gradient HMQC expt.
probe=5mmASW
Pulse Sequence: ghmqc_d0

170

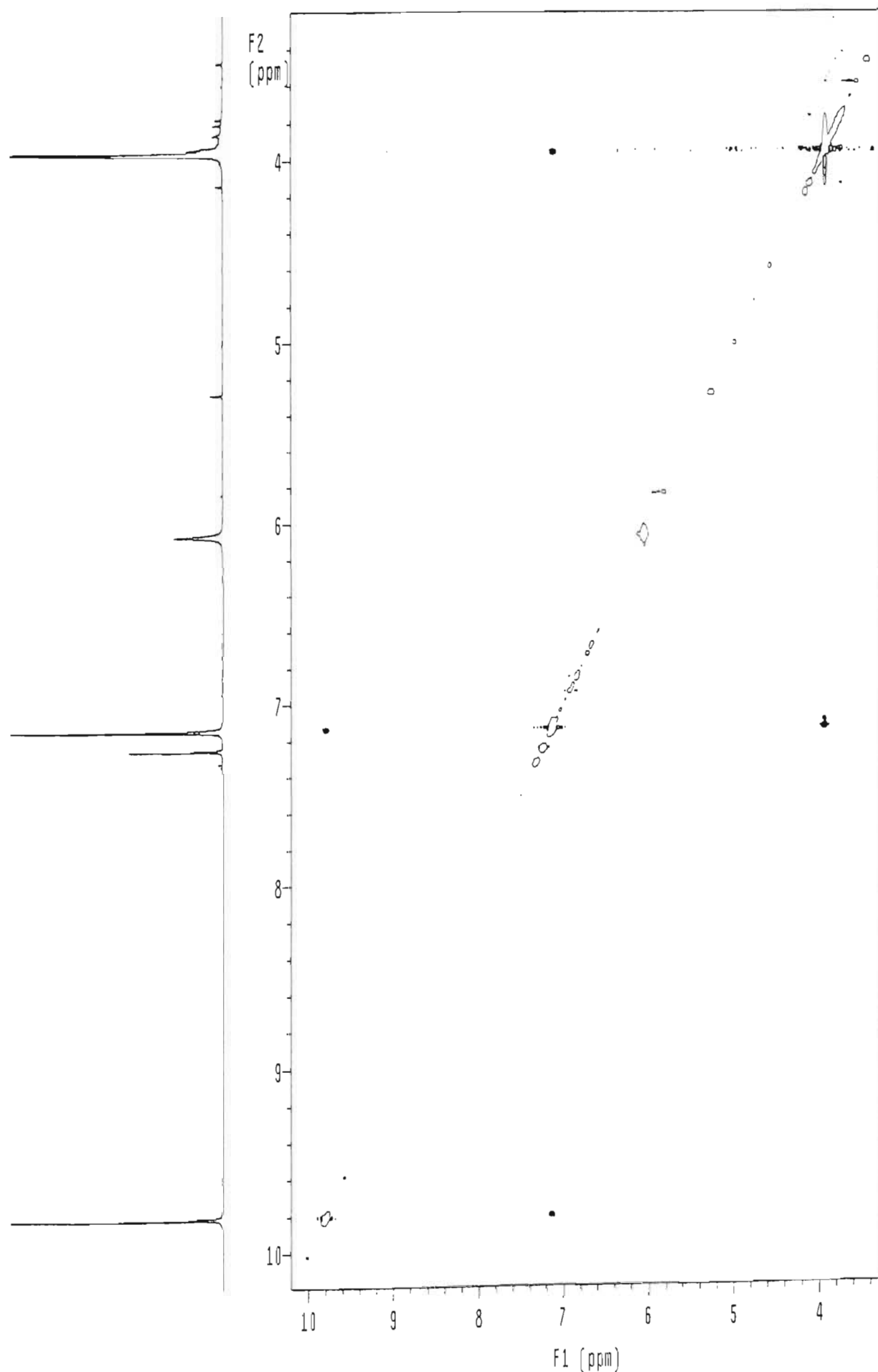


N00009.sse-17/11-20 in cdc13
Gradient NOESY expt.
mix=1sec
probe=5mmASW

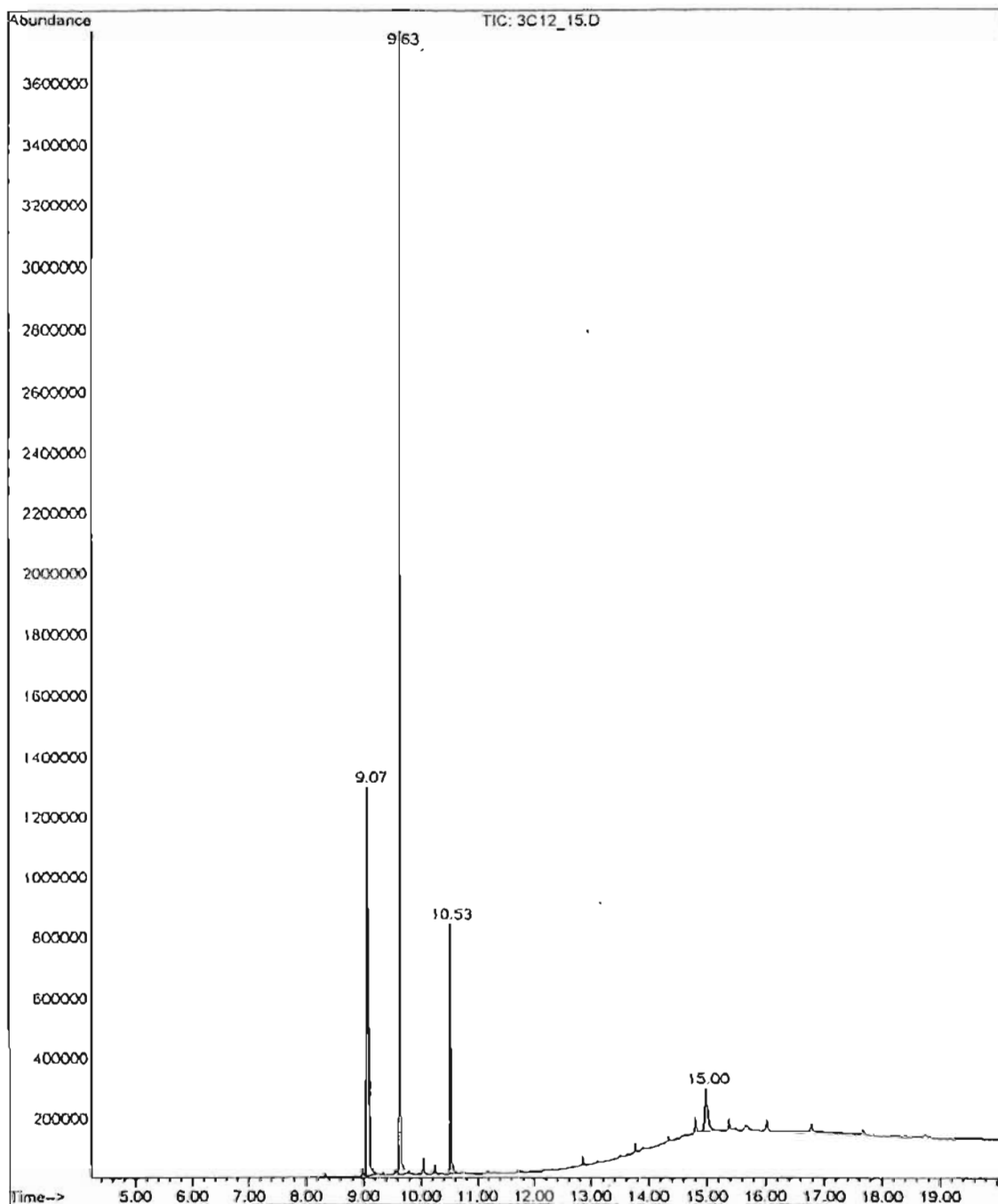
Pulse Sequence: noesy_da



171



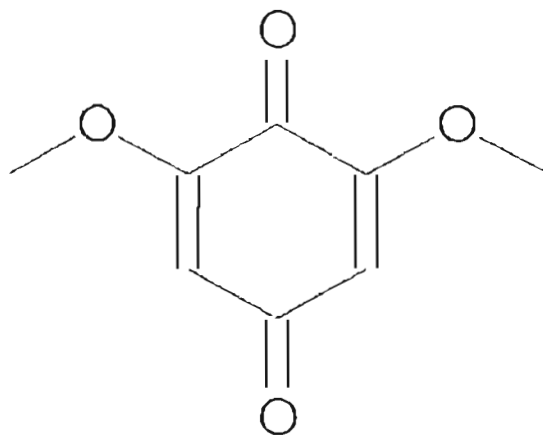
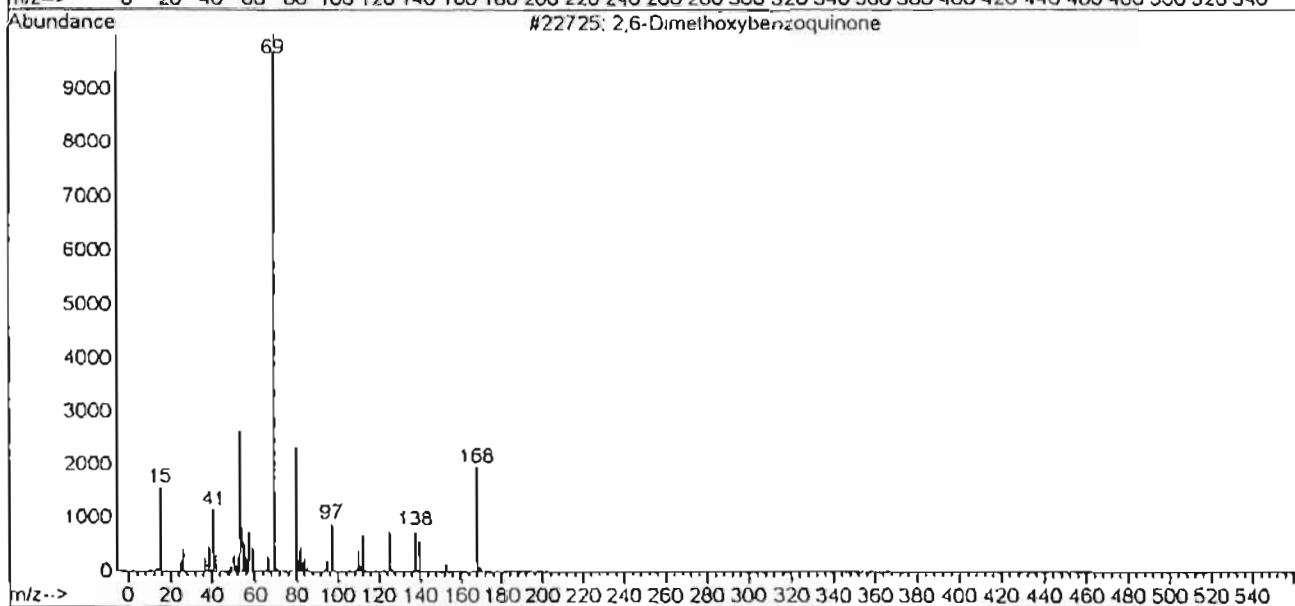
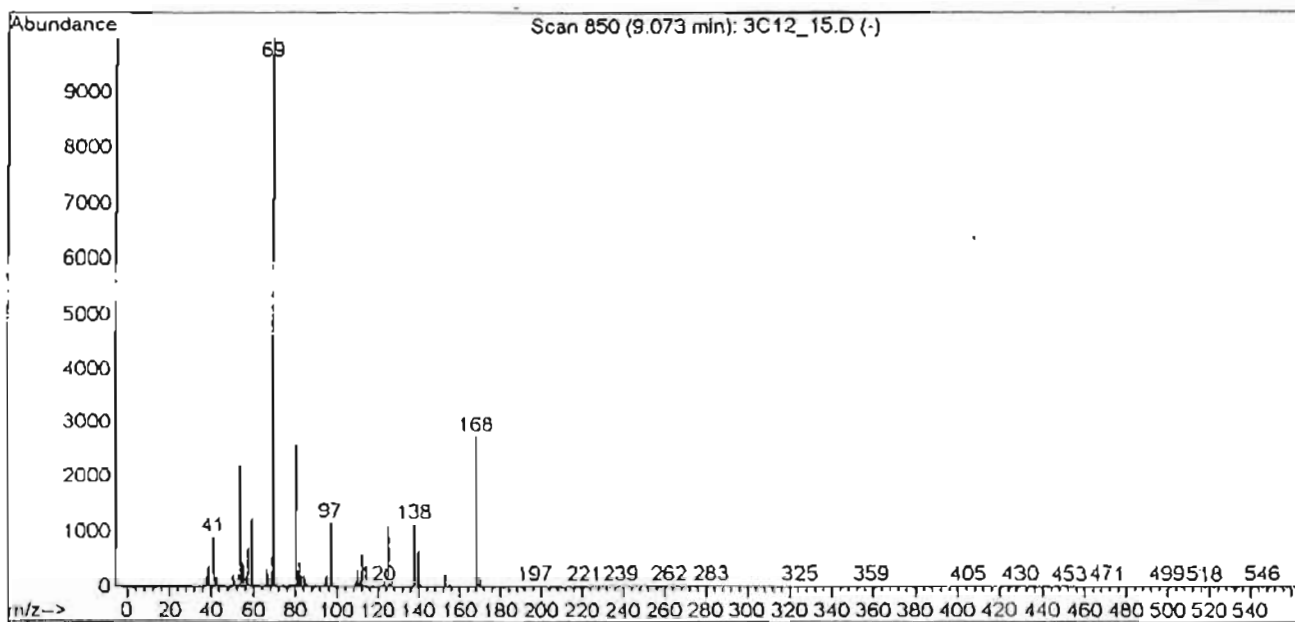
SPECTRUM 41: NOESY NMR spectrum of compound 5, syringaldehyde, in CDCl₃



PK#	RT	Area%	Library/ID	Ref#	CAS#	Qual
1	9.07	32.44	C:\Database\Nist98.1			
			2,6-Dimethoxybenzoquinone	22725	000530-55-2	86
			2-Butenoic acid, 2-propenyl ester	22140	020474-93-5	35
			2-Propenoic acid, 2-methyl-, 1,...	22150	000097-90-5	27
2	9.63	51.78	C:\Database\Nist98.1			
			Benzaldehyde, 4-hydroxy-3,5-dim...	125459	000134-96-3	95
			Dibenzofuran, 4-methyl-	78256	007320-53-8	53
			3,4-Dimethoxy-5-hydroxybenzalde...	78222	029865-90-5	53

SPECTRUM 42 : Gas chromatogram of compound 6, 2,6-dimethoxy-1,4-benzoquinone

Library Searched : C:\Database\Nist98.1
Quality : 86
ID : 2,6-Dimethoxybenzoquinone

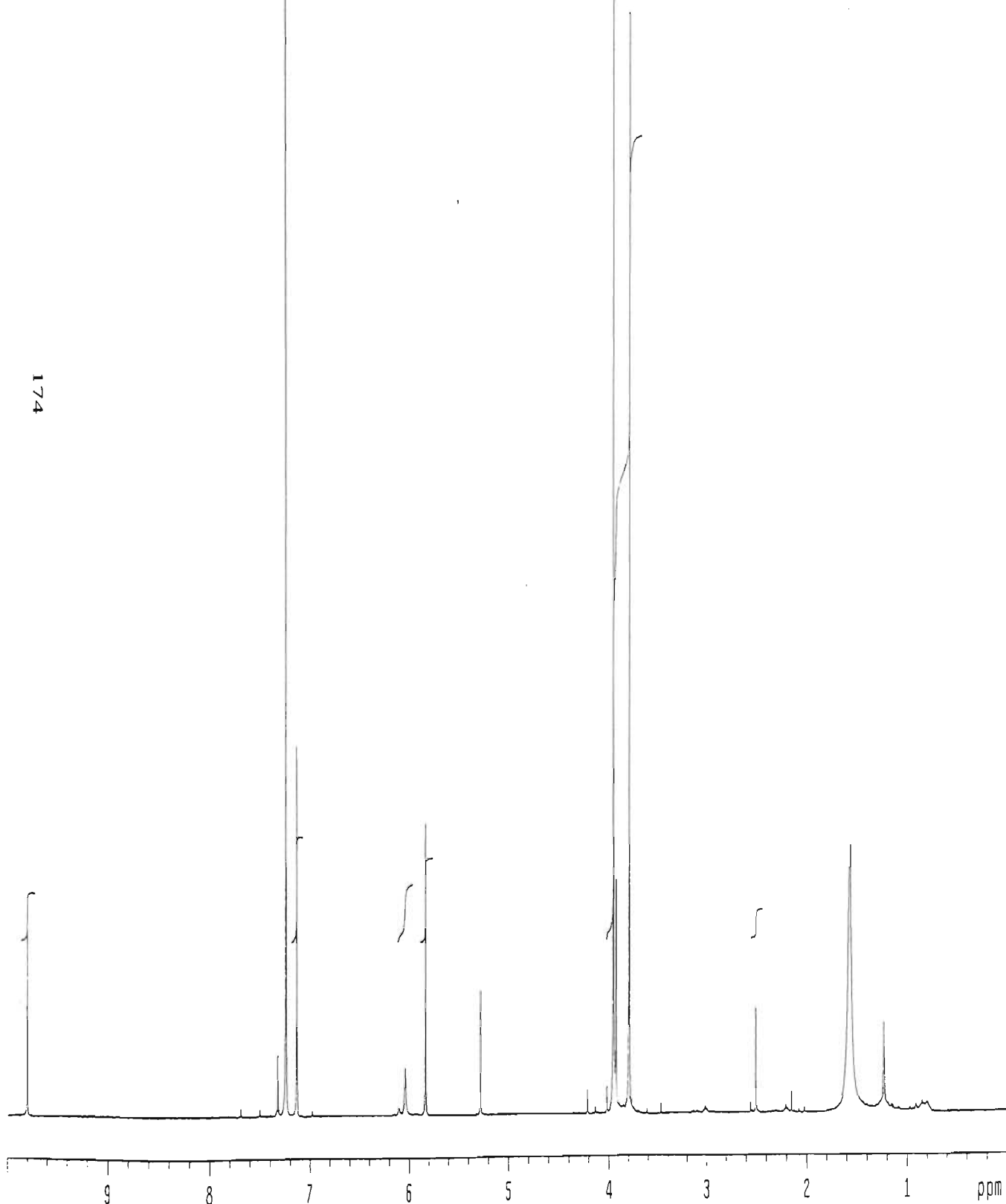
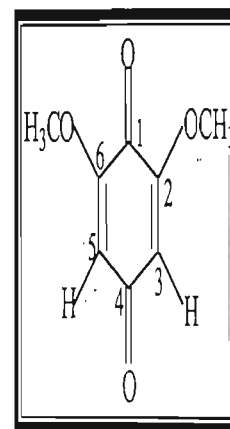


SPECTRUM 43 : Mass spectrum of compound 6, 2,6-dimethoxy-1,4-benzoquinone

hsse3c.sse-3c/12-15 in cdc13

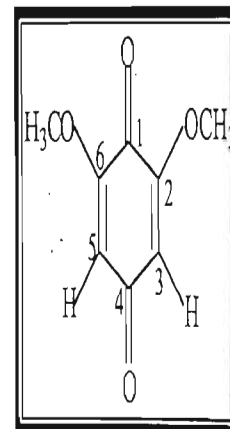
Pulse Sequence: s2pu1

INDEX	FREQUENC	PPM	HEIGHT
1	3920.19	3.802	21.2
2	2927.267	7.319	7.1
3	2835.403	7.240	148.9
4	2853.466	7.135	42.6
5	2414.322	6.037	5.5
6	2333.745	5.835	33.7
7	2111.243	5.279	14.3
8	1582.365	3.956	150.0
9	1576.139	3.941	5.3
10	1571.377	3.929	27.1
11	1520.101	3.801	127.7
12	1000.746	2.502	12.1
13	626.247	1.566	31.0
14	492.196	1.231	10.4

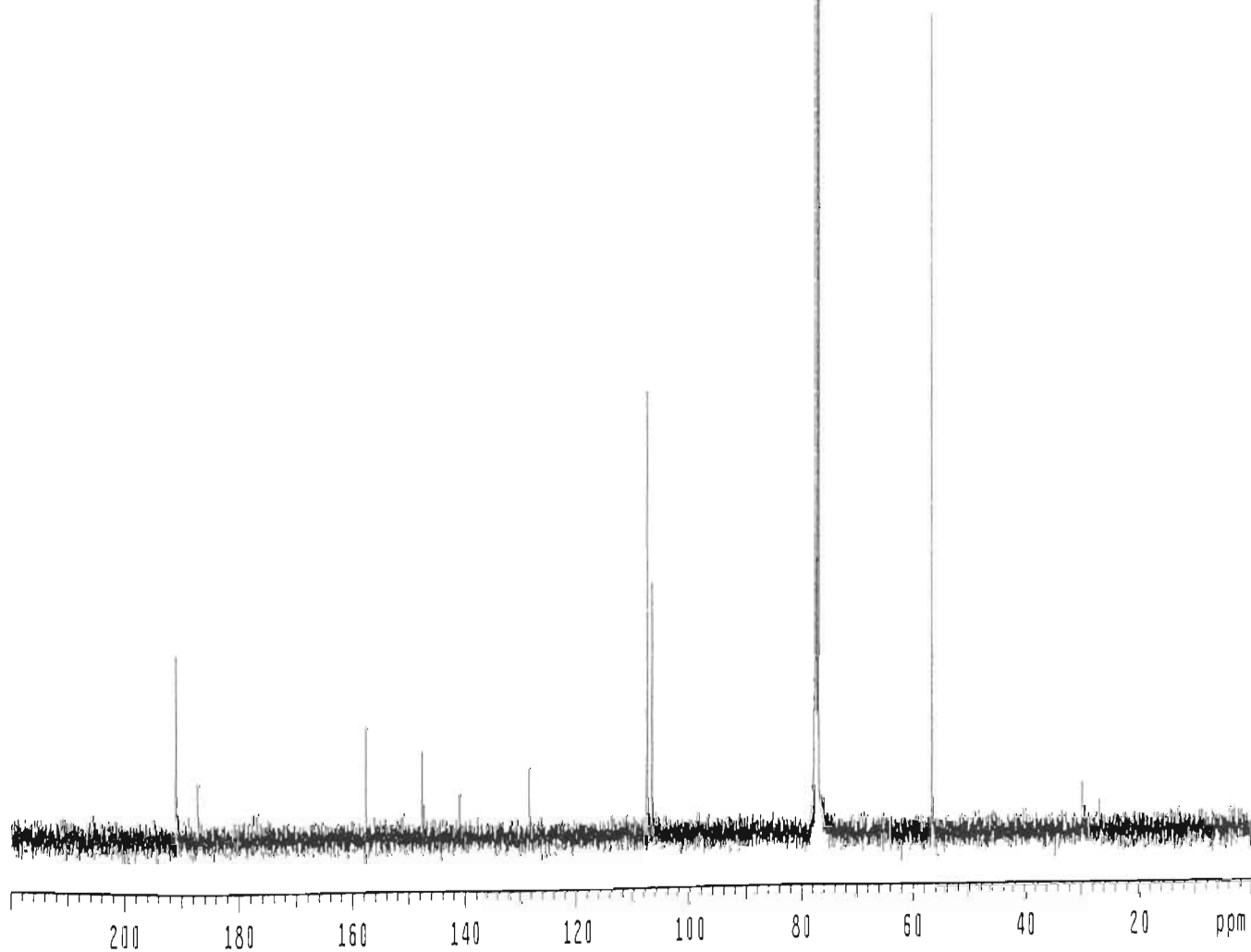


Pulse Sequence: s2pul

INDEX	FREQUENCY	PPM	HEIGHT
1	19182.11	190.743	17.3
2	18790.785	186.851	5.5
3	15819.479	157.305	10.4
4	14815.860	147.325	8.0
5	14156.669	140.770	4.1
6	12913.269	128.406	6.6
7	10817.039	107.562	7.6
8	10802.208	107.414	41.2
9	10726.400	106.661	23.5
10	7775.694	77.320	374.0
11	7764.158	77.205	29.3
12	7743.559	77.000	400.0
13	7711.423	76.680	391.4
14	5679.465	56.475	76.3
15	2985.844	29.690	4.6



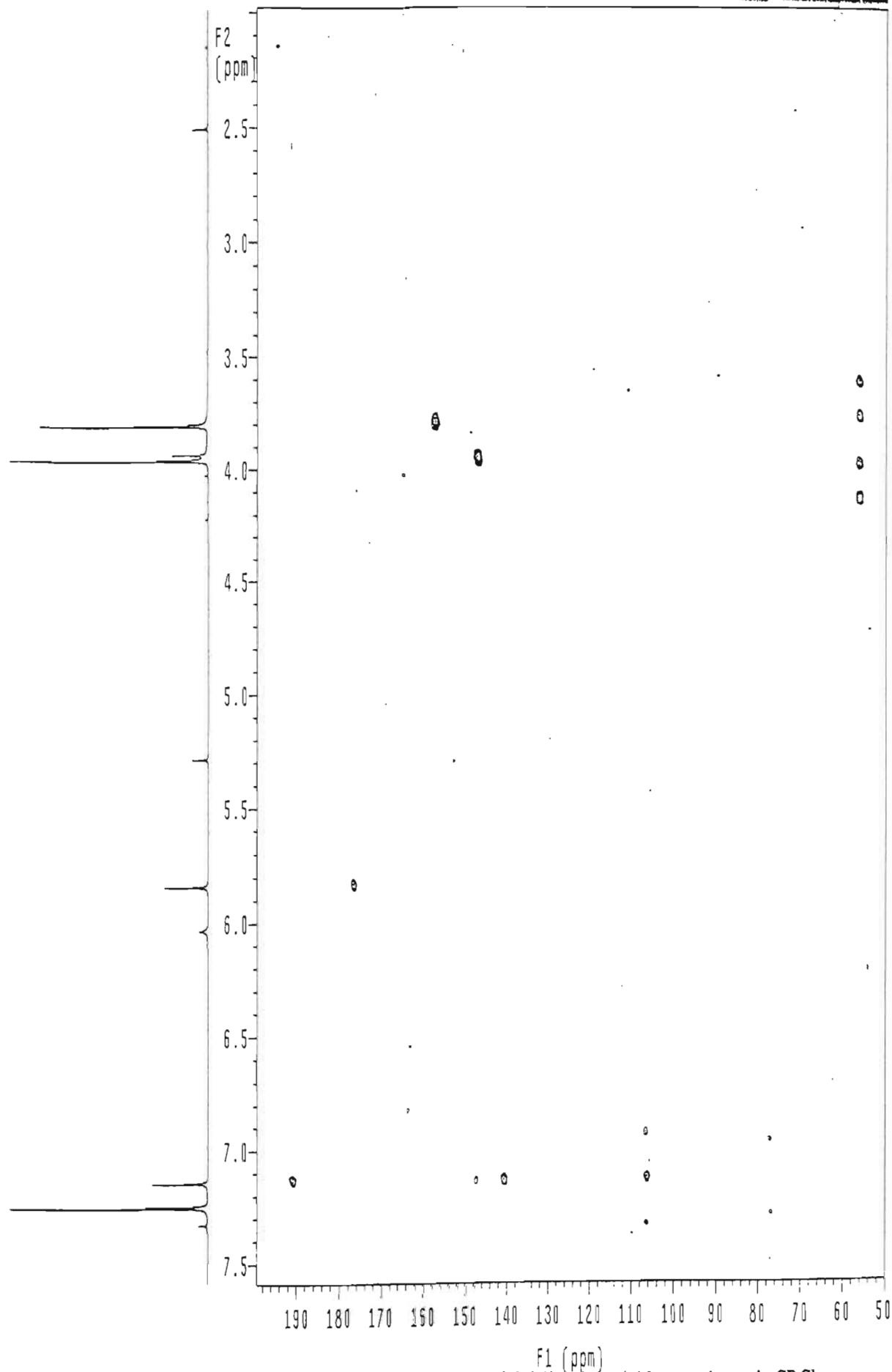
175



H8sse3c.sse-3c/12-15 in cdcl3
Gradient HMBc expt.
probe=5mmASW

Pulse Sequence: ghmqc_da

176

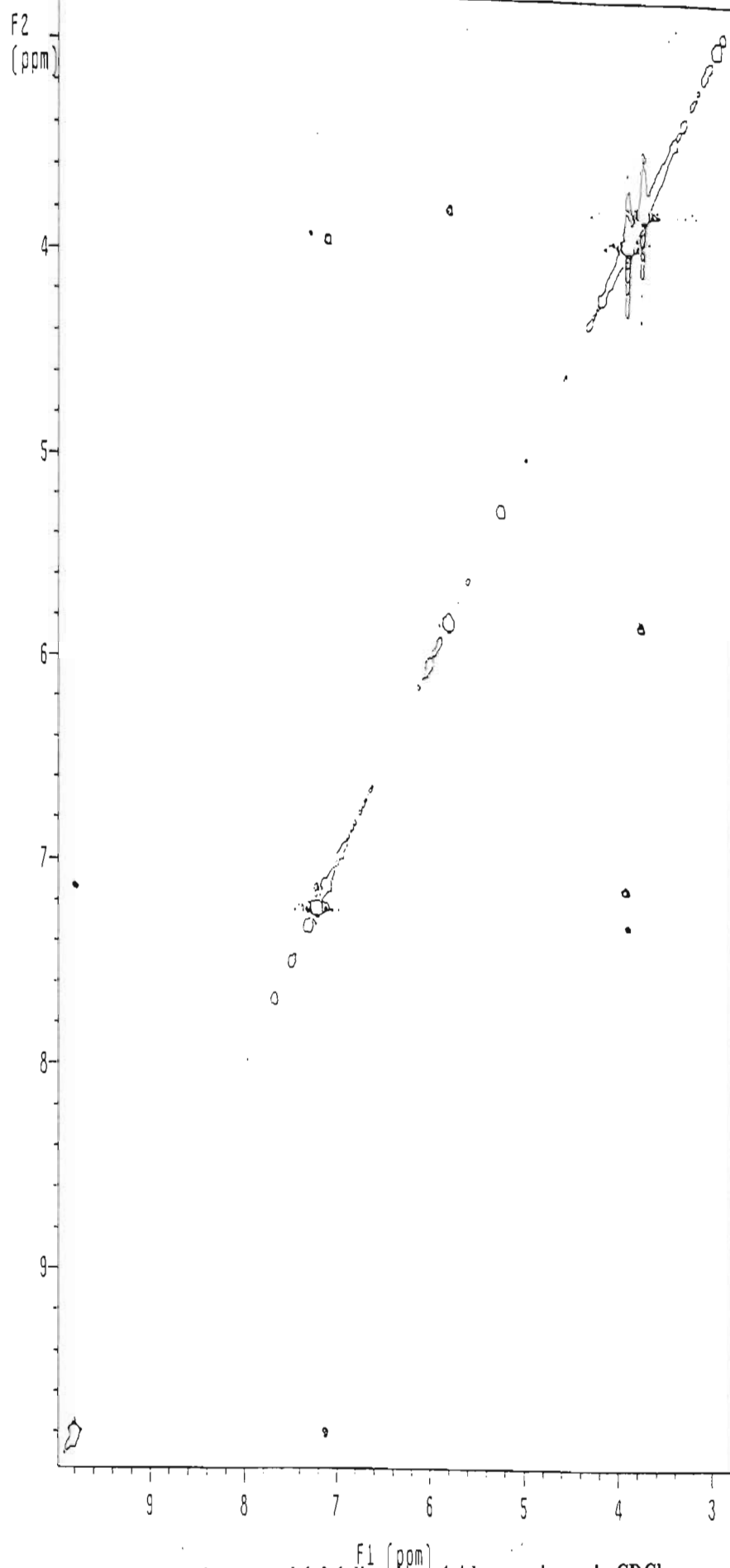


SPECTRUM 46 : HMBC NMR spectrum of compound 6, 2,6-dimethoxy-1,4-benzoquinone, in CDCl_3

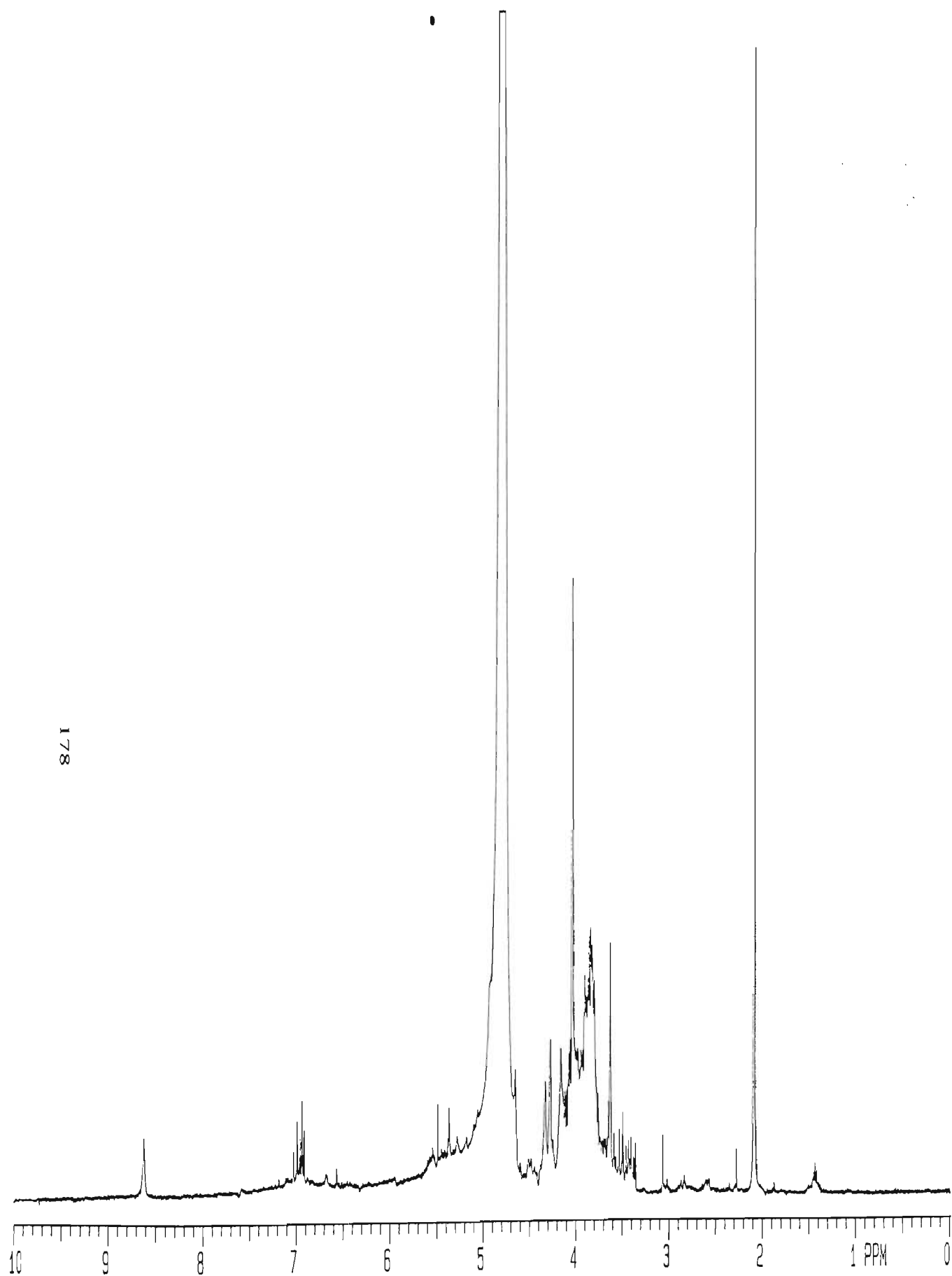
NOSS3C.ssa-3c/12-15 in cdc13
Gradient NOESY expt.
mix=1sec
probe=5mmASW

Pulse Sequence: noesy_da

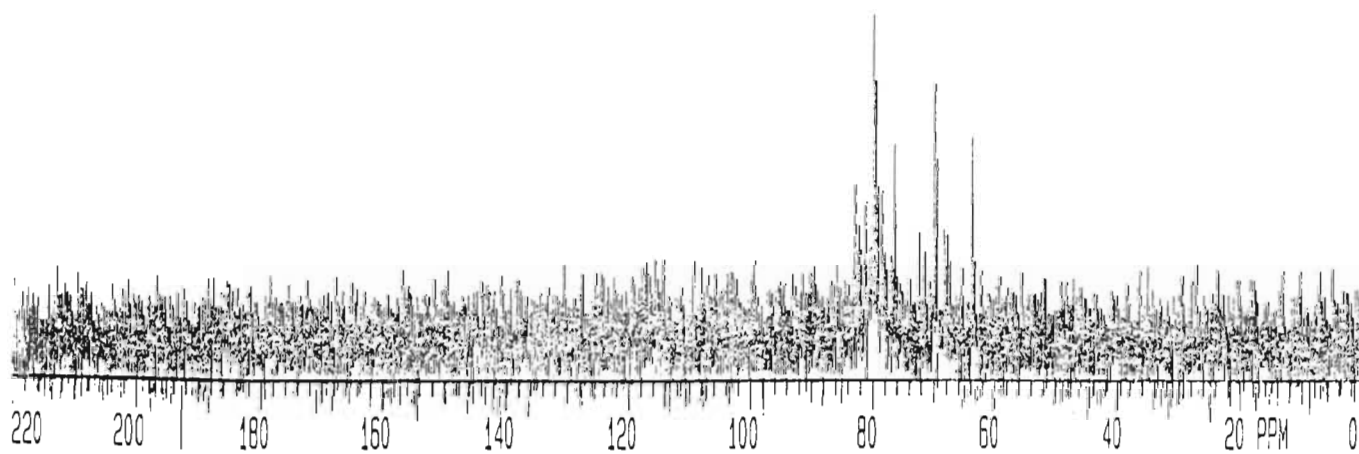
177

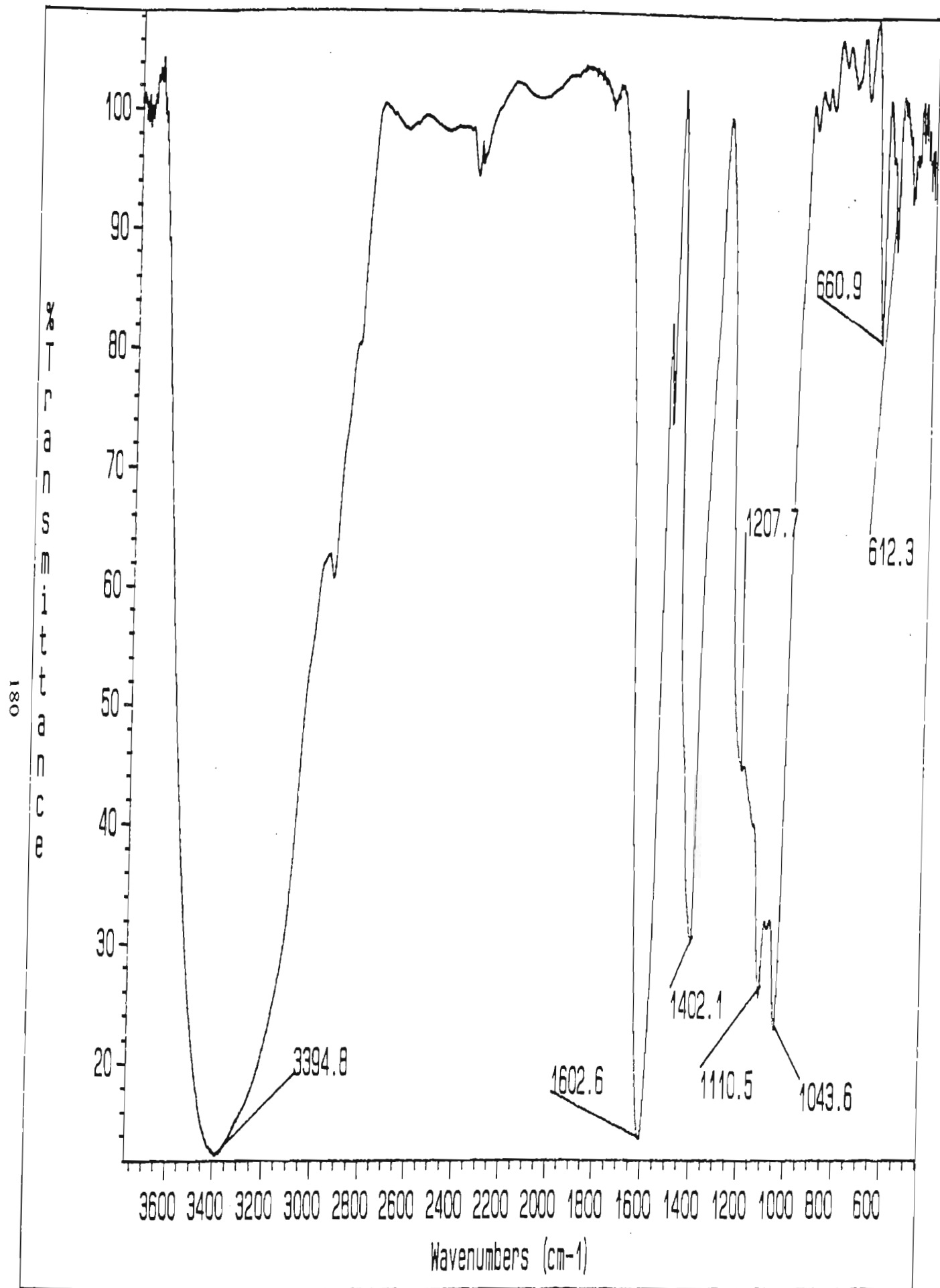


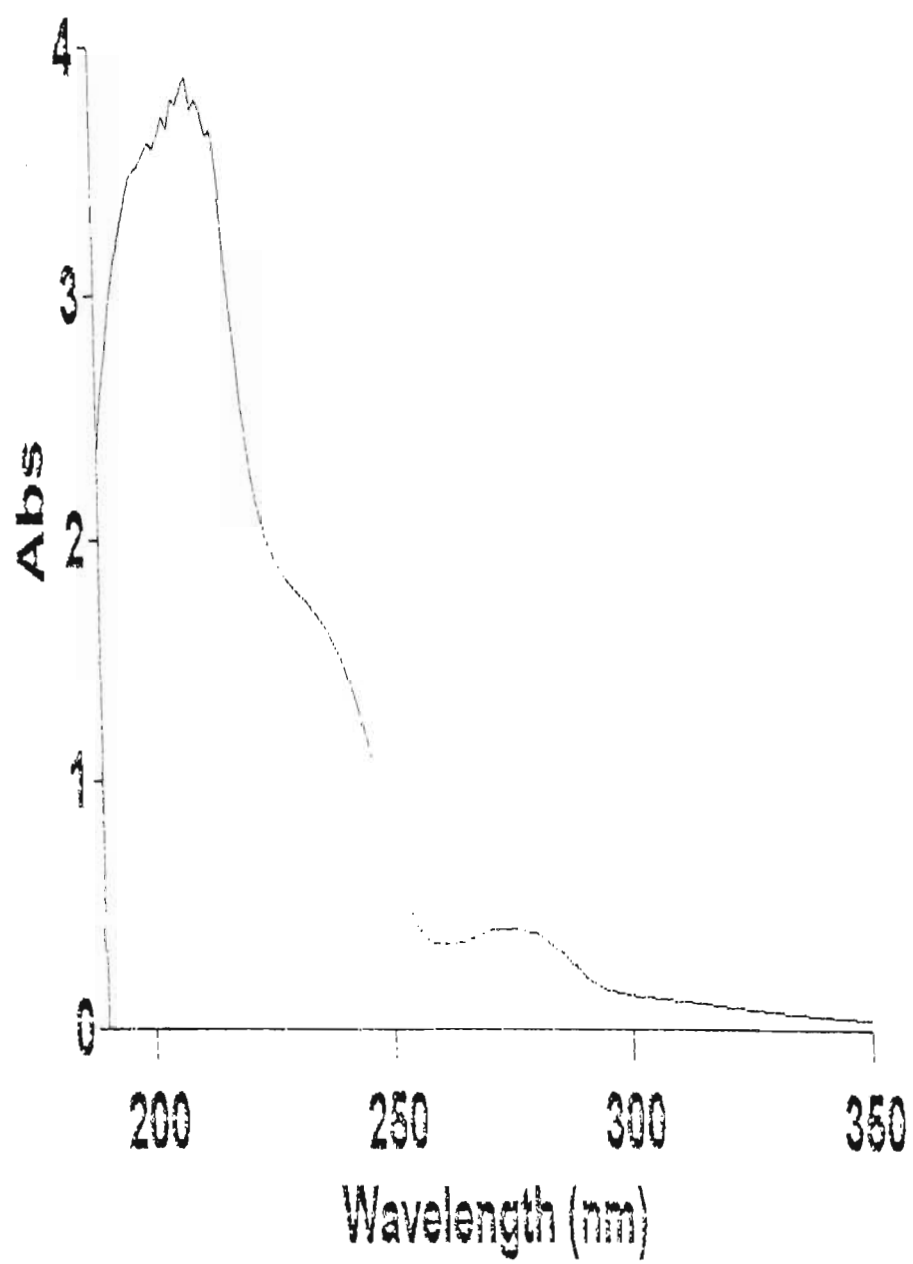
SPECTRUM 47 : NOESY NMR spectrum of compound 6, 2,6-dimethoxy-1,4-benzoquinone, in CDCl₃



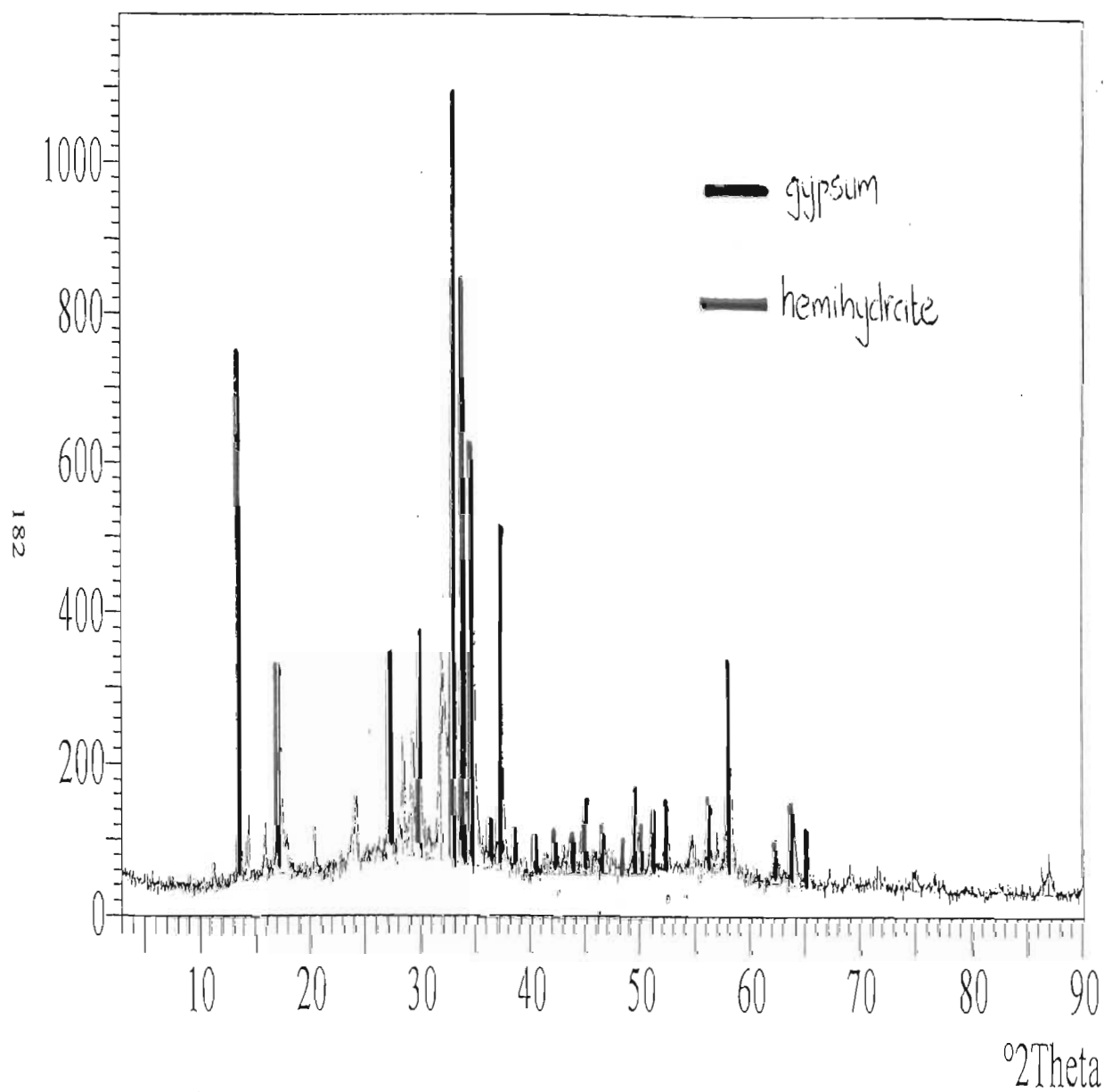
179







counts/s



SPECTRUM 52 : XRD spectrum of residue formed from the calcium - spent liquor effluent

X'Pert Graphics & Identify
(searched) peak list: woodppt

User-1
10/06/2000 14:04

Description:
WOOD PPT

Original scan: woodppt
Description of scan:
WOOD PPT

Used wavelength: K-Alpha

K-Alpha1 wavelength (Å): 1.78897
K-Alpha2 wavelength (Å): 1.79285
K-Alpha2/K-Alpha1 intensity ratio : 0.50000
K-Alpha wavelength (Å): 1.78897
K-Beta wavelength (Å):

Peak search parameter set: As Measured Intensities
Set created: 04/28/1999 12:06
Peak positions defined by: Minimum of 2nd derivative
Minimum peak tip width (°2Theta): 0.00
Minimum peak tip width (°2Theta): 1.00
Peak base width (°2Theta): 2.00
Minimum significance: 0.60

d-spacing (Å)	Relative Intensity (%)	Angle (°2Theta)	Peak Height (counts/s)	Background (counts/s)	Tip Width (°2Theta)	Significance
9.15229	2.36	11.21731	24.03	39.70	0.16000	0.81
7.55751	68.01	13.59456	693.28	45.38	0.08000	5.76
7.16766	7.81	14.33775	79.58	47.19	0.08000	0.62
6.48632	7.07	15.85302	72.09	50.86	0.10000	0.80
6.00071	27.40	17.14524	279.33	53.99	0.08000	1.04
5.06870	4.66	20.32864	47.52	55.70	0.08000	2.13
4.30789	7.69	23.96796	78.37	71.96	0.20000	1.14
4.26901	6.85	24.18954	69.82	72.98	0.12000	1.39
3.79151	25.43	27.29138	259.24	81.47	0.08000	1.89
3.69743	3.93	27.99981	40.06	79.93	0.12000	0.82
3.64294	15.38	28.42733	156.80	79.00	0.12000	2.08
3.54244	14.84	29.25153	151.25	77.21	0.20000	2.66
3.45699	27.20	29.99135	277.27	75.60	0.18000	5.32
3.37506	3.53	30.73712	36.00	73.98	0.20000	0.80
3.25560	21.46	31.89448	218.73	71.46	0.16000	0.82
3.15136	100.00	32.97903	1019.42	69.10	0.22000	23.02
3.06618	75.42	33.92258	768.85	67.05	0.06000	2.40
2.99861	54.94	34.71091	560.08	65.33	0.22000	11.96
2.86996	5.43	36.31985	55.38	61.84	0.12000	0.64
2.81032	39.99	37.11849	407.64	60.10	0.10000	2.13
2.74267	2.05	38.06878	20.85	58.03	0.06000	0.68
2.71314	5.57	38.49937	56.78	57.10	0.10000	0.88
2.59201	2.66	40.37478	27.12	54.89	0.32000	1.83

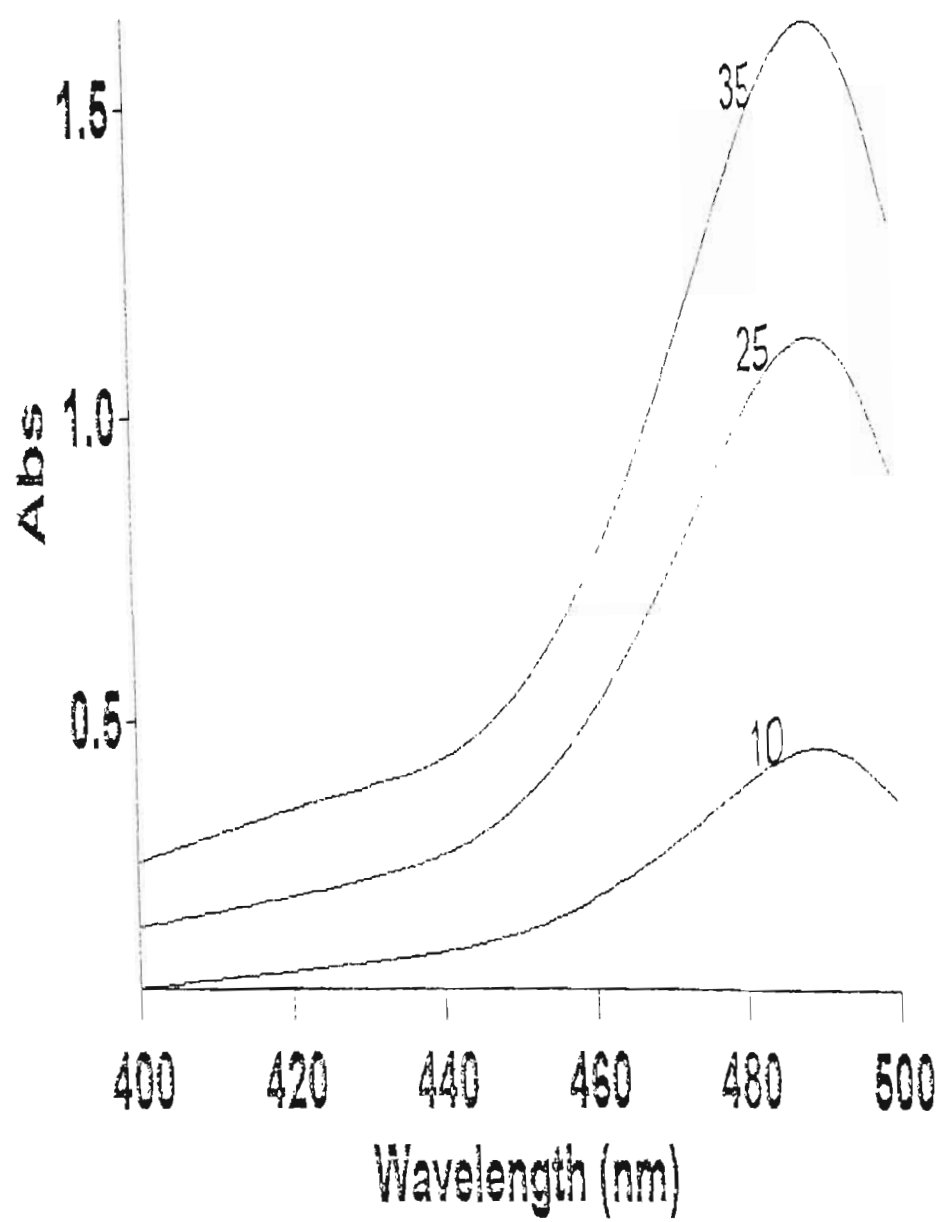
d-spacing (Å)	Relative Intensity (%)	Angle (°2Theta)	Peak Height (counts/s)	Background (counts/s)	Tip Width (°2Theta)	Significance
2.53560	1.80	41.31359	18.34	54.96	0.24000	0.68
2.49387	3.79	42.03744	38.60	55.02	0.20000	0.75
2.44611	3.54	42.89837	36.06	55.09	0.12000	0.84
2.39985	3.82	43.76749	38.92	55.16	0.16000	0.90
2.34279	8.30	44.89081	84.59	55.25	0.20000	1.53
2.30061	2.29	45.75995	23.31	55.33	0.32000	0.69
2.26910	4.02	46.43232	41.02	55.38	0.40000	2.20
2.18404	3.55	48.35360	36.23	55.54	0.16000	1.02
2.13870	9.98	49.44654	101.75	55.63	0.14000	1.77
2.11611	4.24	50.01050	43.19	55.68	0.16000	0.93
2.07363	6.39	51.10788	65.09	55.77	0.20000	1.64
2.02917	8.77	52.31141	89.35	55.87	0.24000	3.77
1.95180	4.52	54.55302	46.09	56.06	0.40000	2.28
1.90009	7.67	56.16711	78.20	56.19	0.06000	1.21
1.87935	4.59	56.84290	46.84	56.25	0.16000	0.73
1.84638	25.98	57.95318	264.82	56.34	0.24000	5.45
1.73316	3.48	62.14181	35.43	43.90	0.32000	1.22
1.69385	8.74	63.75119	89.05	41.61	0.32000	5.28
1.66373	6.89	65.04589	70.24	39.77	0.20000	1.87
1.62012	2.39	67.02383	24.37	37.62	0.24000	1.54
1.58040	2.37	68.94165	24.11	37.36	0.32000	0.87
1.53296	3.20	71.39398	32.59	37.02	0.06000	0.78
1.47661	1.95	74.56839	19.91	34.71	0.48000	2.01
1.44549	1.85	76.45839	18.84	32.19	0.24000	0.73
1.43290	1.27	77.25382	12.95	31.12	0.24000	0.67
1.35548	0.97	82.58484	9.89	28.45	0.48000	1.23
1.32326	0.87	85.05852	8.90	29.54	0.24000	1.12
1.31059	2.11	86.07915	21.47	29.99	0.24000	0.68
1.30238	4.29	86.75584	43.75	30.29	0.16000	0.64

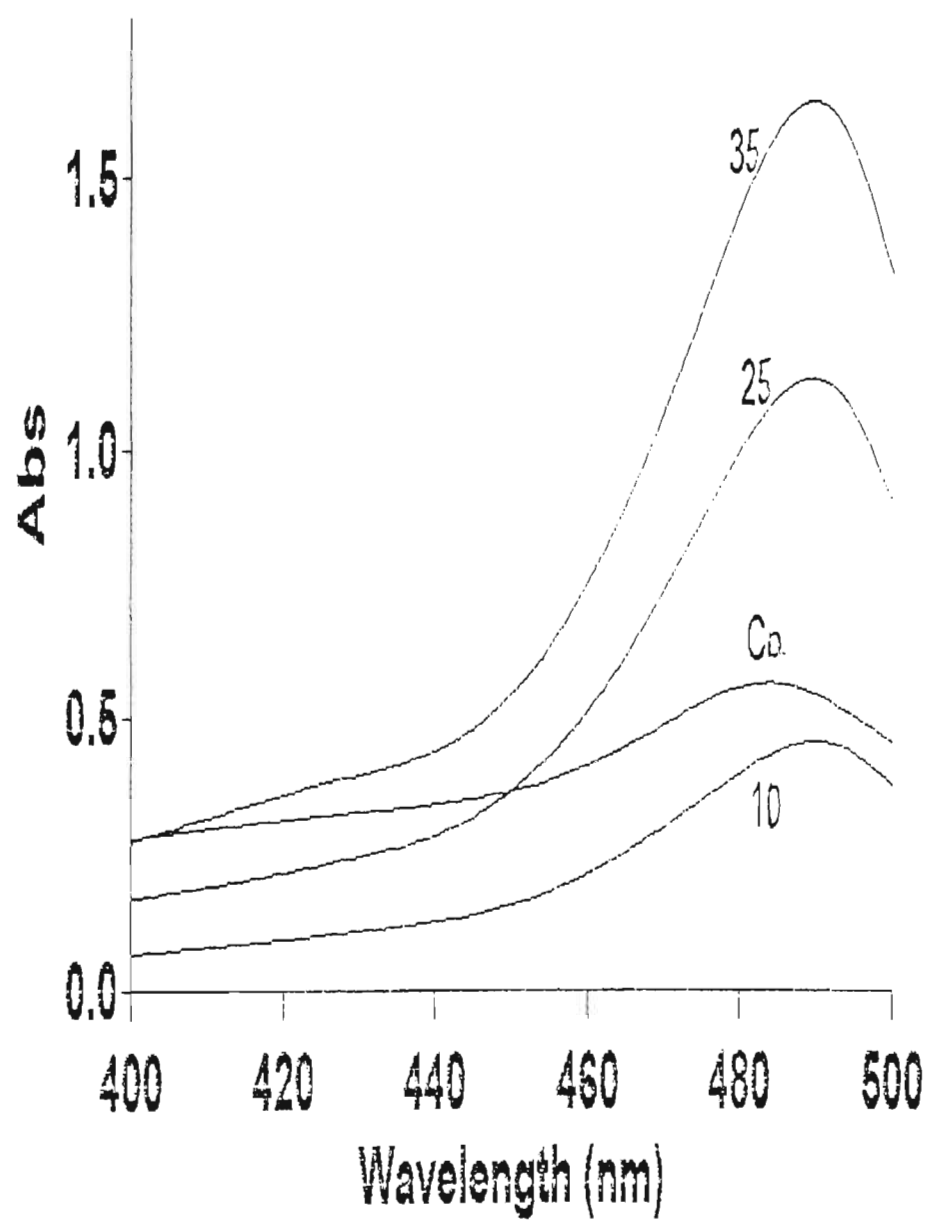
MAJOR ELEMENT COMPOSITIONS - WEIGHT PERCENT

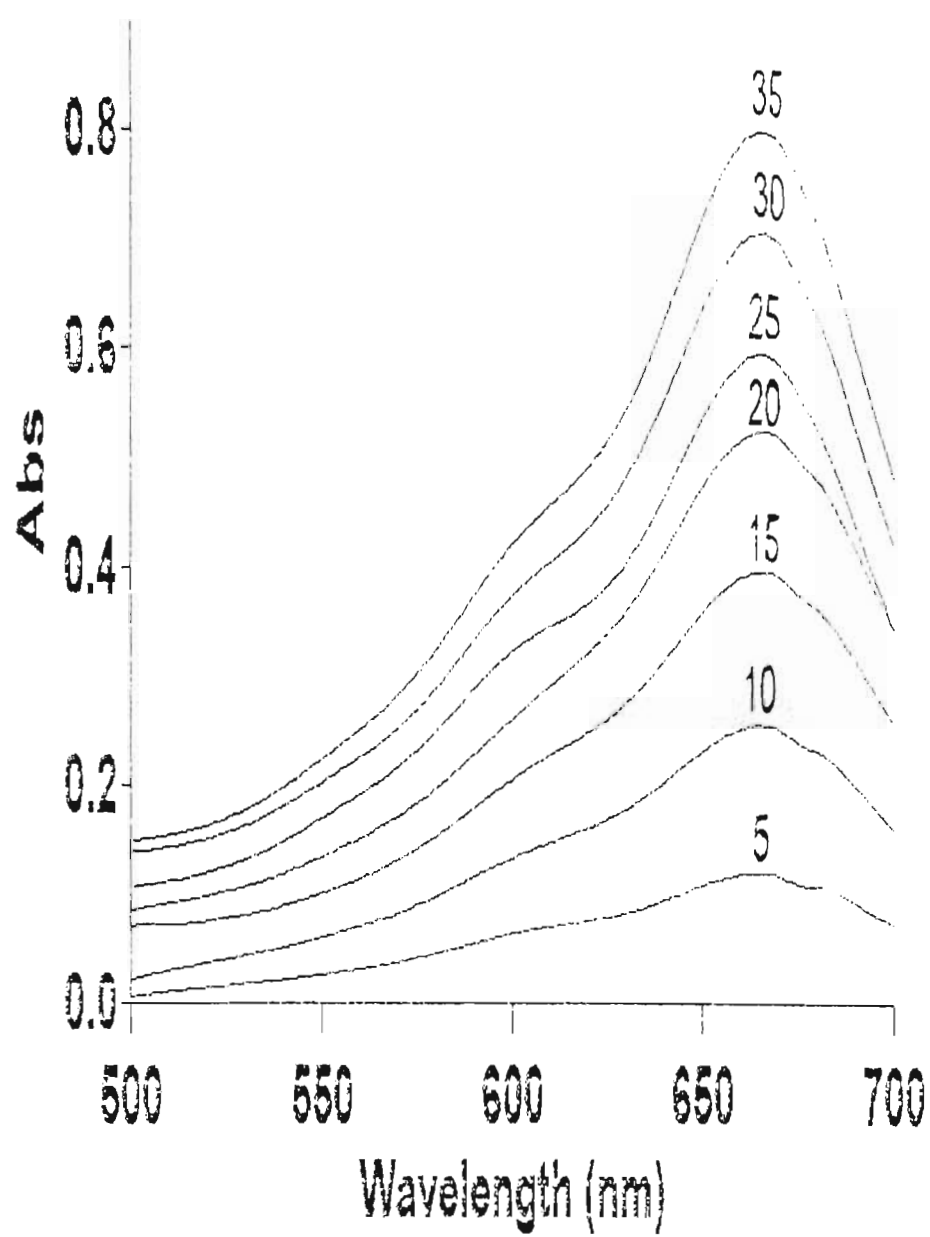
IGNITED	SiO2	Al2O3	Fe2O3	MnO	MgO	CaO	Na2O	K2O	TiO2	P2O5	Cr2O3	NiO	TOTAL	L.O.I.
BRENDA														
WEIGHT PERC OXIDE	5.93	0.23	0.00	0.000	0.25	82.84	1.27	0.00	0.00	0.03	0.0909	0.000	90.64	80.41

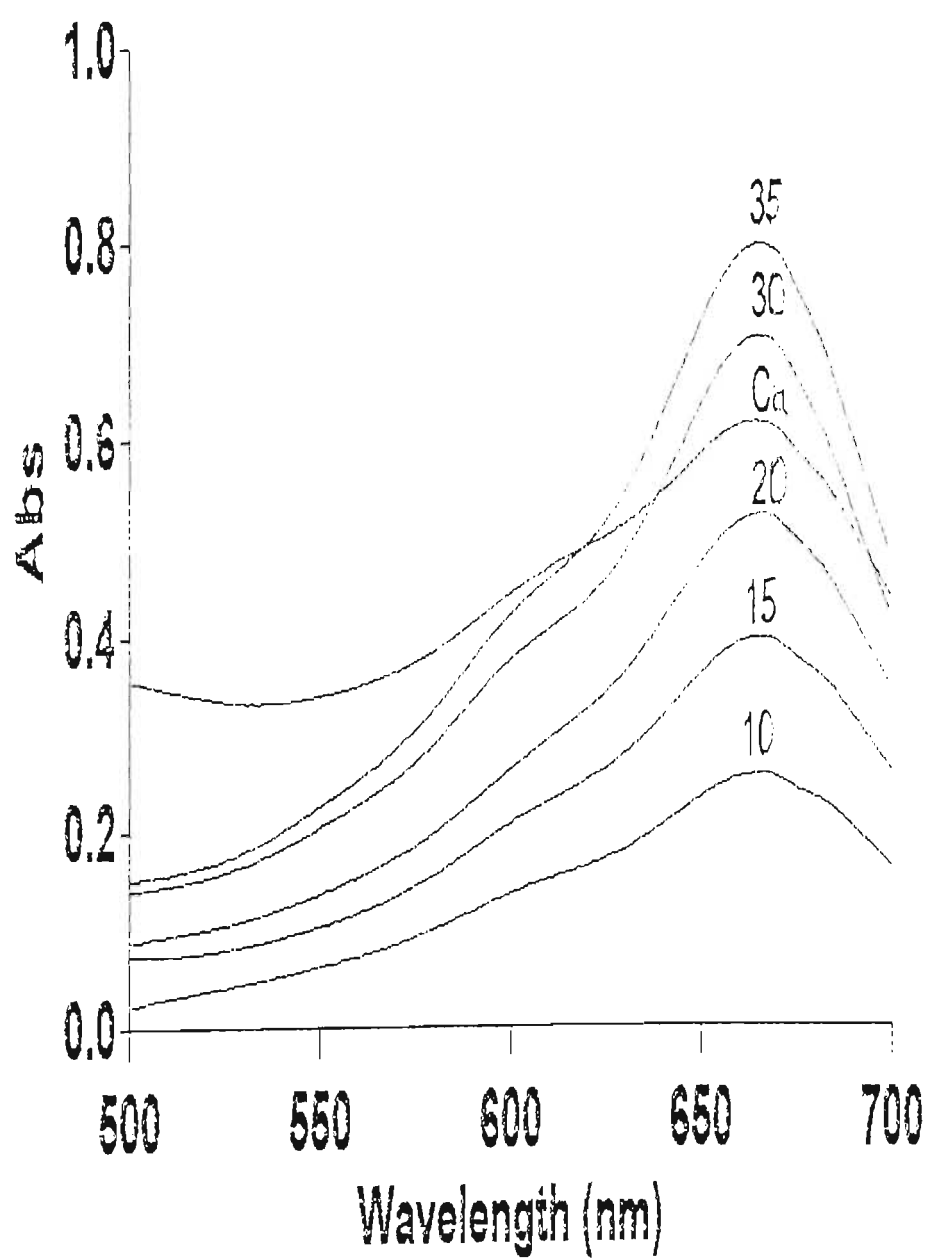
Major elements analysed on fused beads.

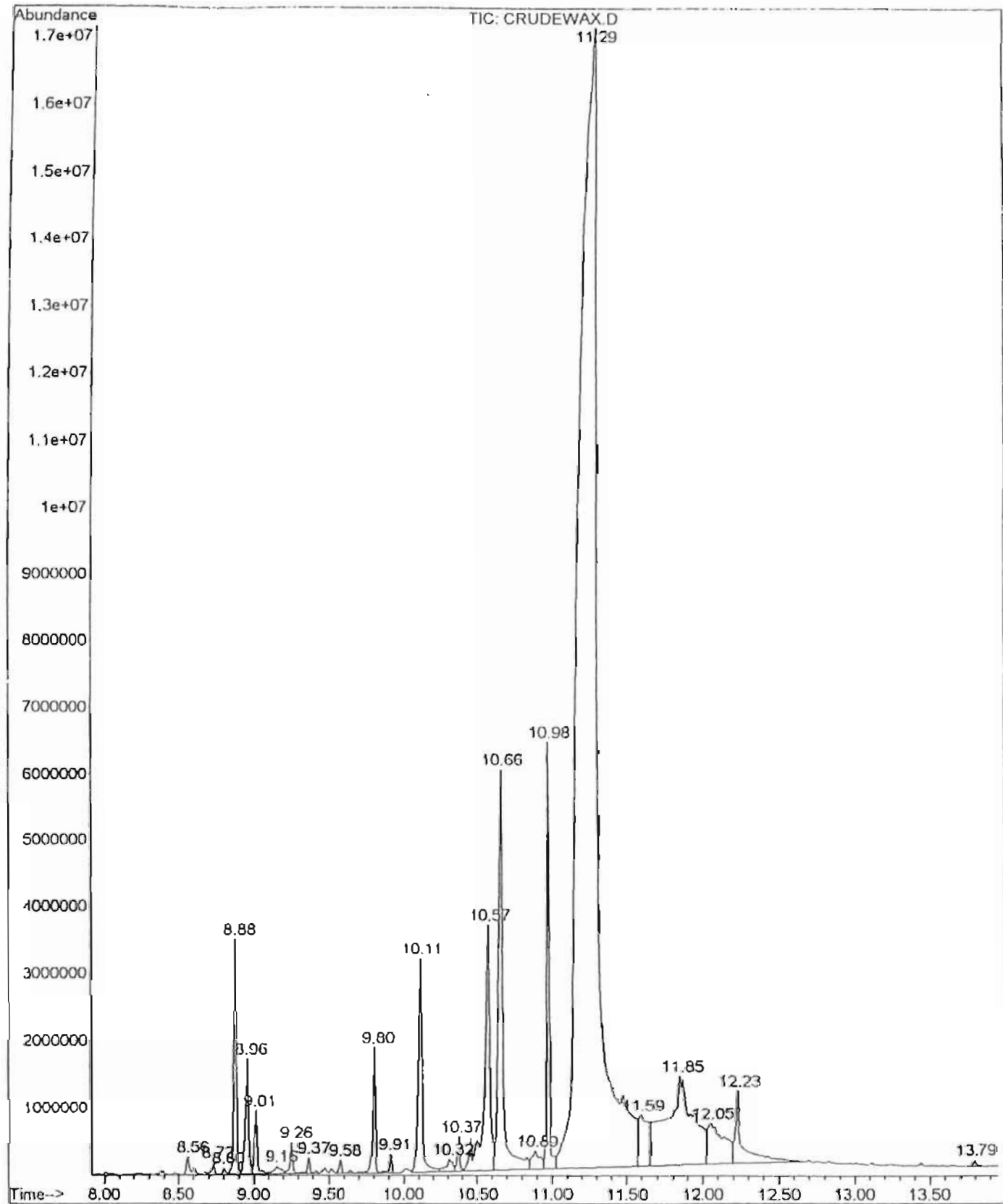
Checked for Sulphur on fused bead and is present in significant amount
and can make up the balance.





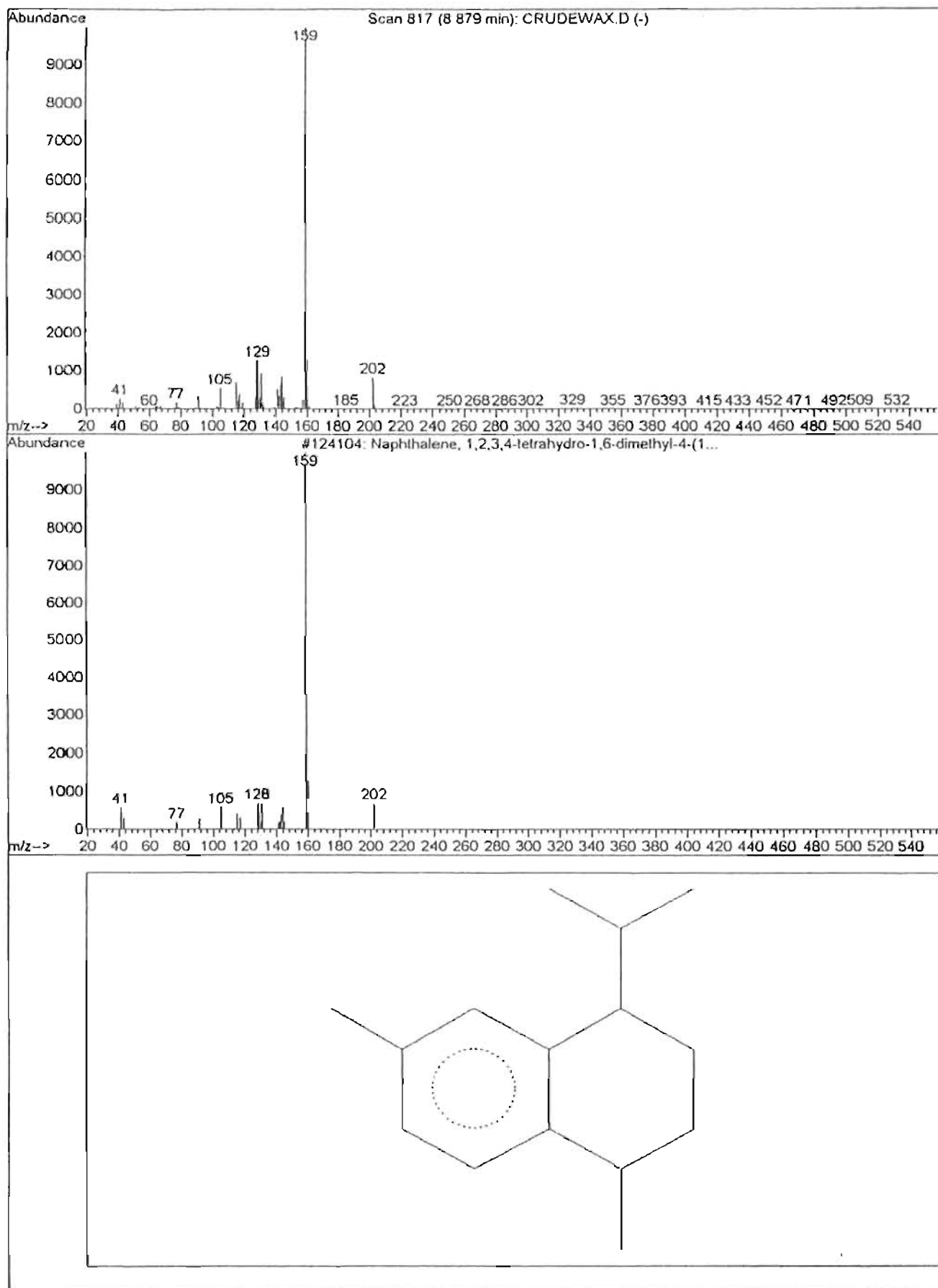






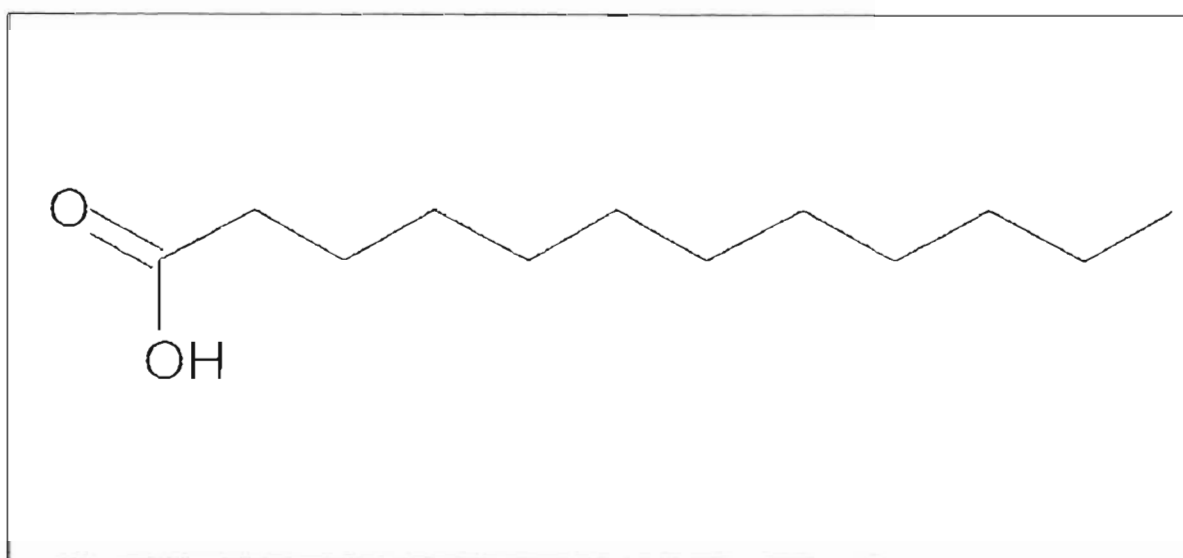
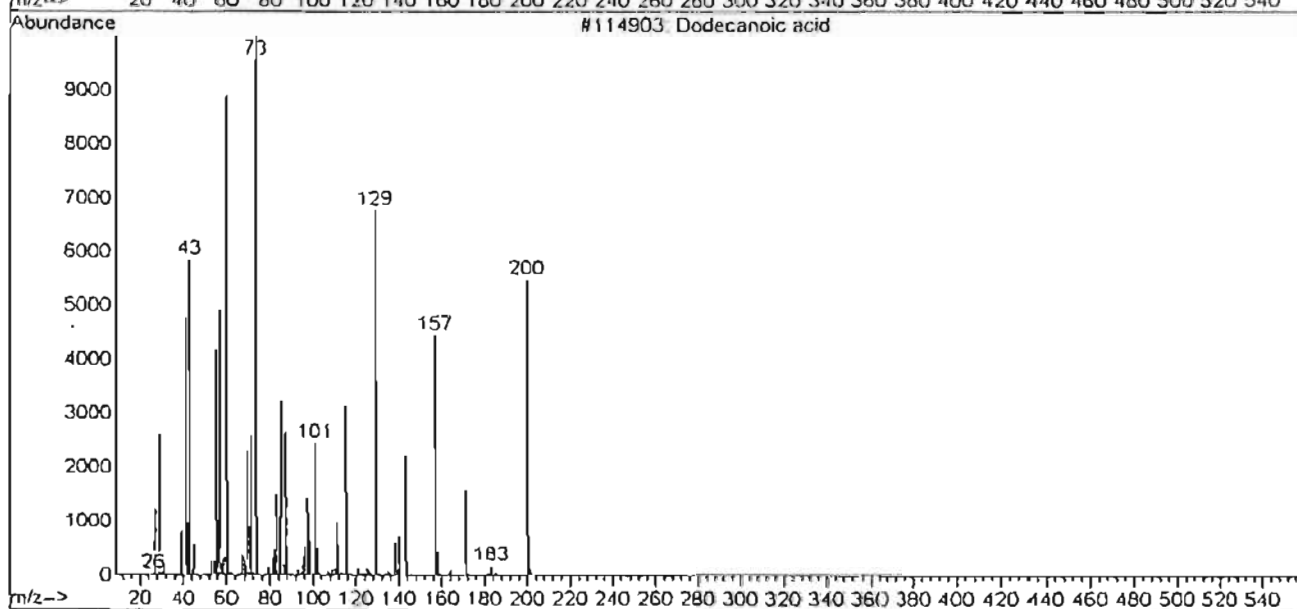
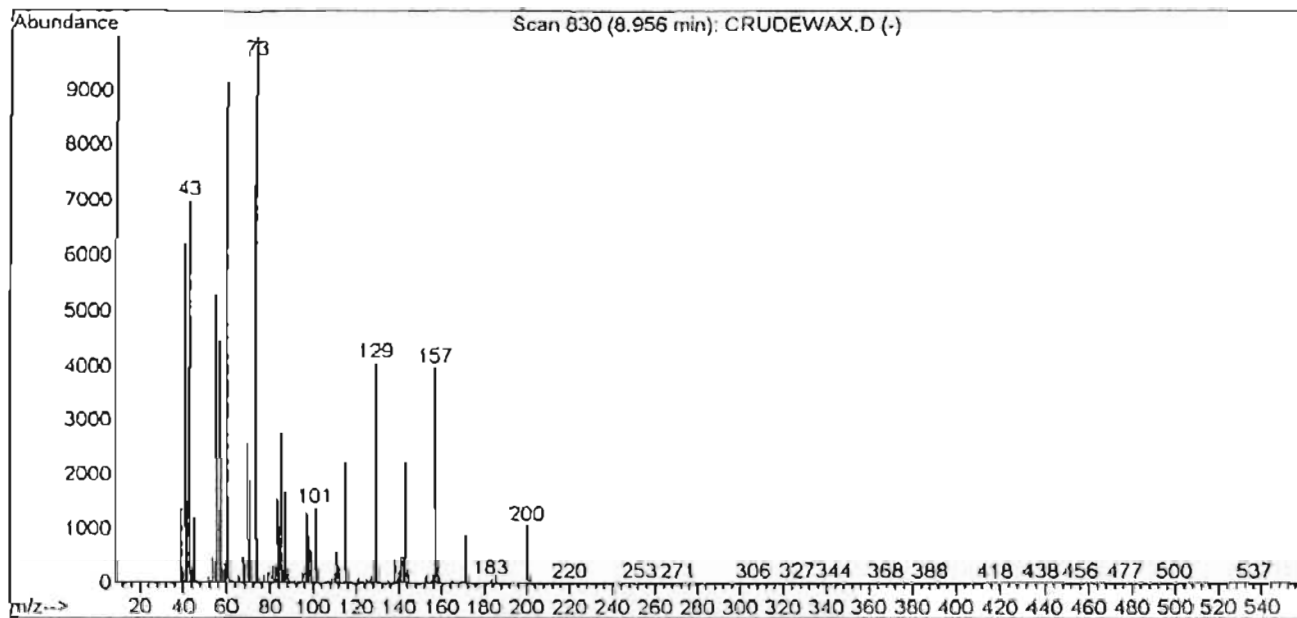
SPECTRUM 57 : Gas chromatogram of the wax balls from the calcium – spent liquor evaporates

Library Searched : C:\Database\Nist98.1
 Quality : 97
 ID : Naphthalene, 1,2,3,4-tetrahydro-1,6-dimethyl-4-(1-methylethyl)-, (1S-cis)-



SPECTRUM 58 : Mass spectrum of 1,2,3,4-tetrahydro-1,6-dimethyl-4-(1-methylethyl)-naphthalene

Library Searched : C:\Database\Nist98.1
Quality : 96
ID : Dodecanoic acid

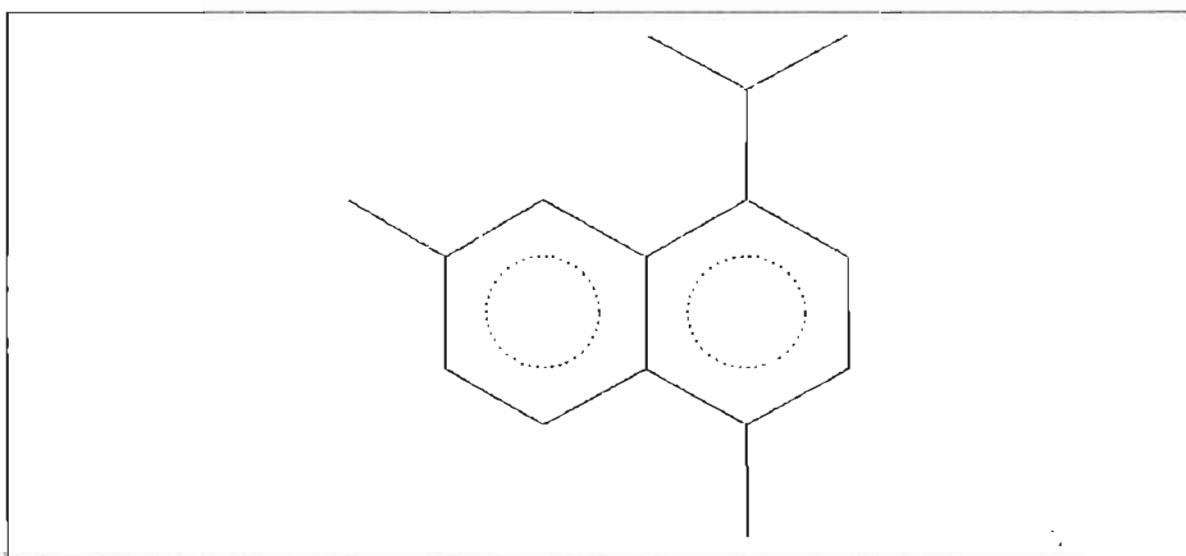
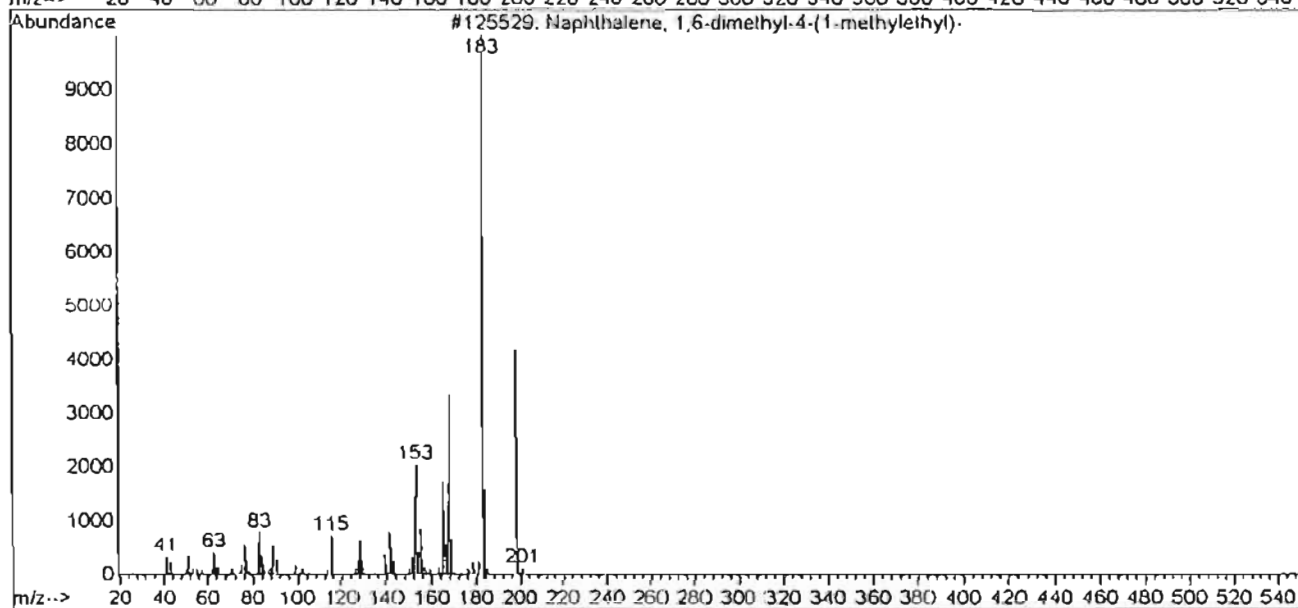
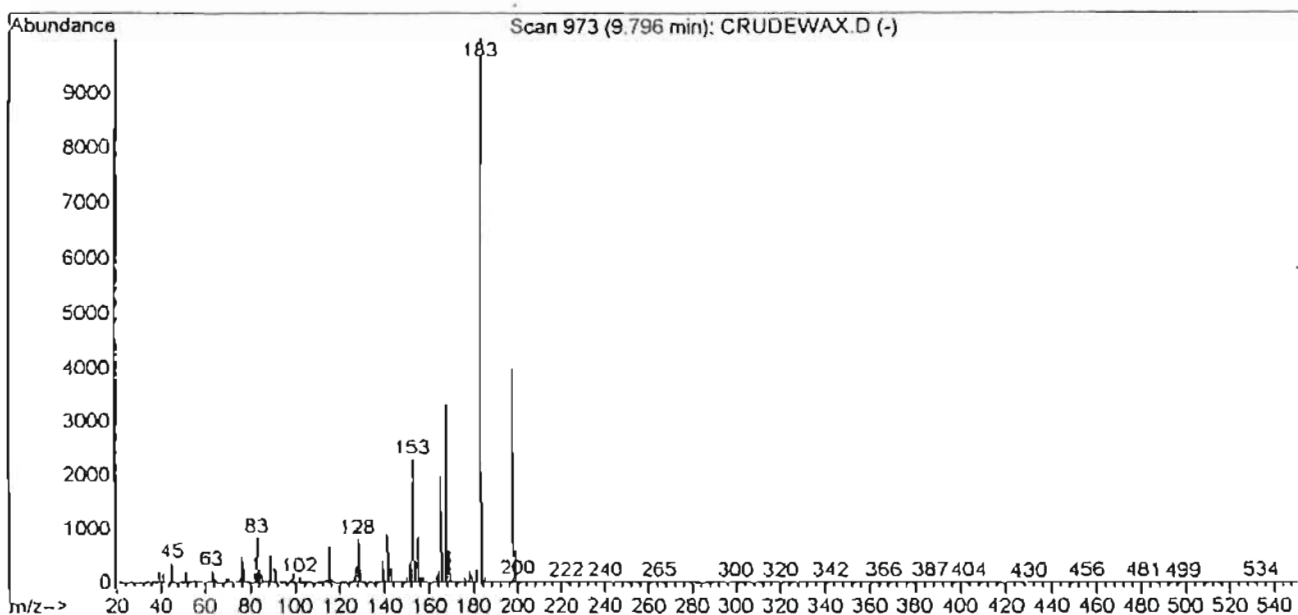


SPECTRUM 59 : Mass spectrum of dodecanoic acid

Library Searched : C:\Database\Nist98.1

Quality : 99

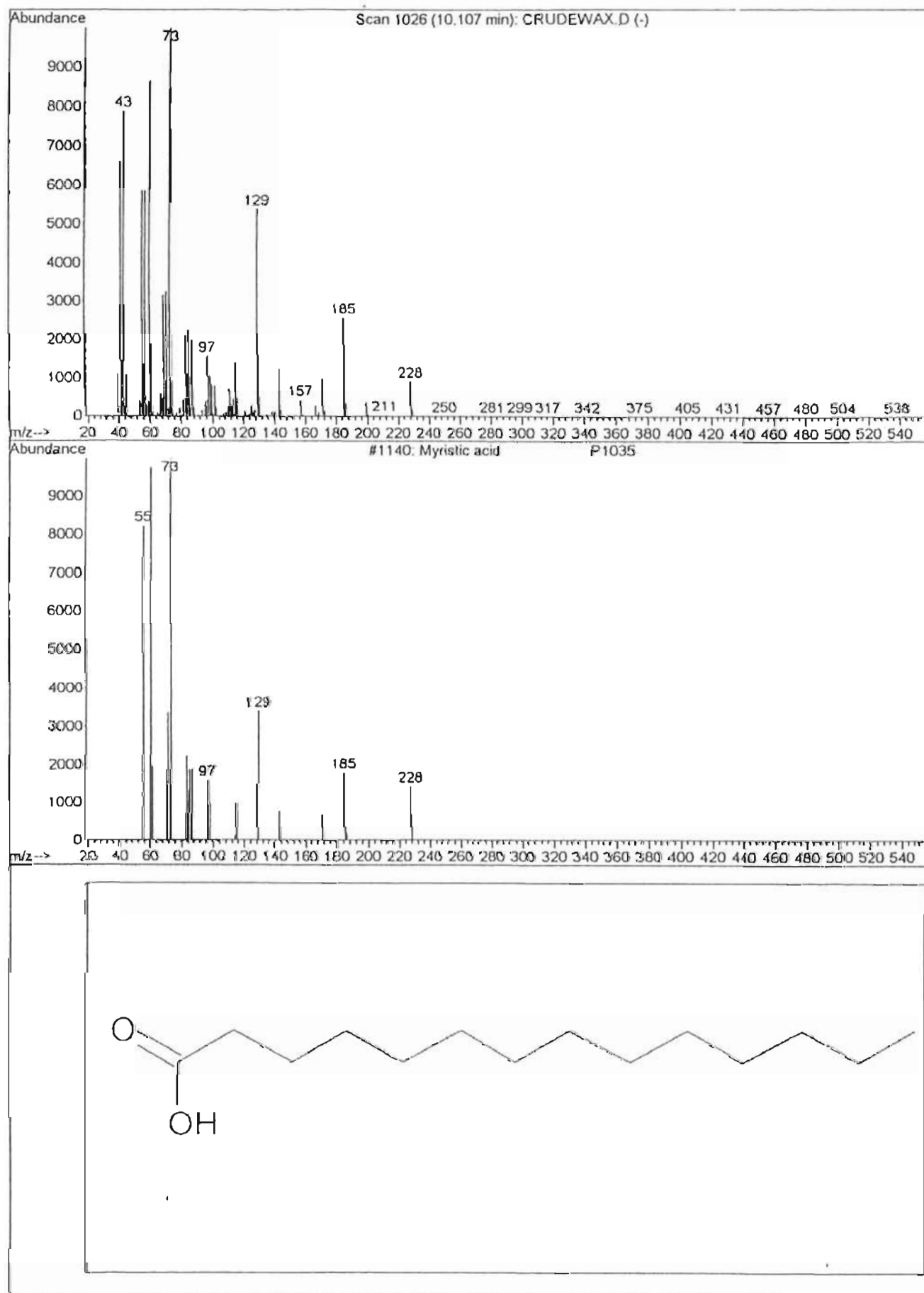
ID : Naphthalene, 1,6-dimethyl-4-(1-methylethyl)-



SPECTRUM 60 : Mass spectrum of 1,6-dimethyl-4-(1-methylethyl)-naphthalene

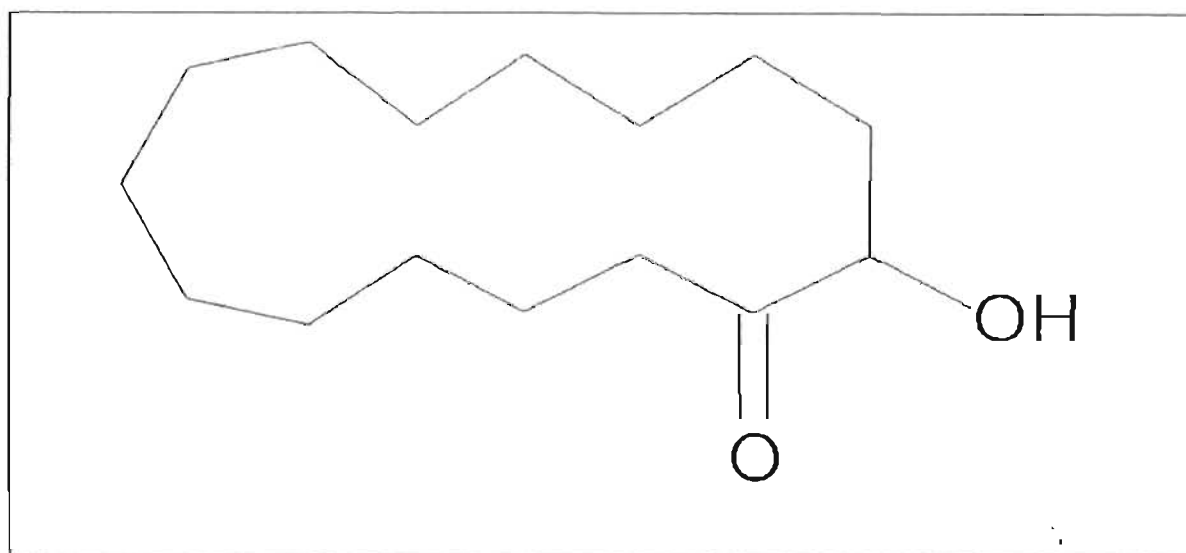
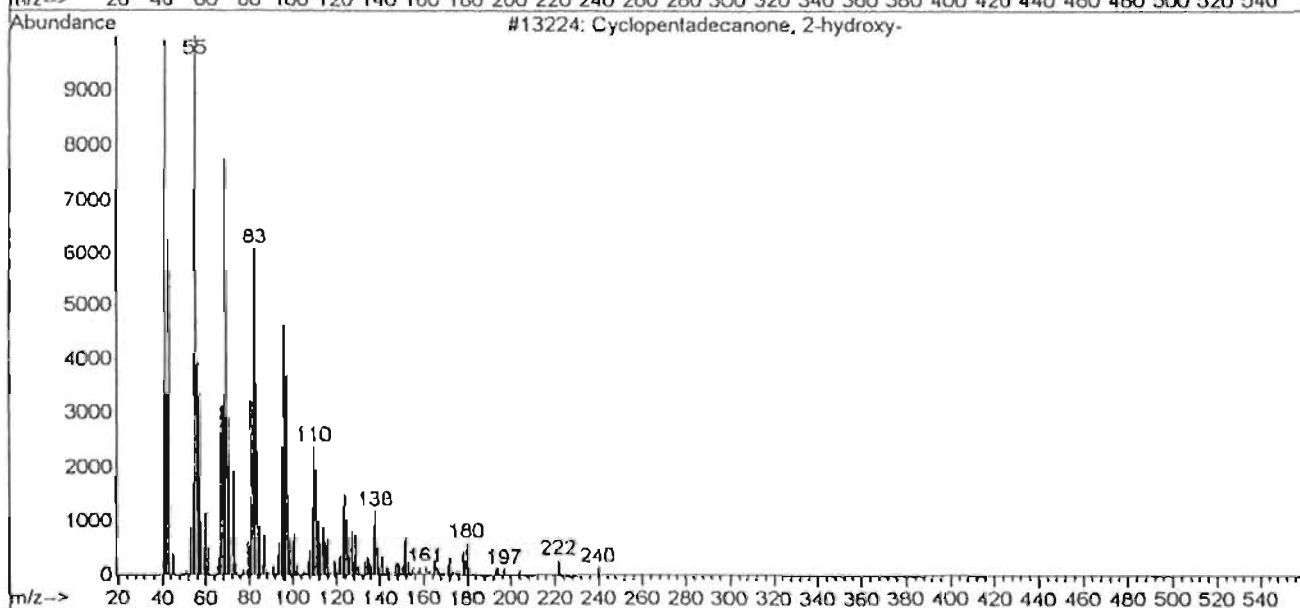
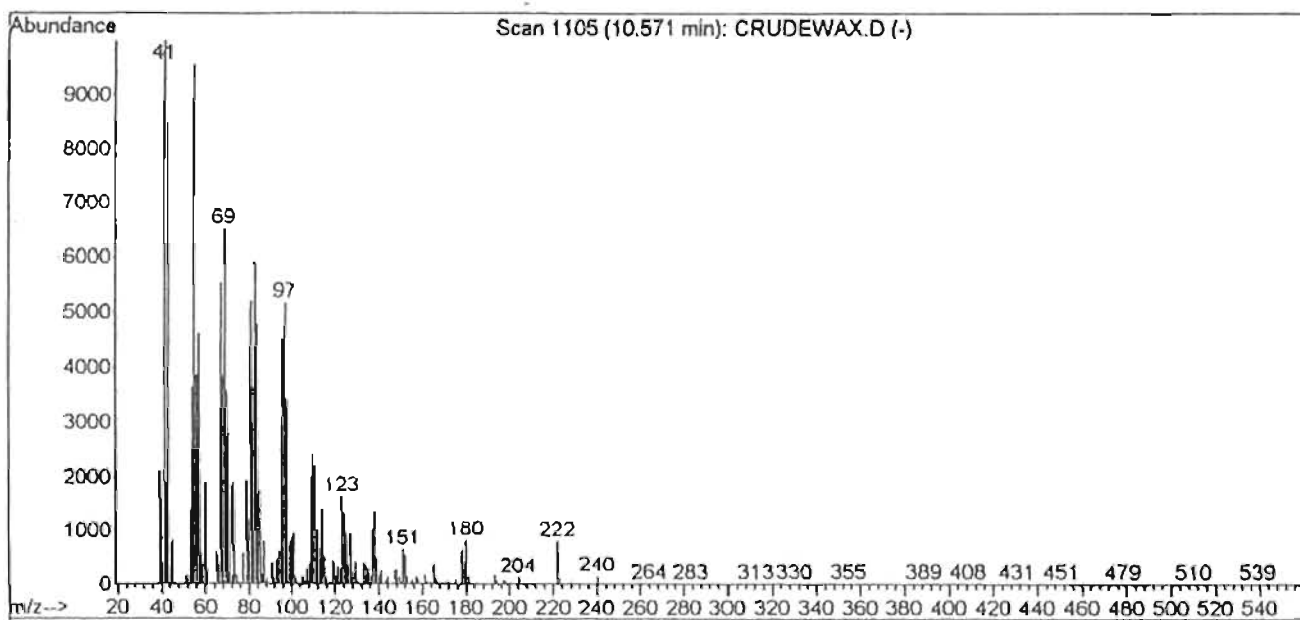
Library Searched : C:\Database\PMW_TOX2.L
Quality : 95
ID : Myristic acid

P1035



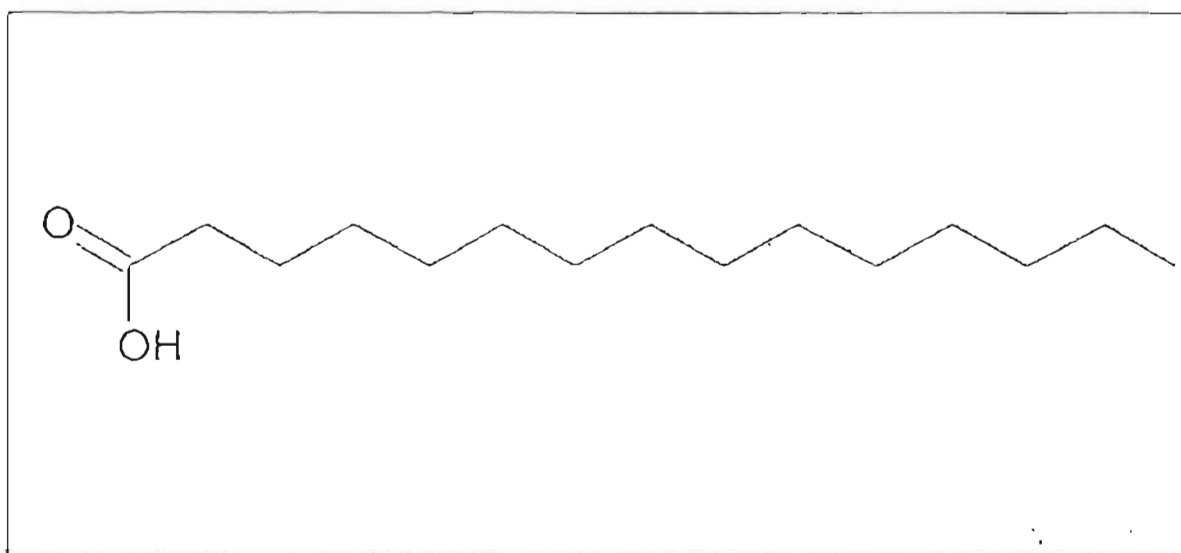
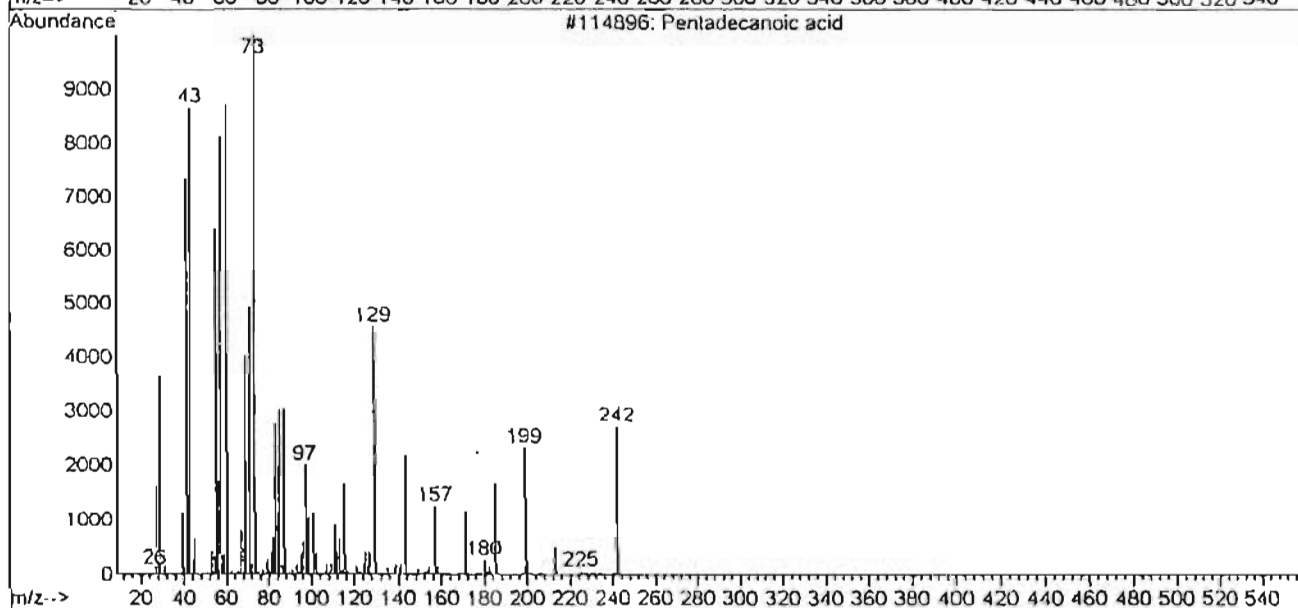
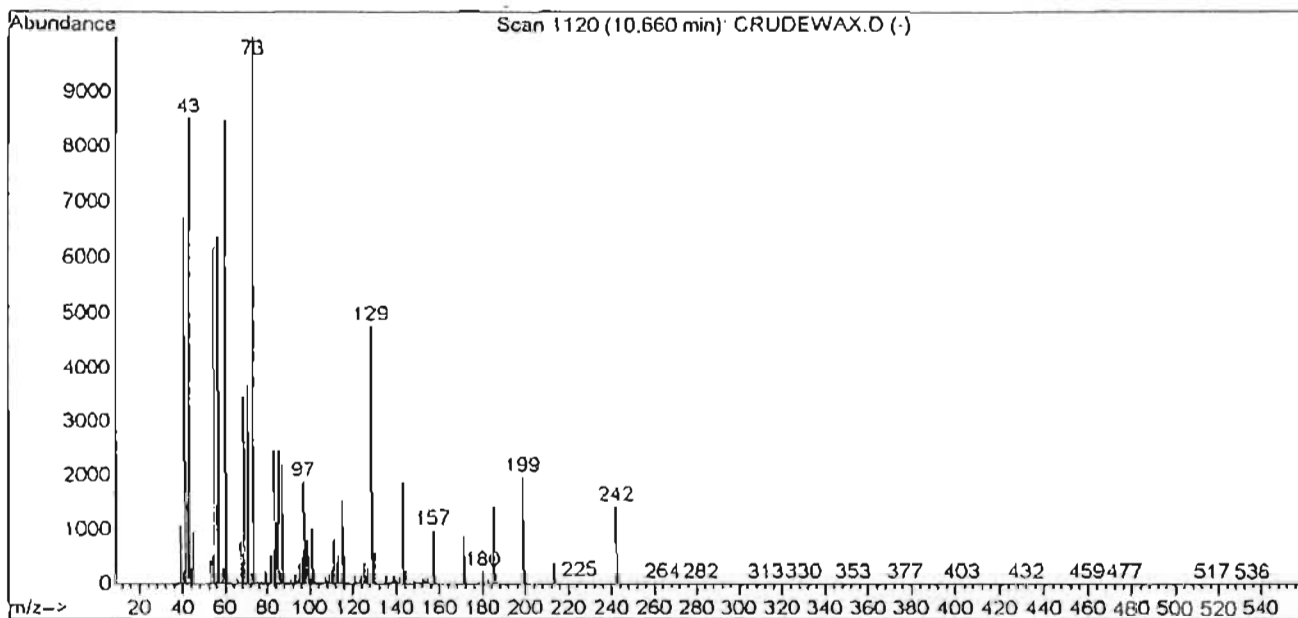
SPECTRUM 61 : Mass spectrum of myristic acid

Library Searched : C:\Database\Nist98.1
Quality : 99
ID : Cyclopentadecanone, 2-hydroxy-



SPECTRUM 62 : Mass spectrum of 2-hydroxy-cyclopentadecanone

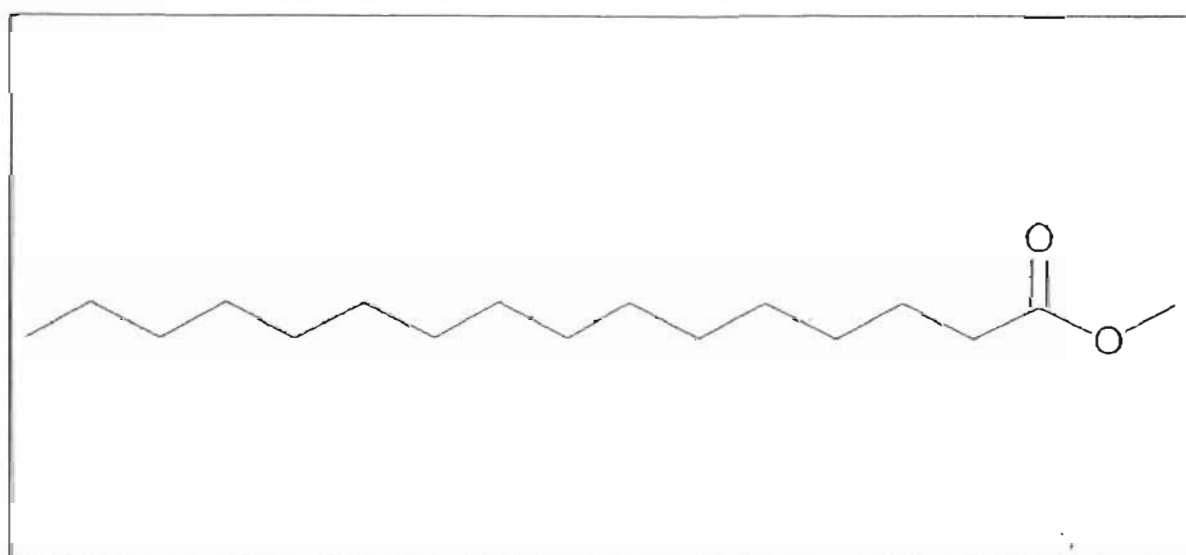
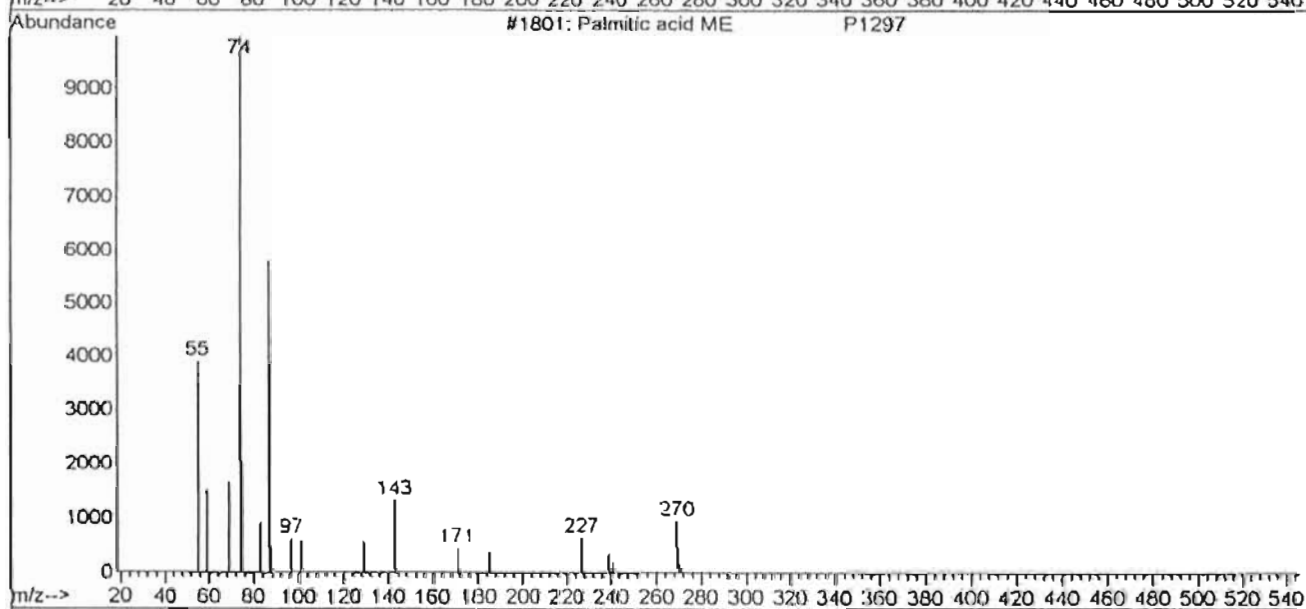
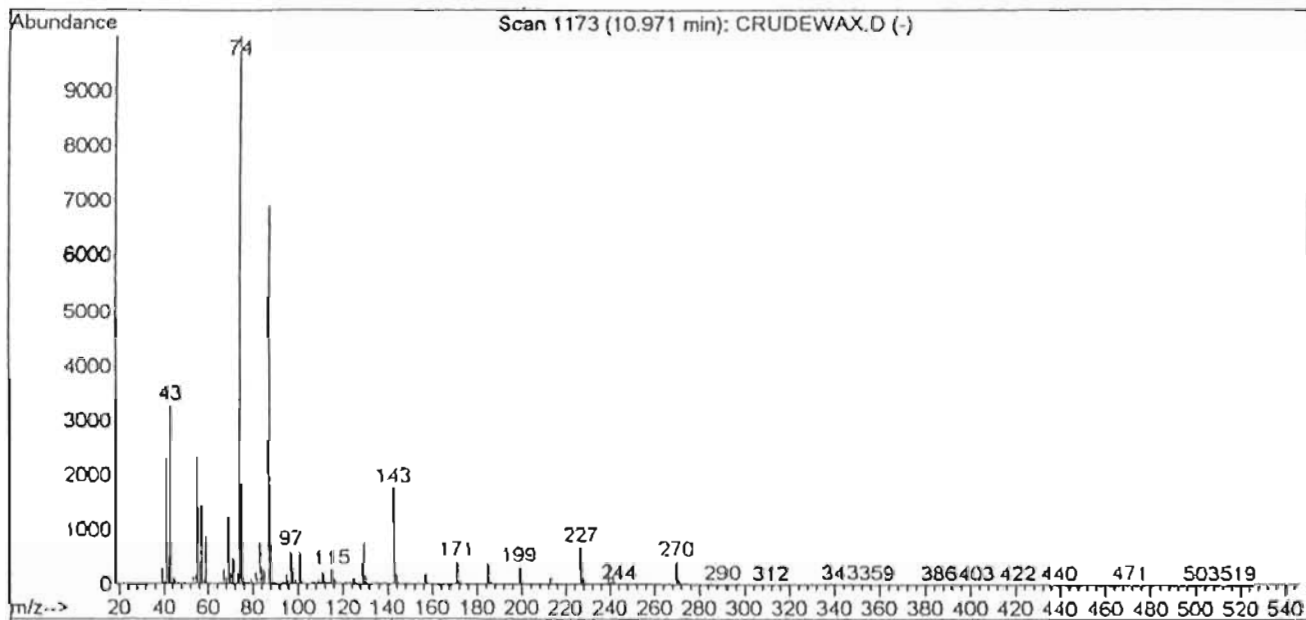
Library Searched : C:\Database\Nist98.1
Quality : 99
ID : Pentadecanoic acid



SPECTRUM 63 : Mass spectrum of pentadecanoic acid

Library Searched : C:\Database\PMW_TOX2.L
Quality : 90
ID : Palmitic acid ME

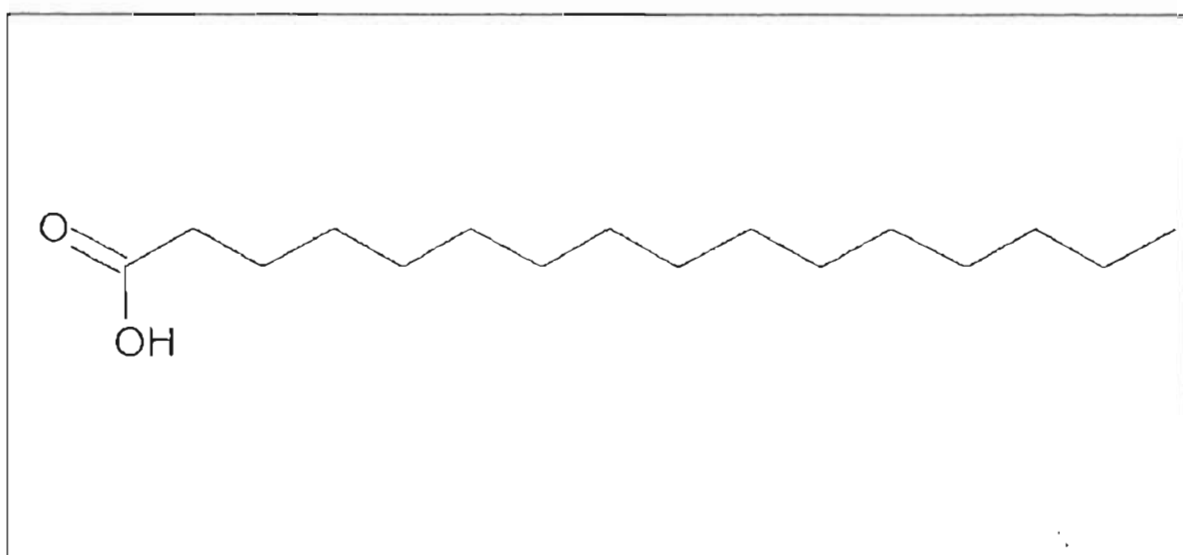
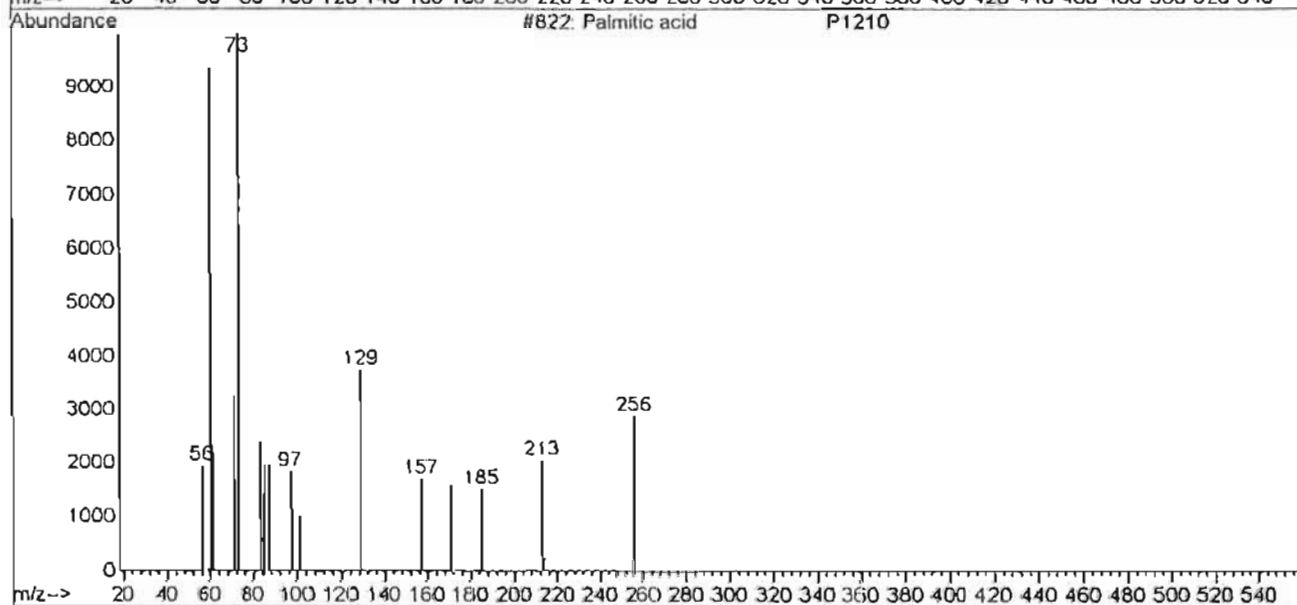
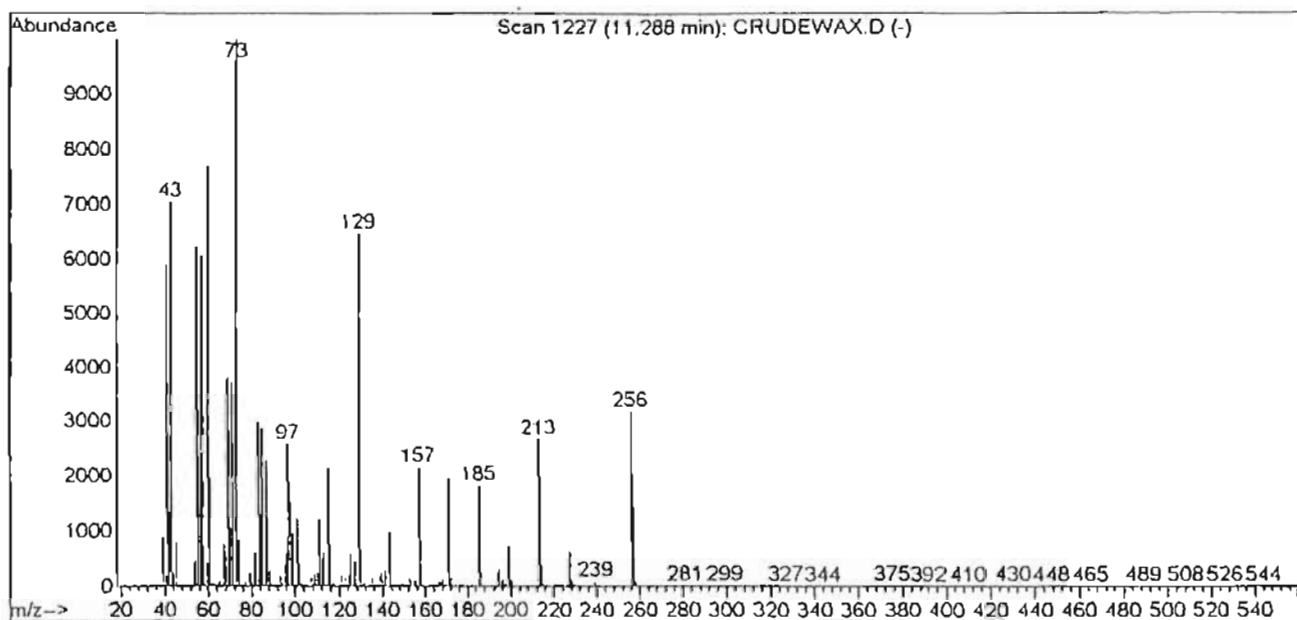
P1297



SPECTRUM 64 : Mass spectrum of palmitic acid methyl ester

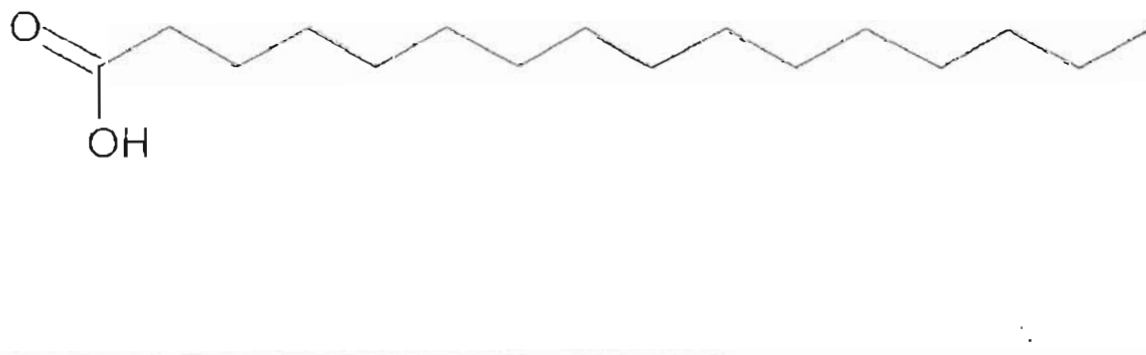
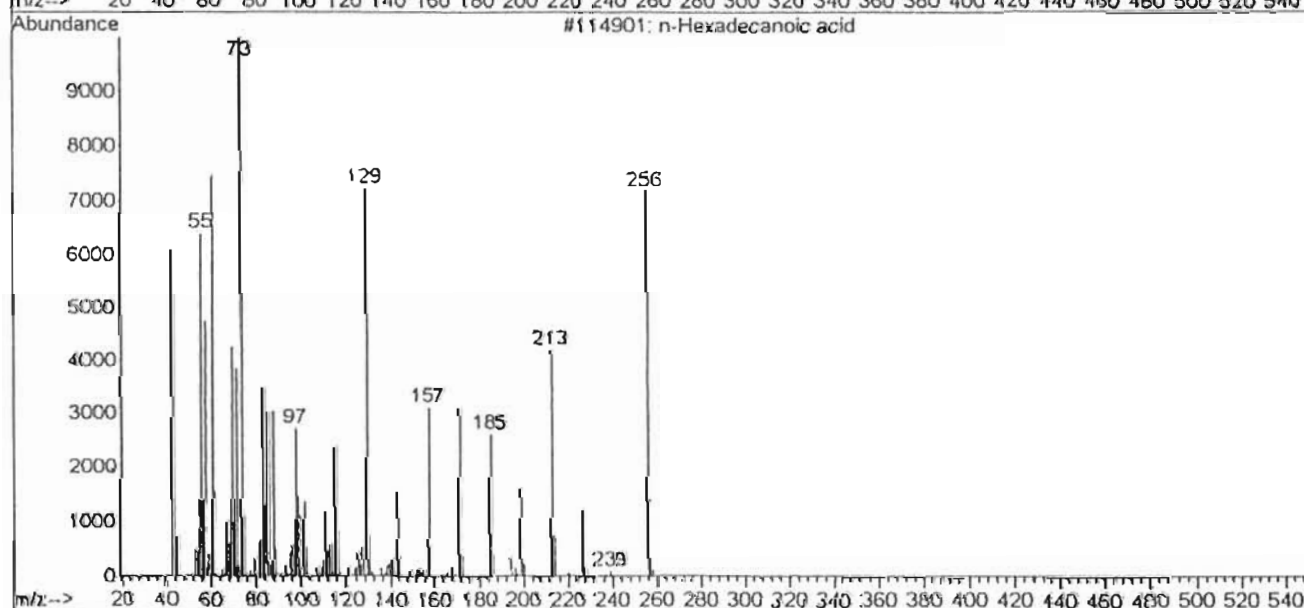
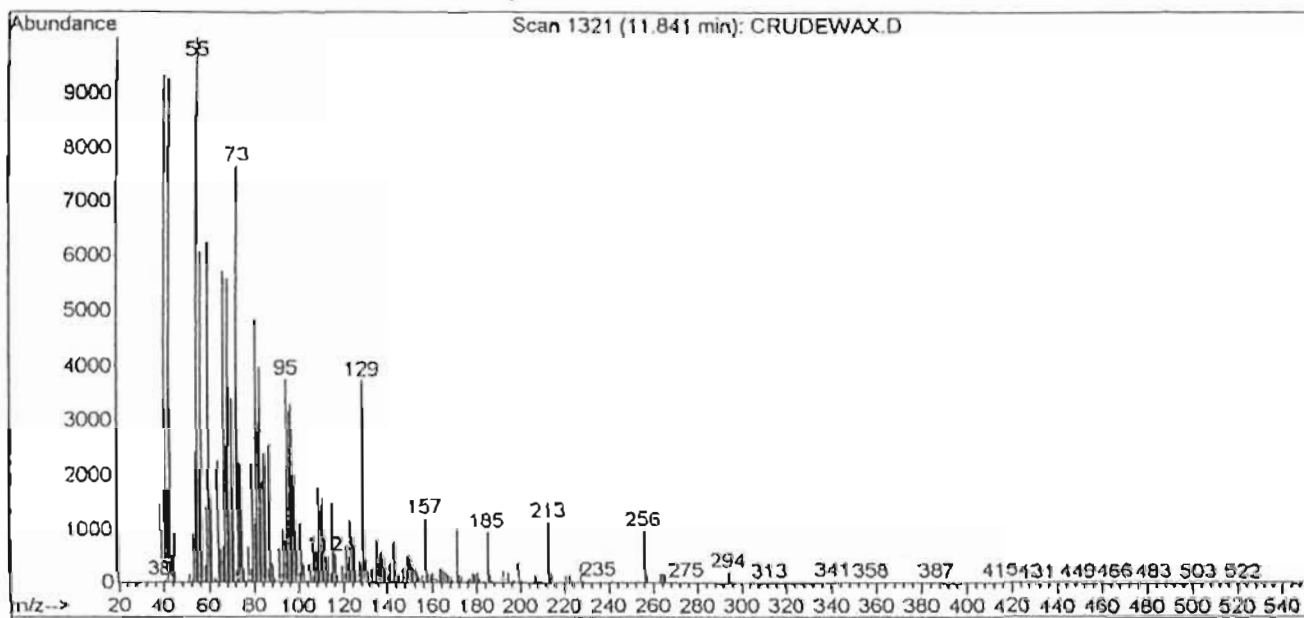
Library Searched : C:\Database\PMW_TOX2.L
Quality : 96
ID : Palmitic acid

P1210



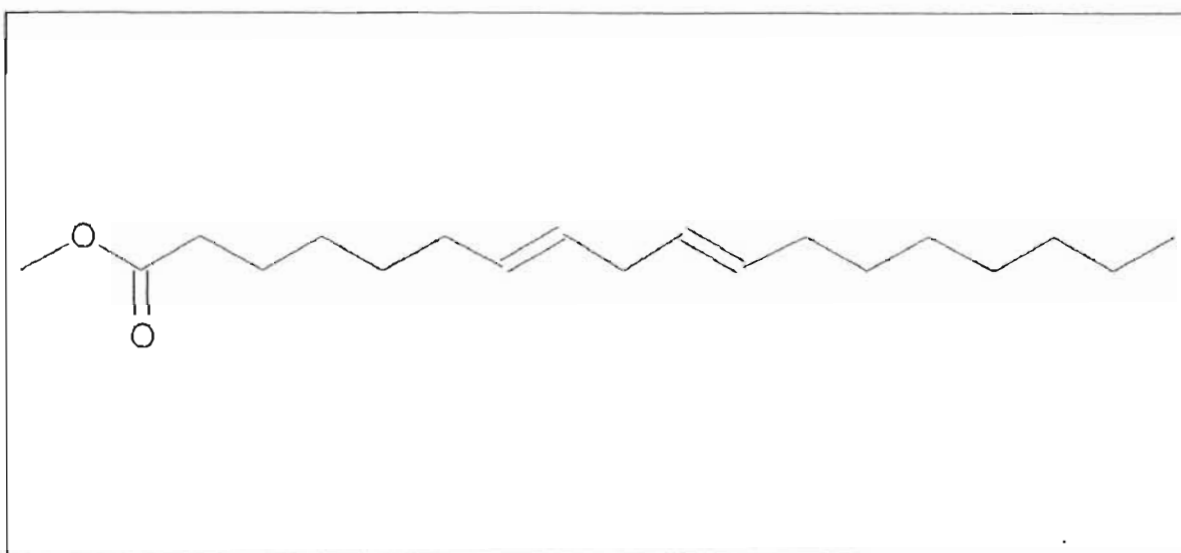
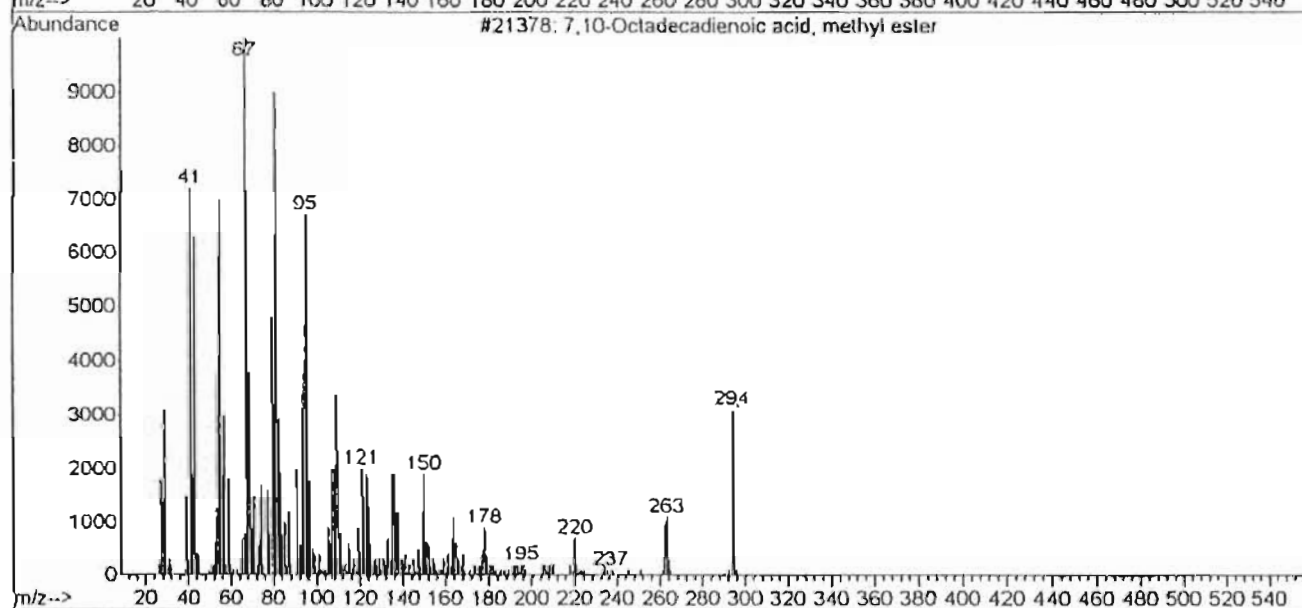
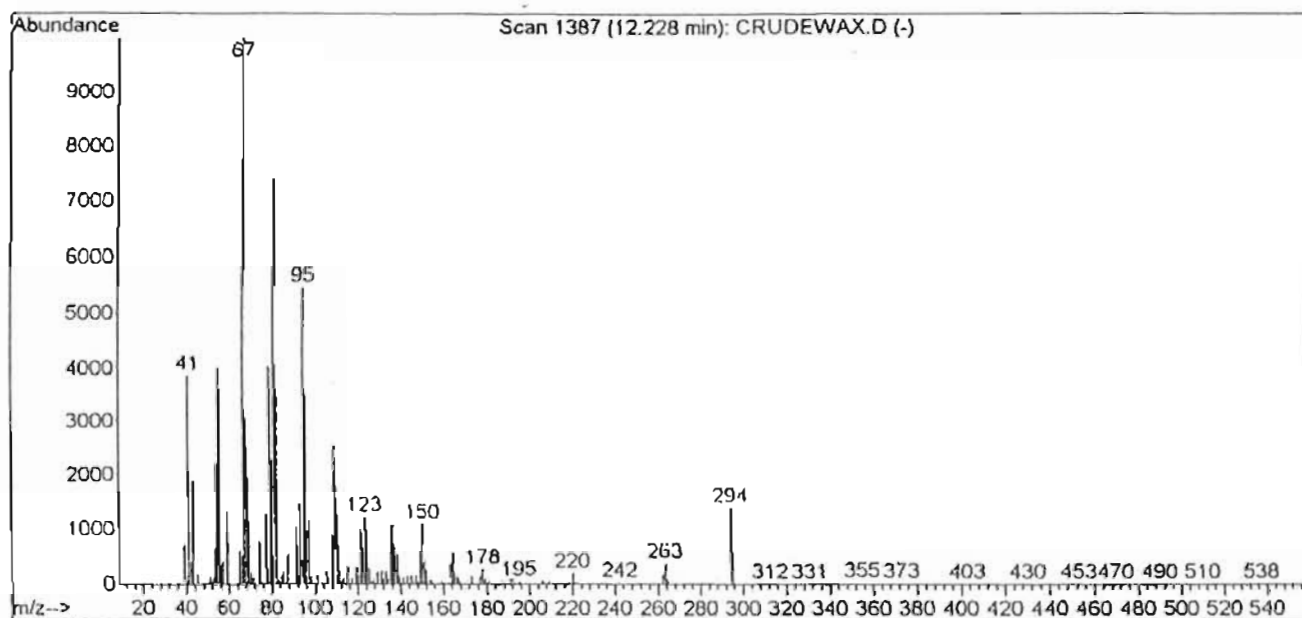
SPECTRUM 65 : Mass spectrum of palmitic acid

Library Searched : C:\Database\Nist98.1
Quality : 96
ID : n-Hexadecanoic acid



SPECTRUM 66 : Mass spectrum of hexadecanoic acid

Library Searched : C:\Database\Nist98.1
Quality : 94
ID : 7,10-Octadecadienoic acid, methyl ester



SPECTRUM 67: Mass spectrum of 7,10-octadecadienoic acid, methyl ester

Data File : D:\BRENDA\CRUDEWAX.D

Vial: 22

Acq On : 4 Apr 2001 15:39

Sample : Crude Wax

Inst : Instrumen

Misc : 1ul inject, 1:75 split, MeCl2, 20dpm

Multiplr: 1.00

Sample Amount: 0.00

MS Integration Params: autoint1.e

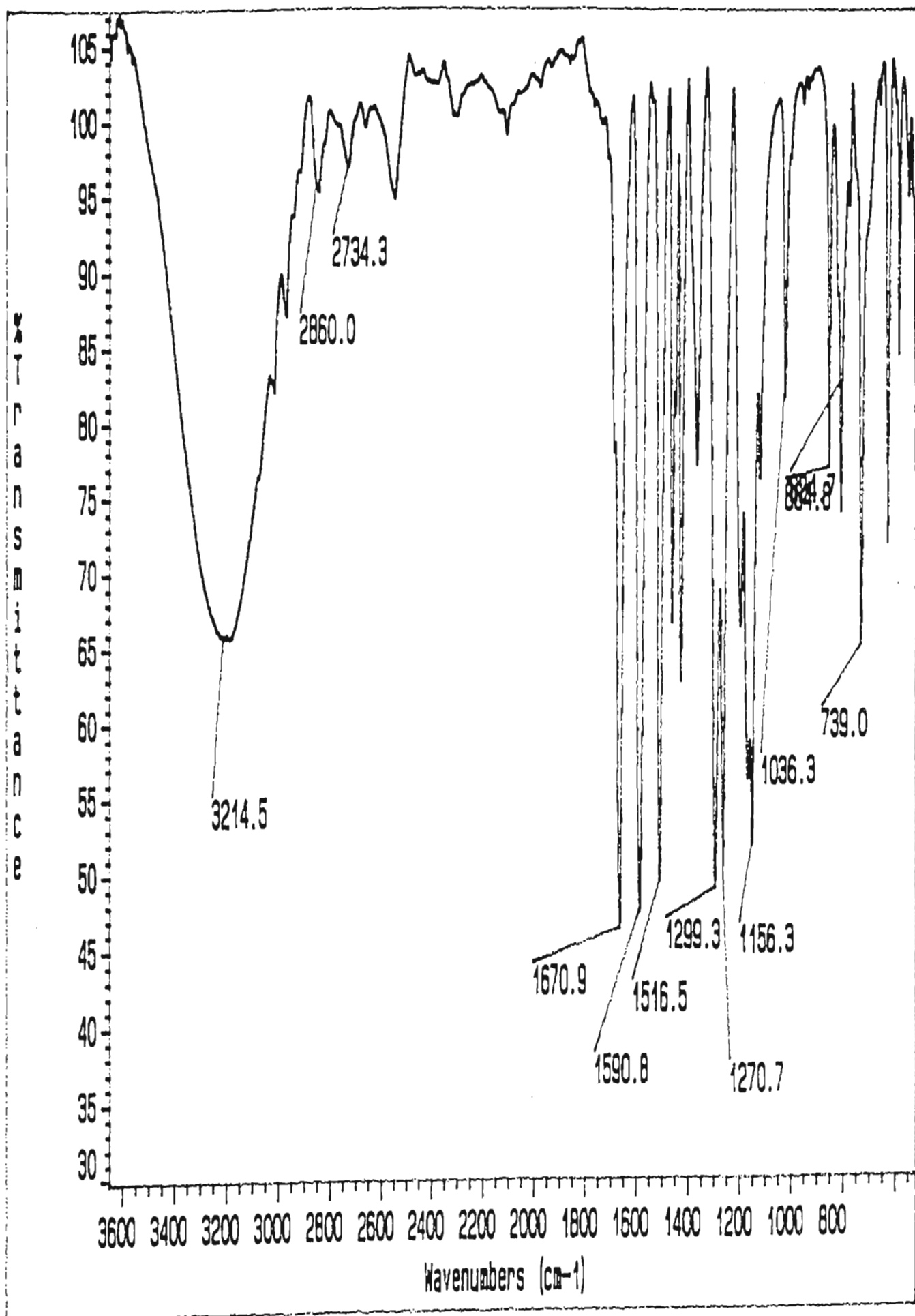
Method : C:\MSDCHEM\1\METHODS\NEW.M (Chemstation Integrator)

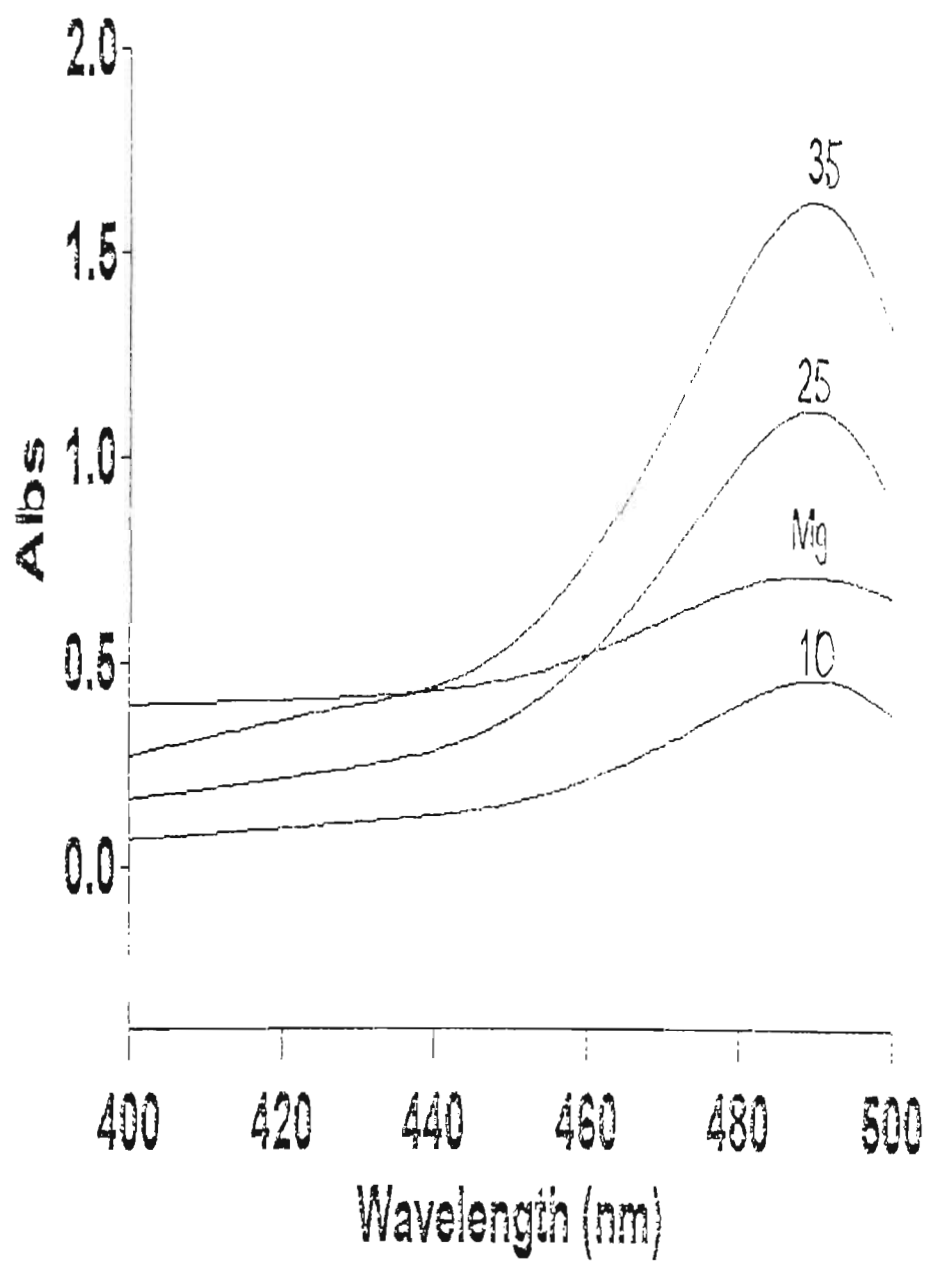
Title :

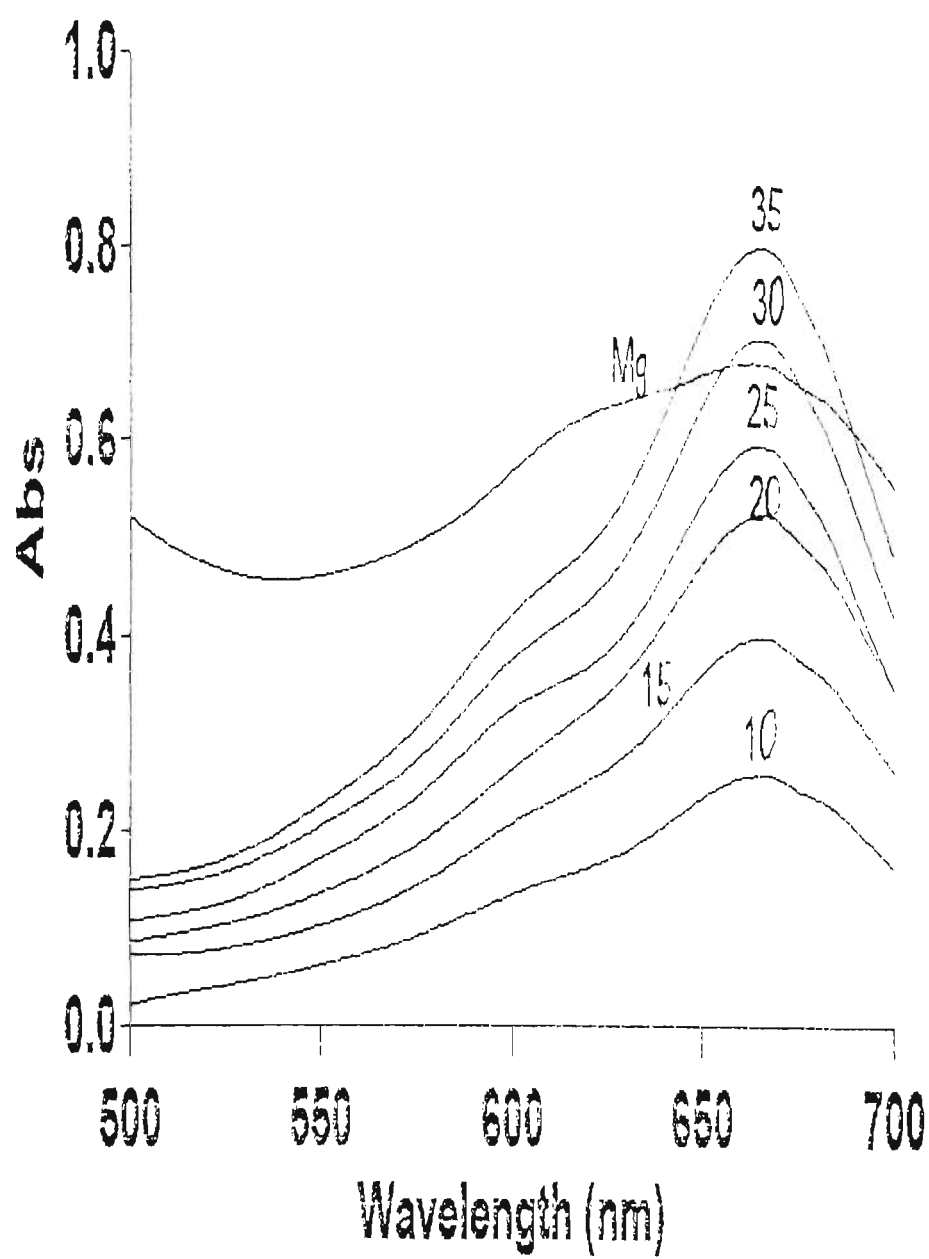
Signal : TIC

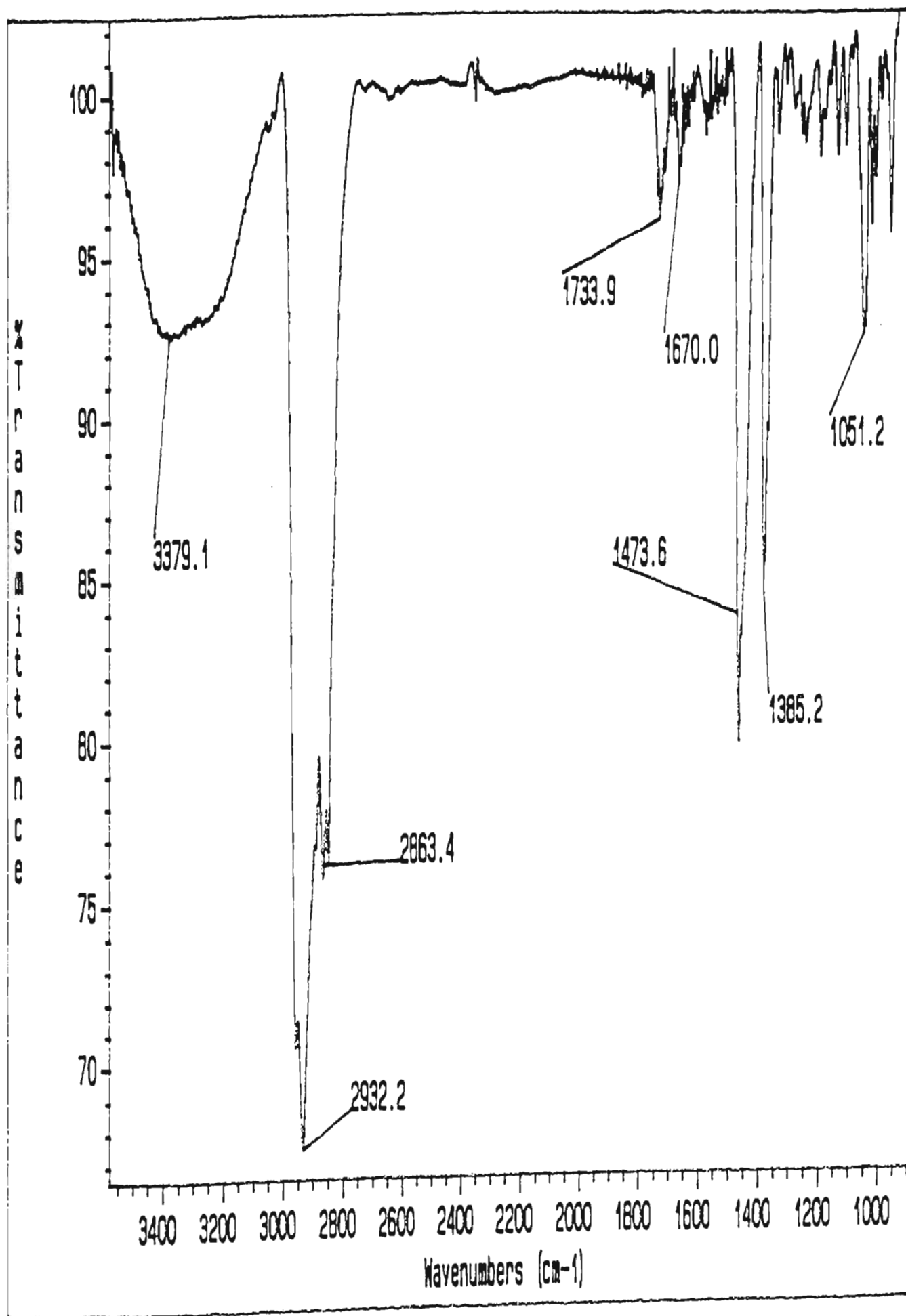
peak #	R.T. min	first scan	max scan	last scan	PK TY	peak height	corr. area	corr. % max.	% of total
1	8.562	755	763	778	VV 3	255779	5071498	0.34%	0.221%
2	8.732	778	792	800	VV 2	176872	2954736	0.20%	0.129%
3	8.803	800	804	808	PV	91551	1145595	0.08%	0.050%
4	8.879	808	817	823	VV	3468683	43411803	2.91%	1.892%
5	8.956	823	830	836	VV 2	1594335	25912763	1.74%	1.129%
6	9.014	836	840	852	VV	937853	12883368	0.86%	0.561%
7	9.161	852	865	873	VV 6	106523	3830047	0.26%	0.167%
8	9.255	873	881	886	VV	438074	5854047	0.39%	0.255%
9	9.373	886	901	913	VV 2	230055	3948493	0.26%	0.172%
10	9.578	930	936	943	VV	195599	2560001	0.17%	0.112%
11	9.802	943	974	981	VV	1806728	23536685	1.58%	1.026%
12	9.907	981	992	1001	VV	263864	3379219	0.23%	0.147%
13	10.107	1016	1026	1048	VV	3044552	60370823	4.05%	2.631%
14	10.319	1048	1062	1067	VV 5	145282	5456119	0.37%	0.238%
15	10.372	1067	1071	1077	VV	462269	6010427	0.40%	0.262%
16	10.571	1077	1105	1112	VV 2	3630514	93931569	6.30%	4.093%
17	10.660	1112	1120	1152	VV	5611919	128914105	8.64%	5.618%
18	10.889	1152	1159	1169	VV 4	257671	10211795	0.68%	0.445%
19	10.977	1169	1174	1183	VV	6338053	74329261	4.98%	3.239%
20	11.288	1183	1227	1275	VV 2	16929180	1491351529	100.00%	64.987%
21	11.594	1275	1279	1289	VV 6	749826	32339324	2.17%	1.409%
22	11.852	1289	1323	1352	VV 8	1204307	166339054	11.15%	7.248%
23	12.052	1352	1357	1382	VV 7	613434	47064939	3.16%	2.051%
24	12.228	1382	1387	1461	VV	1070352	39342324	2.64%	1.714%
25	13.791	1640	1653	1666	BV	92187	1728763	0.12%	0.075%
26	17.322	2231	2254	2268	BV 8	112288	2979731	0.20%	0.130%

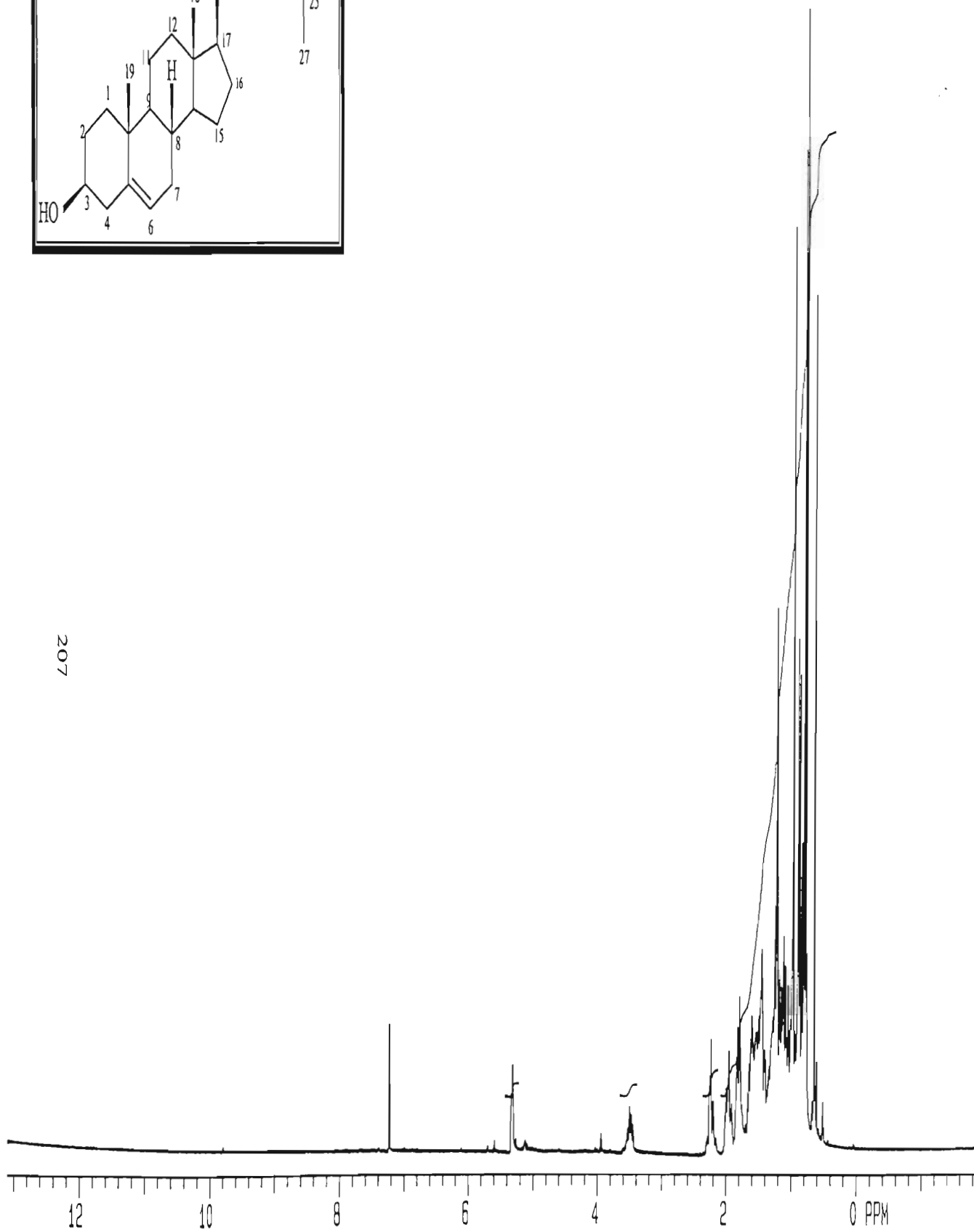
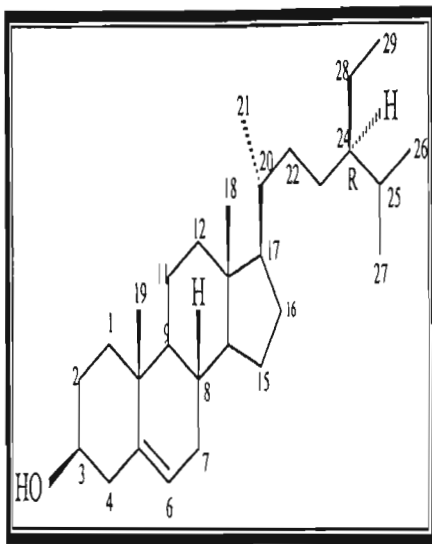
Sum of corrected areas: 2294858017





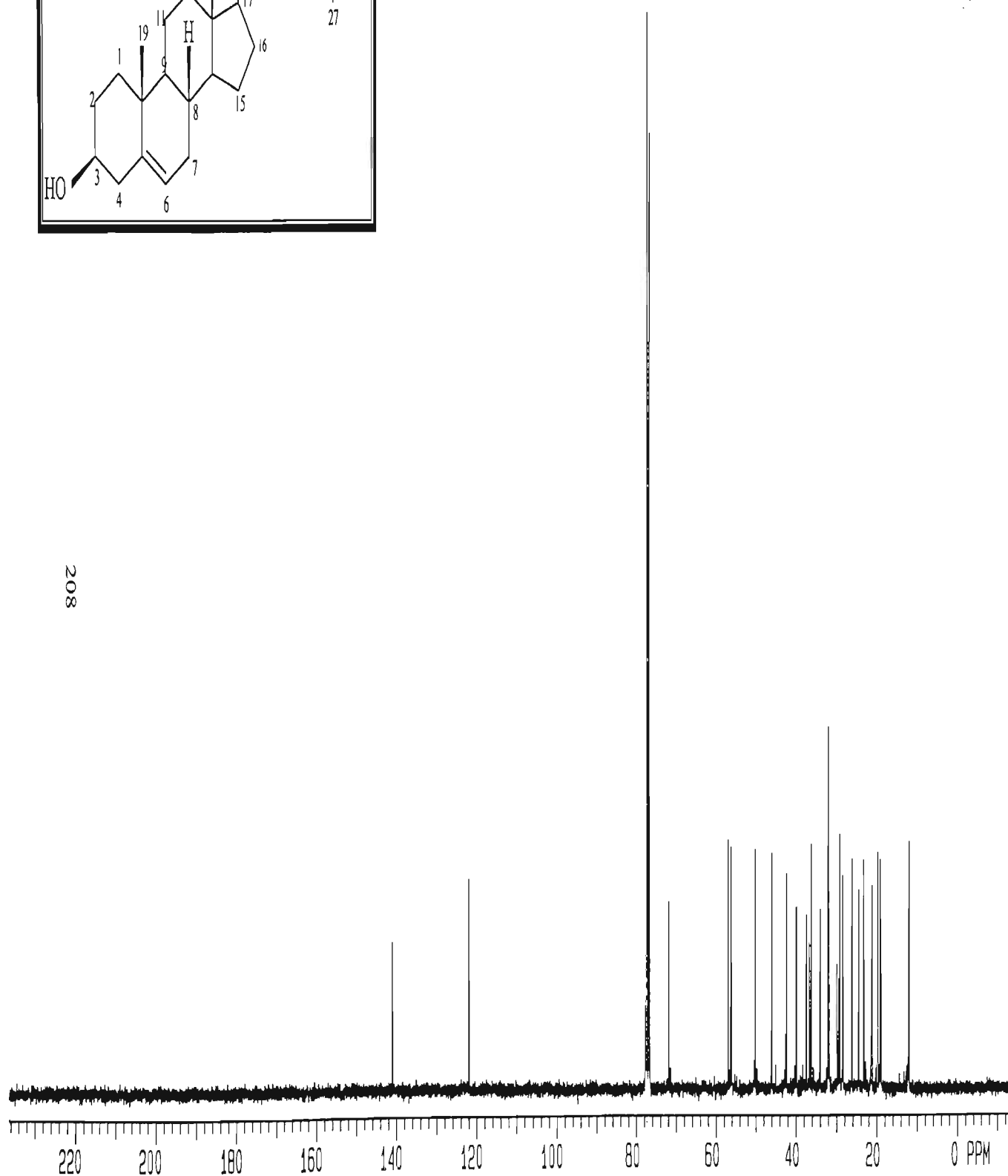
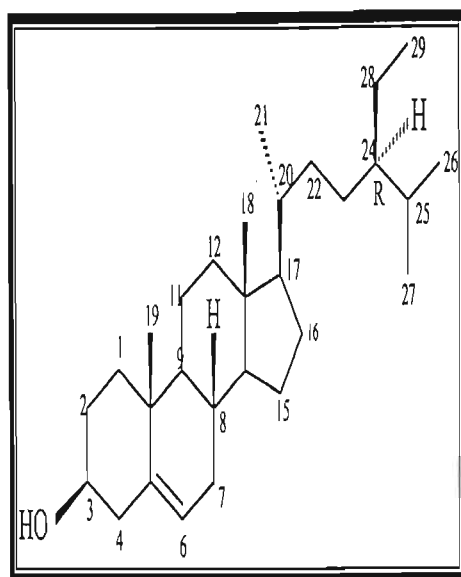


SPECTRUM 72: Infrared spectrum of compound 8, β -sitosterol



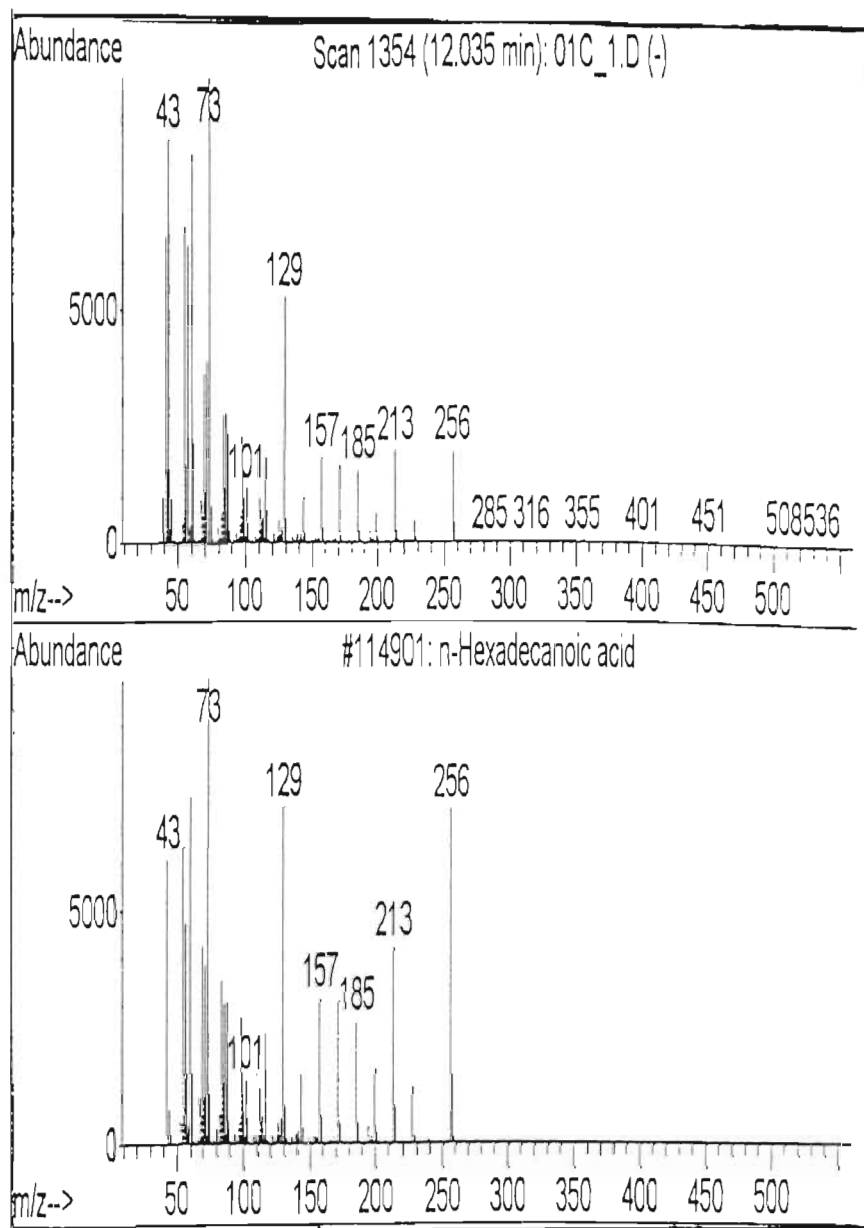
207

SPECTRUM 73: ^1H NMR spectrum of compound 8, β -sitosterol, in CDCl_3

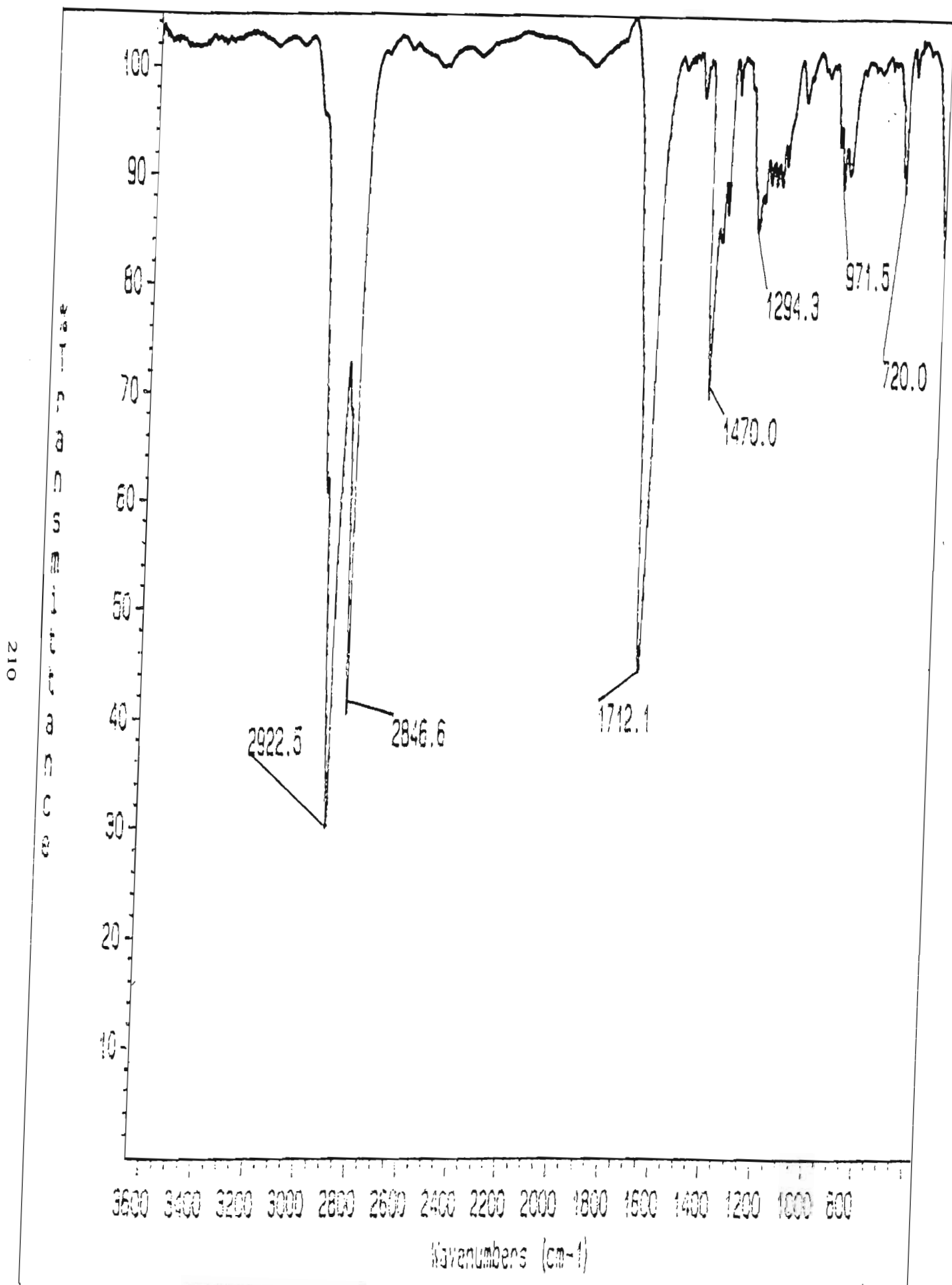


208

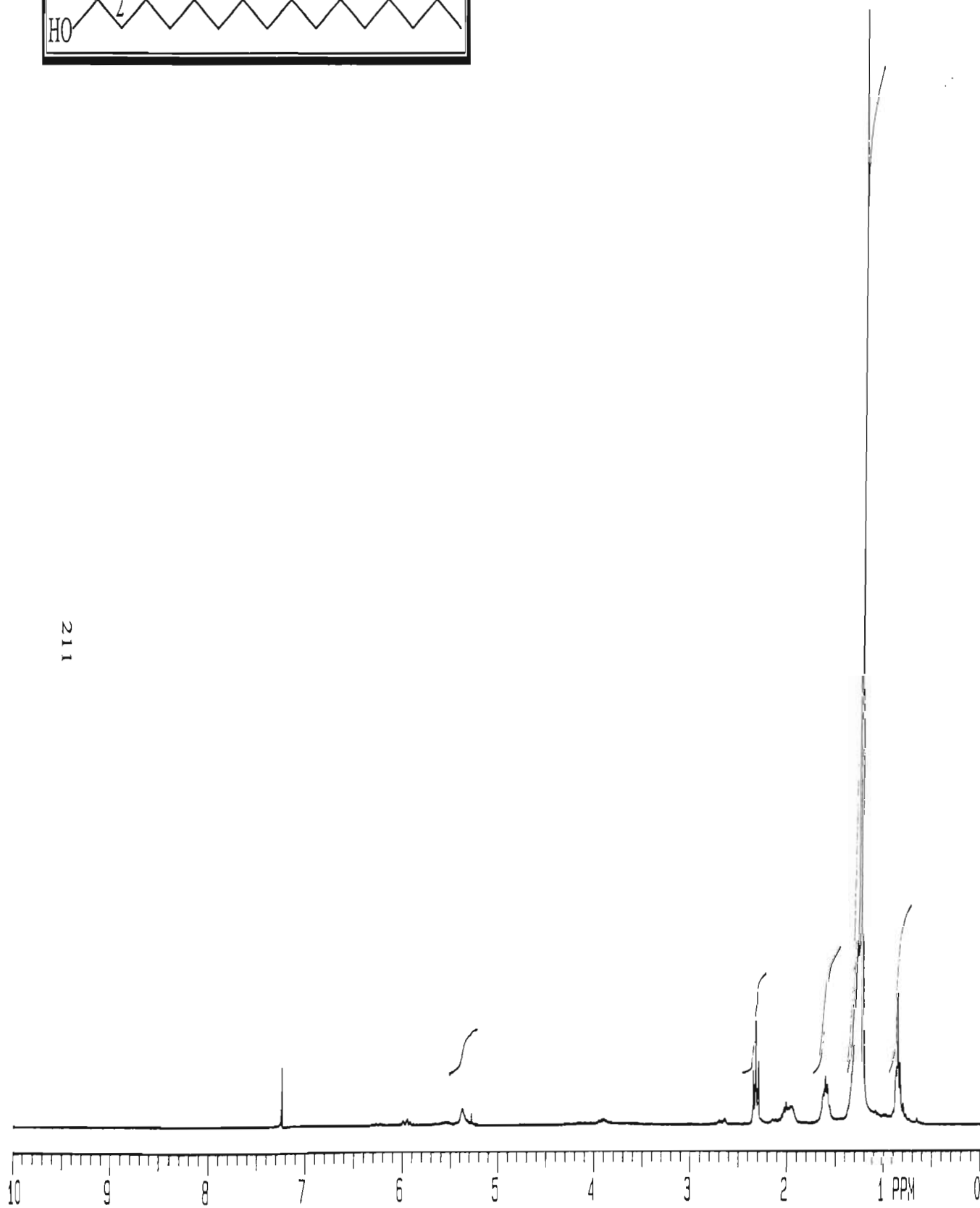
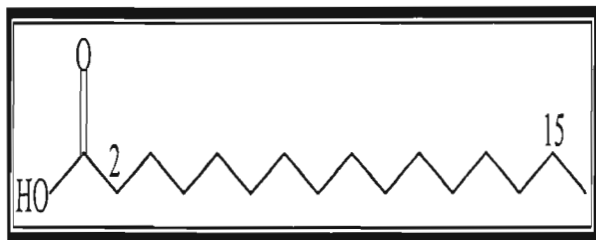
SPECTRUM 71. ^{13}C NMR spectrum of compound 9, *R*-sitosterol, in CDCl_3 .

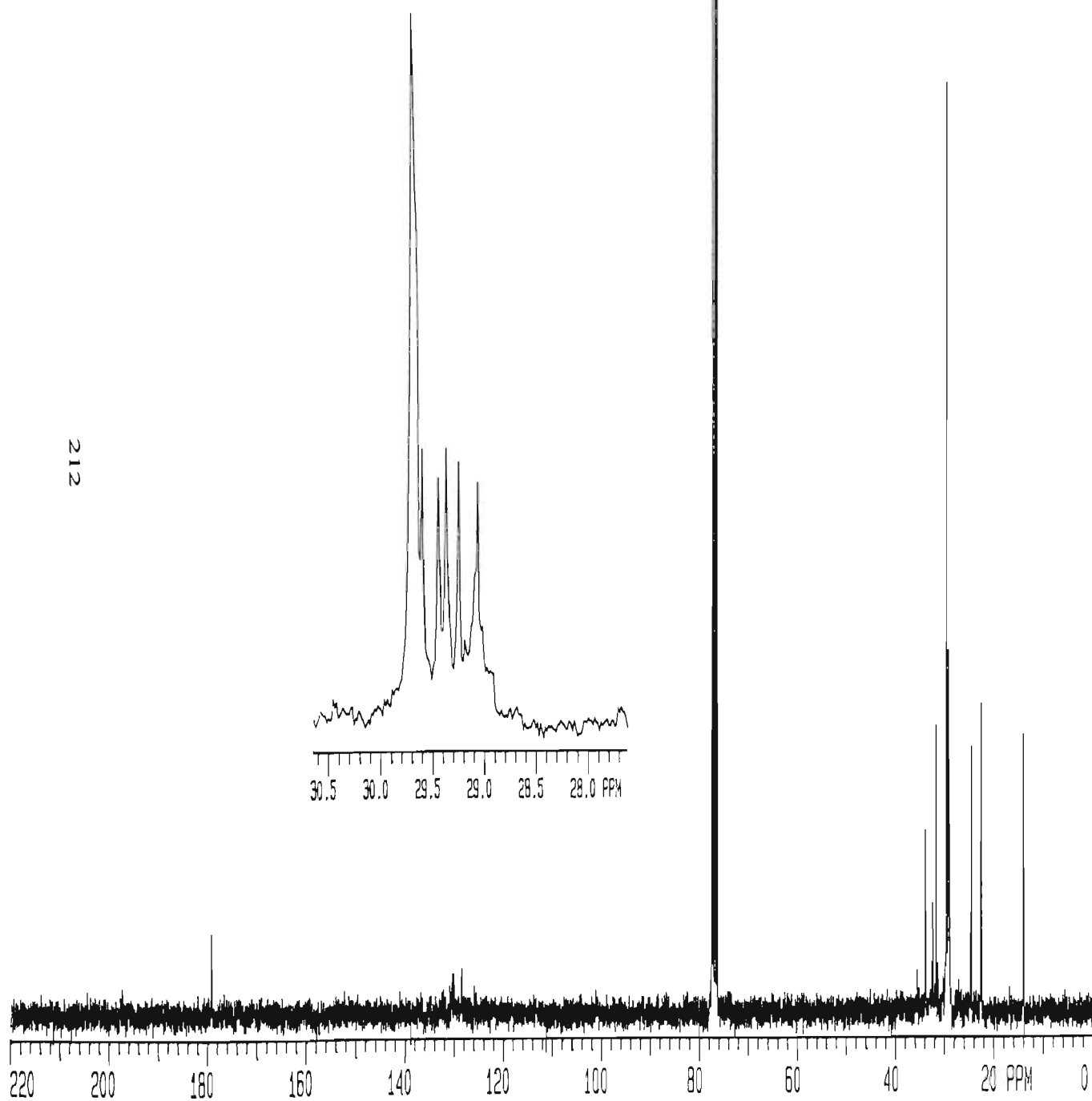
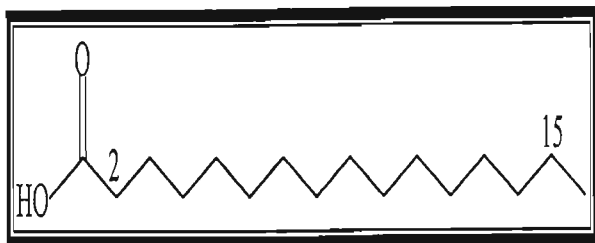


SPECTRUM 75: Mass spectrum of compound 9, hexadecanoic acid

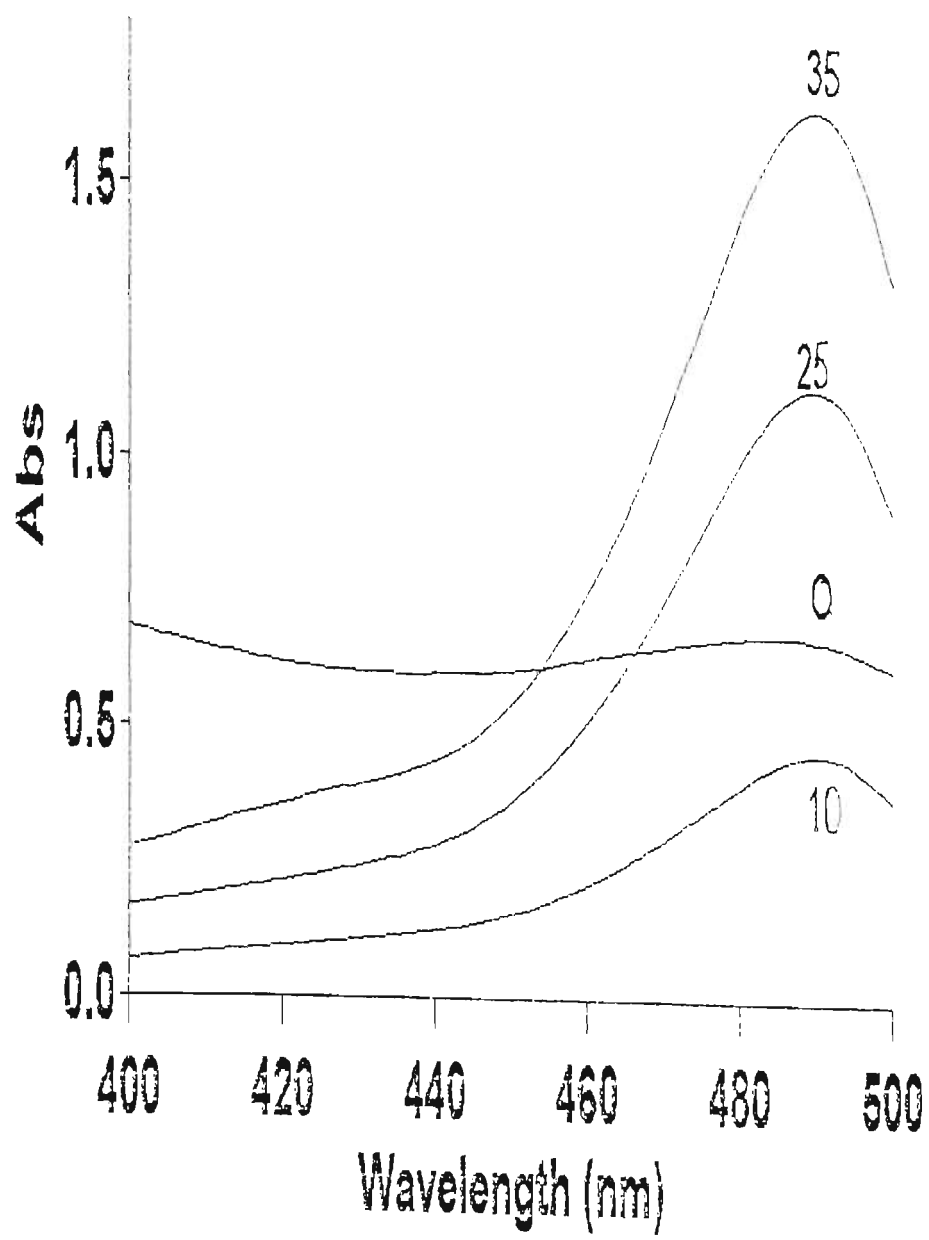


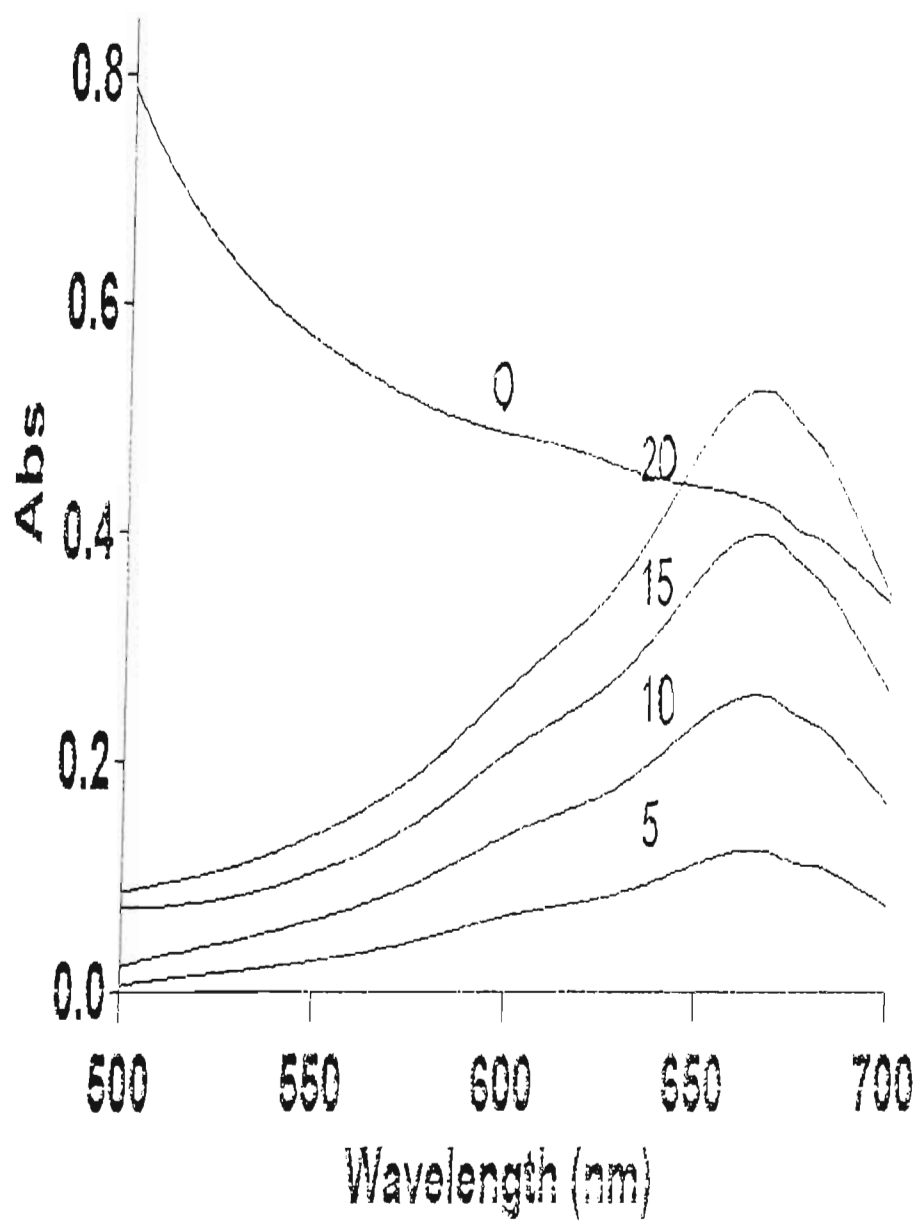
SPECTRUM 76: Infrared spectrum of compound 9, hexadecanoic acid



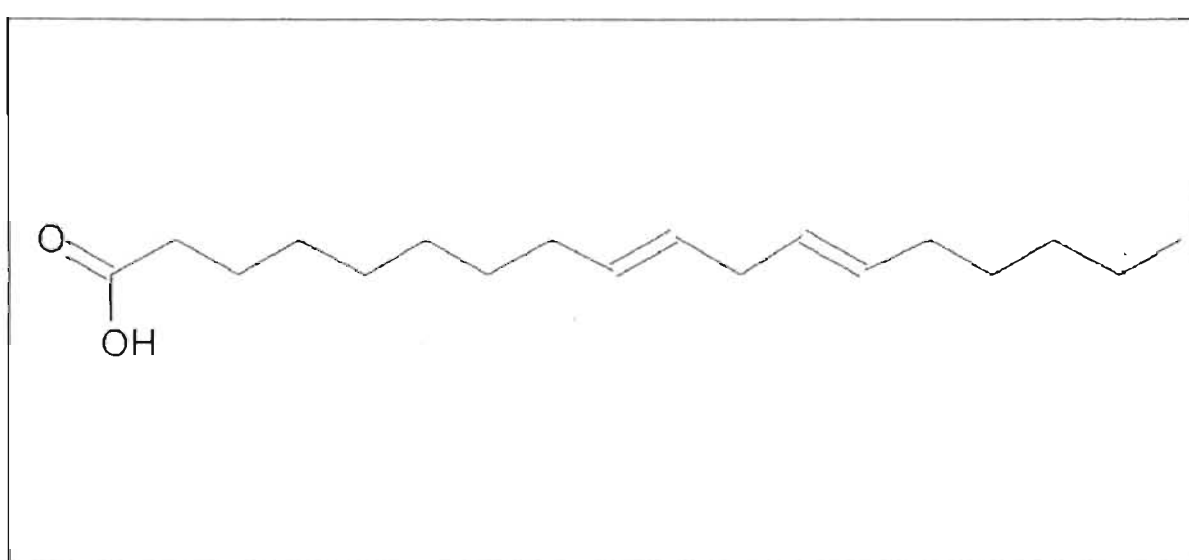
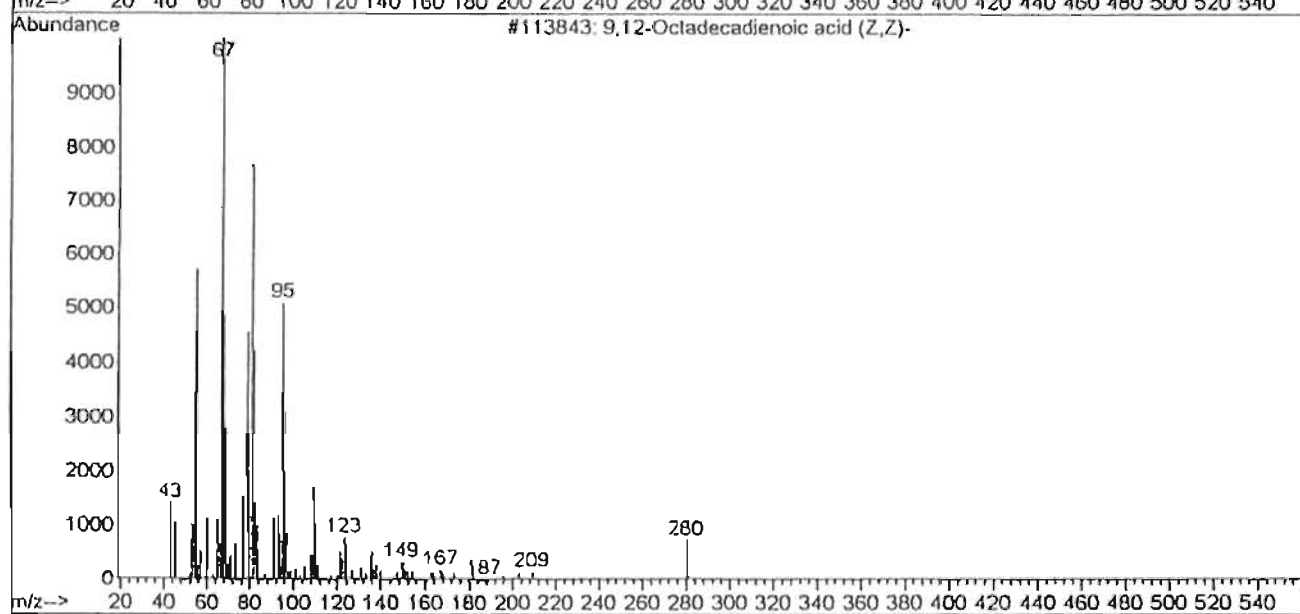
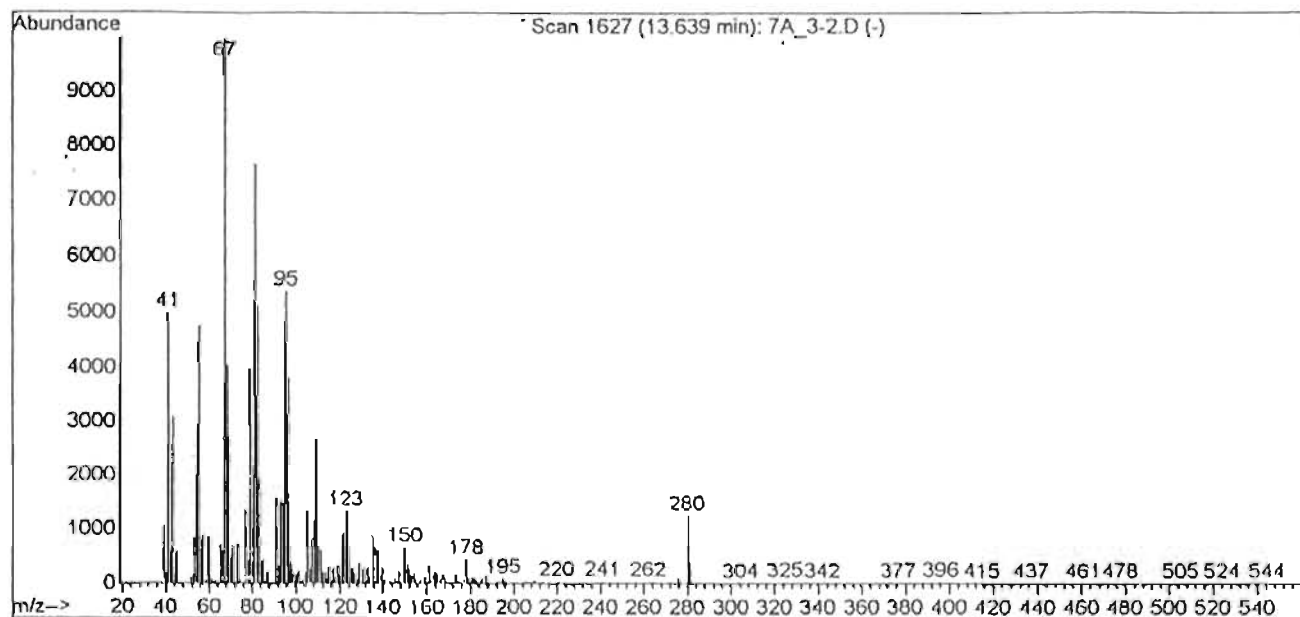


SPECTRUM 78 : ^{13}C NMR spectrum of compound 9. hexadecanoic acid. in CDCl_3

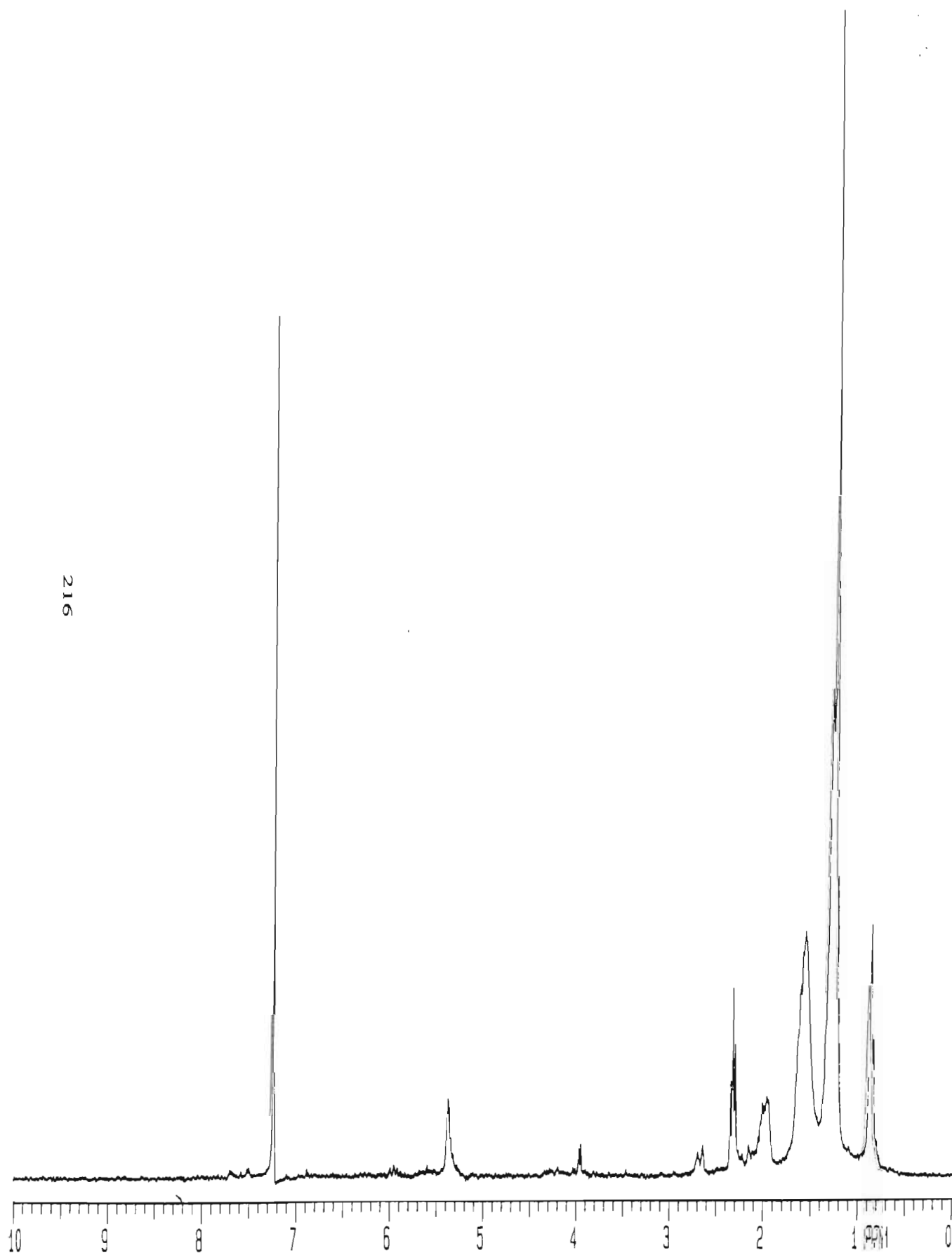
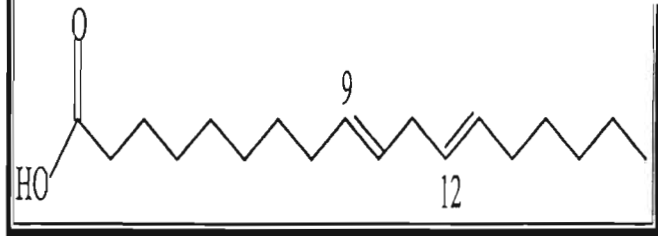




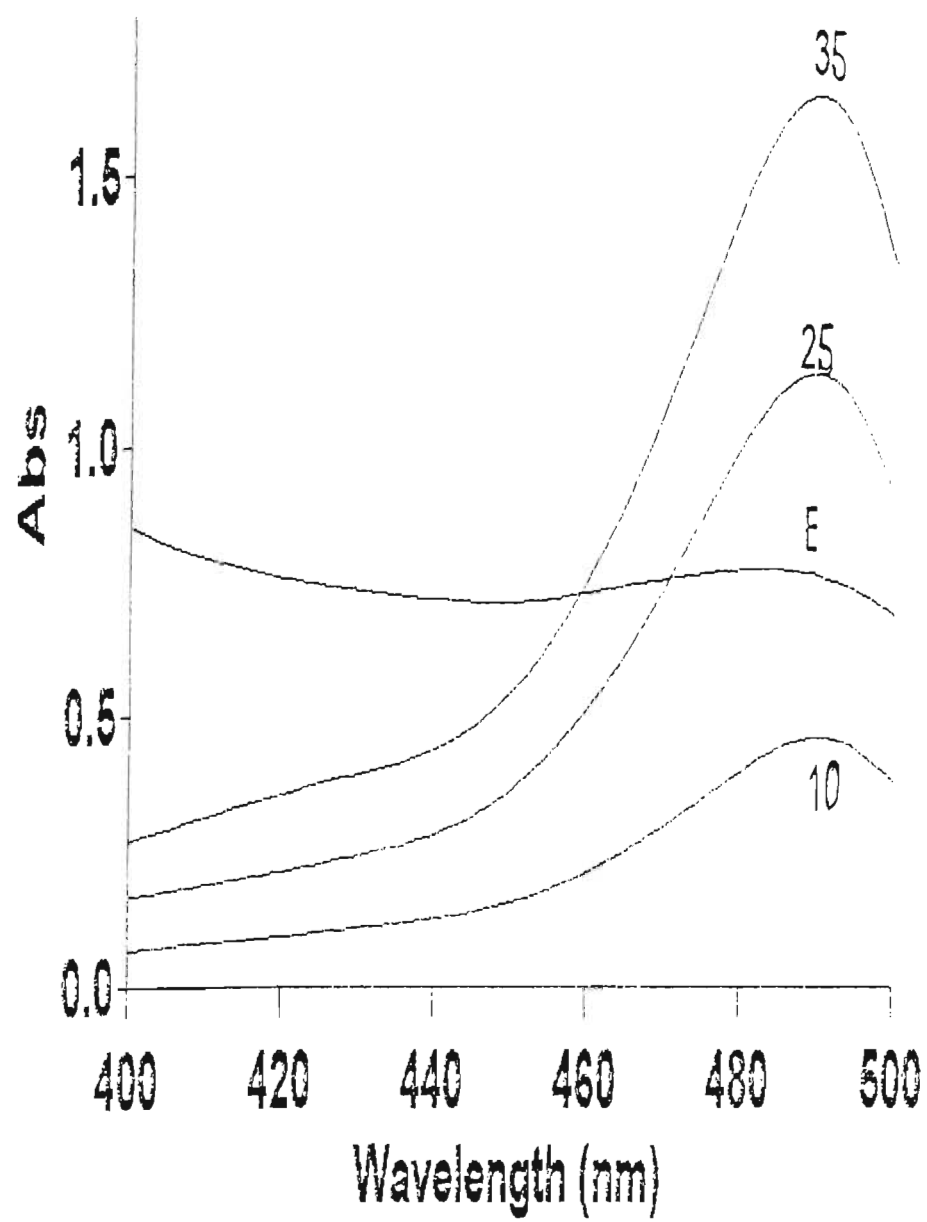
Library Searched : C:\Database\Nist98.1
Quality : 98
ID : 9,12-Octadecadienoic acid (Z,Z) -

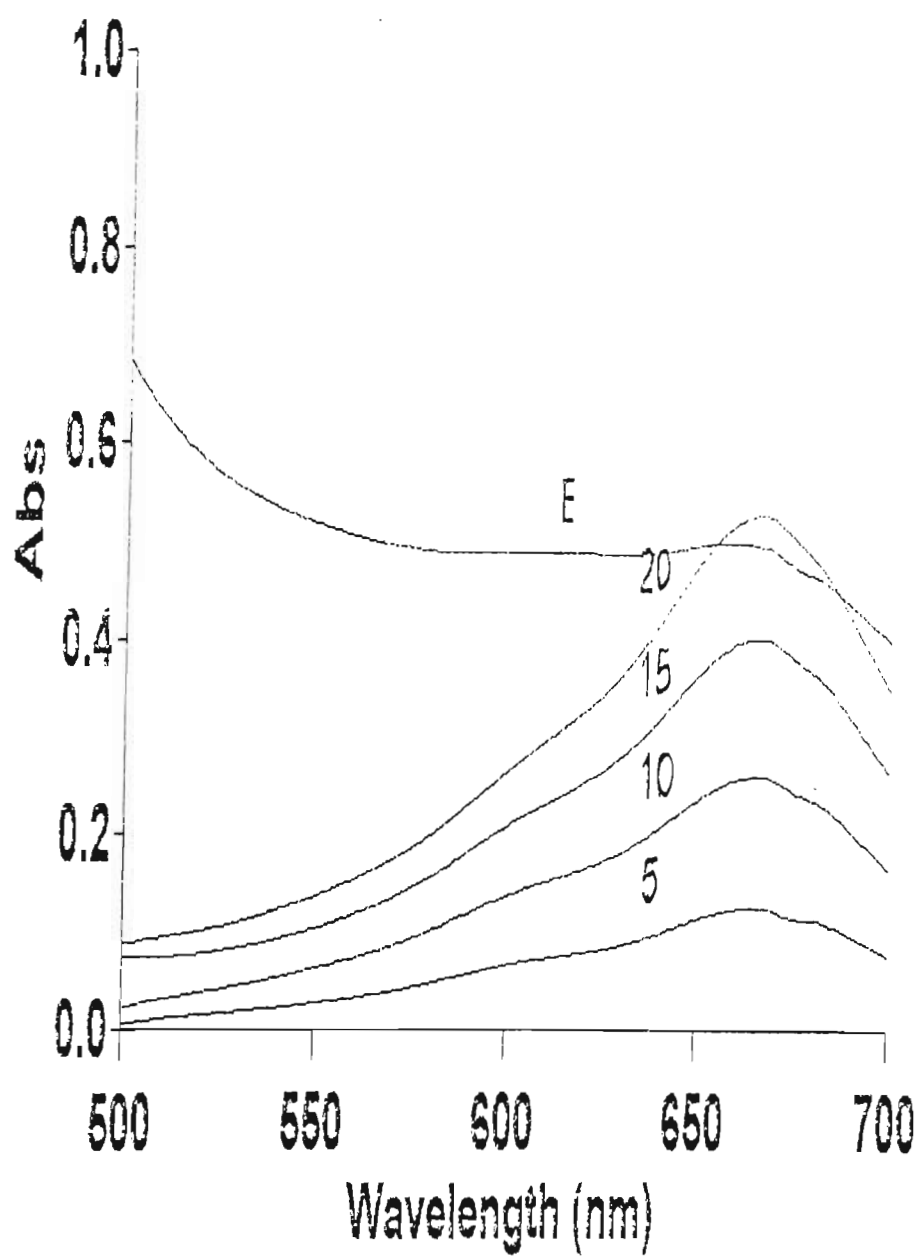


SPECTRUM 81 : Mass spectrum of compound 10, 9,12-octadecadienoic acid



SPECTRUM 82 : ^1H NMR spectrum of compound 10, 9,12-octadecadienoic acid, in CDCl_3





APPENDIX B

LIST OF DATA IN APPENDIX B

Page No.

TABLE 11 : Results of calcium – spent liquor analysis obtained from SAPPI SAICCOR	221
TABLE 12 : Data for the conductivity titration used to determine the sulphonic acid content of the calcium – spent liquor	222-223
GRAPH 1 : Graph of conductance (mS/cm) vs volume of NaOH (ml)	224
Sulphonic acid content calculations	225

SPENT LIQUOR ANALYSIS (CALCIUM BASE)

	<u>% By Weight</u>	
Total dissolved solids	15%	
Ash	1,3%	or 8,1% of solids of which 4,5 is Ca
Sugars (monosaccharides)	2,3%	or 21% of solids of which :- xylose 17,0 galactose 1,4 mannose 1,4 glucose 1,2
Hemicellulose (polysaccharides)	2,4%	or 15% of solids
Lignin	6,4%	or 40% of dry solids
Acetic acid	1,4%	
Formic acid	0,1%	
Acetone	0,1%	
Furfural	0,1%	
Alcohol (ethyl and methyl)	0,5%	
Sulphur (all forms expressed as S)	0,9%	or expressed as SO_4 = 1,8% further split into Free- SO_4 0,2 Loosely combined SO_4 0,6 SO_3 0,1 Permanently linked (sulphates, sulphonates) 0,7

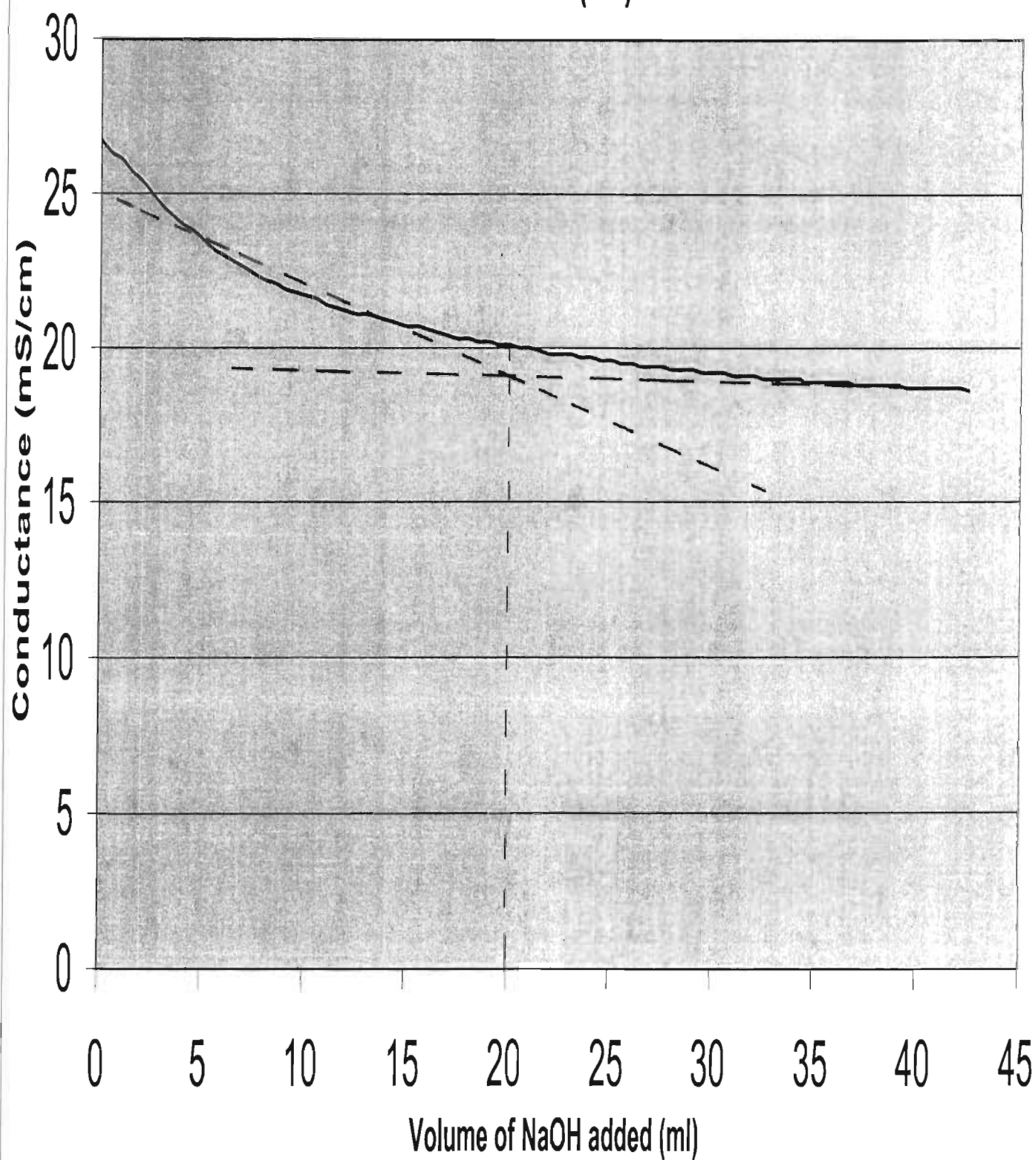
In addition there would be small amounts of a wide range of organic compounds :-
resins, waxes, oils etc.

TABLE 12 : Data for the conductivity titration used to determine the sulphonic acid content of the calcium - spent liquor

NaOH (ml)	Conductance (mS/cm)
0	26.7
0.5	26.3
1	26.1
1.5	25.7
2	25.4
2.5	25
3	24.6
3.5	24.3
4	24
4.5	23.8
5	23.5
5.5	23.2
6	23
6.5	22.8
7	22.6
7.5	22.4
8	22.2
8.5	22.1
9	21.9
9.5	21.8
10	21.7
10.5	21.6
11	21.4
11.5	21.3
12	21.2
12.5	21.1
13	21.1
13.5	21
14	20.9
14.5	20.8
15	20.7
15.5	20.7
16	20.6
16.5	20.5
17	20.4
17.5	20.3
18	20.3
18.5	20.2
19	20.2
19.5	20.1
20	20.1
20.5	20
21	20
21.5	19.9
22	19.8
22.5	19.8
23	19.8
23.5	19.7
24	19.7
24.5	19.6

NaOH (ml)	Conductance (mS/cm)
25	19.6
25.5	19.5
26	19.5
26.5	19.4
27	19.4
27.5	19.4
28	19.3
28.5	19.3
29	19.3
29.5	19.2
30	19.2
30.5	19.2
31	19.1
31.5	19.1
32	19.1
32.5	19
33	19
33.5	19
34.2	19
34.5	18.9
35	18.9
35.7	18.9
36	18.9
36.5	18.9
37	18.8
37.5	18.8
38	18.8
38.6	18.8
39	18.8
39.5	18.7
40	18.7
40.5	18.7
41	18.7
41.5	18.7
42	18.7
42.5	18.6

GRAPH 1: Graph of conductance (mS/cm) vs volume of NaOH (ml)



Sulphonic acid content calculations

Mass of sample = 50.04 g

Temperature $20.7^{\circ}\text{C} - 22.2^{\circ}\text{C}$

From the graph, the inflection point is approximately 20ml of NaOH.

$$\begin{aligned}\text{Number of moles of NaOH} &= \text{concentration} \times \text{volume} \\ &= 0.100 \text{ mol/dm}^3 \times (20 \times 10^{-3} \text{ dm}^3) \\ &= 0.0020 \text{ mol}\end{aligned}$$

no. of moles NaOH : no. of moles sulphonic acid groups is 1 : 1

therefore, no. of moles of sulphonic acid = 0.0020 mol

$$\begin{aligned}\text{sulphonic acid content} &= 0.0020 \text{ mol} / 50.04 \text{ g} \\ &= 3.997 \times 10^{-5} \text{ mol/g}\end{aligned}$$

A 20 % dodecylamine in butanol mixture was made up dissolving 20 g dodecylamine in 100 g butanol.

Molar mass of dodecylamine = 185.35 g/mol

$$\begin{aligned}\text{No. of moles in 1 g of dodecylamine} &= (1 \text{ g} \times 1 \text{ mol}) / 185.35 \text{ g} \\ &= 5.395 \times 10^{-3} \text{ mol}\end{aligned}$$

Now there is 3.997×10^{-5} moles sulphonic acid in 1 g of sample. But equivalent no. of moles as dodecylamine is required, that is 5.395×10^{-3} mol.

$$\begin{aligned}\text{Mass of sample that contains equivalent no. of moles of dodecylamine} &= (5.395 \times 10^{-3} \text{ mol} \times 1 \text{ g}) / 3.997 \times 10^{-5} \text{ mol} \\ &= 134.98 \text{ g}\end{aligned}$$

In order to have excess amine, it was assumed that the amount of sulphonic acid groups was higher than that shown on the graph, that is, 35ml instead of 20ml.

$$\begin{aligned}\text{Sulphonic acid content} &= 0.100 \text{ mol/dm}^3 \times (35 \times 10^{-3} \text{ dm}^3) / 50.04 \text{ g} \\ &= 6.994 \times 10^{-5} \text{ mol/g}\end{aligned}$$

Based on the above calculations,

$$\begin{aligned}\text{mass of sample to be taken} &= (5.395 \times 10^{-3} \text{ mol} \times 1 \text{ g}) / 6.994 \times 10^{-5} \text{ mol} \\ &= 77.13 \text{ g}\end{aligned}$$

Therefore, 77.13 g of spent liquor was mixed with 100 g of 20 % dodecylamine in butanol mixture.